1977-3

Environmental Studies, South Texas Outer Continental Shelf, 1975:

An Atlas And Integrated Summary

Prepared For

THE U.S. BUREAU OF LAND MANAGEMENT

This report has been reviewed by the Bureau of Land Management and approved for publication. Approval does not signify that the contents necessarily reflect the views and policies of the Bureau, nor does mention of trade names or commercial products constitute endorsement or recommendation for use.

FOREWORD

"When we try to pick anything by itself, we find it hitched to everything else in the universe"--John Muir.

The chemical and physical interactions both within and along the margin of earth's oceans are among the most complex phenomena in the natural sciences. Ideally, if the various aspects and processes involved were completely understood, the magnitude and scope of their interactions could be predicted for a given time and place. Unfortunately, the problem is that of solving an equation having many unknowns.

The marine environmental studies of outer continental shelf areas being made under the direction of the Bureau of Land Management are unique in both scope and approach. The regional investigations, multidisciplinary and integrated in plan and in execution, are being carried out simultaneously by teams of scientists representing State, Federal, and private organizations.

As an integrated summary of the results obtained for such a large number of scientific disciplines, this report also is unique in the field of marine science. No source of previous experience could be drawn upon for its preparation because none exists. The atlas format was chosen as the best means of presenting the data because time and space relationships for data of regional scope are more readily apparent in visual displays. Maps provide both a synoptic overview and a time base to which subsequent data similarly processed and compiled can be easily compared. By comparing sequential data covering a series of years, the nature of the processes affecting a region can be qualified and the range of their seasonal and yearly fluctuations quantified.

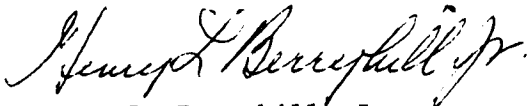

Henry L. Berryhill, Jr.

ENVIRONMENTAL STUDIES, SOUTH TEXAS OUTER CONTINENTAL SHELF, 1975:

AN ATLAS AND INTEGRATED SUMMARY

Henry L. Berryhill, Jr.
Program Coordinator,
Compiler and Editor

Participating Organizations and Principal Investigators:

University of Texas

P. L. Parker
C. Van Baalen
J. S. Holland
D. E. Wohlschlag
R. S. Scalan
N. P. Smith
J. K. Winters

Texas A&M University

C. S. Giam
E. T. Park
W. M. Sackett
B. J. Presley
J. D. McEachran
M. E. Chittenden, Jr.

Rice University

R. E. Casey

National Oceanic and Atmospheric Administration

National Marine Fisheries Service

J. W. Angelovic
R. F. Temple
J. H. Finucane
C. W. Caillouet
W. L. Trent
C. R. Arnold
E. L. Nakamura
R. Juhl
R. S. Armstrong

National Ocean Survey

M. F. Devine

U.S. Geological Survey

H. L. Berryhill, Jr.
G. L. Shideler
C. W. Holmes
S. S. Barnes
G. W. Hill

Prepared for
The U.S. Bureau of Land Management

CONTRACT 08550-MU5-20
SUBMITTED APRIL, 1977

TABLE OF CONTENTS

LIST OF ILLUSTRATIONS

LIST OF TABLES

INTRODUCTION

LOCATION OF AREA AND BATHYMETRY

The South Texas Outer Continental Shelf (OCS) as described herein is the area outlined by the Department of the Interior for oil and gas leasing. The area covers approximately 19,250 sq km and extends northward from the United States-Mexico International Boundary to a midpoint of Matagorda Island, Texas and seaward from the Federal-State territorial boundary 16.6 km to the approximate position of the 200 m isobath, or outer edge of the continental shelf (fig. 1). The lease block grid for the area is shown by figure 2 and subdivisions of the South Texas OCS are shown by figure 3.

The bathymetry of the South Texas OCS is shown by figure 4. The continental shelf off south Texas has an average width of about 88.5 km and a relatively gentle seaward gradient that averages about 2.3 m/km. The primary topographic features outlined by the bathymetric contours on the map are the deltaic bulge seaward of the Rio Grande, the comparable outline of an ancestral delta near the shelf edge seaward of Matagorda Bay and the broad ramplike indentation on the outer shelf between the two deltaic bulges. Second order topographic features are the north-to-northeastward trending low ridges, terraces and low scarps over the ancestral Rio Grande delta, the series of small closures associated with a band of irregular topography along the ramp between water depths of 64 to 91 m and the terracelike area along the outer shelf beginning at the 91 m isobath. The secondary features seem to be relicts of late Pleistocene and early Holocene deposition and erosion associated with migration of the shoreline. The small topographic closures

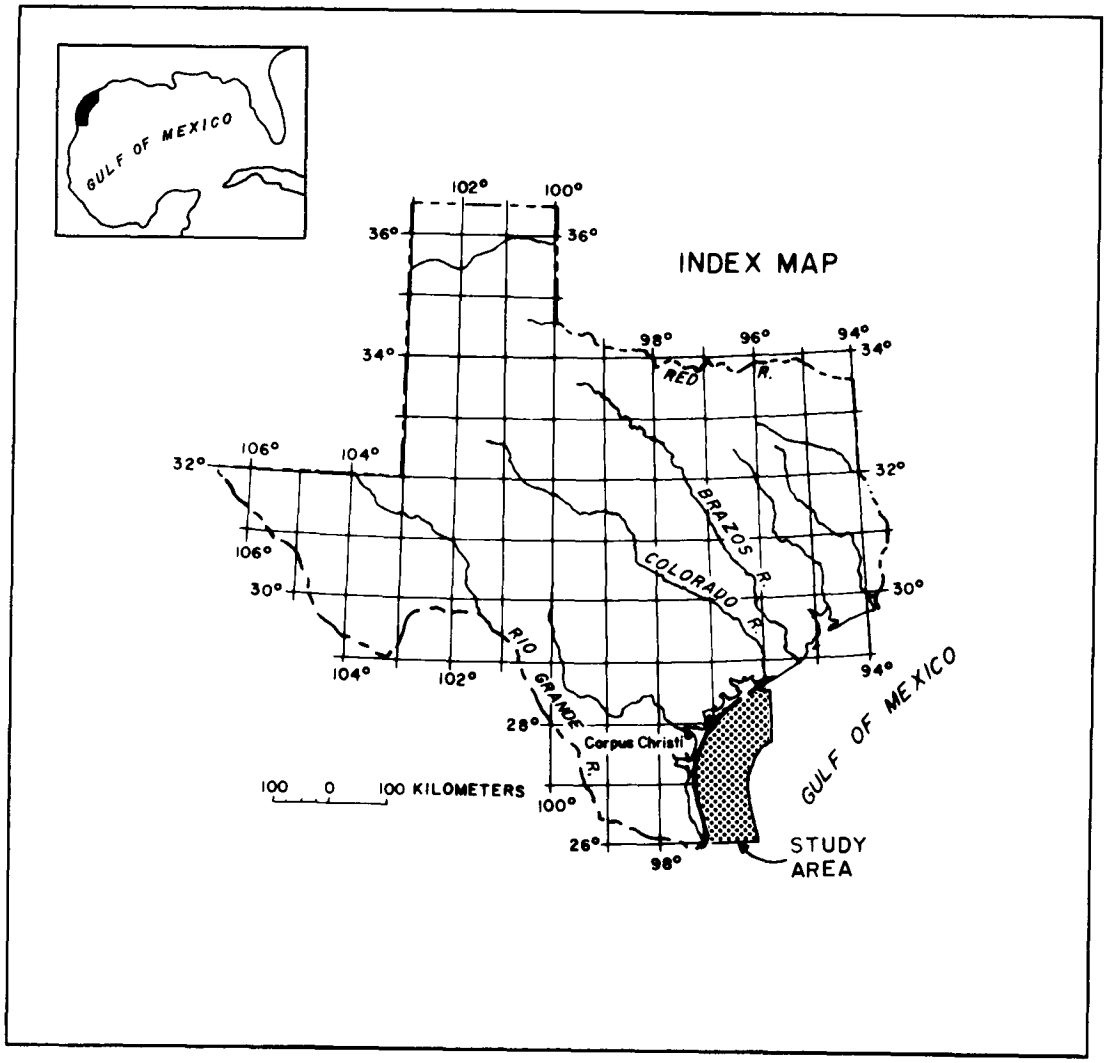

Figure 1. Location of the study area.

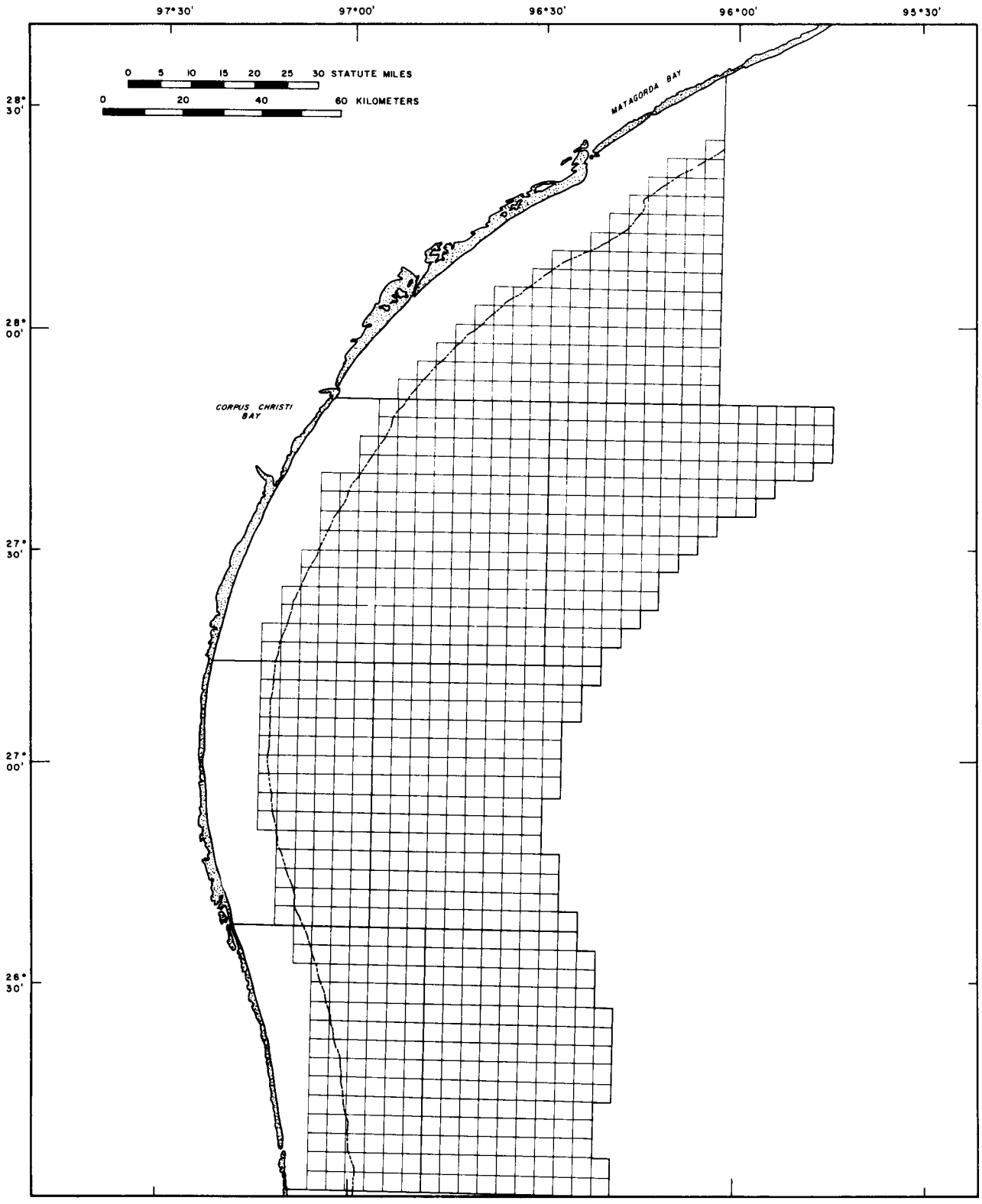

Figure 2. Petroleum lease block grid for the South Texas Outer Continental Shelf.

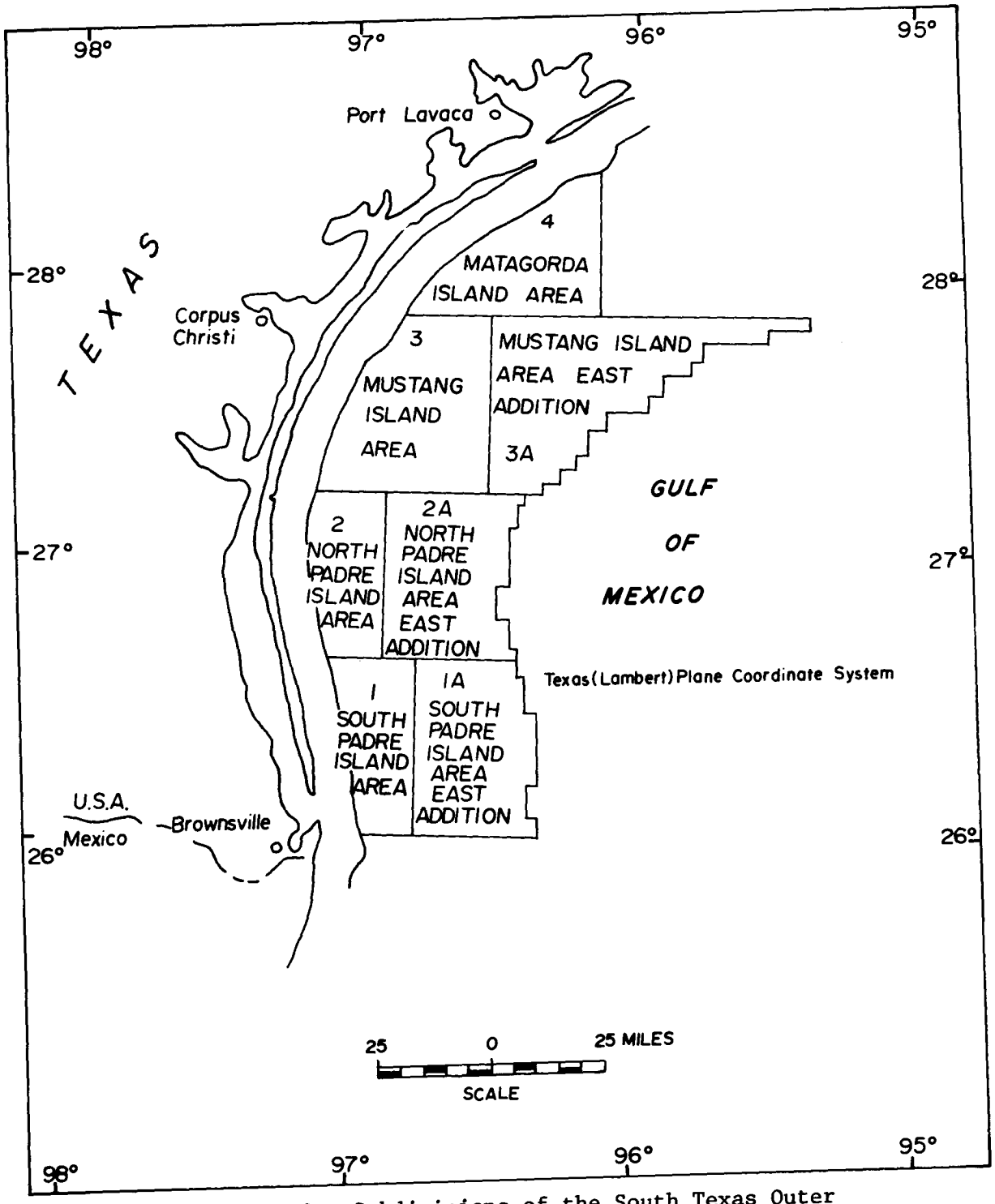

Figure 3. Subdivisions of the South Texas Outer Continental Shelf lease area.

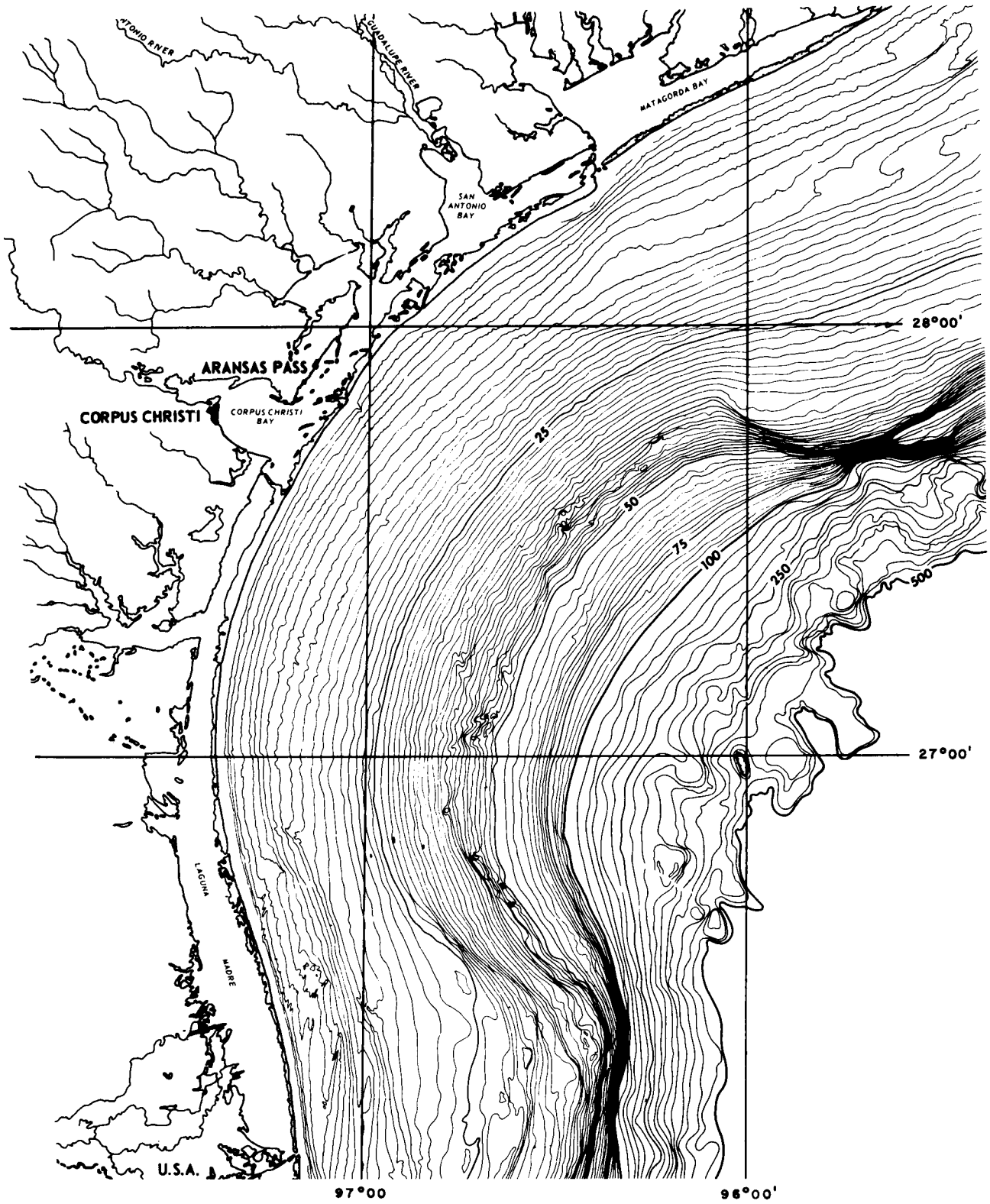

Figure 4. Bathymetry of the South Texas Outer Continental Shelf (depth in fathoms). From Berryhill and others, 1976, Part I, figure 3.

on the outer shelf have been identified as carbonate reefs that formed during the last low stand of sea level in late Pleistocene/early Holocene time. The locations of the reefs are shown by figure 5.

PURPOSE AND NATURE OF STUDIES

General Statement

In 1974, the Bureau of Land Management was authorized to initiate a National Outer Continental Shelf Environmental Studies Program to include all OCS areas considered by the Federal Government for future petroleum leasing and development. The primary objectives of the program, as stated by the BLM are:

- to provide information about the OCS environment that will enable the Department of the Interior and the Bureau of Land Management to make sound management decisions regarding the development of mineral resources;
- to provide a basis for predicting the impact of oil and gas exploration and development on the marine environment;
- to establish a basis for predicting the impact of OCS oil and gas activities in frontier areas;
- to provide impact data that might result in modification of leasing regulations, operating regulations, or operating orders.

To accomplish the stated objectives, the BLM developed an operational plan that will eventually include four phases of effort in those segments of the OCS that yielded oil and gas. The phases are: I, summary of existing knowledge; II, baseline sampling and gathering of supporting descriptive and predictive data based on consideration of data gaps indicated by review

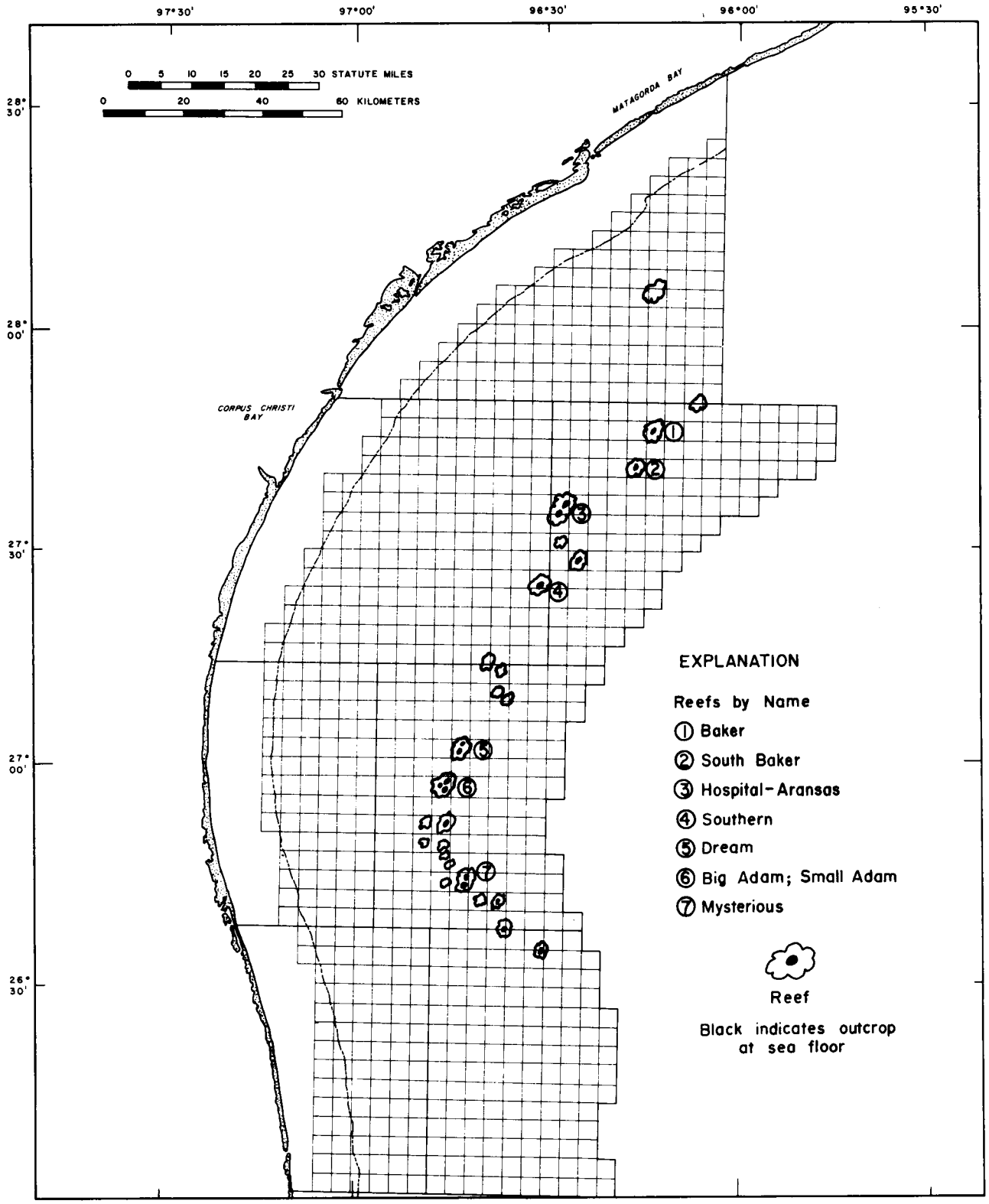

Figure 5. Location of carbonate reefs on the outer part of the continental shelf.

of existing knowledge; III, special topical and additional descriptive and predictive studies as directed by the initial studies; and IV, environmental monitoring after oil and gas exploration and development have begun.

Work Plan

Baseline Sampling

Following review of the status of knowledge for the South Texas OCS in the summer of 1974, a plan for sampling and scientific study was developed that would provide a comprehensive data base from which the status of pre-development environmental conditions (baselines) for an offshore region could be determined and the possible impact of petroleum development predicted. The rationale for the baseline concept as the initial type of field study is based on the firm premise that future impacts cannot be detected, measured, and assessed unless the nature of the environment and some of its intricacies are known and understood beforehand. Aspects of the environment specified by the BLM for study relative to the determination of baselines are listed below.

Water Mass

- Hydrography and physical oceanography: water mass structure; movement and variations; severe conditions;
- Biology: planktonic populations; biomass; productivity levels; macro-organisms; taxonomy;
- Chemistry: trace metals and hydrocarbons in particulates and in organisms; hydrocarbons in solution; micronutrients; dissolved oxygen; salinity.

Sediments

- Biology: identification of benthic communities; total biomass; species diversity; extent of bioturbation;

- Chemistry: trace metals; hydrocarbons; organic carbon; carbonate;
- Geology: texture and mineralogy of unconsolidated sediments; structural features with emphasis on faults and chronology of faulting; seeps; slumps.

In developing the plan of study for the South Texas OCS, the scientific investigations were coordinated in an interdisciplinary manner so that the results would not only reveal baseline conditions but also yield some understanding of the magnitude, scope, and interaction of the marine processes operative over the region as well. As a supplement to the field sampling and acquisition of new data, pertinent historical data of two types were used: a) sample material previously collected but not analyzed; and b) analytical data available but not extensively published. The historical data are so identified in the text.

The work plan for the South Texas OCS provides for several years of study: an initial year to determine the environmental conditions prior to the beginning of drilling; and subsequent years to confirm the results for the first year and to provide a base for future monitoring of operations. The work was continued in 1976 and sampling for 1977 is about to begin.

Time Frame For Field Studies

The South Texas OCS region was selected for study by the BLM in the summer of 1974. The field investigations for the first year began in late October 1974 and ended in mid September 1975.

The geologic field investigations were completed between late October and late December 1974; the biological and hydrographic field work was done seasonally, beginning in November 1974 and ending in September 1975. Seasonal sampling was continued in 1976 and will be carried out again in 1977.

Participants

The scientific investigations for the first year of study were carried out by 2 Federal agencies and 3 universities, under contractual arrangement with the BLM. The participating organizations were: the University of Texas Marine Science Institute, Port Aransas; Texas A&M University; Rice University; The National Oceanic and Atmospheric Administration; and the U.S. Geological Survey, Corpus Christi office.

The study involved some 110 persons at one time or another during all phases of the first year's effort. The management structure included a program manager, 3 element leaders responsible for organizational increments of the study, and 28 principal investigators, who bore the responsibility for completion of the scientific analytical synthesis and for preparation of topical reporting assignments. The organizational structure for the study and the names of principal investigators, listed according to organization represented and scientific responsibility, were as follows:

Program Manager

Henry L. Berryhill, Jr.

U.S. Geological Survey

Element Leaders

Patrick L. Parker

University of Texas

for work done by
- University of Texas Marine Science Institute at Port Aransas
- Texas A&M University
- Rice University

Assisted by
C. S. Giam
Texas A&M University

Joseph W. Angelovic

National Marine Fisheries Service, Gulf Fisheries Center

for work done by
National Oceanic and Atmospheric Administration:
- National Marine Fisheries Service
- National Ocean Survey
- (Texas A&M University by subcontract)

Henry L. Berryhill, Jr.

U.S. Geological Survey

Principal Investigators

Listed by organization represented and by discipline or topic of study responsibility

University of Texas Marine Science Institute, Port Aransas

Hydrography	Ned P. Smith
Phytoplankton and chlorophyll	Chase Van Baalen
Neuston	J. Selmon Holland
Benthic invertebrates	J. Selmon Holland
Demersal fishes	Donald E. Wohlschlag
High-molecular-weight hydrocarbons:	
Water	Patrick L. Parker Richard S. Scalan J. Kenneth Winters
Neuston	
Zooplankton	
Sediment	

Texas A&M University

Zooplankton	E. Taisoo Park (Moody College of Marine Sciences and Maritime Resources)
Low-molecular-weight hydrocarbons and nutrients	William M. Sackett
High-molecular-weight hydrocarbons	
Benthos	C. S. Giam
Trace metals: neuston, zooplankton, benthos	Bobby J. Presley

Rice University

Microzooplankton and microzoobenthos	Richard E. Casey

National Oceanic and Atmospheric Administration:

National Marine Fisheries Service

Larval shrimp (historical)	Robert F. Temple
Ichthyoplankton	John H. Finucane
Shrimp catches (historical)	Charles W. Caillouet, Jr.
Pelagic fishes	W. Lee Trent
Recreational fishes	W. Lee Trent Connie R. Arnold
Billfishes	Eugene L. Nakamura
Hydroacoustic survey (fishes)	Rolf Juhl
Physical Oceanography (climate) (historical): Seasonal temperature, salinity and circulation	Reed S. Armstrong Robert F. Temple

Texas A&M University

Zooplankton (historical)	E. Taisoo Park
King mackerel and Spanish mackerel larvae	John D. McEachran
Ichthyofauna (historical)	Mark E. Chittenden, Jr.

National Ocean Survey

Climate; wind; tides; currents	Michael F. Devine

U.S. Geological Survey, Corpus Christi, Texas

Benthic sediments: texture, mineralogy and general sedimentation	Gerald L. Shideler
Benthic sediments: trace metals content; carbonate; organic carbon; and clay mineralogy	Charles W. Holmes
Benthic sediments: stratification and depositional structures	Henry L. Berryhill, Jr.
Suspended sediments: distribution and texture	Gerald L. Shideler
Suspended sediments: clay mineralogy	Charles W. Holmes

Suspended sediments: trace metals content - - - - - - - - - - - - - Stephen S. Barnes

Biogeology: infaunal communities and biogenic structures in benthic sediments - - - - - - - - - - - - Gary W. Hill

Geologic framework and sea floor stability - - - - - - - - - - - - - Henry L. Berryhill, Jr.

Field Investigations

Biological surveys

The biological surveys, which included also sampling for hydrography and benthic infauna, were repeated three times to provide seasonal coverage: December 1974-January 1975; April-May 1975; and August-September 1975. The biological surveys were planned jointly by the University of Texas Marine Science Institute, Port Aransas; Texas A&M University and the National Marine Fisheries Service. The surveys were made under the auspices of the University of Texas Marine Science Institute, Port Aransas, and scientists from Texas A&M and NMFS participated in the cruises.

Survey vessel--The biologic and hydrographic sampling at sea were made aboard the R/V LONGHORN owned by the University of Texas. The LONGHORN is a steel-hulled 80 ft by 24 ft, 7 ft draft ship carrying a crew of 5 and a scientific party of 10.

Navigation and sample station locations were plotted by LORAN A. Water depth was measured by a SIMRAD fathometer. Persons who served as chief scientist during the cruises were: Gerald P. Pfeiffer, Ned P. Smith, Richard K. Tinnin, and J. Selmon Holland.

Sample stations--The sampling grid consisted of 12 stations located on 4 transects, as shown on figure 6. As noted previously, each station was

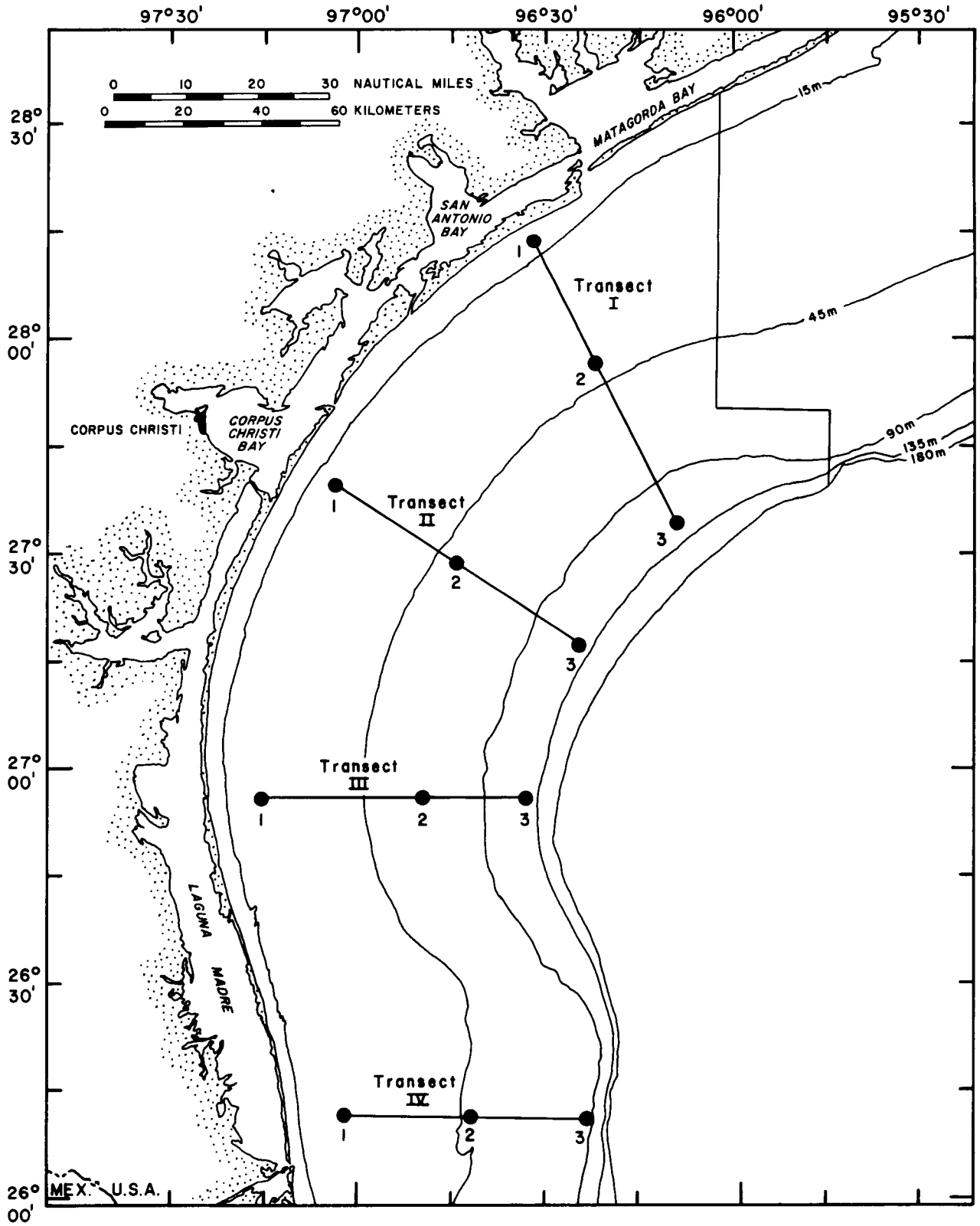

Figure 6. Location of stations for biologic and hydrographic sampling.

occupied 3 times during the 1-year study period to allow for seasonal variations. The coordinate location of each of the 12 biologic-hydrographic stations is shown by table 1. For utility, the geologic sampling station number (fig. 7) that corresponds to the biologic station has been added to the table. The geologic stations, though not in every case in exactly the same position as the biologic stations, are nevertheless close.

Table 1. Station locations and depths for the biologic-hydrographic sampling. Number in the right hand column is the corresponding number of the geologic sampling station.

Transect number	Station number	Latitude	Longitude	Depth (meters)	Geologic sta. no.
I	1	28°12.0'	96°27.0'	18	10
	2	27°54.5'	96°19.5'	42	32
	3	27°33.5'	96°06.5'	134	85
II	1	27°40.0'	96°59.0'	22	70
	2	27°30.0'	96°44.5'	49	95
	3	27°17.5'	96°23.0'	131	115
III	1	26°57.5'	97°11.0'	25	165
	2	26°57.5'	96°48.0'	65	160
	3	26°57.5'	96°32.5'	106	156
IV	1	26°10.0'	97°00.5'	27	246
	2	26°10.0'	96°39.0'	47	250
	3	26°10.0'	96°24.0'	91	255

The rationale for the sampling grid was based on the working experience of the scientists in the South Texas OCS region. The geographic positions of the transects and the depth position of individual stations along the transects were preselected on the basis of the generally uniform changes in bottom topography, both in a seaward direction and from north to south, and in the physical and chemical parameters. The seasonal sampling periods were selected to permit study of the water column during a cold period, during a period of mixed temperatures, and during a time of temperature maximum.

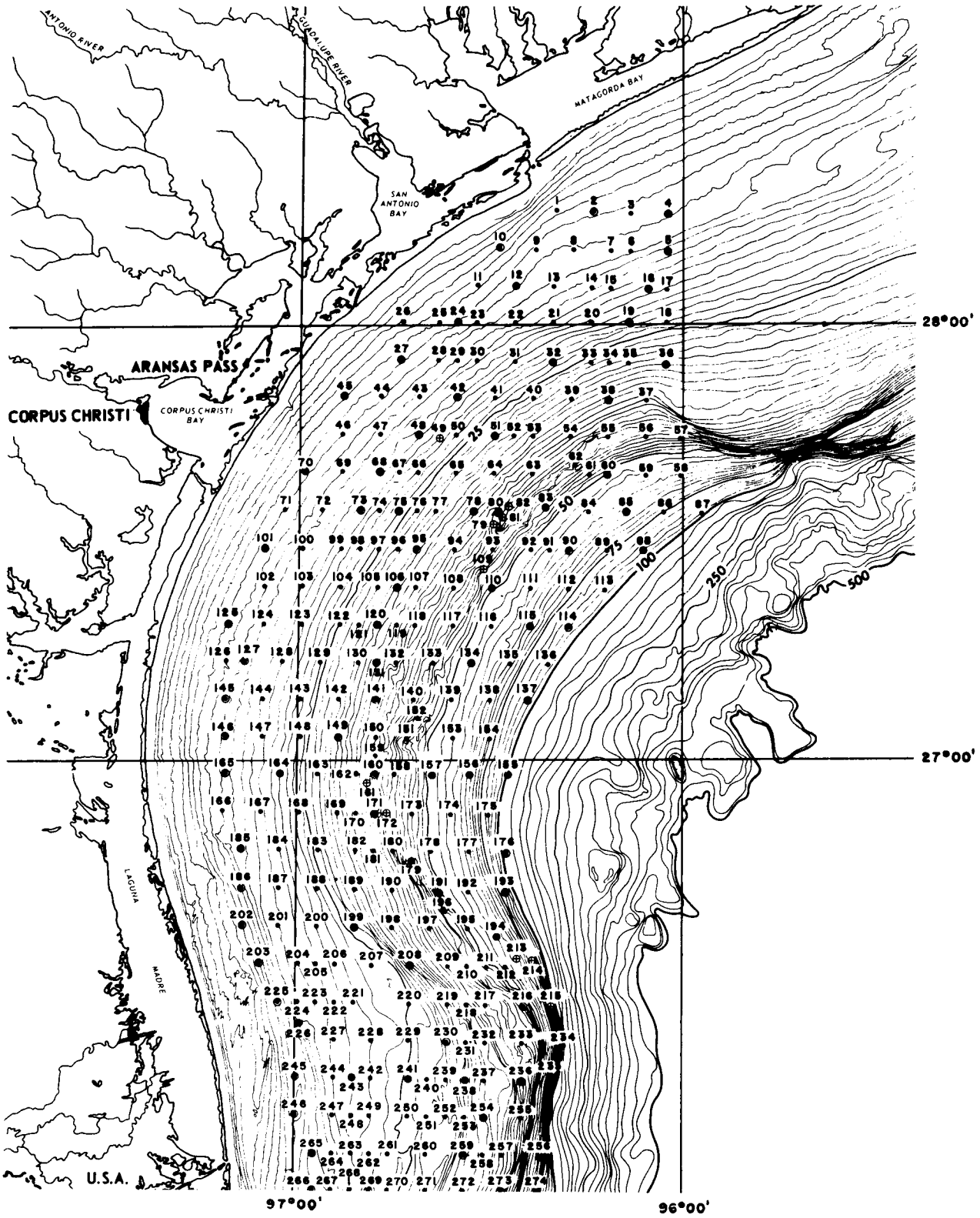

Figure 7. Location of benthic sample stations for geologic studies. • indicates bottom grab; ◉ indicates both pipe core and box core in addition to bottom grab; ⊕ indicates pipe core only.

Sampling techniques

1. Hydrography - A PLESSEY salinity-temperature-depth (STD) self-contained profiling system was lowered at each of the 12 stations. The resulting salinity and temperature profiles provided a general characterization of the water mass. The profiles were supplemented with surface calibration data, using a bucket thermometer for temperature and a BECKMAN RS-7 laboratory salinometer for salinity.
2. Primary productivity - Water samples were taken with NISKIN bottles at two depths (surface and one half the photic zone) for phytoplankton and at three depths (the above two depths and at near-bottom depth) for nutrients, chlorophyll a, ATP, low-molecular-weight hydrocarbons and dissolved oxygen. The photic zone was determined by use of a SECCHI disc.
3. Zooplankton (Mesozooplankton and Ichthyoplankton) - Two oblique tows were made for zooplankton, day and night, using 250 µm nets equipped with flowmeters and a BENTHOS time-depth recorder; vertical tows were made using a 30 cm, 74 µm mesh net. Water samples were taken at several depths for microzooplankton studies.
4. Neuston - The sea surface was only sampled during the day. A 1 m, 153 µm net was towed at the surface by a sled. No flowmeter was used.
5. Benthic fauna - Three types of benthic samples were taken: a) the epifaunal invertebrates were sampled both day and night using a 10.7 m standard otter trawl; b) the demersal fish were sampled day and night using a conventional Gulf coast 10.7 m standard flat trawl; c) the bottom sediments were sampled for infauna using a SMITH-MACINTYRE grab sampler with a capacity of 0.0125 m^3. Four replicate samples were taken with the grab sampler at each station so that in-station variability could be determined.

6. Hydrocarbons - Water, zooplankton, neuston, epifauna, bottom sediment, and macronekton samples were taken for hydrocarbon analysis. Subsamples of 30-l water bottle casts were reserved for dissolved low-molecular-weight hydrocarbon determination; special 19-l water samples were collected for dissolved high-molecular-weight hydrocarbon determination. Zooplankton nets were towed day and night using a standard 1 m net mounted on a specially constructed metal-free frame. Subsamples of sediments were taken from the benthic grabs. Neuston net tows were made with a 0.5 m net equipped with noncontaminating grommets and mounted on a sled constructed of fiber glass. Epifaunal samples, consisting of crustaceans, molluscs and fishes, were collected with the otter trawl. All material collected, both biologic and bottom sediments, was frozen aboard ship in glass containers. The preservative used for the water samples was mercuric chloride.
7. Trace metals - The collections of zooplankton, neuston, and benthic fauna taken for hydrocarbon analysis were also subsampled for trace metal analysis. All samples were frozen aboard ship in plastic bags and maintained in this state until analyzed.

Summary of samples collected--A summary of samples collected is given in table 2.

Table 2. Listing of biologic-hydrographic samples by type and number.

Type	Number
Phytoplankton	72
Zooplankton	144
Neuston	36
Benthos (epifauna and infauna)	324
Hydrography	72
Light hydrocarbon	146
Heavy hydrocarbon	395
Trace metal	348
Microzooplankton	432
Primary productivity	147
Quality control	140
TOTAL	2,256

Geological surveys

The geological survey was subdivided into a series of three cruises or surveys: the first beginning on October 29, 1974 and the third ending on December 21, 1974. The geologic field investigations included, in addition to the sampling of benthic sediments and sediment particulate suspended in the water column, expendable bathythermograph (XBT) casts and the release of surface drifters. In addition some 1,600 km of high resolution seismic reflection profiles were collected as a means of relating the near-surface geologic conditions to the regional geologic framework of the continental terrace.

Survey vessel--The vessel used for the geologic investigations at sea was the R/V KANA KEOKI, leased by the USGS from the University of Hawaii. The R/V KANA KEOKI has an overall length of 156 ft and beam of 36 ft, carries an operating crew of 15, and has accommodations for a scientific crew of 15. Chief scientists for the three cruise legs were Charles W. Holmes, Gerald L. Shideler and Henry L. Berryhill, Jr.

Field positioning for the sampling and vessel navigation for the geophysical surveying for most of the work was provided by Decca Survey Systems, Inc. on a subcontract to USGS. The precision system was HI FIX operating in a hyperbolic mode with a lane transmitting separation of 50 ft. Use of LORAN A and satellite navigation in lieu of HI FIX during parts of cruise leg three was necessary because of sky wave problems during the night hours.

Sample stations--A sampling net of 274 bottom stations spaced along 27 transects was established for the geologic sampling. The locations of the benthic sample stations are shown by figure 7. The rationale used in

establishing the bottom station net was: adequate regional coverage; spacing to provide a station for each of the blocks nominated for petroleum lease bid; the geologic nature of the area to the extent known prior to the study, including the physiography of the sea floor and general sedimentological patterns; and sufficient density to determine if distributional characteristics of the bottom sediments such as texture might indicate long-term net movement patterns of shelf water.

Sampling format and techniques

1. Bottom sediments

   a) Bottom grab samples - At 264 of the 274 bottom stations a grab sample was taken using a SMITH-MACINTYRE sampler having a 0.0125 m^3 capacity. From each grab sample, seven subsamples were taken for the various analyses to be made and for the archives: texture; clay mineralogy; percent heavy minerals; carbonate content; organic carbon content; and trace metals content (barium, cadmium, copper, chromium, iron, manganese, nickel, lead, vanadium, zinc). The subsamples were taken by inserting plastic tubes 15 cm long and 3.8 cm in diameter into the sediment. The tubes were capped with plastic CAPLUGS and sealed. The subsamples for organic carbon, carbonate and archiving were frozen aboard ship.

   b) Biogeologic samples - After completion of the subsampling from each of the 264 bottom grab samples, the remaining sediment was washed through a specially constructed 46 cm diameter aluminum hopper containing a large-sized sieve for catching the macro-infaunal organisms and a 0.5 mm mesh SARAN bag acting as a screen at the terminal end to catch all other organisms in the sediment.

The bag sample was gently washed to remove the fine sediment and stored in a glass jar in 5 percent buffered formalin. The biologic samples were removed from the ship after each cruise leg and transferred to a 45 percent isopropyl alcohol solution until such time as they could be sorted, counted and identified. Similar treatment was given to the sediment remaining in each of the box cores, thus providing an additional sample for checking variability of infaunal communities at a station. The locations of the sample stations for biogeologic studies are shown by figure 7a.

c) Pipe cores - At 90 stations, a pipe core was obtained for studying sediment stratigraphy and textural variations with depth below the sea floor surface: 80 cores at grab sample stations; 10 at stations other than grab sample stations where special bottom features were indicated. The sediments were cored by use of a gravity-fall pipe corer constructed of stainless steel and loaded by a 500 lb head. The core was retained in a plastic liner having an inside diameter of 7 cm. The actual length of the sediment cored was recorded, the probable maximum penetration of the corer was approximated from the mudline on the corer and recorded, and the cores were capped and sealed aboard ship. The cores were stored aboard ship in vertical racks under refrigeration and were subsequently maintained under refrigeration until processed in the laboratory for study. The location of the pipe cores is shown by figure 8.

d) Box cores - At 74 of the 90 pipe core stations, a box core was taken using a sampler of 0.028 m^3 capacity employing a 1000 lb head. The sampler was able to penetrate up to 45.7 cm into the sea floor. The

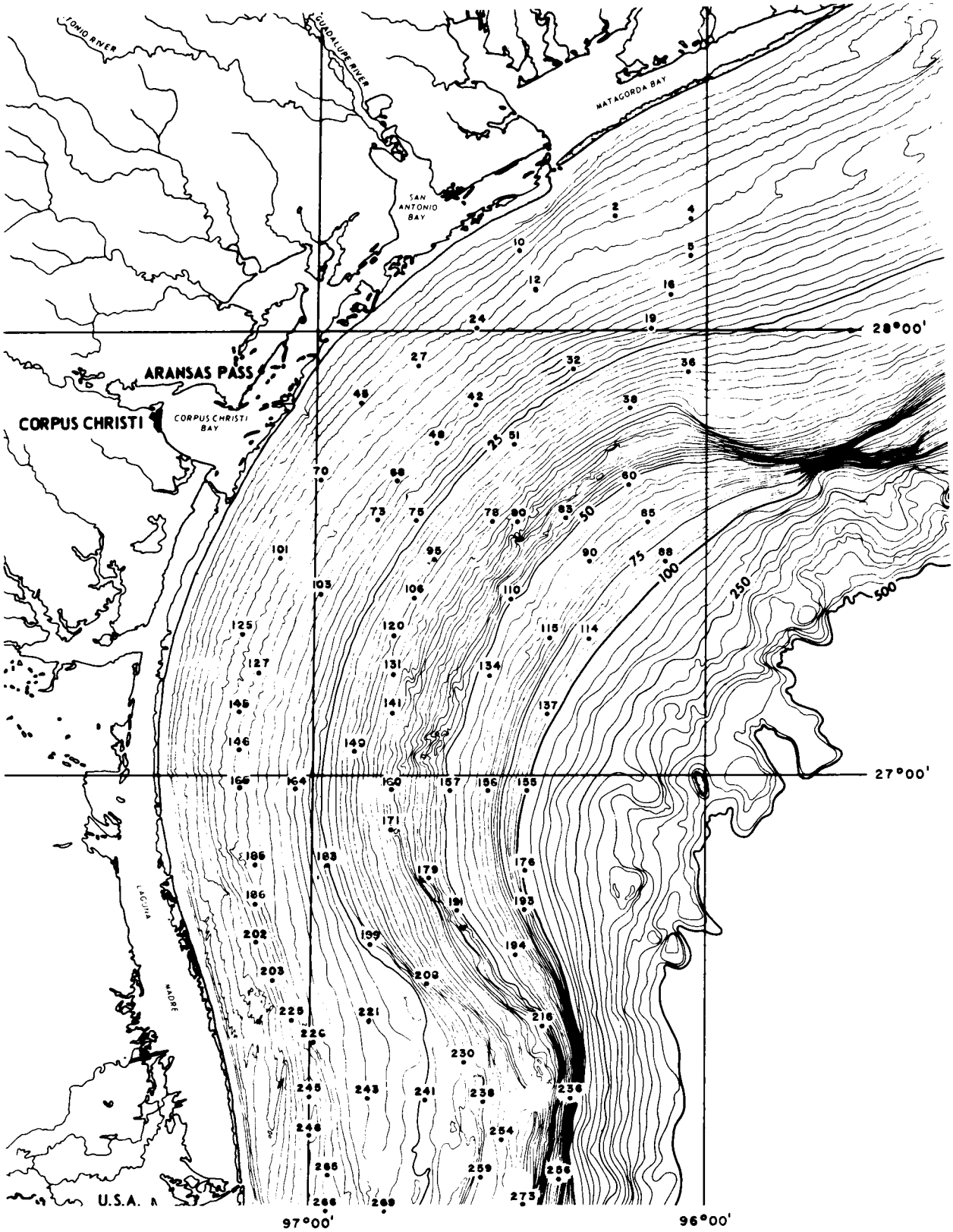

Figure 7a. Location of sample stations for biogeologic studies.

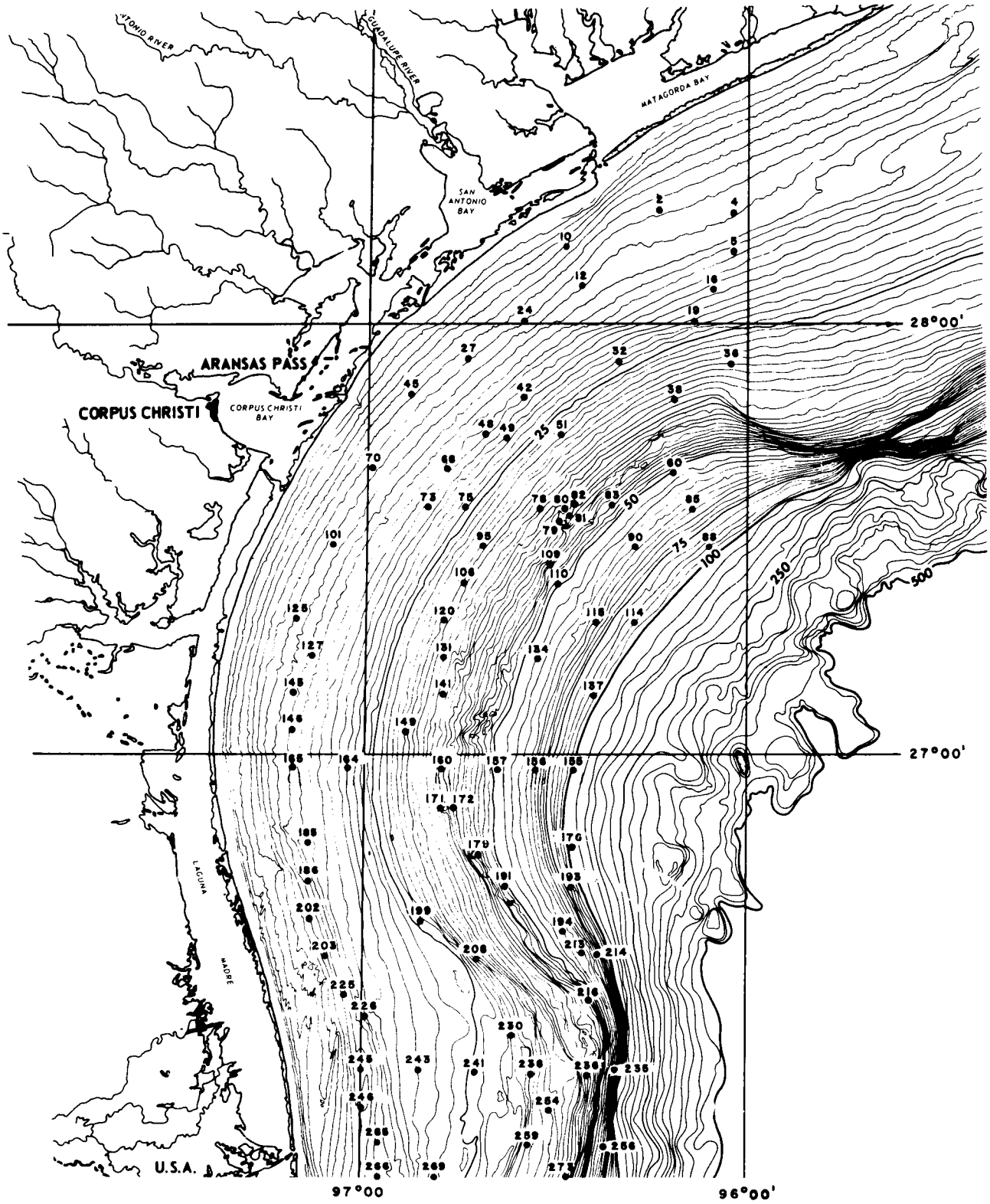

Figure 8. Location of pipe core stations.

sediment was cored to document depositional sedimentary structures and biogenic structures. The box cores were slabbed, photographed aboard ship and stored under refrigeration. Before the cored sediment was slabbed, a backup sample for hydrocarbon analysis was taken and frozen aboard ship. The location of the box core stations is shown by figure 8a. Although they are included on figure 7, the locations of the pipe core and box core stations are repeated in figures 8 and 8a for clarity and utility.

2. Suspended sediments

At 24 of the 264 bottom grab stations, samples were taken at 3 depths in the water column for suspended sediment: surface, mid-water depth, and near bottom. Water samples were obtained in NISKIN bottles and transferred to plastic bottles for further processing aboard ship. The water for sediment texture studies was put into 1 gallon jugs, buffered with 5 percent formaldehyde solution to prevent organic growth and stored under refrigeration. A one-to-one 3-1 aliquot of each sample showing turbidity was filtered through a preweighed SELAS FLOTRONICS silver filter having a 0.45 μm nominal pore diameter, washed with 100 ml of deionized water in order to remove the salts, and frozen for return to the laboratory. The locations of sample stations for suspended sediments are shown by figure 9.

3. Hydrography and physical oceanography

To augment the hydrography and physical oceanography studies, XBT casts were made at 128 of the 264 bottom grab stations and surface drifter bottles were released at 79 stations. The XBT graphs were turned over to NOAA for use in their compilation. The locations of the XBT and surface drifter cast stations are shown by figures 10 and 11.

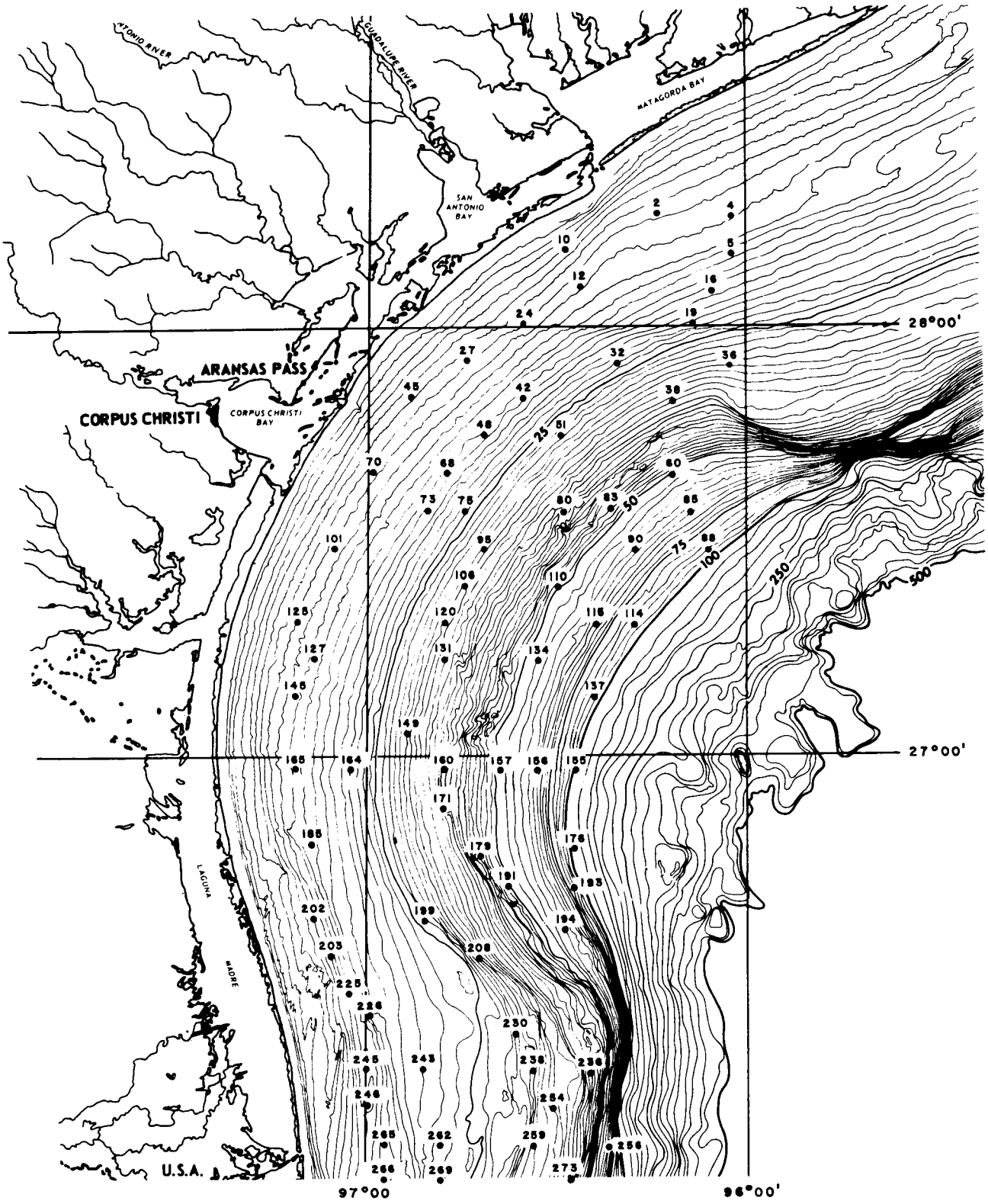

Figure 8a. Location of box core stations.

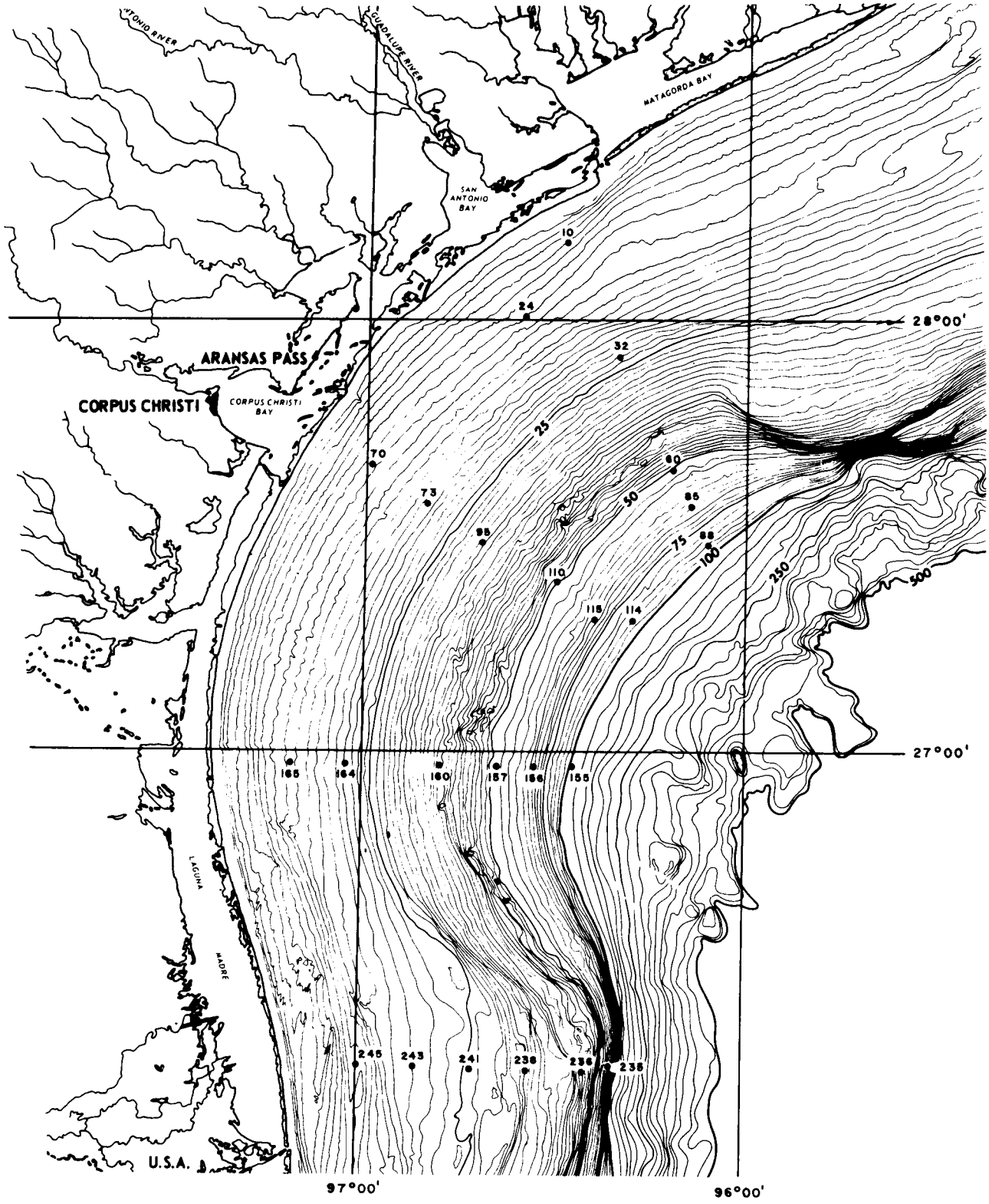

Figure 9. Location of sample stations for suspended sediments.

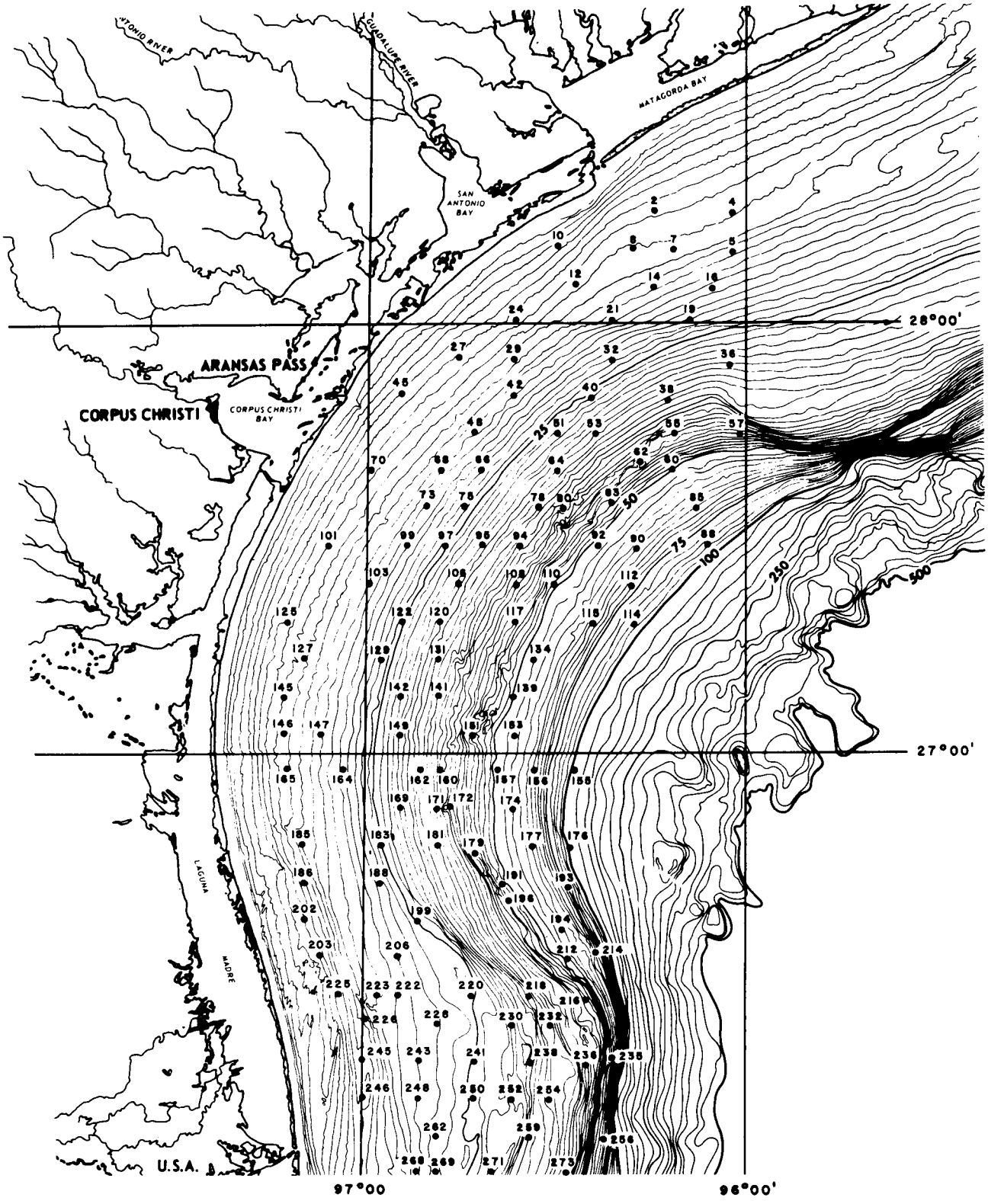

Figure 10. Location of XBT stations.

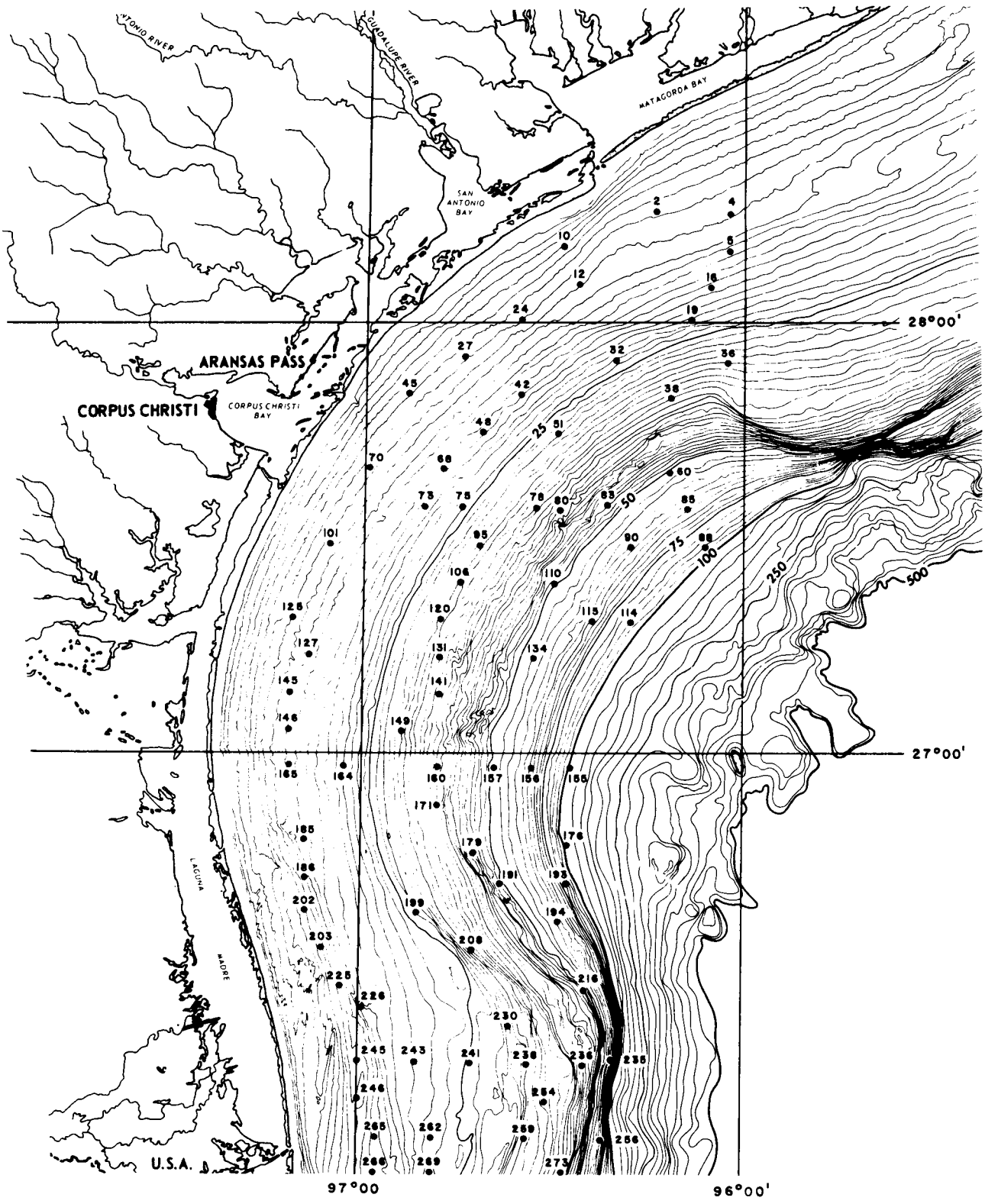

Figure 11. Location of surface drifter cast stations.

Summary of samples collected--A listing of samples collected by type and number is shown by table 3.

Table 3. Listing of geological and associated samples by type and number.

Benthic sediments for trace metals analysis	264
Benthic sediments for textural analysis	264
Benthic sediments for clay mineralogy	72
Benthic sediments for percent heavy minerals	72
Benthic sediments for carbonate analysis	264
Benthic sediments for organic carbon analysis	264
Pipe cores for textural stratification, depositional structures and biogenic structures	90
Box cores for near-surface depositional and biogenic structures	72
Infaunal samples from benthic sediments for biogeologic studies	338
Suspended sediment samples for trace metals and clay mineralogy	72
Temperature/depth (XBT)	128
Sediment samples as backup for hydrocarbon analysis	74
Bottom grab samples, archives	264
Box core slabs, archives	74
TOTAL	2,612

Geophysics--The geophysical data used for compiling the geologic framework were 11,260 km of high-resolution seismic reflection analog profiles. These data include 8,860 km made available by the Conservation Division of USGS and 1,600 km collected on the third geological cruise.

No commitment for a specific amount of acoustic profiling was stated in the USGS contract with the BLM. As originally planned, the third geological cruise was to have been devoted entirely to geophysical surveying. However, continuing night sky wave problems with the HI FIX navigation system plus loss of the box corer halfway.through the second geological cruise pushed some 10 days of station work into the third cruise, thus decreasing the amount of geophysical data ultimately obtained.

The systems used for collecting the geophysical data were: ACOUSTIPULSE, transmitting 1000 joules and recording at a sweep rate of 250 ms; ANALOG REFLECTION sparker, transmitting 900 joules and recording at a sweep rate of 1000 ms; sparker, transmitting 10,000 joules and recording at a sweep rate of 1000 ms; and SUB-BOTTOM PROFILER, transmitting 10 kw (3.5 kHz frequency) and recording at a sweep rate of 500 ms. The navigational fixes taken at intervals of 305 m along most of the traverses and at 610 m along others provided some 37,000 precisely located points for plotting of the geophysical data. The locations of the acoustic profiles coded as to the several types of acoustic data obtained are shown by figure 12.

Historical Surveys

General statement

From January 1963 to December 1965, a unique set of time-series surveys was conducted in and adjacent to the South Texas OCS by the Galveston Laboratory of the U.S. Bureau of Commercial Fisheries, now the National Marine Fisheries Service, using the R/V GUS III. The surveys were part of an extensive shrimp research program in the northwestern Gulf of Mexico. During the 3 years, key stations arranged in transects across the continental

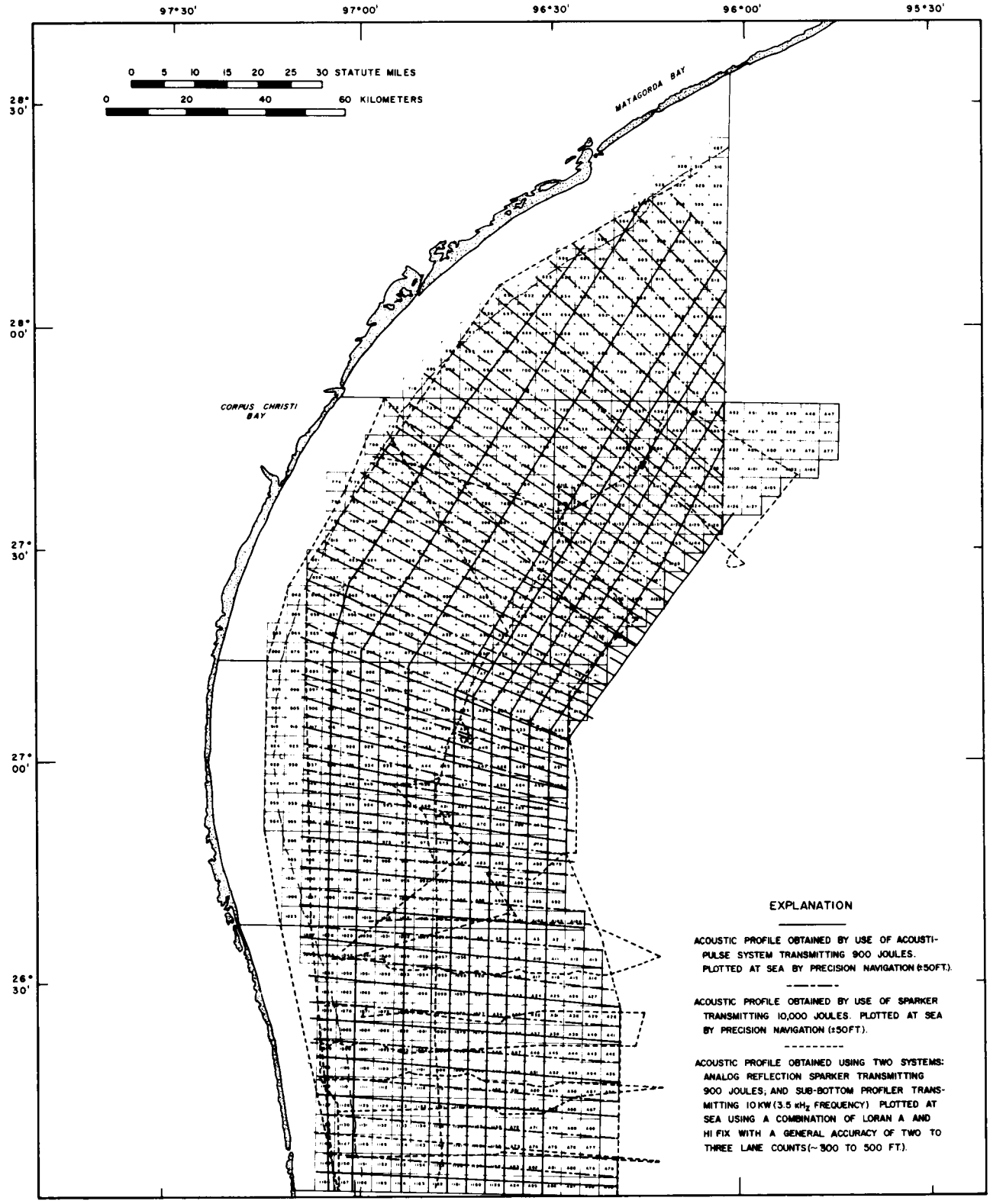

Figure 12. Location of geophysical track lines.

shelf off Texas and Louisiana were occupied monthly. Work at each station included biologic sampling and hydrographic observations. The locations of stations on the three transects that are within the South Texas OCS are shown by figure 13.

Since 1965, some of the data collected during the 1963 to 1965 cruises have been analyzed and published, while other material has not been analyzed. The data from the GUS III cruises have been included in the South Texas OCS environmental study because: 1) the amount of data available is significant and the data are pertinent to the study; and 2) the historical data provide a time-lapse comparison with results from the 1974-1975 study.

The historical data have been analyzed for the South Texas OCS environmental studies by scientists representing the National Marine Fisheries Service and the National Ocean Survey of NOAA. Their report also included a historical summary of the regional climatology, both onshore and offshore, as well as historical data on hydrography and physical oceanography collected and supplied by members of the Department of Oceanography, Texas A&M University.

Biology

Zooplankton--The historical zooplankton samples collected on the South Texas OCS during the GUS III cruises came from stations 22, 23, 24 and 58 (fig. 13) and the collections were made on a monthly basis. The samples were collected with a GULF-V plankton net made of 200 μ mesh wire screen with a mouth diameter of about 40.5 cm. Tows were step-oblique of about 20 minutes duration from 3 m above bottom to the sea surface. The amount of water filtered during each tow was estimated from a flowmeter positioned in the center of the net mouth.

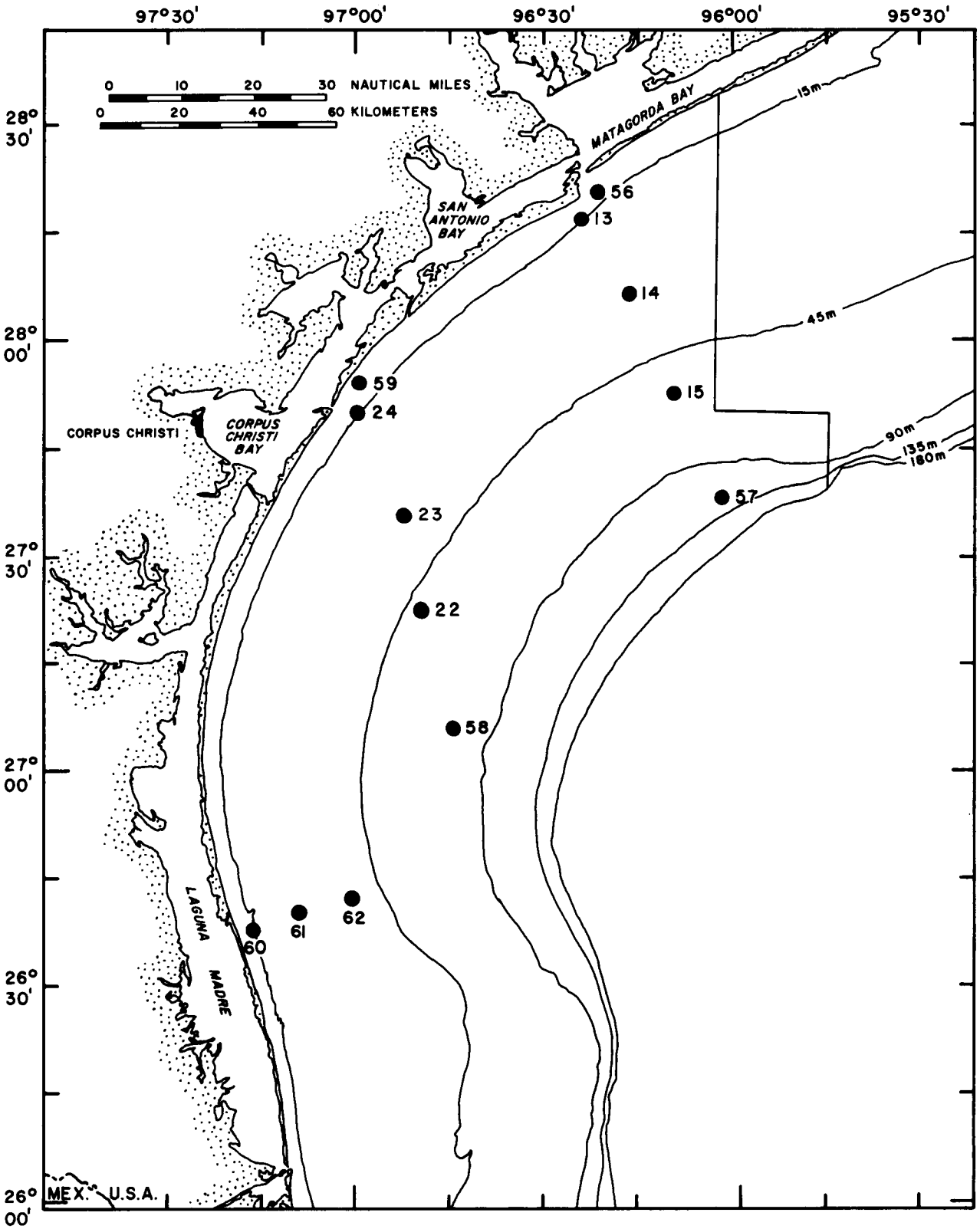

Figure 13. Location of sampling stations for historical data collected by Bureau of Commercial Fisheries (now National Marine Fisheries Service), 1962-1965; hydrographic and biologic.

Larval shrimp (Penaeus spp.)--Sampling for larval shrimp also was carried out during the 1963 to 1965 cruises. The stations sampled for shrimp larvae were the same as those sampled for zooplankton (fig. 13).

Samples were obtained with a GULF-V plankton net consisting of a conical, monel net (mesh size of 31.5 strands per cm) attached to a metal frame. The plankton was collected in a cup attached to the end of the net; following each tow the net was washed down and the plankton was removed and preserved in 5 percent formalin. Estimates of water volume filtered were calculated from a flowmeter positioned in the center of the net mouth. Oblique-step tows were made at each station at tow speed averaging 4.6 kmph. Each of 4 depths was fished for 5 minutes during each tow: 3 m above bottom, 2 intermediate depths, and 3 m below the surface.

Physical oceanography/hydrography

1. A surface drifter survey was conducted by the Bureau of Commercial Fisheries, Galveston, during 1962 and 1963. Surface drift bottles were released from a ship each month at the stations shown on figure 14. Operations were similar between years except that fewer stations were occupied in 1963 and one vessel was used to cover the entire study area rather than two as in 1962. Although the rate of bottle recovery varied between months, cumulative totals for the 2 year period indicate that 20.3 percent of the bottles released were recovered within 30 days.
2. A surface and bottom drifter project was started in 1970 by the USGS office in Corpus Christi, in cooperation with the U.S. Coast Guard Rescue Unit stationed at the Corpus Christi Naval Air Station. The

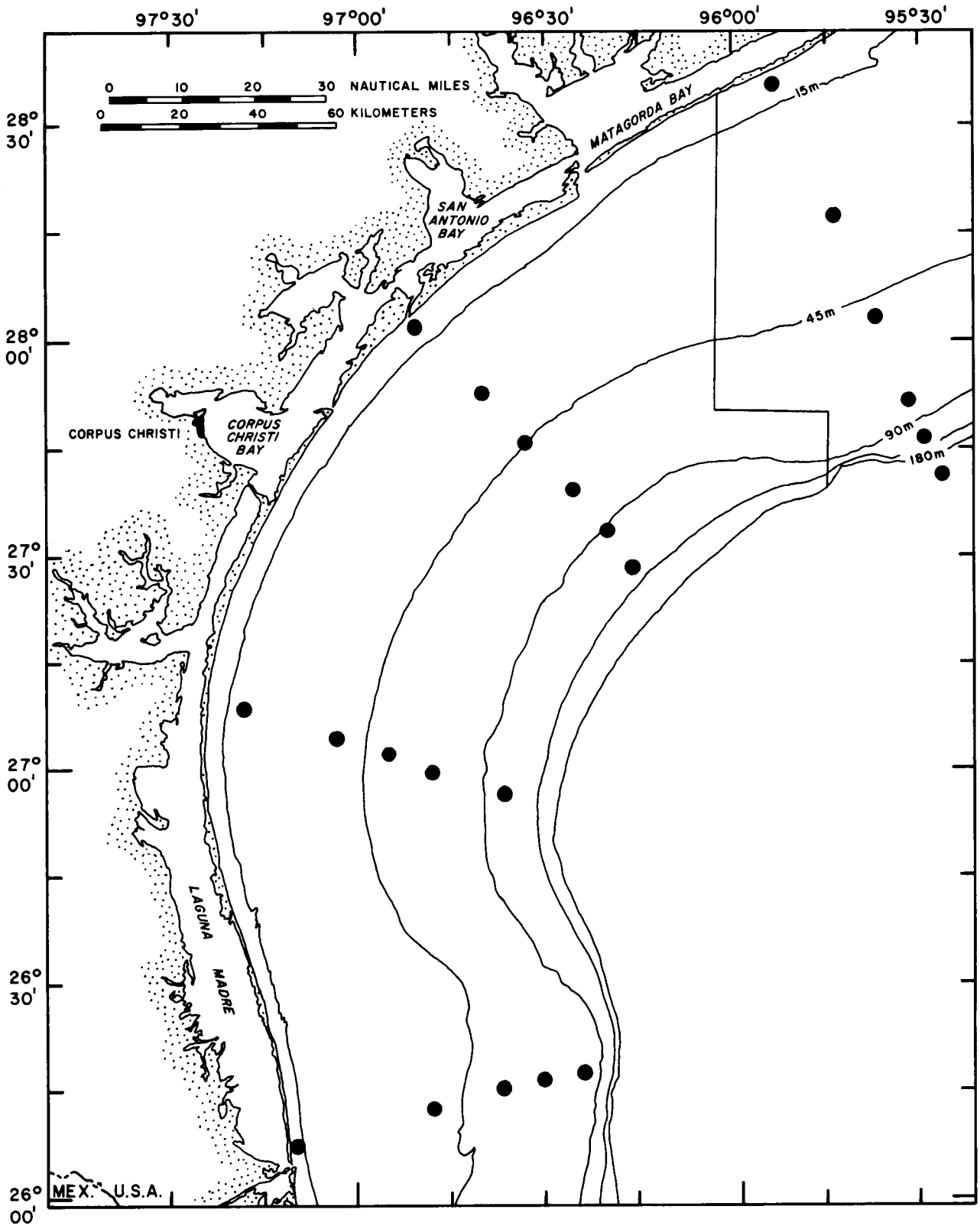

Figure 14. Location of stations for release of surface drifters, 1962-1963.

surface and bottom drifters were dropped from an airplane whose location was fixed by LORAN A or by TACAN. The release points (48) were 22 km (12 nautical miles) apart along 4 lines paralleling the coast between Port Aransas, Texas and the mouth of the Rio Grande. These lines were 2, 19, 37 and 56 km offshore in water depths averaging 9, 27, 40 and 58 m. Releases were made seasonally from January 1970 to April 1973 with the exception of a gap in the winter of 1971. In 1973 the area of study was extended northward to the entrance to Galveston Bay. The overall average recovery was 20 percent of the drifters released during the 1970 to 1973 period.

3. Monthly temperature and salinity measurements were made vertically through the water at each station as a part of the shrimp research project. The temperatures were recorded by mechanical bathythermographs that sounded bottom in all casts. Surface bucket temperatures were taken for correction purposes with stem thermometers graduated to 0.1°C. Surface water was sampled for salinity determinations from the bucket samples used for bathythermograph reference temperatures. Subsurface waters were sampled at depths of 3, 11, 24, 43, 70, and 107 m in NANSEN bottles. All samples were drawn into 200 mm culture tubes having POLYSEAL caps. As soon as possible after each cruise, chlorinity was determined in the laboratory by the Knudsen method.

   Additional hydrographic data gathered by Texas A&M University are included in the resumés of historical data.

4. The statistics used to summarize the regional weather characteristics for the onshore coastal area of south Texas came from the long-term weather records of the National Weather Service recorded at coastal

weather stations located in Corpus Christi and Brownsville, and at several subordinate stations. Offshore climatic data were accumulated over the years from ships' records, from ephemeral offshore observation stations and from specific studies and observations of hurricanes.

The data for tides, tidal currents and sea level came from the coastal tidal recording stations at Port Isabel, Brazos Santiago, Port Aransas and Galveston, although Galveston lies north of the South Texas OCS. Of the tidal recording stations within the South Texas OCS region, the one at Port Aransas does not provide a continuous historical sequence of data, as numerous gaps exist in the records.

Quality Control Analyses

Of vital importance to any baseline studies program is the quality of the analyses performed. Consistent and state-of-the-art analytical techniques both within a laboratory and between laboratories, and precision of results within very narrow limits are mandatory if the baselines are to be meaningful and useful in any subsequent monitoring efforts.

Every effort was made during the planning of the South Texas OCS Environmental Studies Program not only to insure the use of up-to-date techniques widely recognized and used in the scientific community, but also to require a standardization among the various scientists and laboratories that would produce not only precision but consistency as well. Consequently, for each discipline of study that required analytical chemical quantification of the sample material obtained, a specific number of samples was designated for quality control analysis. The number of samples for each discipline and the geographic spread of the samples to be used for quality control were designated

by the BLM. The quality control sample was taken as a subsample at sea from the primary field sample, was handled and prepared aboard ship in the same manner as other subsamples from the same primary sample, and then was sent directly to the quality control laboratory by the investigator. Quality control laboratories, one for trace metals analysis and another for hydrocarbons, were selected by the BLM. The quality control laboratories are independent of the South Texas OCS Environmental Studies Program and have no investigative role in it themselves, nor any connection with the principal investigators. The quality control analyses provide to the BLM a check against the analytical results supplied by the individual investigators.

Reporting of Data

Data management

Comprehensive programs of the geographic scope of the several OCS environmental studies now underway generate a large volume of data. Such a quantity of data requires a management system that not only must be internally standardized for effective data synthesis but also must provide the basic analytical results expeditiously to the BLM and to the public.

To insure maximum utility of the basic data produced, the management plan for the South Texas OCS adheres to that established by the BLM for the overall National Environmental Studies Program. All data generated are transferred in accordance with established deadlines as interim inventory listings to the BLM. These data are supplied in a computer format that lists each sample by number, location (by geographic and X-Y coordinates), water depth and other pertinent descriptors. All analytical results obtained

for the sample are also recorded. Data for each discipline of study are reported separately but are formulated in a manner that will provide for cross-correlating analytical results within a major category of study, such as within biology or within geology.

As the means of making the basic analytical data available to the public on a timely basis, the investigators are required to submit the properly formulated data to the Environmental Data Service (EDS) of the National Oceanographic Data Center (NODC) of NOAA, where the public may obtain the data upon request. The time frame for submitting basic analytical data to the EDS is approximately one year from the terminal date of the field investigations. All basic analytical data produced during the first year (1975) of the South Texas OCS environmental study have been submitted to the EDS, with the exception of biological taxonomic data which will be prepared according to the numeric code now being formulated by the Institute of Marine Science, University of Alaska on a grant from NODC along with BLM support. The numeric code is intended to be applicable on a world-wide basis to higher taxa so that genera and species can be fitted into it.

Element reports

The element report is a second level of reporting established by the BLM to provide a synthesis and interpretation of the basic data, resulting in an overview of regional characteristics on a topical basis. Prepared under the guidance and coordination of the element leader, the element report includes the analytical results and interpretations prepared by each principal investigator.

Results of the first year of study for each of the three elements of the South Texas OCS study (UT/A&M/RU, NOAA and USGS) have been released in

three separate reports that cover the topical responsibilities undertaken. The titles of the reports and their availability are as follows:

1. Angelovic, J. W., and others, 1976, Environmental Studies of the South Texas Outer Continental Shelf, 1975: vol. I, Plankton and Fisheries Investigations, 425 p., 40 figs., 45 tables; vol. II, Physical Oceanography, 290 p., 174 figs., 14 tables (NOAA). Available from the U.S. Bureau of Land Management Regional Outer Continental Shelf Office, New Orleans, La.: Hale Boggs Federal Bldg., 500 Camp Street, Suite 841 (70130).

2. Parker, P. L., and others, 1976, Environmental Studies, South Texas Outer Continental Shelf, 1975, Biology and Chemistry: text, 598 p., 181 figs., 83 tables; 2 vols. of appendices listing analyses (UT/A&M). Available from the BLM office, New Orleans, see address above.

3. Berryhill, H. L., Jr., and others, 1976, Environmental Studies, South Texas Outer Continental Shelf, 1975: Geology: Pt. I, 353 p., 114 figs., 21 tables; Pt. II, Analytical data, 83 p. Available by direct order from the National Technical Information Service, Springfield, Va., 22161; price $10.75.

A fourth report, complementary to those listed above but not included in the integrated summary, covers a separate and continuing study of the topographic highs or offshore reefs on the South Texas OCS. The results of the topographic highs studies made in 1975 are in Bright, Rezak and others (1976). The report is available from the BLM office in New Orleans.

Integrated report

The third level of reporting established for the OCS environmental study areas is the integrated report, a summary synthesis of the data in the element reports to provide a regional interdisciplinary overview and characterization plus an understanding of the extent, magnitude, and interaction of the various processes that make up the marine environment of the continental shelves. The integrated report is both a descriptive resumé of the data for each discipline presented within an integrated outline and

an interpretive synthesis of all the data to highlight the most significant findings and their regional relations.

The essence of the format chosen for the integrated report, South Texas OCS, is a series of small-scale summary maps. The maps represent a translation of the basic analytical data from the original tabular form prepared by the principal investigators to maps which permit greater utility in comparing and correlating data. Furthermore, the maps presented herein provide a time base to which data from the subsequent years of study, similarly plotted, can be compared quickly and easily. A series of such maps, spanning several years of study, will provide a means for determining the significant long-term regional trends, the maximum ranges of variation that can be expected from one year to another and the degrees of interrelationship for the various marine processes.

The maps are arranged in various series in this report to convey the intended purposes which are to demonstrate regional variability within a given aspect of study as a function of season and water depth and to compare the distributional pattern for a single environmental aspect to that of another.

In most cases, the mapped analytical data have been extrapolated by use of contours to make any apparent regional trends more visible. In cases where a regional trend seems apparent, shading has been used for accentuation. The contours and shading used to highlight the patterns represent my interpretive judgement concurred with by the principal investigators.

The integrated report emphasizes the most significant results of the first year of study and the relation of one aspect of data to another. Consequently, the large volume of tabulated basic analytical data in the

element reports is not repeated, nor are the numerous references to the literature cited by the various investigators. The reader who wishes to obtain the precise coordinate location of a sample, to examine the analytical data as originally compiled, or to read the principal investigator's original interpretation and background of research, should consult the element reports. The discussions that follow are the integrated results for the year 1975.

Glossary for symbols and terms used to record and report units of measurement

Physical oceanography and hydrography

°C - degree centigrade*

°/oo - parts per thousand

σt - density anomaly

gm/cm^3 - gram per cubic centimeter

MLD - mixed layer depth

cm - centimeter*

cm/sec - centimeter per second

km/h - kilometer per hour

m - meters*

mph - miles per hour

m/sec - meters per second

l - liter*

ml - milliliter*; one thousandth of a liter

ml/l - milliliters per liter

Geology

μm - micron; one millionth of a meter

mm - millimeter; one thousandth of a meter

Ø - phi; particle size diameter expressed as the negative logarithm to the base 2 of the diameter in millimeters. As the particle size decreases the Ø unit increases.

ms - milliseconds*, one thousandth of a second

gm - gram*

μg - microgram*, one millionth of a gram

cm^3 - cubic centimeters

ppm - parts per million*

kHz - kilohertz; a frequency of 1000 cycles per second

joule - unit of energy expended in one second by a current of one ampere at a potential of one volt

BP - before present

Chemistry

at/l - moles per liter, or micrograms divided by atomic weight divided by volume (liter)

µg-at/l - micrograms per atom liter

µg/l - micrograms per liter

nm - nanometer, one billionth of a meter

nl - nanoliter, one billionth of a liter

nl/l - nanoliter per liter

µl - microliter, one millionth of a liter

µg/gm - micrograms per gram

ppmv - parts per million volume

mg/kg - milligrams per kilogram

(*Indicates unit used in more than one discipline of study)

CLIMATE

COASTAL CLIMATOLOGY

General

The climate of south Texas is subtropical and is characterized by short mild winters and hot summers; however, significant variations occur from north to south. The climate becomes progressively drier southward and most of the south Texas coastal area is classed as semi-arid. Compared to an average of 106.20 cm of rain at Galveston, Corpus Christi receives an average of 71.98 cm and Brownsville an average of 67.95 cm. Monthly averages of weather measurements for Corpus Christi and Brownsville are given in table 4.

Pressure and Winds

The general circulation of air near the surface over the south Texas coastal region follows the sweep of the western extension of the Bermuda high pressure system throughout the year. The Bermuda pressure system becomes dominant during the spring months, as the influence of northern anticyclones disappears. Mean pressure falls as the equatorial trough migrates northward and the low pressure system over Mexico deepens. The minimum mean pressure of 1014 mb occurs in summer.

Beginning in September, the equatorial trough migrates southward, the Mexican low pressure system fills, and the Bermuda high pressure system decreases in strength. Accompanying this trend, continental high pressure systems to the north intensify as winter approaches. As barriers weaken to the south, the high pressure systems moving from the north reach the

Table 4. Monthly long-term averages of weather measurements made at Corpus Christi and Brownsville.

Corpus Christi (27°46' N., 97°30' W.)

Type Measurement	J	F	M	A	M	J	J	A	S	O	N	D	ANNUAL
Temperature, °C	13.9	15.6	18.3	22.2	25.6	27.8	28.9	28.9	27.6	23.3	17.8	15.0	22.2
Monthly mean (°F)	(57.0)	(60.1)	(64.9)	(71.7)	(78.1)	(81.7)	(84.0)	(84.0)	(81.7)	(73.9)	(64.0)	(59.0)	(71.7)
Precipitation in	4.1	4.1	3.6	5.3	7.6	6.1	5.8	7.1	11.2	7.1	4.3	5.3	71.9
cm (in)	(1.6)	(1.6)	(1.4)	(2.1)	(3.0)	(2.4)	(2.3)	(2.8)	(4.4)	(2.8)	(1.7)	(2.1)	(28.3)
Days with precipitation	8.0	7.0	6.0	5.0	6.0	5.0	4.0	5.0	9.0	7.0	6.0	7.0	75.0
Mean wind speed	17.6	20.1	20.1	20.9	20.9	20.1	17.6	16.6	16.6	16.6	20.9	16.6	
in km/hr (Mph)	(10.9)	(12.5)	(12.5)	(13.0)	(13.0)	(12.5)	(10.9)	(10.3)	(10.3)	(10.3)	(13.0)	(10.3)	
Prevailing wind direction	N	SE	SE	SE	SE	SE	SE	SE	SE	SE	N	N	

Brownsville (25°54' N., 97°30' W.)

	J	F	M	A	M	J	J	A	S	O	N	D	ANNUAL
Temperature, °C	16.1	17.8	20.0	23.3	26.1	28.3	28.9	28.9	27.2	24.4	20.0	17.2	23.3
Monthly mean (°F)	(61.0)	(64.0)	(68.0)	(73.9)	(79.0)	(82.9)	(84.0)	(84.0)	(81.0)	(75.9)	(68.0)	(62.8)	(73.9)
Precipitation in	3.6	3.8	2.5	4.1	6.1	7.6	4.3	7.1	12.7	8.9	3.3	4.3	68.3
cm (in)	(1.4)	(1.5)	(.9)	(1.6)	(2.4)	(3.0)	(1.7)	(2.8)	(5.0)	(3.5)	(1.3)	(1.7)	(26.9)
Days with precipitation	7.0	6.0	4.0	4.0	5.0	5.0	4.0	7.0	10.0	6.0	6.0	6.0	70.0
Mean wind speed	19.4	19.4	22.3	22.3	20.9	19.4	17.6	17.6	16.6	16.6	17.6	17.6	
in km/hr (Mph)	(12.0)	(12.0)	(13.8)	(13.8)	(13.0)	(12.0)	(10.9)	(10.9)	(10.3)	(10.3)	(10.9)	(10.9)	
Prevailing wind direction	SE	SE	SE	SE	SE	SE	SE	SE	SE	SE	SE	N	

lower latitudes and produce maximum mean pressure of 1020 mb in winter. The high pressure systems and their associated extratropical cyclones are responsible for the wide pressure ranges in winter.

The surface winds of the south Texas coastal region are dominated by the general circulation of the Bermuda high pressure system throughout the year. In March and April, alternating strong north winds and increasingly persistent strong southeast winds produce the highest annual average wind speeds. The warmer months are dominated by persistent southeasterly winds. South-southwest winds reach a maximum frequency in June and July. The lowest mean wind speeds occur during the late summer and early fall when the monthly average is 16 km/h. As winter approaches, the winds become more variable in both velocity and direction. During winter, northerly winds associated with the intensified North American continental high pressure systems produce a maximum in the frequency of wind speeds greater than 50 km/h. Although the frequency of northerly wind increases during winter, the south Texas coastal region is sufficiently far south to remain under the dominance of the Bermuda high pressure system and its prevailing southeasterly winds. The mean wind vectors for the period 1965 to 1974 for 9 of the 12 months of the year are shown on figure 15. Comparison of the mean wind velocities for the 10 year span 1965 through 1974 with those for the considerably longer time span covered by the statistics in table 4, show that velocities for the more recent years have been higher. For example, the mean wind speed for January in table 4 is 17.6 km/h; that for January in figure 15 is 25.5 km/h. Velocities for other months in figure 15 are similarly higher.

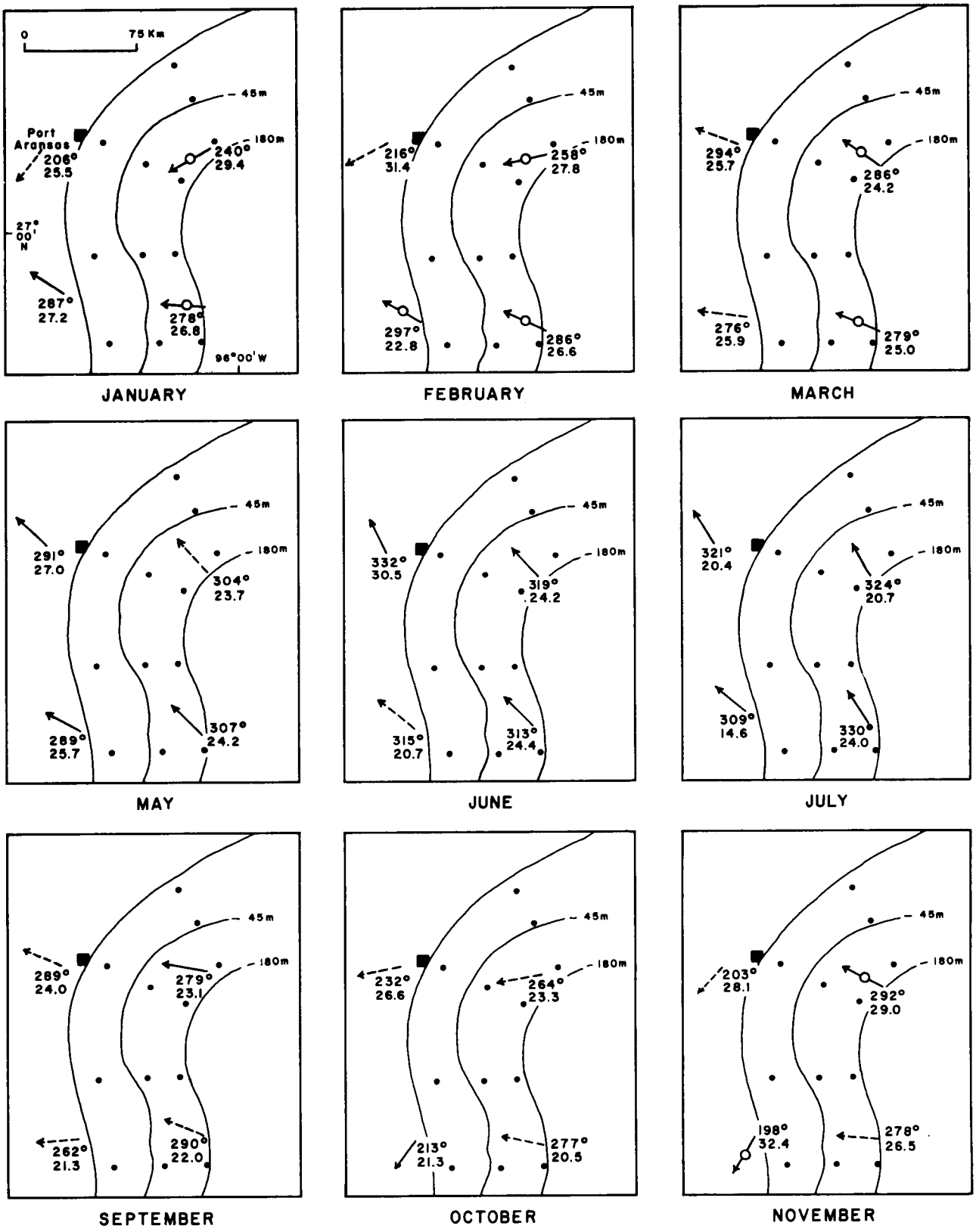

Figure 15. Monthly mean wind vectors, onshore and offshore, 1965-1974. Upper number is mean direction of air flow; lower number is mean wind speed in km/h. Pattern of arrows indicates steadiness, or ratio of the directional mean to the velocity mean: $\geq .67$ ↗ ; $< .67$ ↗ ; $< .33$ ↗.

Temperature and Precipitation

Air temperature extremes for the south Texas area are tempered significantly by the combined effects of prevailing southeasterly winds and the large area of the Gulf waters. Low temperatures occur when strong northerly winds associated with cold fronts penetrate the area. Freezing temperatures normally occur in near-coast areas at least once each winter. The highest summer temperatures occur when there is a shift of wind direction from the prevailing southeasterlies to south and southwest.

The south Texas area is semi-arid. Peak precipitation months are May and September. Tropical cyclones may add large amounts to the monthly rainfall totals for the period June to October and may cause normally higher saline bays to freshen drastically in a period of a few hours. The winter months have the least rainfall. Winter precipitation comes mainly from frontal activity and low stratus clouds. Because of the semi-arid conditions not only along the coast but landward for more than a hundred miles, no major stream flows to the Gulf of Mexico along the south Texas coast between Port Aransas and the Rio Grande, 135 miles to the south. This factor has a direct influence on the pattern of marine processes on the South Texas OCS.

The long-term monthly averages for temperature and precipitation at Corpus Christi and at Brownsville are shown by table 4.

OFFSHORE CLIMATOLOGY

General Statement

Compared to the adjacent land area, offshore winter temperatures are higher and average wind velocities are greater. Offshore summer conditions

are more similar to the onshore climate, but with some diurnal differences: the daily temperature range is smaller and the afternoon wind speed maximum is less pronounced offshore than at coastal land stations.

The offshore area, unlike the coastal area, is not rainy at any season. Rain is most frequent in December and January with a secondary maximum in August and September. Based on rain frequency, the driest season in the area is March-June with an average of less than 3 percent of ships' weather observations reporting rain.

Seasonal Conditions

Winter: Mean monthly surface air temperatures over the area vary from 68°F in December to 64°-65°F in January and February. More than 90 percent of the actual observations are within ±10°F of the mean. Isotherms have an east-west orientation across the Gulf, but they bend to follow the contour of the Texas coastline. The air near the coast is colder than that over the outer continental shelf. The mean offshore sea surface temperature is 4°-5°F warmer than the air in December, decreasing to 2° warmer in February.

Spring: The mean monthly surface temperatures over the area are 67°-68°F in March, 71°-72°F in April, and 77°-78°F in May. The temperature gradient characteristic of the winter season prevails through March. During April, the area becomes dominated mostly by tropical maritime air and there is less contrast in surface air temperature from north to south. Approximately 90 percent of the actual surface air temperature observations in the Gulf are within ±10°F of the mean (72°F) in April, when frontal passages still occur, compared to ±5° of the mean (78°F) in May, when little frontal activity occurs. The temperature varies little from north to south by May. The mean sea surface temperature is about the same as the air temperature by mid-April.

Summer: Mean monthly surface air temperature varies little during the summer months. The mean for June is 82°F and for both July and August, 84°F. Approximately 90 percent of the actual observations are within ±5°F of the mean. During the summer season, the mean monthly air surface temperature, the daily air surface temperature and the daily sea surface temperature are virtually the same. An exception may be the possible upwelling conditions near Brownsville where sea surface temperatures are occasionally 5° to 10°F colder than the air temperature.

Fall: Both sea surface and air temperatures are warmer during September, just as in the summer months. Mean surface air temperature is 83°F with little geographic variation. During October, surface air temperature isotherms begin to show a weak south to north gradient. The mean monthly temperature is 78°F near Corpus Christi and 80° to 82°F farther south. The November pattern of mean monthly surface air temperature isotherms is almost identical to April's; the mean sea surface temperature in October-November is about 3°F higher than the air temperature with a weak north-south gradient.

Winds

Mean wind conditions over the OCS area for the period 1965 through 1974 are shown by the series of maps in figure 15 that cover nine months: January, February, March, May, June, July, September, October, and November. The mapped wind directions graphically demonstrate the regional synoptic patterns described and also indicate the differences and similarities in patterns of air movement from north to south across the South Texas OCS: the southwestward orientation of the mean wind vectors over the northern half reflecting

the frequent frontal passages from the north during the winter months; the parallelism of air flow across the entire area during the summer months; and the beginning of the turnaround of the mean vector from northwesterly to westward and southwestward in the fall months. High winds of more than 17 knots occur most frequently in the winter months, about 20 percent of the time, and are most frequently from the north during the 12 to 24 hour period after passage of a cold front. Winds of velocity greater than 28 knots occur 2 percent of the time.

Wind velocities and their time-frequency patterns and strengths are related directly to wave heights caused by the winds. The median values of monthly wind velocities recorded in the South Texas OCS between 1884 and 1973 are shown by figure 16. The median values of monthly wave heights during the same period are shown by figure 17.

Severe Weather

Hurricanes

The largest and most destructive storms affecting the Texas coastal and offshore areas are tropical cyclones. The intensity of tropical cyclones may range from weak to large and intense storms with maximum winds reaching 320 km/h. Virtually all tropical cyclones affecting the Texas coast originate in the Gulf of Mexico, the Caribbean Sea, or the southern part of the North Atlantic Ocean. The season for tropical storm development extends from June to October; storms are most frequent in August and September and rarely affect the Texas coast after the first days of October.

The average frequency of tropical cyclones for the entire Texas coast is one every two years; they were most frequent in 1886 and 1933, with four

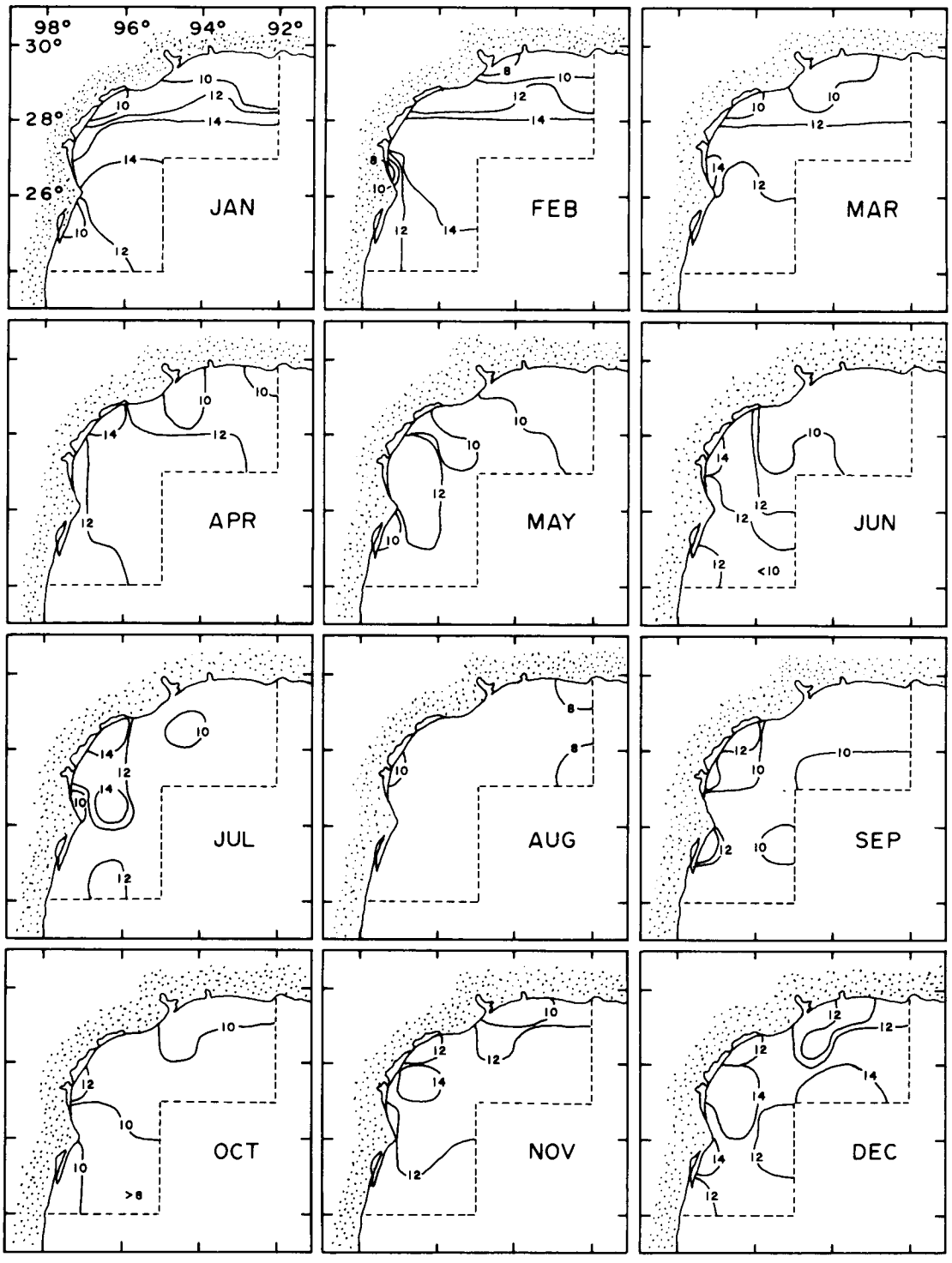

Figure 16. Median values of monthly wind velocities (in knots) recorded between 1884 and 1973, South Texas.

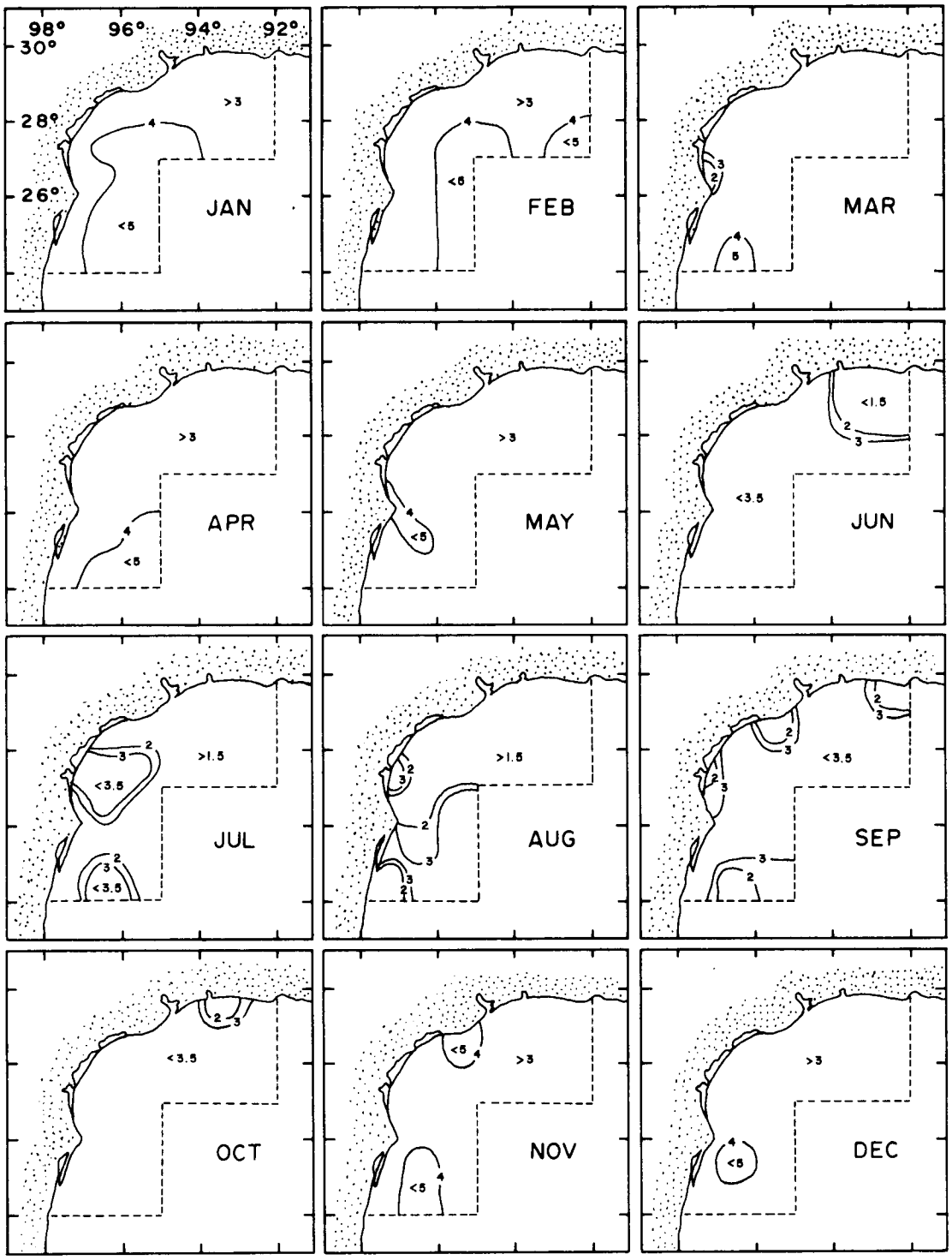

Figure 17. Median values of monthly wave heights (in feet) recorded between 1884 and 1973, South Texas.

in each of those years. A total of 37 hurricanes affected Texas during the period 1900 through 1974; all occurred from June to October. Of these, nine were severe in the South Texas OCS lease area, all occurring in August and September. The paths of all hurricanes traversing the South Texas OCS during the period from 1871 through 1967 and the positions of landfall are shown by the maps in figure 18.

Although hurricane winds cause a large amount of damage and loss of life in coastal areas, study of past hurricanes indicates that the storm tides cause more destruction and a larger number of deaths. In offshore areas, high waves are most destructive. The most extreme storm tides are near and to the right of the point at which the storm makes landfall. The extent of storm tides along the coast depends on the size and intensity of the individual hurricane. Tide heights in bays, especially near the heads where water can be trapped, usually are much higher than tides along the shoreline of the open Gulf in the same area. Storm tides of 5 to 6 m have been recorded in Corpus Christi and Matagorda Bays. Storm tides on the Gulf of Mexico shoreline have been somewhat lower, but 3 to 3.5 m heights have been recorded, and Padre Island has been inundated several times.

Offshore, in water depths of 100 m or more, fully developed hurricane waves can reach significant heights of 12 to 15 m and extreme heights of 20 to 25 m. As the waves move into shallow water they are modified due to shoaling, refraction and bottom friction, which cause an attenuation of 50 percent or more as the waves move over the outer shelf. In the inner shelf, with mean depths of 10 to 15 m, breaking waves with heights of 0.78 percent of the water depth become important. The storm surge can be quite significant, as much as 2 to 3 m, which in turn increases the height of breaking waves.

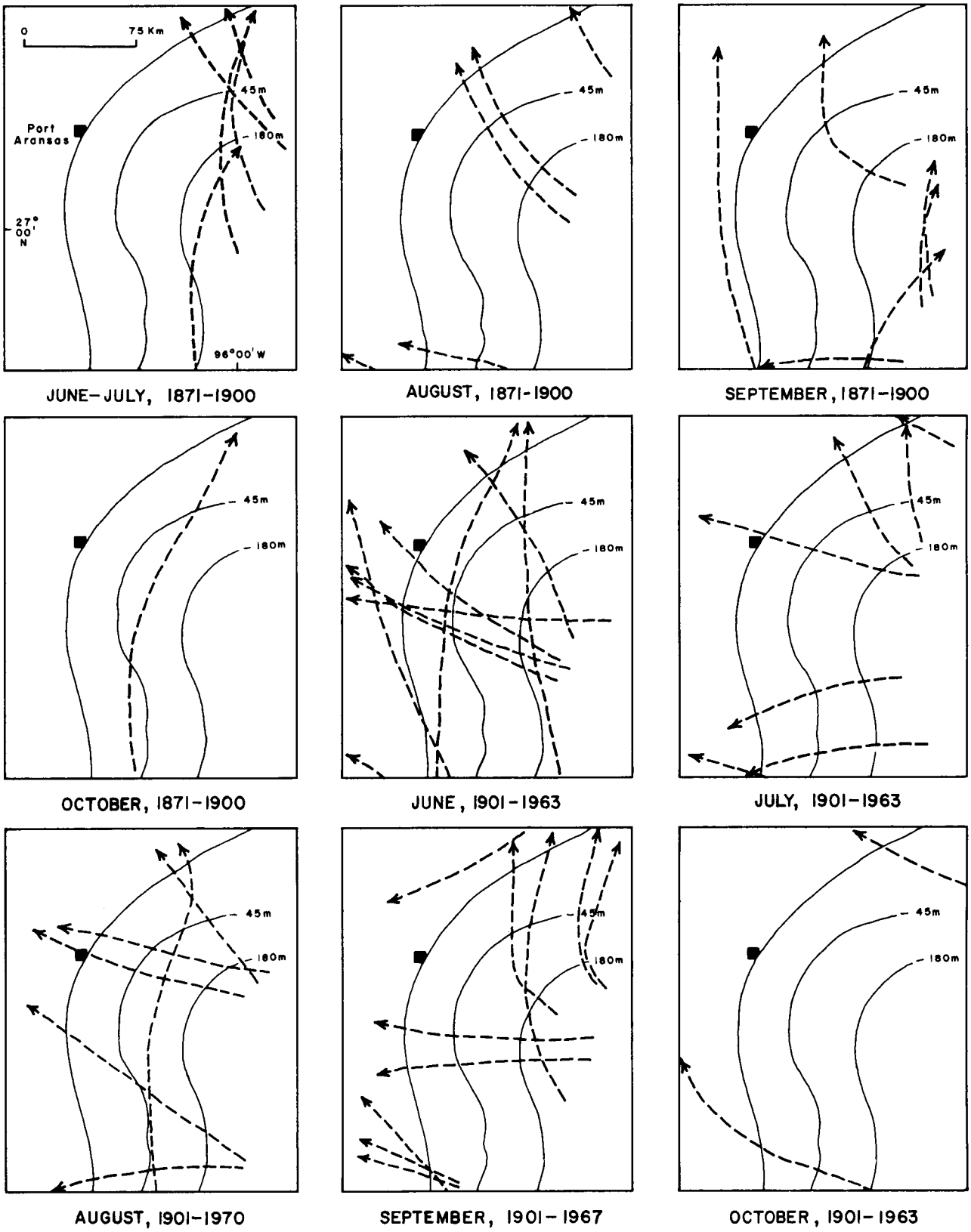

Figure 18. Paths and points of landfall for hurricanes traversing the South Texas OCS area from 1871 through 1967. From Carr, J. T., Jr., 1967.

The wind velocities and sea conditions accompanying the most severe storms that have impacted the South Texas OCS are listed in table 5.

Table 5. Wind velocities and sea conditions accompanying the most severe storms that have impacted the South Texas OCS. Data from Carr, 1969.

Date	Direction of movement and point of landfall	Wind velocity	Height of storm surge
1875 Sept. 14-19	NW, Matagorda Bay	160 km/h, estimated	No record
1880 Oct. 12-13	NW, Brownsville	No record	Brownsville virtually destroyed
1916 Aug. 18-19	NW, Corpus Christi	160 km/h, estimated	1.8 m, Corpus Christi
1919 Sept. 13-14	NW, just so. of Corpus Christi	160 km/h, estimated	4.9 m, Corpus Christi 3.7 m, Port Aransas
1933 Sept. 3-5	W, Brownsville	170 km/h, maximum 192-200 km/h	3.7-4.6 m, Brownsville 2.7 m, Corpus Christi
1942 Aug. 29-30	NW, Matagorda Bay	192 km/h, estimated at Port Lavaca	4.6 m, Matagorda 4.6 m, Port Lavaca
1945 Aug. 26-27	NNW, Matagorda Bay	216 km/h, Port Lavaca 200 km/h, Port Aransas	4.6 m, Port Lavaca 3.0 m, Matagorda
1961 Sept. 10-12	NW, Matagorda Bay	280 km/h - gusts	5.2 m, Port Lavaca 3.0 m, Port Aransas
1967 Sept. 19-21	NW, Port Isabel (Brownsville)	174 km/h; gusts to 192 km/h	5.5 m, Padre Island 2.4 m, Corpus Christi
1970 Aug. 3-5	WNW, Corpus Christi	208 km/h; gusts to 258 km/h	2.7 m, Port Aransas 1.5 m, Corpus Christi
1971 Sept. 9-13	Parallel to coast	160+ km/h; gusts at Port O'Connor	1.2-1.8 m

Statistical probabilities for the occurrence of extreme winds and waves can be generated from past hurricane data and wave conditions provided by wave hindcast techniques. Estimates of extreme wind and wave recurrence probabilities for the South Texas OCS are given in table 6.

Table 6. Statistically estimated extreme wind and wave probabilities for the South Texas OCS by recurrence interval.

	Recurrence interval in years			
	10	25	50	100
Winds in km/h				
-Highest one hour	99	122	141	156
-Highest one minute	129	152	171	191
Wave heights in meters				
-Highest significant	10.4	12.5	14.0	15.6
-Highest	17.7	21.0	23.5	25.9

Such estimates of probability of recurrence must be used with caution, however, as the more severe hurricanes have tended to cluster in time, as indicated by table 5. Several characteristics of the storms listed in the table are worthy of note:

1. although hurricanes can occur in the northwestern Gulf from June to October, all have come in August and September with a single exception;
2. long periods can occur without a given area being struck;
3. the most severe hurricanes have tended to cluster: 1875 to 1886, three; 1887 to 1915, none; 1916 to 1919, two; 1920 to 1932, none; 1933 to 1945, three; 1946 to 1960, none; 1961 to 1971, four.

The general characteristics of all tropical storms that have affected the South Texas OCS in the period 1886 to 1971 are given in table 7 by 80 km coastline segments.

Table 7. Tropical storm characteristics, 1886 to 1971 (by 80 km coastal segments north from the Mexican border to the mid-Texas shelf). Sector 2 terminates just south of Corpus Christi Bay; sector 4 terminates midway between Matagorda and Galveston Bays.

	Coastal Sector			
	1	2	3	4
Earliest storm	August 4	June 23	June 23	June 22
Latest storm	Sept. 22	Sept. 20	Oct. 16	Sept. 11
Number of tropical cyclones (winds of 80-120 km/h)	8	10	11	10
Number of hurricanes (winds >120 km/h)	7	6	6	8
Number of great hurricanes (winds of 160 km/h or greater)	2	4	3	3

Northers

Some 30 to 40 polar air masses penetrate the North American continent to the Gulf of Mexico each winter. During a given year some 15 to 20 of these generally bring strong northerly winds to the Gulf and are referred to as northers.

The norther, or cold front, is associated with a strong anticyclone and with cold air masses descending from the north; it should not be confused with the northerly winds in the western quadrants of tropical cyclones which approach from the east. Local usage has corrupted the term norther to apply to any wind shift to the north accompanied by a drop in temperature. A wind velocity increase to at least 37 km/h is typical of the passage of a norther. Velocities ranging from 46 to 92.5 km/h are characteristic of severe northers

and from 1 to 6 northers per year are likely to be severe over the open Gulf. Northers generally occur from November to March and are most severe from December to February; however, the number, frequency patterns, and strengths of northers vary from year to year. The severe northers can generate sufficient wind strength and wave height to hamper operations at sea for periods lasting 12 to 24 hours.

SHELF WATER

PHYSICAL OCEANOGRAPHY AND HYDROGRAPHY

The historical data for sea surface and water column hydrography compiled by NOAA plus the hydrographic data collected by the University of Texas during the 1974-75 baseline sampling were used in preparing the resumés of physical oceanographic and hydrographic characteristics of the South Texas OCS. The water temperature and salinity data collected by Texas A&M University during the baseline studies were recorded in the discussion of nutrients, as these data were collected as a part of the nutrient study and more properly relate to nutrients on time-sequence and cause-and-effect bases. The geographic distribution of the historical hydrographic data used in the following summaries is relatively sparse; the number of observations south of Port Aransas are few. Consequently, conclusions regarding regional hydrographic patterns on a historical basis should be treated cautiously.

Sea Surface Temperature

Monthly variations in sea surface temperature over the South Texas OCS for 1962 and 1963 are shown by figure 19. The months of April, August and December have been omitted from the figure; April and August do not differ significantly from the immediately preceding month and December is intermediate between November and January. With the exception of June, July and August, the isotherms are parallel to the coast. The sea surface temperature gradient reaches a maximum during January. Through the following four-month period it progressively flattens under the influence of increasing seasonal

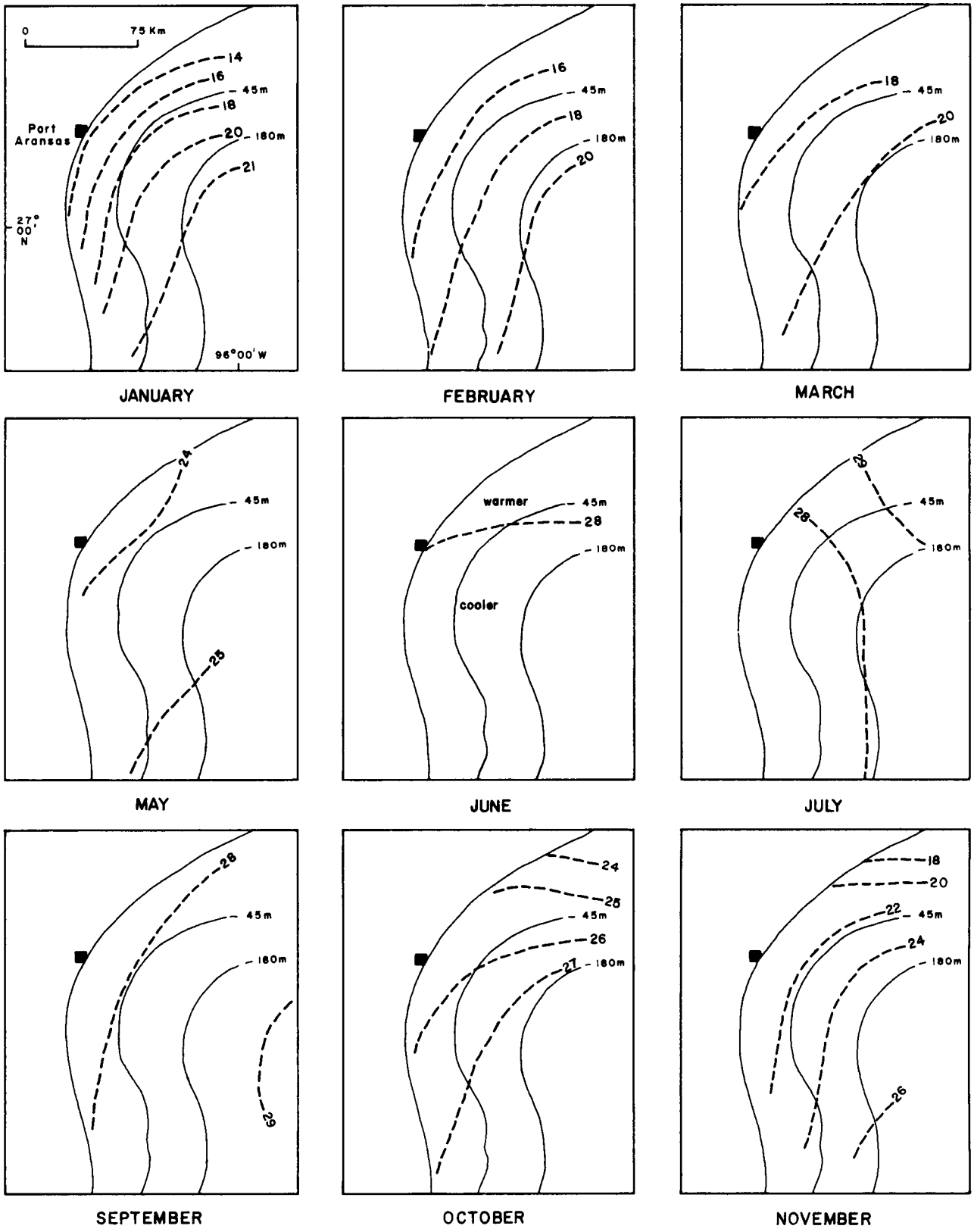

Figure 19. Monthly sea surface temperature patterns over the South Texas OCS, 1962-1963. Isotherms in °C.

heating. From June through September inclusive, the sea surface is in a nearly isothermal condition. During October, November and December, seasonal cooling produces an increasing gradient.

For most of the year, cooler water is found nearshore and the temperature increases progressively southward along the coast. The exception is the period June through August when the surface temperature increases from south to north over the entire shelf.

Sea Surface Salinity

Areal Patterns

The monthly pattern for isohalines is similar to that for the isotherms. They are shown by the series of maps in figure 20. From January through April the 36.4 °/oo isohaline is over the outer edge of the continental shelf and the isohalines are parallel to the coast. Beginning in May the isohalines begin a clockwise rotation relative to the coast and become normal to it by July. By September the isohalines approach parallelism and by October are once again parallel to the coast.

The trend of salinities indicated by the data gathered during the 1974-75 baseline sampling does not follow that indicated by the historical data; however, as noted previously, the historical data are more sparse and were not collected in the same months. During the late 1974 through 1975 sampling period, the isohalines in all seasons paralleled the coast and the salinity of inner shelf water at both the surface and at intermediate depths was in the 20's (°/oo) during the April/May sampling period along the entire coastline. Furthermore salinity readings in the high 20's (°/oo) were recorded along the southern part of the inner South Texas OCS during

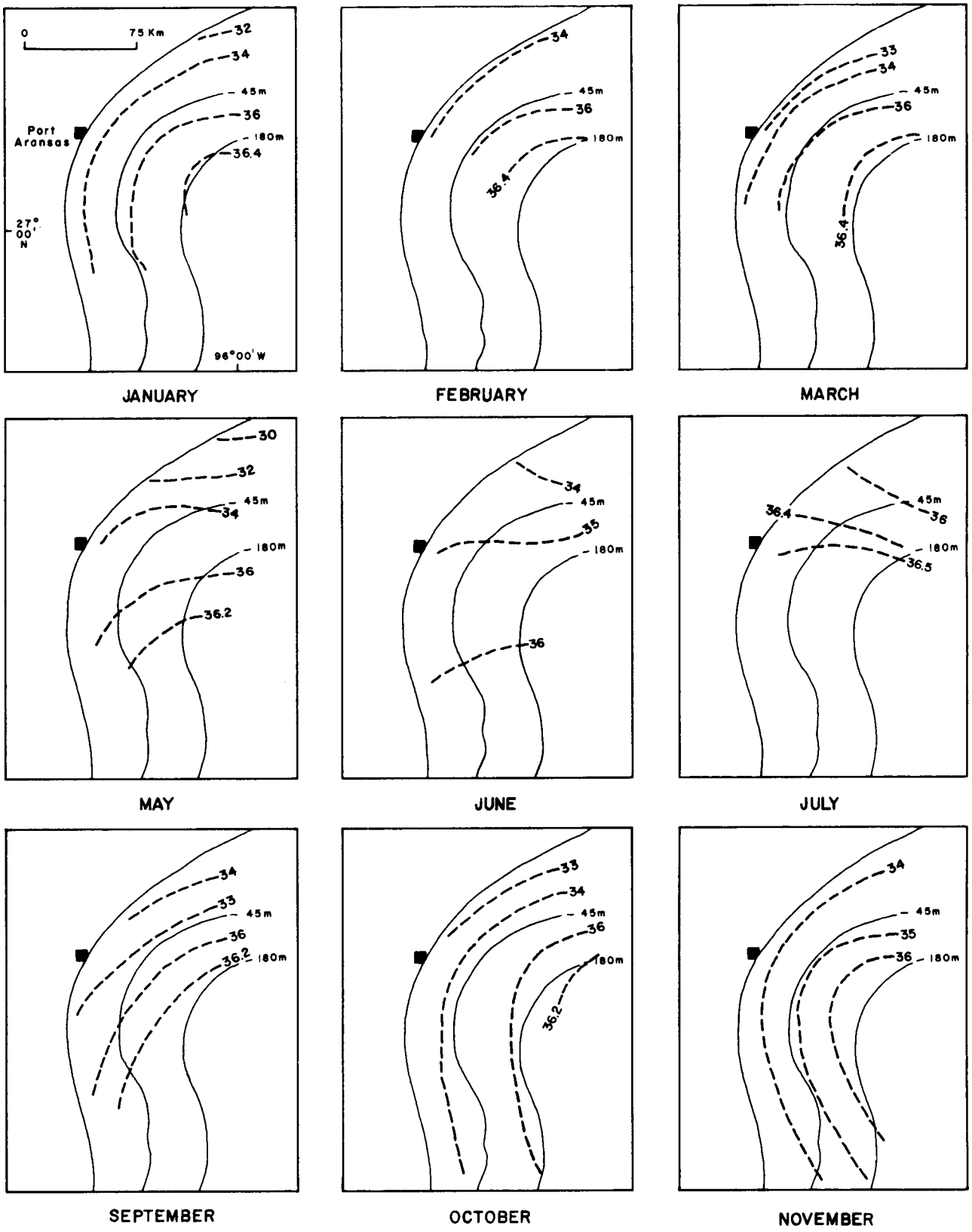

Figure 20. Monthly sea surface salinity patterns over the South Texas OCS, 1962-1963. Isohalines in $^{o}/oo$.

August. The historical data indicate no salinity readings less than 32 °/oo for the South Texas OCS at any time during the year. For a comparison of salinity patterns during 1974-75 with those indicated by the historical data, see figure 62 in the section on hydrographic aspects of primary productivity.

Determining whether the difference between the historical data and the recent data is due to the sparsity of the historical data over much of the South Texas OCS or whether the recent data represent either an anomalous year or a longer term change in regional salinity conditions must await results of the continuing studies on the South Texas OCS.

Influences of Rivers

The amount and distribution of stream discharge into marine waters of the continental shelf, both seasonally and geographically, have great bearing on regional salinity patterns. In summarizing the sources of fresh water affecting the salinities over the northwestern Gulf shelf, Angelovic and others (1976) concluded that the fresh water appears to come principally from the Mississippi and Atchafalaya Rivers. The 20 year (1950-1970) mean monthly discharge rates of the Mississippi and Atchafalaya Rivers and the sum of the monthly means of all the rivers west of the Atchafalaya to the Rio Grande are shown by figure 21. The combined discharge of the Mississippi and Atchafalaya Rivers, as shown by the graph, so overwhelms the combined discharge of the other rivers flowing into the northwestern Gulf that the logical assumption can be made that the salinity patterns for a part of the year are controlled largely by fresh water from the two rivers. Indeed, evidence from the 1974-75 baseline sampling, discussed more fully later,

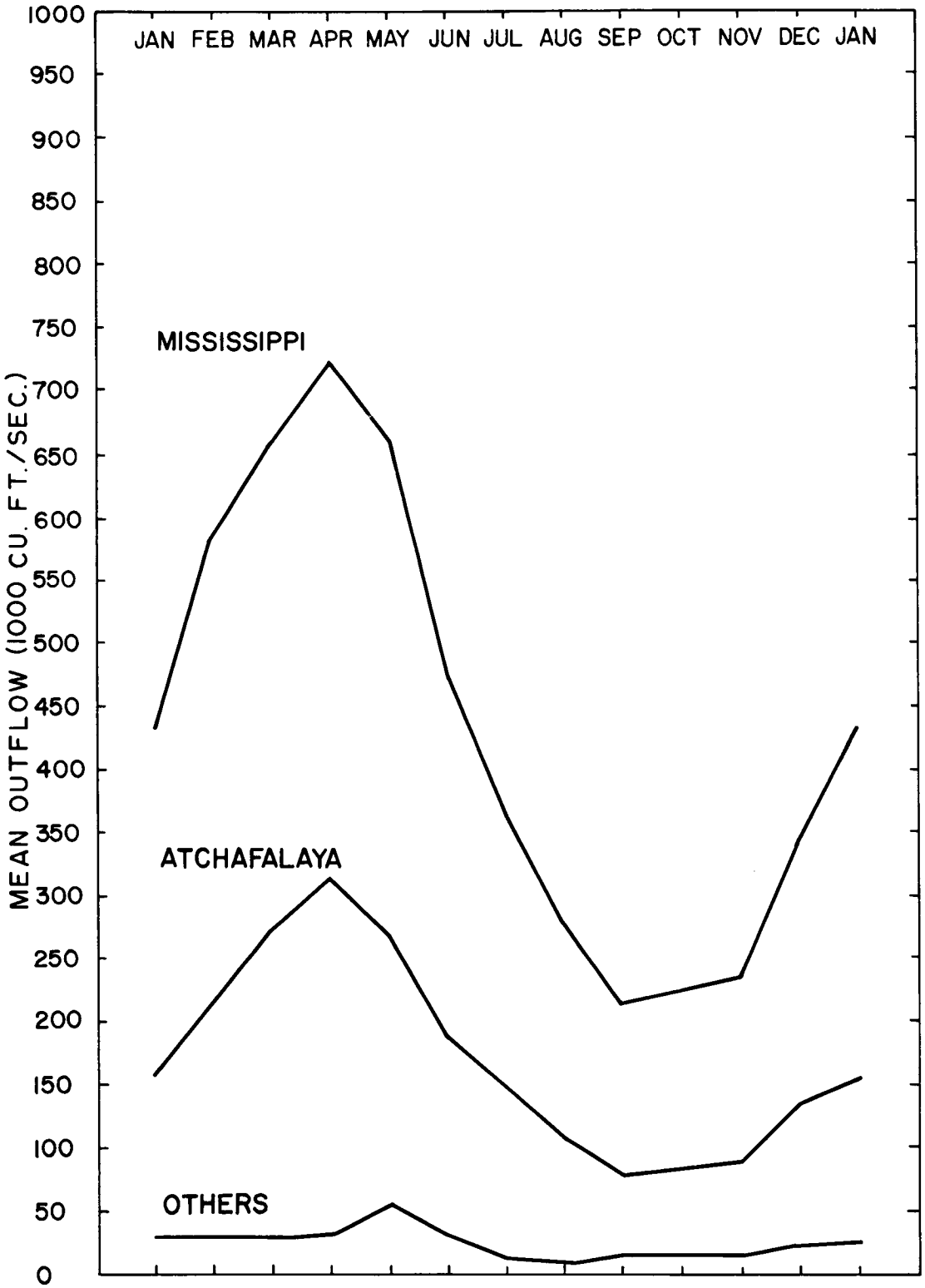

Figure 21. Monthly mean river discharge from the Atchafalaya and Mississippi Rivers and the sum of the mean offings of the rivers west of the Atchafalaya to the Rio Grande. From Angelovic and others, 1976, vol. II, figure 25.

also suggests the presence of Mississippi River water in the northwestern-most part of the South Texas OCS area during a part of that time. However, before the entire band of fresher water (<30 $^{o}/_{oo}$) along the inner OCS during the spring of 1975 can be conclusively attributed to the Mississippi River, further documentation covering a longer time span is needed; hopefully this documentation will come from the continuing studies. Regional patterns for both surface temperature and salinity, which relate directly to climatic conditions that are affected by diurnal, seasonal, annual and long-term cyclic atmospheric changes, can be expected to fluctuate from year to year. Predominant regional trends can be established only by continuous, long-term systematic monitoring.

Surface Density

The monthly distribution of surface density (the density anomaly σ_t) is necessarily similar to the distribution of surface temperatures and salinities. Moreover, the monthly densities show the same general strengthening of gradients from September through March, followed by a rapid erosion of the gradients from April through August. The November surface density is anomalous in this respect: during November the density gradients relax, but the density increases over the entire area. The patterns for surface density are shown by figure 22.

Vertical Sections: Temperature and Salinity

Historical Data

Historical data for water temperature and salinity are so sparse that vertical sections cannot be constructed on either a monthly or bimonthly

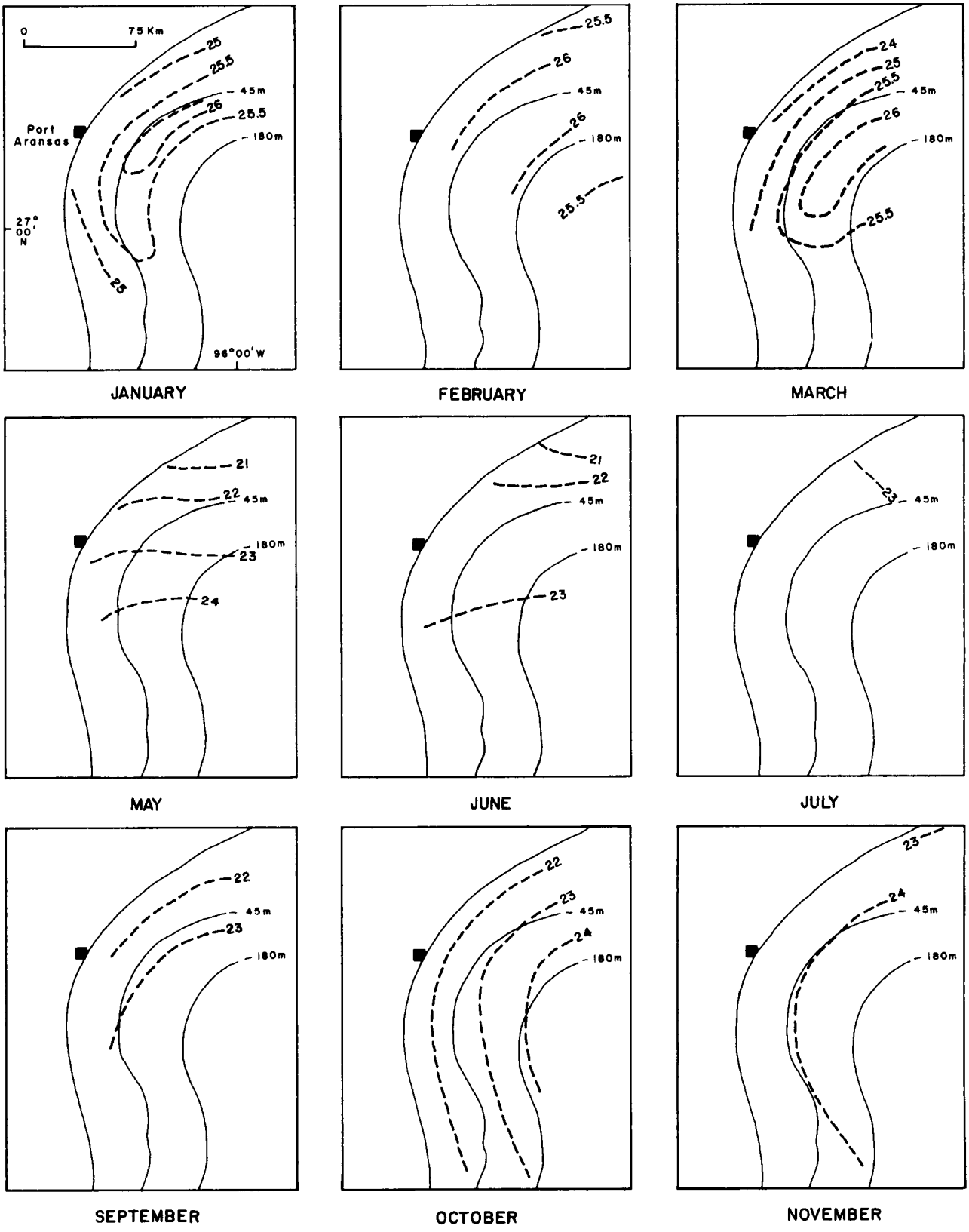

Figure 22. Monthly sea surface density anomaly (10^{-3} gm/cm^3), 1962-1963.

basis. Prior to 1975, the Texas continental shelf had not been surveyed seasonally along the same traverses, with one exception. The exception is the series of observations made by the Bureau of Commercial Fisheries, Galveston, during the period 1963 to 1965. Profiles have been prepared from the data collected during 1964 to show the nature and magnitude of the seasonal cyclic changes in temperature and salinity that take place vertically in the water column during a year. The profiles are shown by figures 23 and 23a. Those in figure 23 are off Port Aransas; those in 23a are off Matagorda Bay. The locations of the two traverses are shown by figure 13. The geographic differences in the two sets of data also are indicated by figures 23 and 23a, but the fact that the stations on the two traverses were not occupied in the same months, except for May, should be noted.

Data Collected During 1974-1975

The temperature and salinity of the water relative to depth were measured seasonally when the biological and chemical samples were being collected along the four traverses shown by figure 6. These data have been compiled as profiles; temperatures are shown by figure 24 and salinities, by figure 25. The salinity-temperature-depth (STD) profiles form a two-dimensional cross-section of the hydrographic characteristics of the shelf along the four traverses.

The three sampling cruises (winter, spring, and fall) provide an overview of the annual variability that can be expected for temperature and salinity throughout the South Texas OCS. Hydrographically, two seasons can be defined for waters of the region. In late winter or early spring,

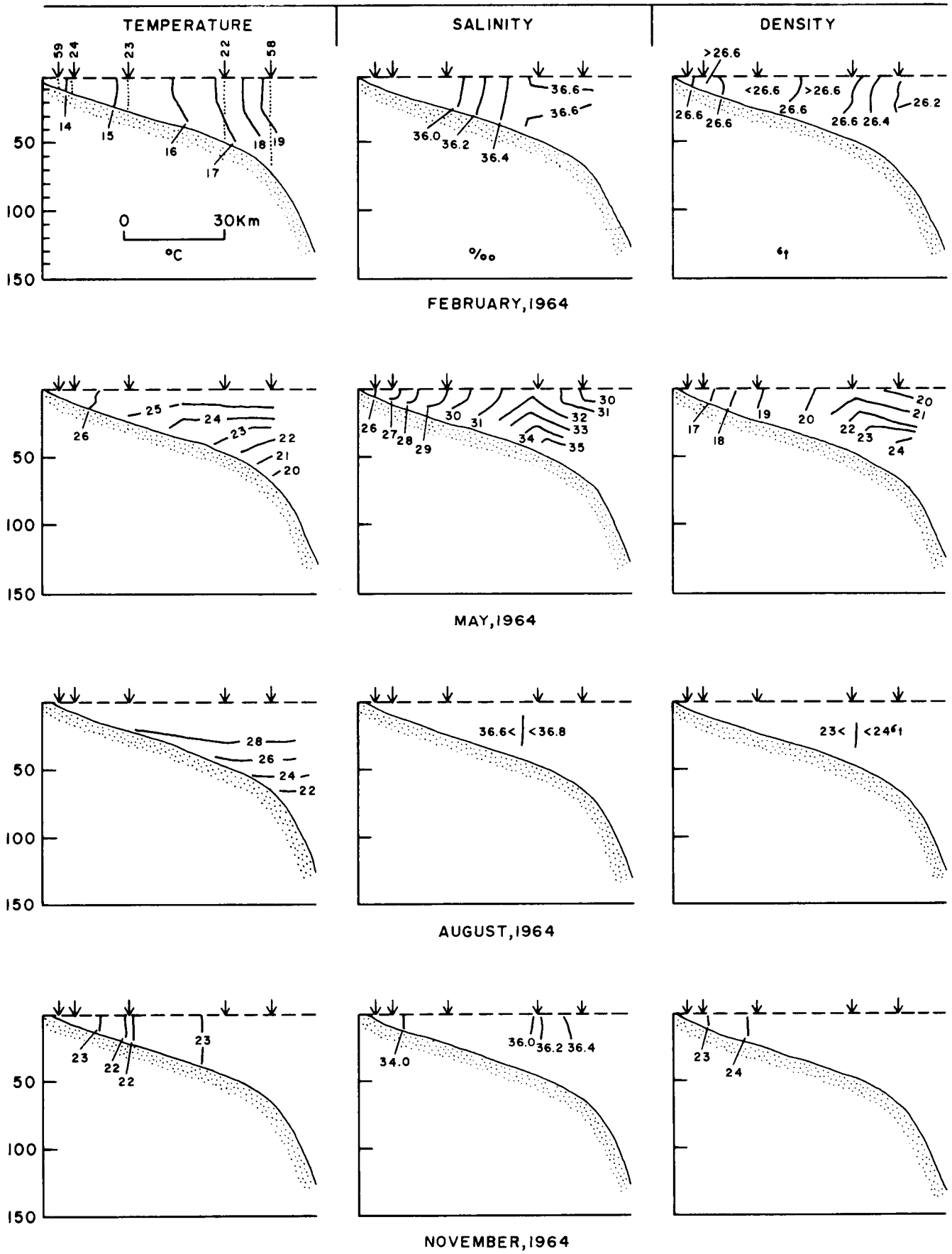

Figure 23. Temperature, salinity and density variations in the water column, South Texas OCS, along a traverse seaward of Port Aransas, 1964. See figure 13 for location of stations. Depth in meters.

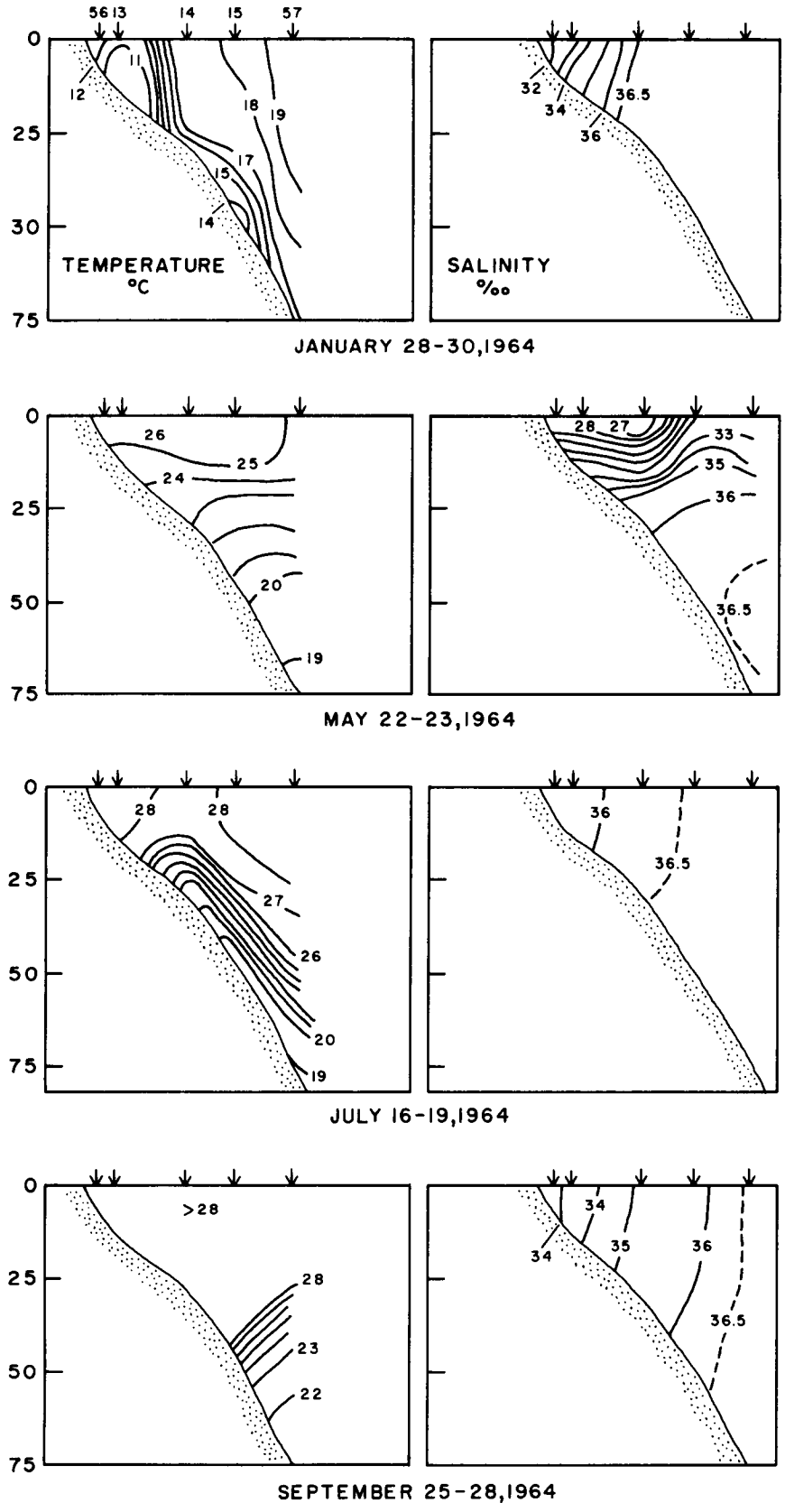

Figure 23a. Temperature and salinity variations in the water column, South Texas OCS, along a traverse seaward of Pass Cavallo (Matagorda Bay), 1964. See figure 13 for location of stations. Depth in meters.

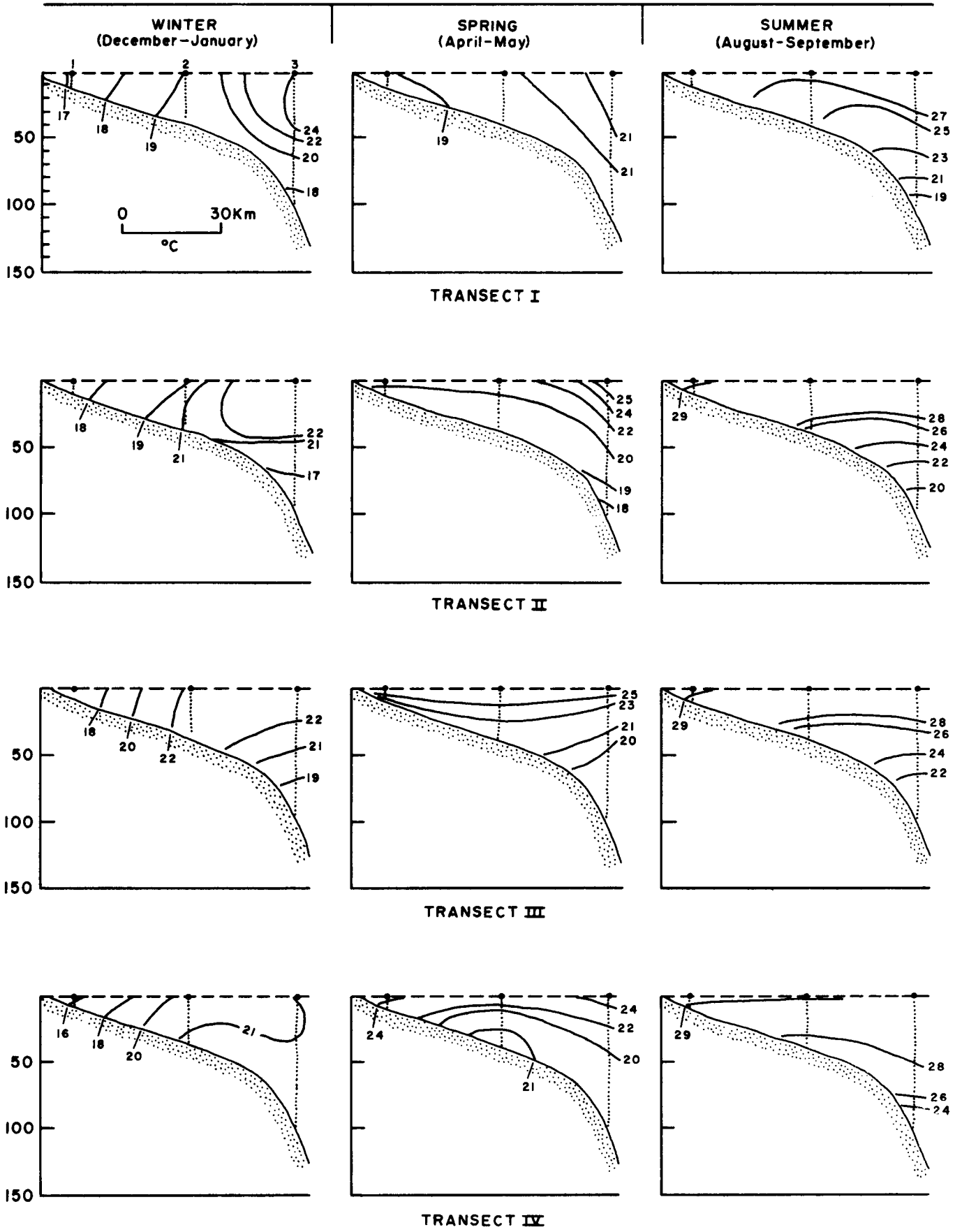

Figure 24. Seasonal temperature variations in the water column, South Texas OCS, December 1974-September 1975. Depth in meters.

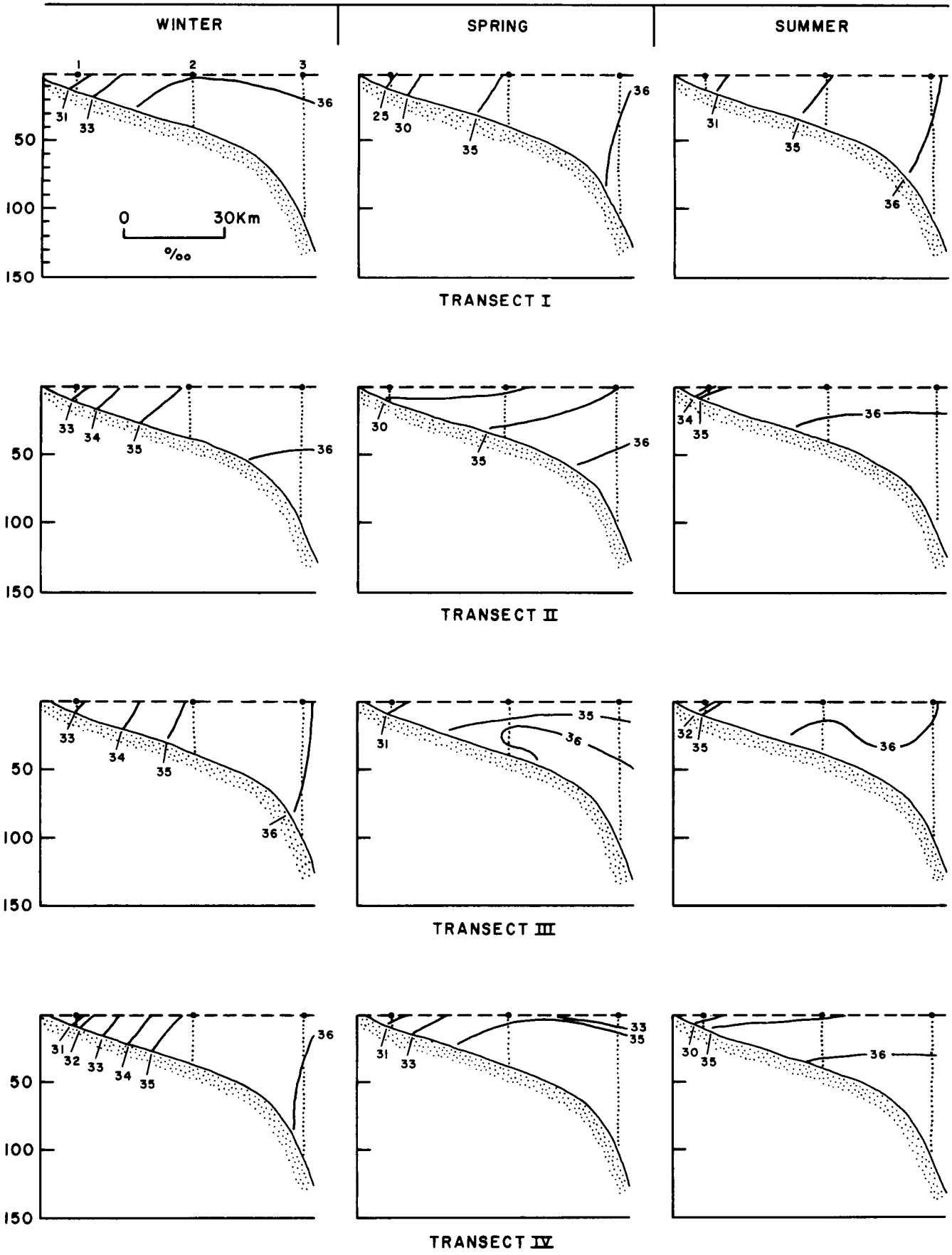

Figure 25. Seasonal salinity variations in the water column, South Texas OCS, December 1974-September 1975. Depth in meters.

the water begins to stratify in response to increasing daily amounts of incoming solar radiation (insolation) and to warm water coming from the shallow bays and estuaries. A pycnocline forms and begins to descend, perhaps as a series of steps as insolation continues to increase and as intermittent periods of intense wind mixing occur. The 1975 data indicate that a seasonal thermocline descends to the 30 to 40 m level by late August or early September.

The hydrographic data are best suited to depicting the long-period annual variations in shelf waters. Caution must be taken in interpreting, for example, the composite of surface temperatures and salinities as a snapshot of an instantaneous, synoptic pattern. Nevertheless, the spring salinity data for 1975 along the Texas coast do define a surface layer of lower salinity that probably came from the Mississippi River. In places, the lower salinity water was measured at mid shelf nearly 60 km from the shoreline. The geographic distribution of the lower salinity water during the spring of 1975 is shown by figure 62. The conclusion that this water came from the Mississippi River must remain tentative, as no current measurements were made to document the direction of water movement west of the mouth of the Mississippi River. As has been pointed out, the volumes of river discharges graphed in figure 21 lend considerable strength to the conclusion that Mississippi/Atchafalaya River waters do reach the northwestern Gulf. However, the extent to which these waters penetrate onto the South Texas OCS probably varies from year to year.

The seasonal profiles constructed from the baseline data (figs. 24 and 25) cannot be directly compared to the profiles constructed from the historical data (fig. 23) for several obvious reasons: 1) the historical data

represent a single traverse; 2) the orientation of the single traverse is oblique to the shoreline, but the baseline traverses are normal to the shoreline; and 3) the seasons during which data were collected for the two different surveys are not exactly the same. Nevertheless, the two sets of data used together point up some regional characteristics. Stratification or partitioning of the water on the basis of both distance from shore and variations in depth change on a seasonal basis. During the colder months of winter, in the late fall and in the early spring, the variations with distance from shore are most significant; during the warmer months, horizontal layering and variations with depth are characteristic. Furthermore, comparison of the four profiles for 1975 shows that differences in temperature from north to south over the South Texas OCS were greatest during the winter sampling period and were less variable geographically during the warmer months. The salinities, by similar comparison, show greater geographic variations from north to south and from east to west over the shelf during all three seasonal sampling periods. The pattern of migration of the 36 $^{o}/oo$ isohaline gives a suggestion of the interplay between the shallower shelf waters, which undergo changes more rapidly in response to coastal influences, and the more stable water of the deeper Gulf.

Comparison of the 1964 and 1975 data shows that the magnitudes of temperatures and salinities can vary significantly over the South Texas OCS from year to year.

Seasonal Variation of the Mixed Layer

Maps in figure 26 show the historical mixed layer depths over the South Texas OCS for 9 of the 12 months. The mixed layer depth (MLD) is

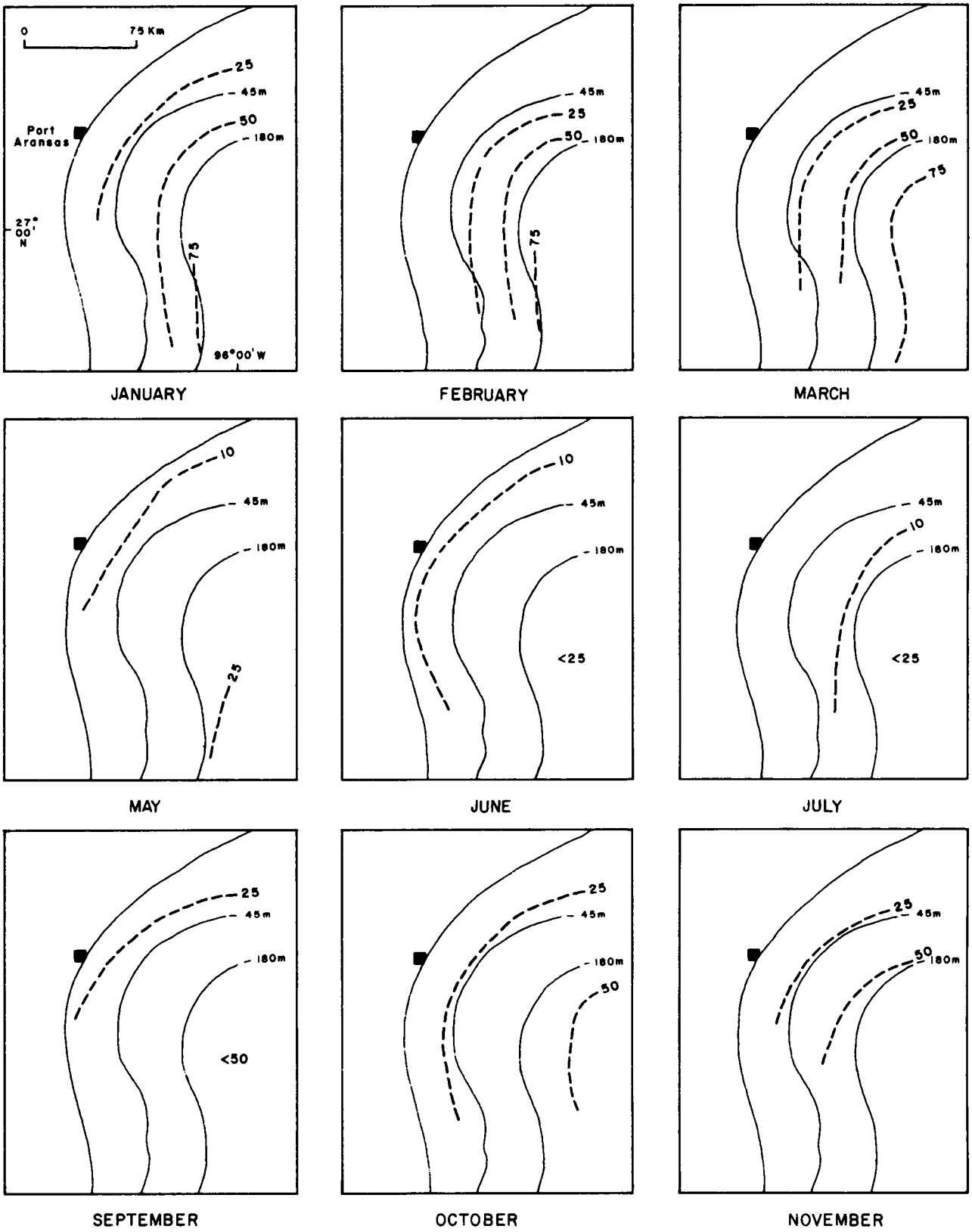

Figure 26. Historical depth ranges of the mixed layer, 1962. Depth in meters.

defined as the depth at which the temperature has decreased by 1.1°C from the surface temperature. Both the annual course of isotherms and the MLD maps (fig. 26) show a seasonal trend in which the MLD is deep in the winter and shallow in the summer.

Generally the period November through February is marked by increased wind velocities and seasonal cooling. During this period, the MLD deepens under the combined effects of instability produced by seasonal cooling and more vigorous vertical mixing by surface waves. Moreover, as the evaporation rates far exceed the precipitation during this period, the mixing process is enhanced. From April to June, the MLD decreases under the influence of subsiding winds and increased heating. By June surface heating and light winds have produced a thin mixed layer above a strong thermocline. The mixed layer slowly deepens in the period July through October. The thermocline remains strong through October, but strengthening winds, seasonal cooling and an increasing dominance of evaporation over precipitation cause the MLD to deepen more rapidly.

Water Movement

Tides, Tidal Currents and Sea Level

Astronomical tides in the South Texas OCS are of relatively small magnitude, as are such tides in the Gulf of Mexico generally. They are diurnal near times of maximum declination of the moon and mixed semi-diurnal near times of zero declination. The diurnal range is 40 to 50 cm along the coast. A small phase difference exists between Port Aransas (27°50' N., 97°03' W.) and Brazos Santiago (Port Isabel) (26°05' N., 97°09' W.).

The controlling dynamics of the tides in this part of the Gulf are not clear. Two hypotheses have been advanced: 1) the principally diurnal tide in the western Gulf is due to cooscillation with the Atlantic Ocean; and 2) it is resonant oscillation with diurnal forcing.

Tidal current observations along the coast of South Texas are sparse. The diurnal speeds of tidal currents in the vicinity of Port Aransas are 45 cm/sec at flood and 60 cm/sec at ebb. Tidal current velocities decrease to 15 cm/sec or less on the open shelf.

Seasonal and synoptic effects cause important variations in sea level. Over the South Texas OCS, the annual nonastronomic variation is larger than the astronomic. At Galveston, north of the South Texas OCS area, long-term records of monthly highest and lowest tides show an annual range of 1.5 to 2.5 cm, although heights of 4 to 6 cm have been recorded during severe hurricanes. Storm surges associated with tropical storms account for the very high levels while most of the abnormally low levels are associated with set-down and drainage out of Galveston Bay during northers. The set-down effect is similar but less pronounced in the South Texas OCS area. The inverse barometer effect is the most elementary factor in sea level fluctuations, both synoptically and seasonally. A 1 mb rise or fall in sea level pressure will cause a 1 cm fall or rise in sea level. In some areas, this effect alone can account for a 10 cm or more increase in sea level from winter to summer.

Steric effects, or changes in the molecular dimensions of seawater because of temperature and salinity fluctuations, usually are of considerable importance in coastal areas. Lighter water will tend to stand higher and denser water lower. Sufficient long-term qualitative data are not available for calculating the steric effects for the South Texas OCS area.

Mean monthly sea level and sea level differences are shown for Galveston and Brazos Santiago for the period 1966 to 1973 by figure 27. The indicated characteristic spring sea level rise, summer lowering, late summer and early autumn rise, and the late autumn fall can be correlated with changes in the wind and density patterns. The spring rise is attributable to high river runoff, the summer lowering to increased density and the south-southeasterly winds and the late summer rise to a shift in winds to the eastern quadrant. The sea level patterns and perhaps also the mean current pattern are subject to considerable year-to-year variation as shown by comparison of figures 28 and 29, where records for 1970 and 1971 are given. Among other features, the high September-October 1971 level and the distinctly different winter patterns in 1970 and 1971 are noteworthy.

Figure 30 shows the cause-and-effect relationship of winds and sea level fluctuations. The data graphed in the figure were obtained by applying a 39-hour low-pass filter to a tide record to remove the astronomical component while retaining the short-term large-scale effects which typically last several days. The highest sea level (March 6-7) was associated with more than a week of sustained winds from the east-southeast quadrant. Reversals in current direction probably were associated with these winds and with the sea level shifts. The lowered sea level in the early part of the period August 15 to September 15 was associated with persistent southeasterly winds. The later shift of winds to the eastern quadrant between August 25 and September 1 caused a strong rise in sea level.

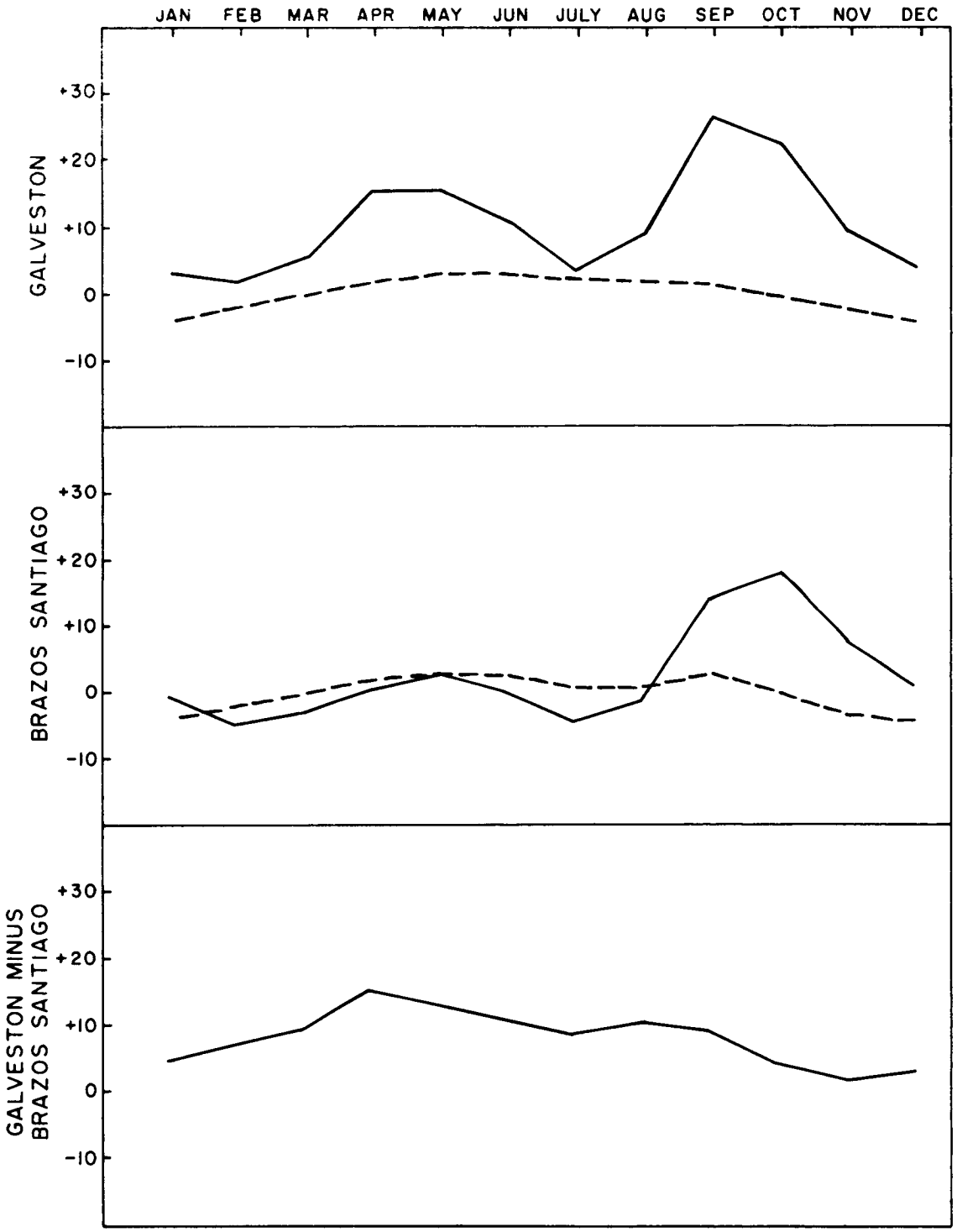

Figure 27. Mean monthly sea levels at Galveston and Brazos Santiago, 1966-1973. Dashed line indicates inverse barometer effect. The coastal station Brazos Santiago is in the southern part of the South Texas OCS. Elevation in centimeters.

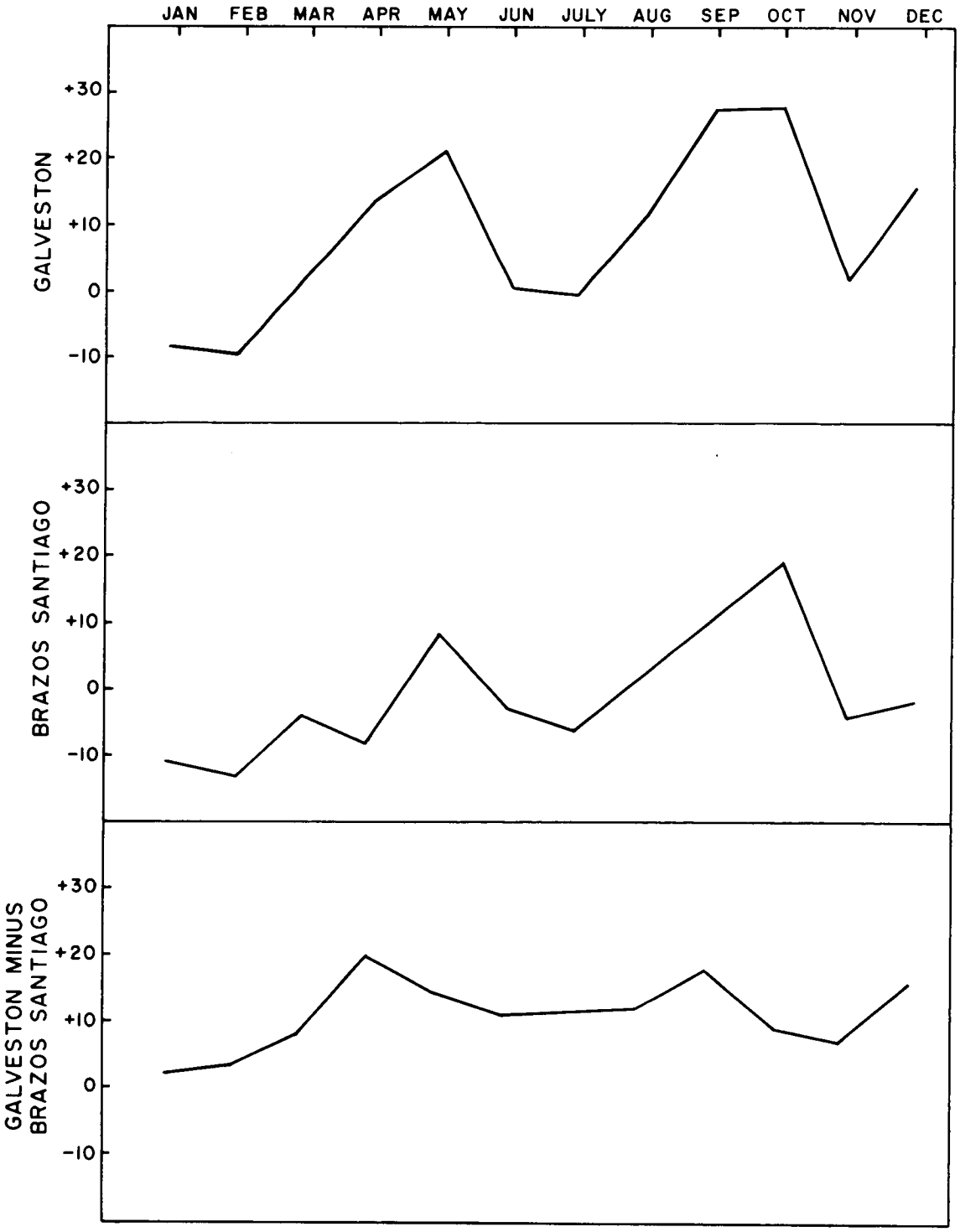

Figure 28. Mean monthly sea levels at Galveston and Brazos Santiago, 1970. The coastal station Brazos Santiago is in the southern part of the South Texas OCS. Elevation in centimeters.

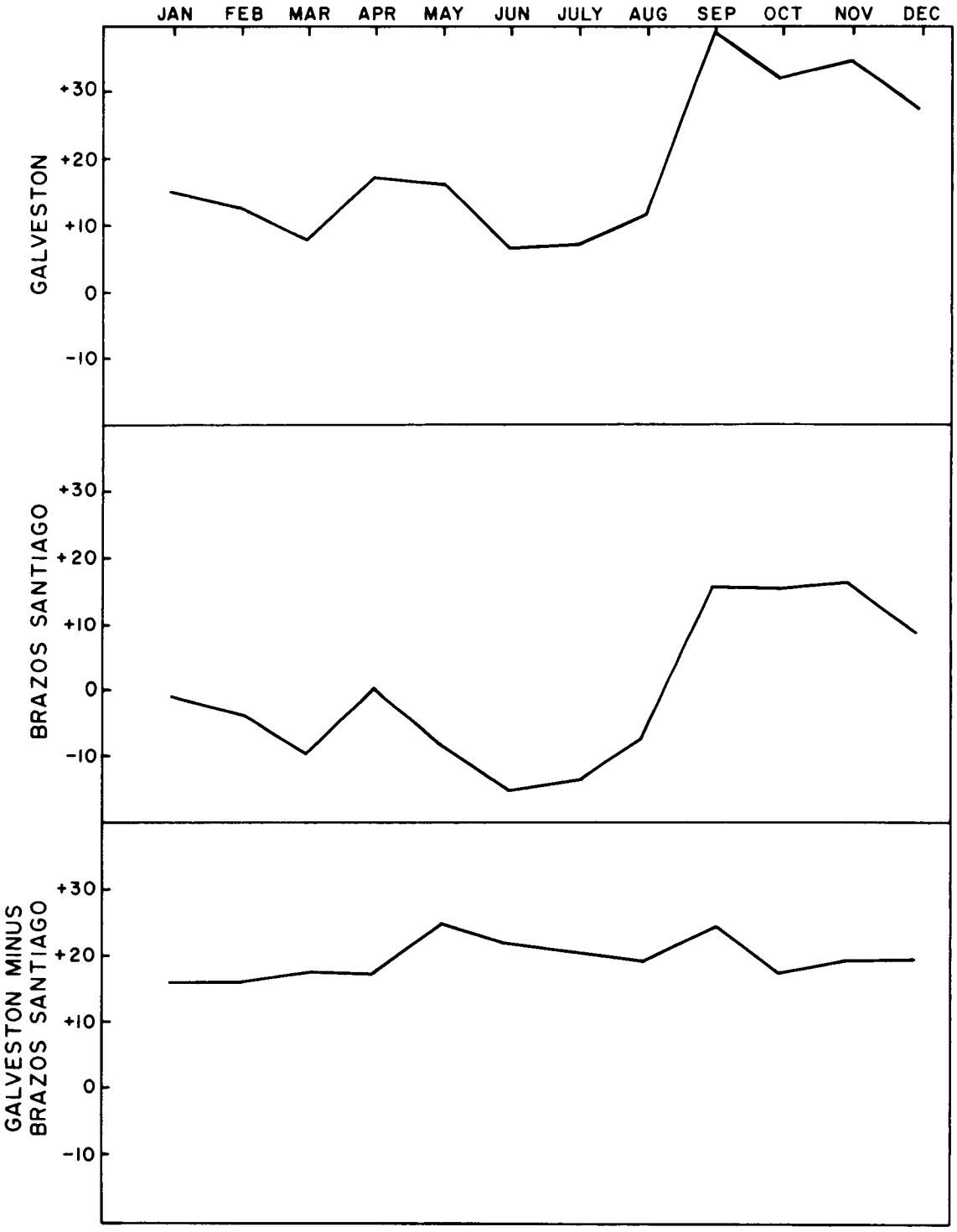

Figure 29. Mean monthly sea levels at Galveston and Brazos Santiago, 1971. The coastal station Brazos Santiago is in the southern part of the South Texas OCS. Elevation in centimeters.

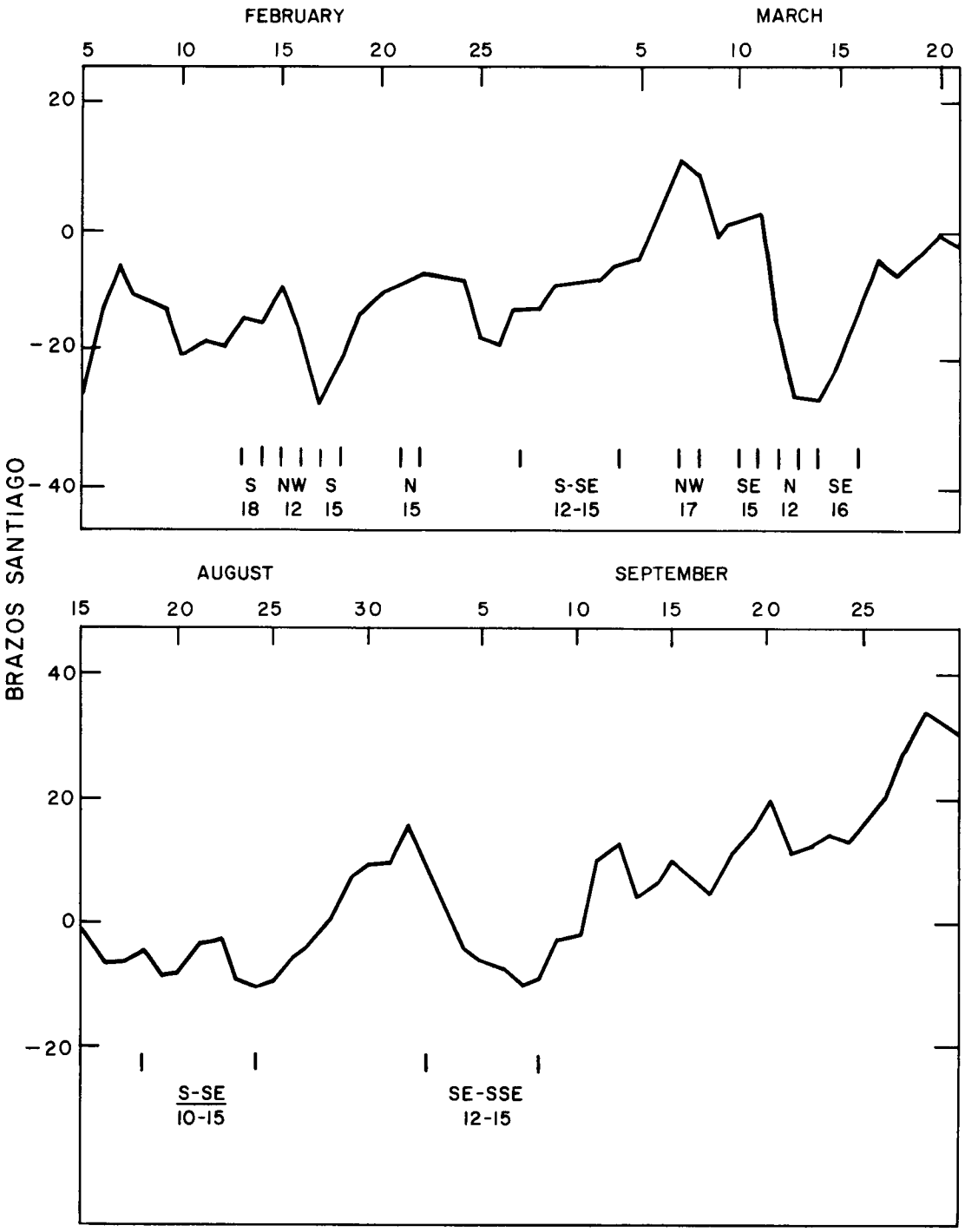

Figure 30. Daily sea level heights and significant steady winds at Brazos Santiago for February-March and August-September, 1970. Elevation in centimeters; winds in mph.

Waves

The data for the long-term median wave heights shown by the maps on figure 17 have been placed in the climate section of the report adjacent to a similar regional summary for offshore wind velocities (fig. 16). The cause-and-effect relationship of wind and waves is so intimate that the two types of data were placed in adjacent figures for greater ease in making comparisons.

The wave heights are at a minimum during the summer, predominantly during July and August. South of 28° N. the wave heights reach a maximum during the winter months from December through February. The maximum observed wave heights in the western Gulf of Mexico not associated with hurricanes have exceeded 6.4 m and have occurred in February. Regionally, wave heights increase from north to south and seaward during all months. In May, July, and August, wave heights increase nearshore off the Texas coast south of 28° N. and in November north of 28° N. Median wave heights average between 0.9 and 1.5 m from November through May and between 0.45 and 1.1 m from June through October. Ninety-five percent of all wave height observations were below 2.1 m from November through February. The statistics show a decrease in maximum wave heights from March to July when minimum heights range from 1.2 to 1.8 m.

Approximately 55 percent of most months wave heights range from 0.9 to 1.8 m. During July and August, this figure falls below 50 percent when calm waters with wave heights of 0 to 0.6 m predominate. Calm conditions exist about 25 percent of the time from October through May. Wave heights greater than 1.8 m occur 24 percent of the time in February and 4 percent in August.

Currents

Existing knowledge about the movement of water over the South Texas OCS has come almost exclusively from drifter studies. Except for a brief period of monitoring at one locale about 6 miles off Port Aransas, no current meter data have been gathered. Consequently, no hourly or daily time data on flow velocities and directions exist for the region.

Drifter Surveys, 1962-1963

The drifter studies carried out by the Bureau of Commercial Fisheries, Galveston, involved release of surface bottle drifters at stations arranged along three transects that crossed the South Texas OCS. A fourth transect further north has been included because of its proximity to the study area. The locations of the release stations and transects are shown by figure 14.

The results of the 1962-1963 drifter surveys, carried out on a monthly basis, are summarized on the series of maps shown on figures 31, 32, and 33. The maps have been arranged on the figures to the extent possible in a way that will permit comparison of results for 1962 with those of 1963. Because the release dates for a given month varied from one year to the other, comparison on a month-to-month basis between the 2 years is not possible. However, the results do allow comparisons on a seasonal basis. In transferring the drifter results from the original compilations on larger scale maps to the smaller scale maps used in figures 31 through 33, space limitations did not permit transfer of all vectors. Where several vectors from a station had similar trends, one vector has been shown as representative.

Monthly surface currents were markedly similar between the 2 years, both in net direction and in speed of drift, even though the number of

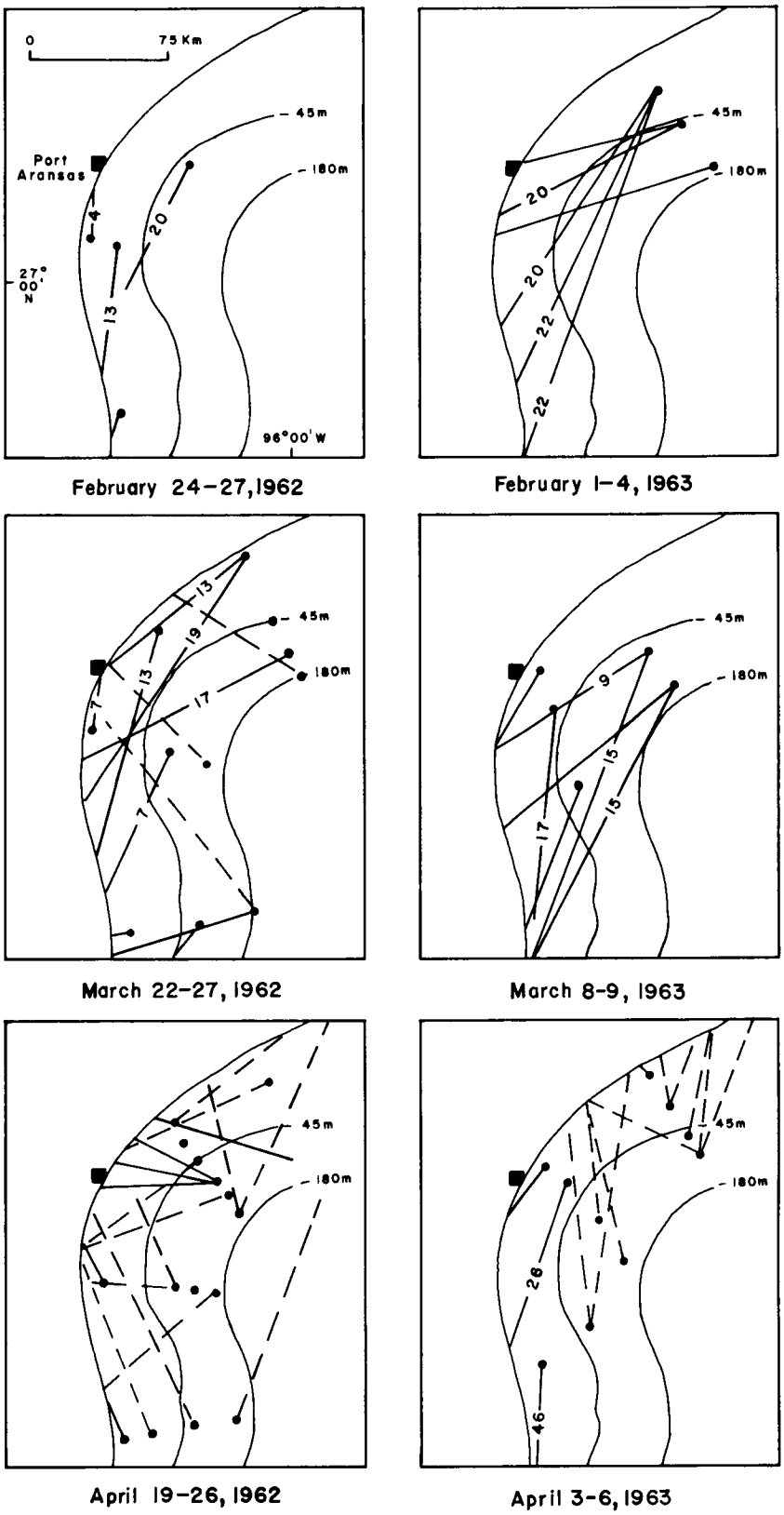

Figure 31. Results of surface drifter releases, February-April 1962 and February-April 1963. Date is period of drifter release. Dot indicates point of release. Vector is net direction of drift; number is indicated net speed of drift in km/day. Solid line indicates landfall or pickup in 0-15 days; broken line, 16-30 days.

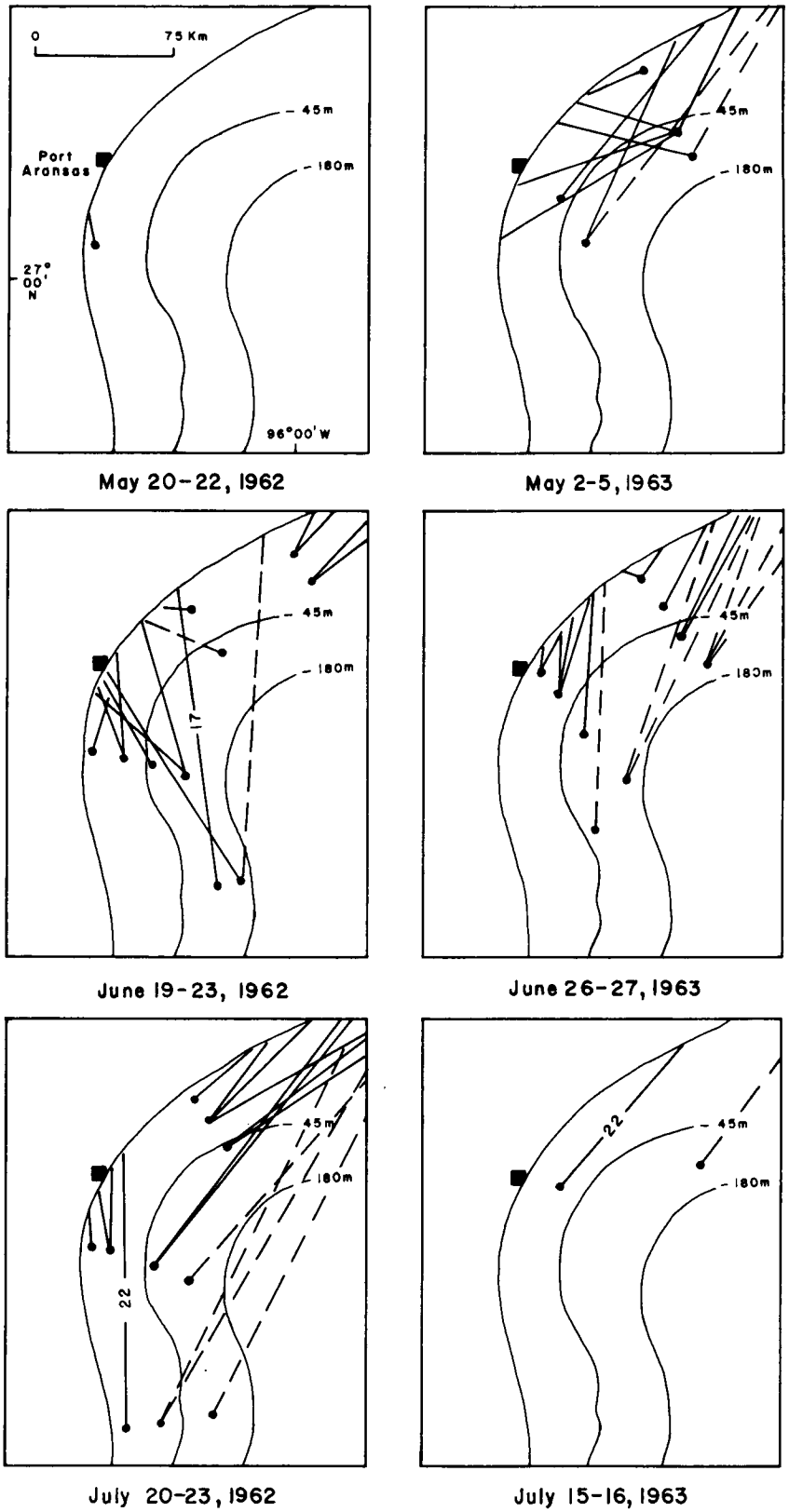

Figure 32. Results of surface drifter releases, May-July 1962 and May-July 1963. Date is period of drifter release. Dot indicates point of release. Vector is net direction of drift; number is indicated net speed of drift in km/day. Solid line indicates landfall or pickup in 0-15 days; broken line, 16-30 days.

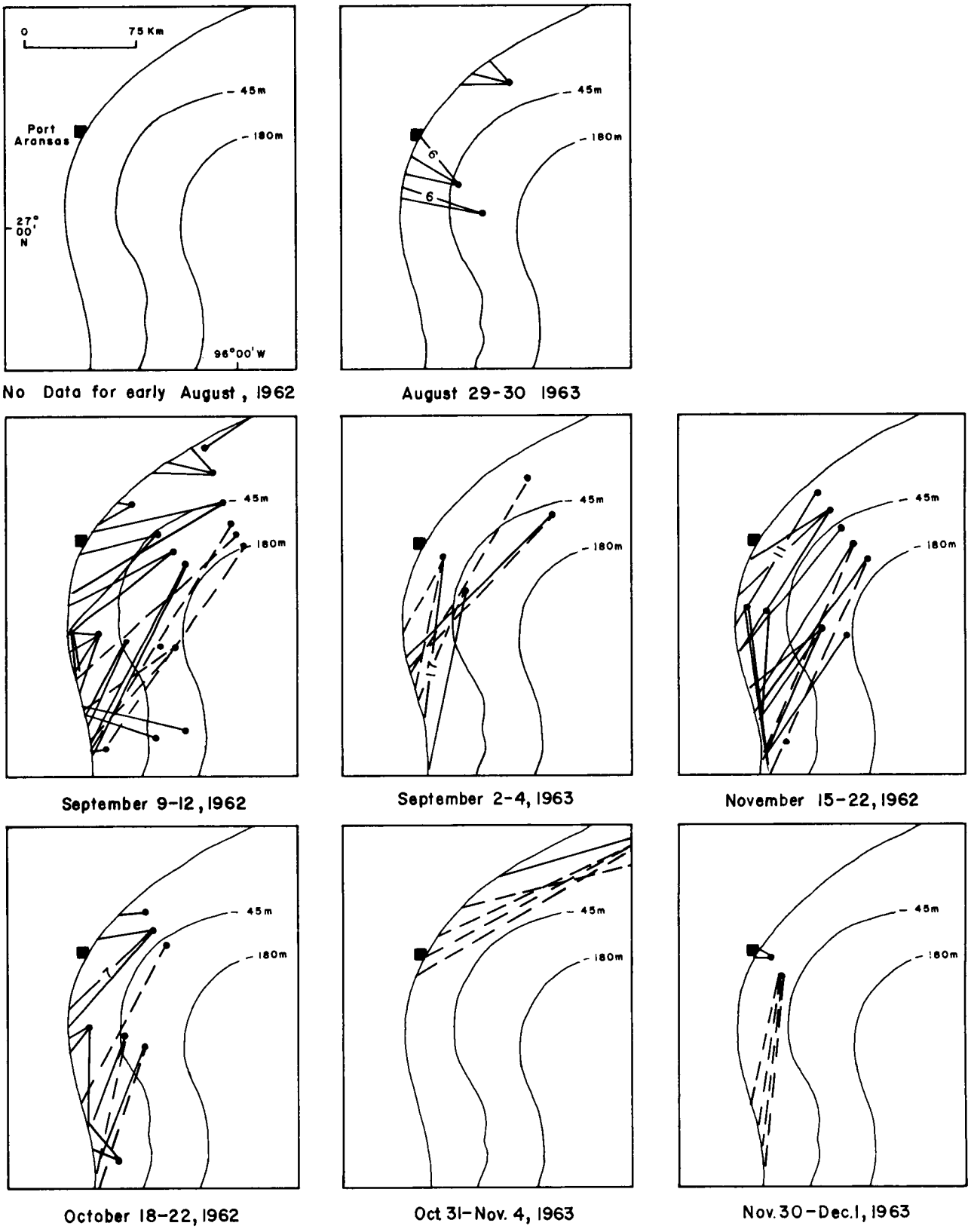

Figure 33. Results of surface drifter releases, September-November 1962 and August-December 1963. Date is period of drifter release. Dot indicates point of drifter release. Vector is net direction of drift; number is indicated net speed of drift in km/day. Solid line indicates landfall or pickup in 0-15 days; broken line, 16-30 days.

drifters and the release stations represented varied considerably. The seasonal characteristics of surface drift and the variation in patterns of drift from season to season are well-demonstrated by the results shown on the series of maps.

When analyzed by season, the following characteristics were indicated by the drifter data gathered from 1962 to 1963:

Winter: Net drift was southwest somewhat oblique to the coastline with a few exceptions mainly near shoreline, where drift was locally northward;

Spring: During April and May, net directions of drift were decidedly less consistent;

Summer: During June and July, the indicated drift was strongly northward, but the return from the southern part of the region was very poor; no releases were made in August 1962 and returns for August 1963 were too few to have much meaning;

Fall: Beginning in September and extending to December, drift was predominantly southerly with local deviations to a westerly direction in the early fall.

Drifter Surveys, 1970-1973

In 1970 the USGS office at Corpus Christi began continuing studies of water movement over the continental shelf off Texas. Release of both surface and bottom drifters on a seasonal (quarterly) basis began in January 1970 over the part of the South Texas OCS extending from Port Aransas southward to the Mexican border. In 1973 the area of study was extended northward beyond the South Texas OCS nearly to Galveston. Some of the results of the drifter releases during 1970 to 1972 are shown by figures 34, 35 and 36.

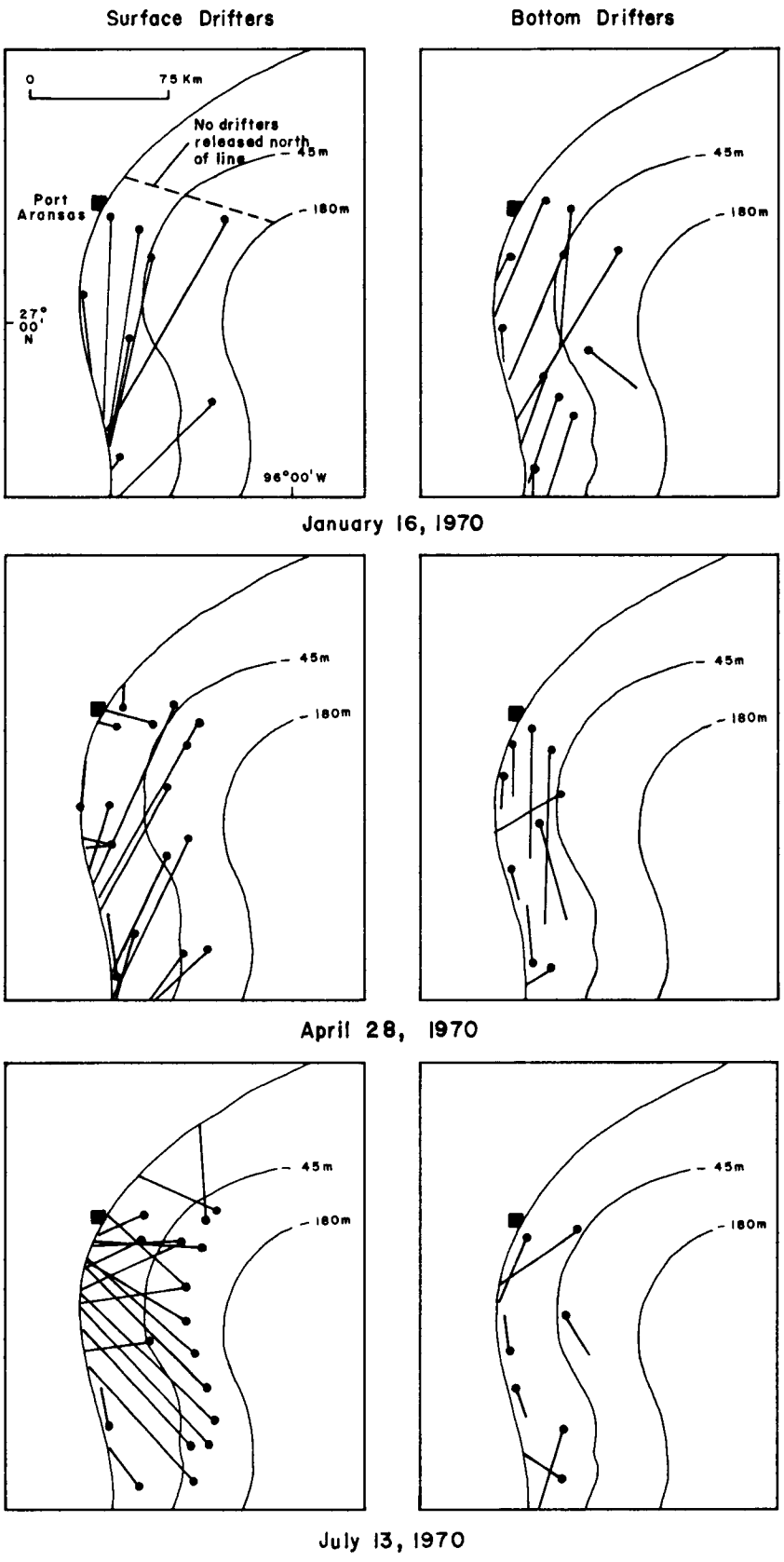

Figure 34. Results of drifter releases, surface and bottom, January, April and July 1970. Dot indicates point of drifter release. Vector is net direction of drift.

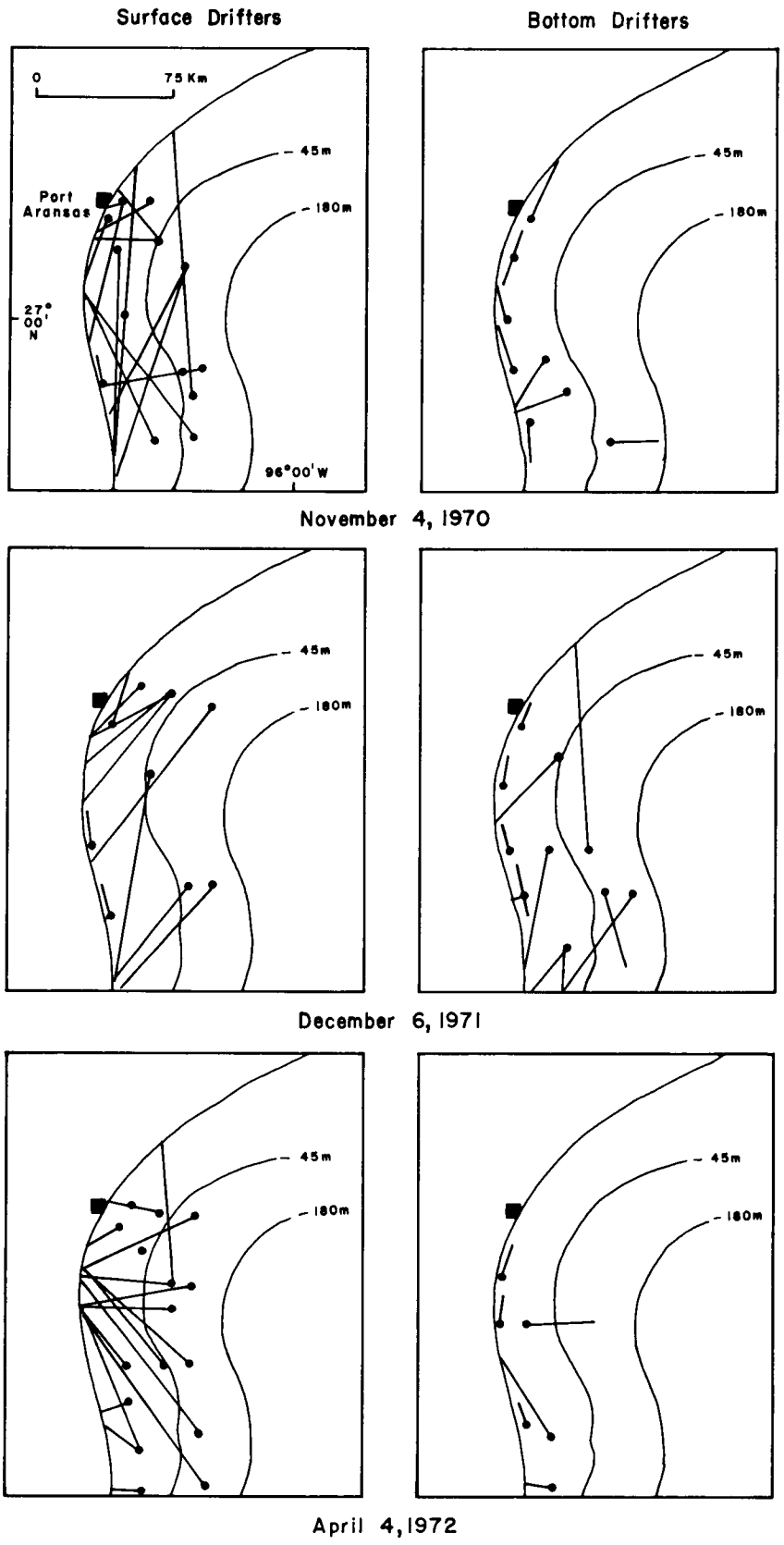

Figure 35. Results of drifter releases, surface and bottom, November 1970, December 1971 and April 1972. Dot indicates point of drifter release. Vector is net direction of drift.

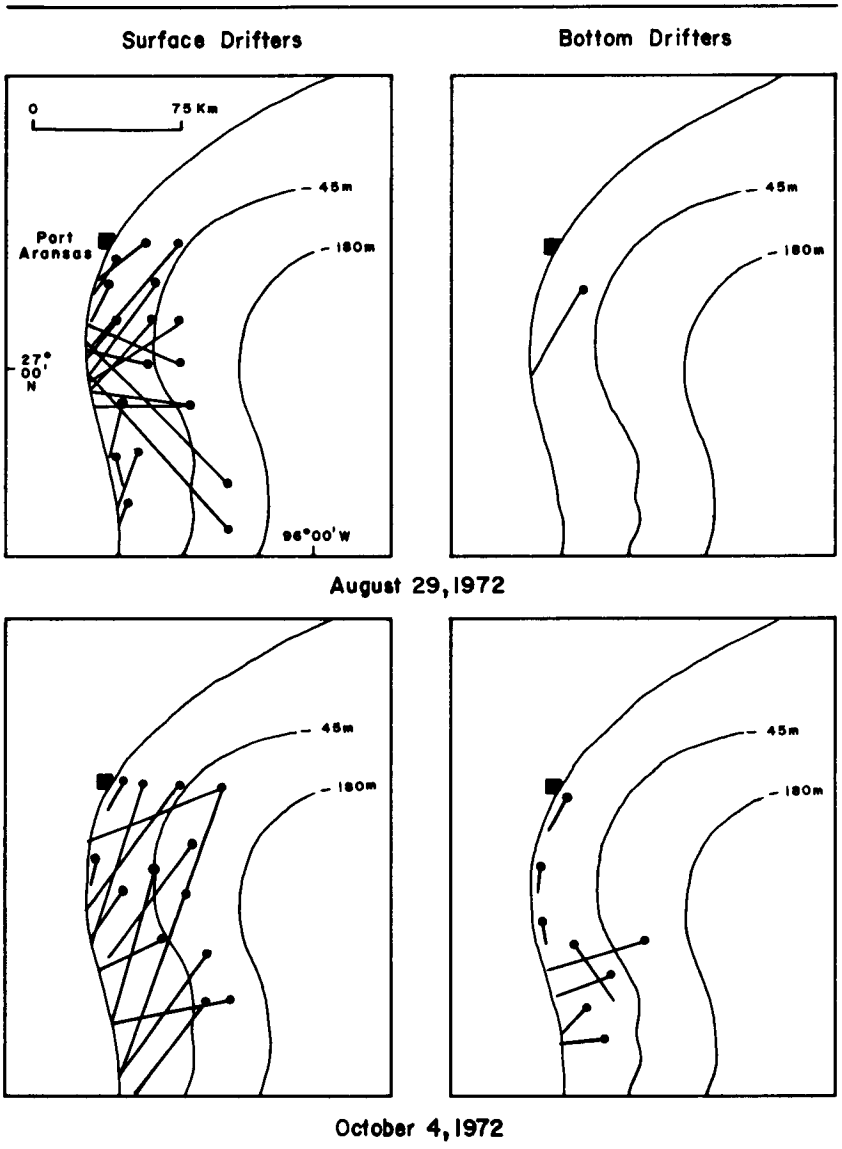

Figure 36. Results of drifter releases, surface and bottom, August 1972 and October 1972. Dot indicates point of drifter release. Vector is net direction of drift.

In broadest terms, the results for 1970 through 1972 indicated a changing pattern of surface drift that accompanied the change from a winter wind regime to a summer wind regime. Transitional periods of directional changes in drift were the spring and fall when prevailing surface currents were in opposition to the prevailing winds. These conditions formed a convergence on central Padre Island (fig. 35, April 4, 1972) that shifted to the north in the spring and to the south in the fall. The pattern of bottom drift, during the same periods of the year, also indicated a bottom convergence zone that at times was several kilometers south of the surface convergence zone, and, at other times was north of the surface convergence zone. The USGS studies also indicated a greater percentage of bottom drifter recovery during the winter.

When analyzed by season, the following regional characteristics were indicated by the 1970 to 1972 data:

Winter: Surface and bottom drift was southward except nearshore where drift was northward;

Spring: Surface drift was predominantly southward for the northern part of the study area and northward in the remainder in April. By May the surface drift was predominantly northward over the entire area. Southerly surface drift was indicated in the extreme northern part of the study area. Bottom drift was southward in 1970 and northward in 1971 and 1972. (Drift was southward again in 1973);

Summer: Surface drift was primarily northward except locally in the northern part of the study area where drift was slightly southward;

Fall: During early fall, surface and bottom drift were southward; during late fall the drift pattern was less consistent with a tendency toward

southward drift in the northern part of the area and northward in the southern part.

The two sets of drifter data, 1962 to 1963 and 1970 to 1972, do not permit comparisons of water movement on a monthly basis because the releases during 1970 to 1972 were seasonal rather than monthly. Furthermore, the dates of release within each of the four months of seasonal release during 1970 to 1972, with but one or two exceptions, did not fall within the same part of the month as the 1962 to 1963 releases. Nevertheless, the two surveys spaced nearly a decade apart reveal two significant characteristics of water movement over the South Texas OCS as a response to the regional wind patterns: 1) surface drift has predictable seasonal patterns - southward during the winter months, northward during the summer months and transitional during the fall and spring months; and 2) the magnitude of drift, specific directions of drift, and the beginning and ending of the transitional or turnaround periods vary from year to year. The latter circumstance is a result of yearly variations in such weather conditions as frequency and strength of northers, date of onset of strong northers in late summer or early fall, cessation date of strong northers in the spring, and prevailing strength and direction of winds in general.

Shelf Circulation

Seasonal temperature and salinity structure

The profiles for temperature and salinity shown in figures 23, 23a, 24 and 25 display diagrammatically the changing dynamics of the water over the South Texas OCS from season to season. This is shown best by the data off Matagorda Bay in the northern part of the South Texas OCS where the

seasonal changes were most pronounced (fig. 23a). During the winter, surface cooling produced cold water (~17°C) nearshore which sank and flowed offshore along the bottom. Concurrently, warmer and more saline surface water (>36.5 °/oo) from offshore drifted landward producing a packing of isotherms around the 25 m isobath and a westward flowing geostrophic current over the outer shelf.

In May (fig. 23a) upwelling along the bottom extended shoreward as far as the innermost station (56). In the upper waters a divergence formed nearshore and a convergence offshore, such as would be associated with a general flow to the east. The water of lower salinity in the spring was carried offshore by offshore or eastward drift.

The July eastward flow was indicated by the distinct upwelling which extended to the surface over the 25 m isobath. By late September, the slope of the isotherms had reversed, indicative of convergence toward shore at the surface and offshore drift along the bottom. For geostrophic balance, this circulation would require a return to westward flow.

Circulation patterns

The general pattern of circulation for the northern half of the South Texas OCS has been inferred from the temperature, salinity, and density (σ_t) data collected during the GUS III cruises conducted from 1963 through 1965. The surface salinity measured during each of the GUS III cruises and the water circulation patterns inferred from the hydrographic data are shown by the maps on figures 37 through 42. The maps are arranged in chronological order, beginning with January 1963 and ending with December 1965 (not every month is included). The South Texas OCS south of the 27° parallel was not covered by the study.

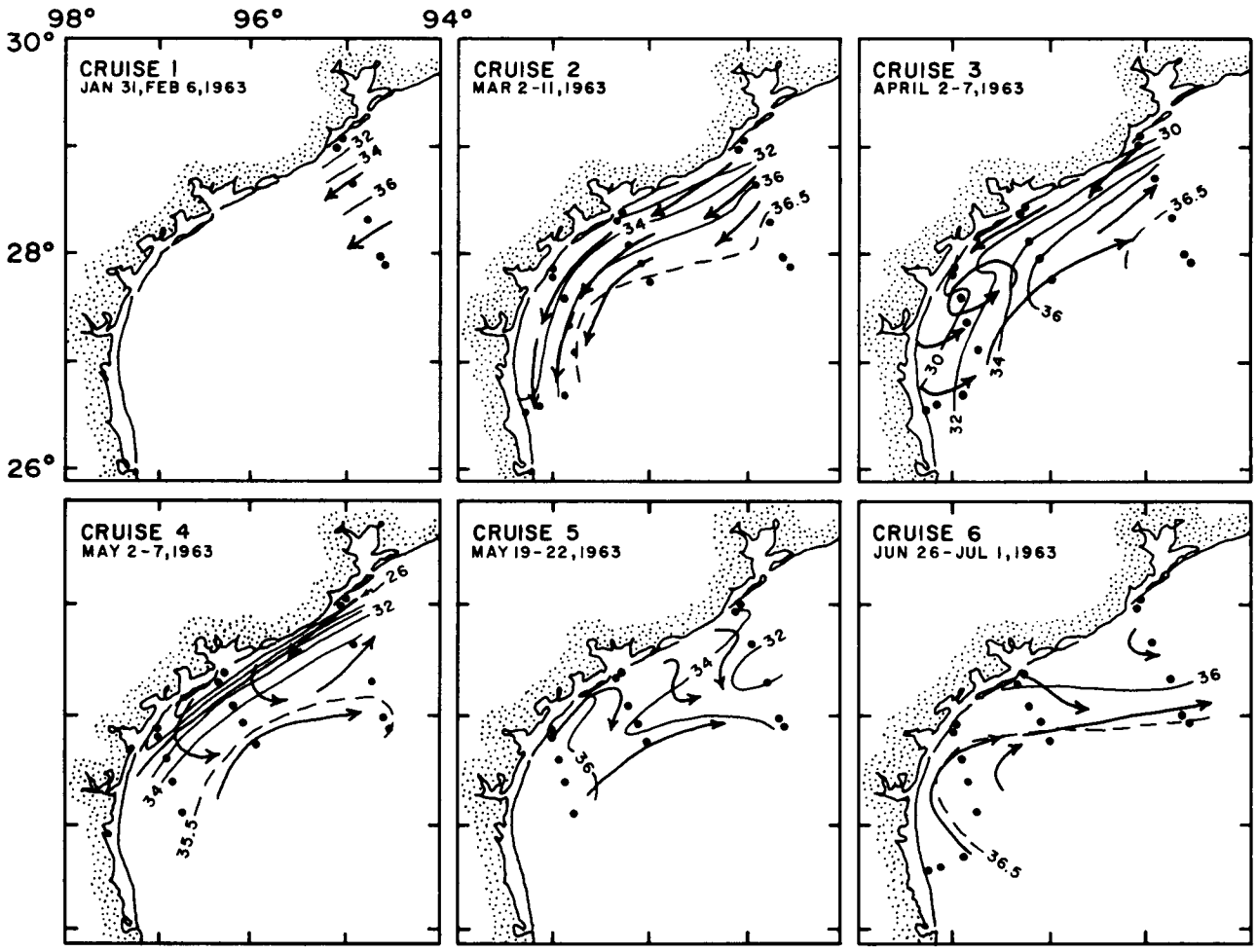

Figure 37. Surface salinity and inferred shelf water circulation for GUS III cruises, January 31-July 1, 1963. Salinity in $^{o}/oo$.

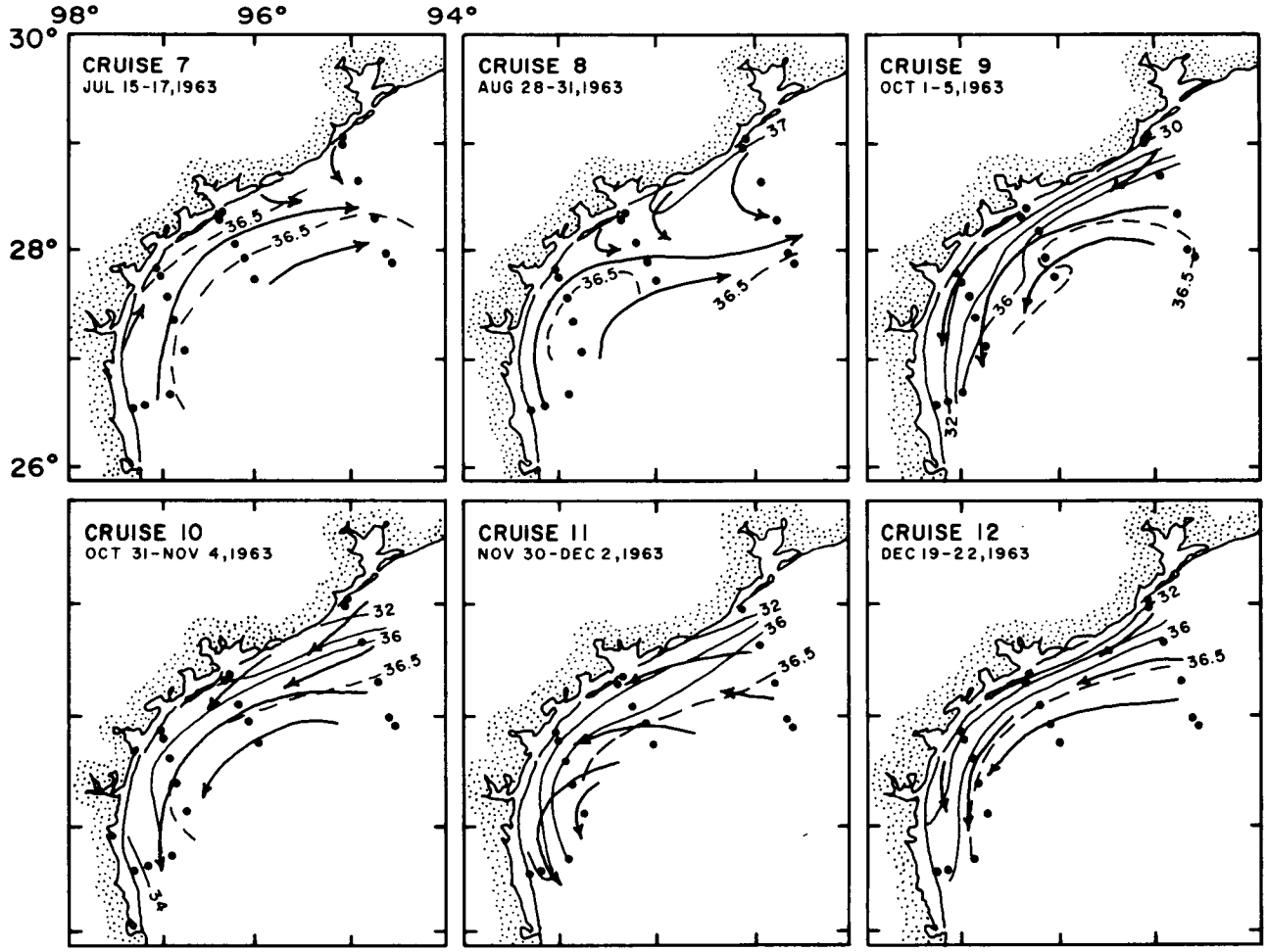

Figure 38. Surface salinity and inferred shelf water circulation for GUS III cruises, July 15-December 22, 1963. Salinity in $^{o}/oo$.

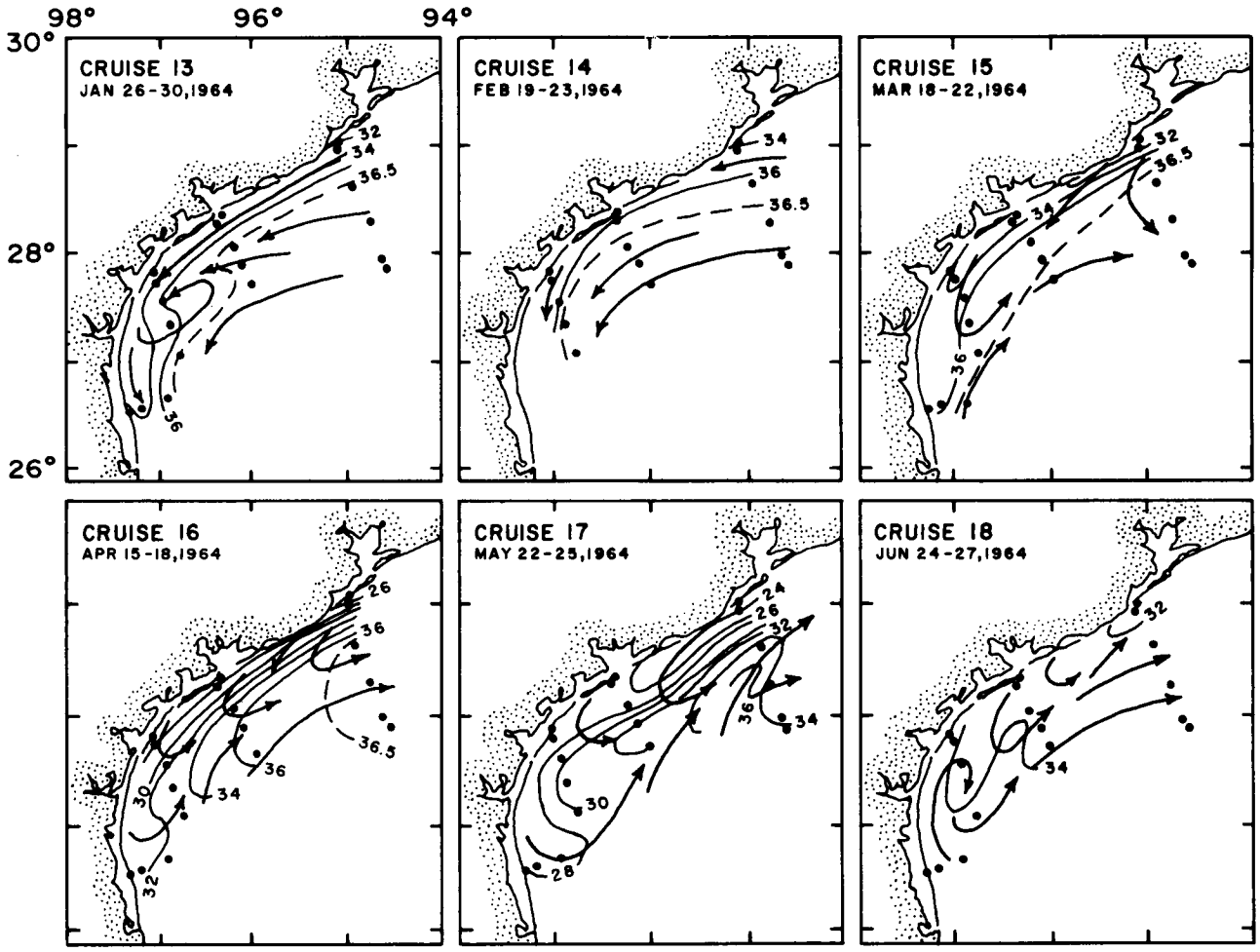

Figure 39. Surface salinity and inferred shelf water circulation for GUS III cruises, January 26-June 27, 1964. Salinity in $^{o}/oo$.

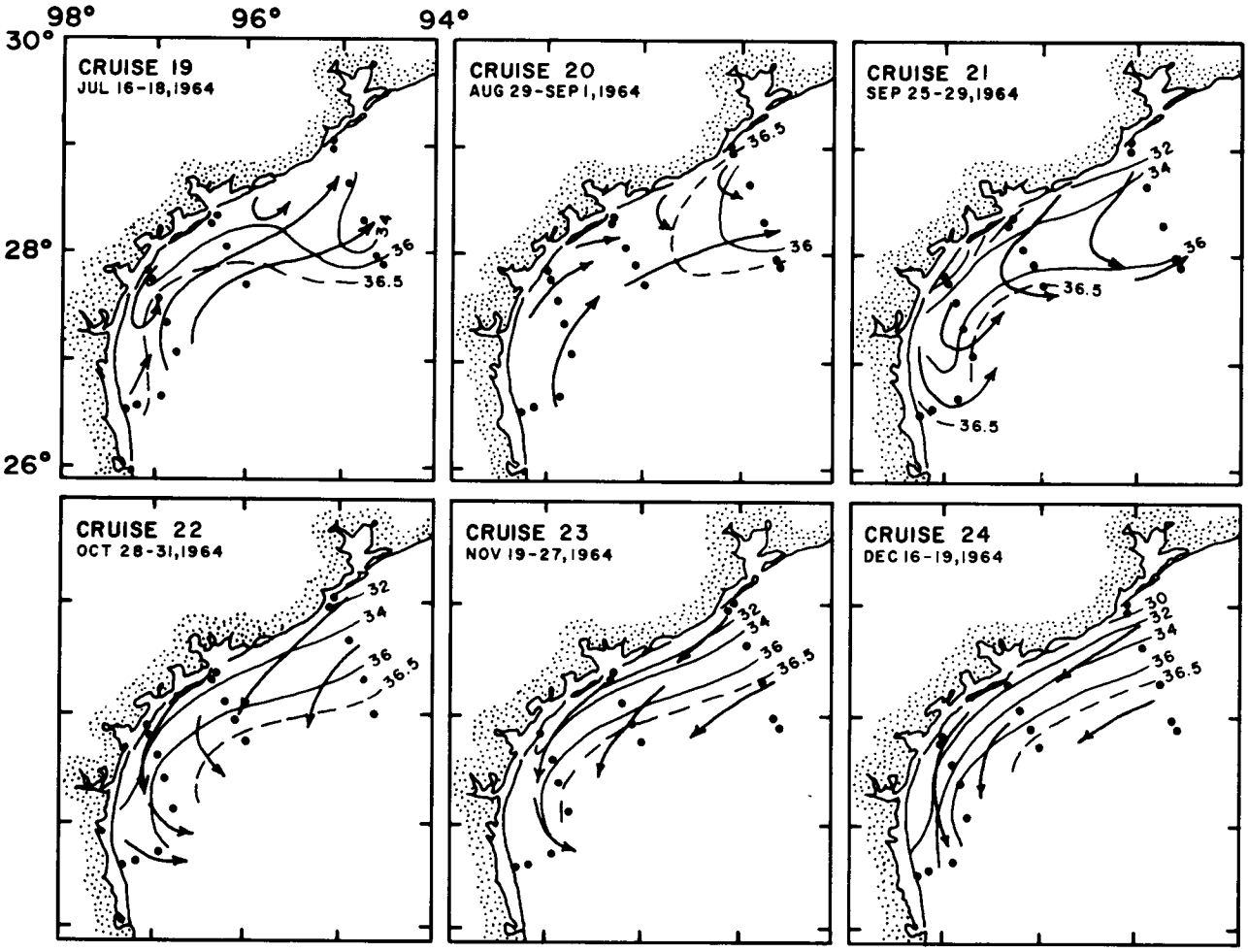

Figure 40. Surface salinity and inferred shelf water circulation for GUS III cruises, July 16-December 19, 1964. Salinity in $^{o}/oo$.

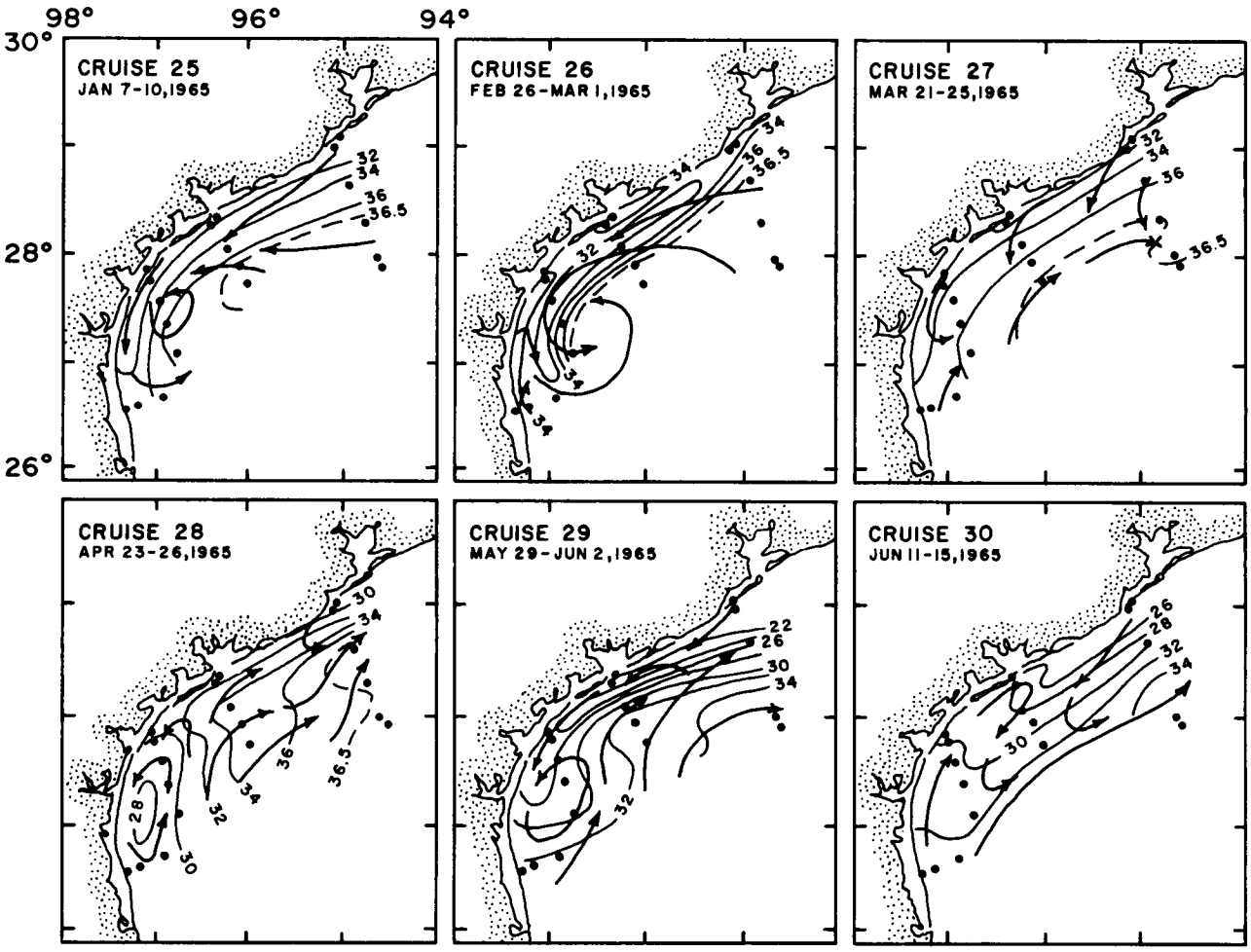

Figure 41. Surface salinity and inferred shelf water circulation for GUS III cruises, January 7-June 15, 1965. Salinity in $^{o}/oo$.

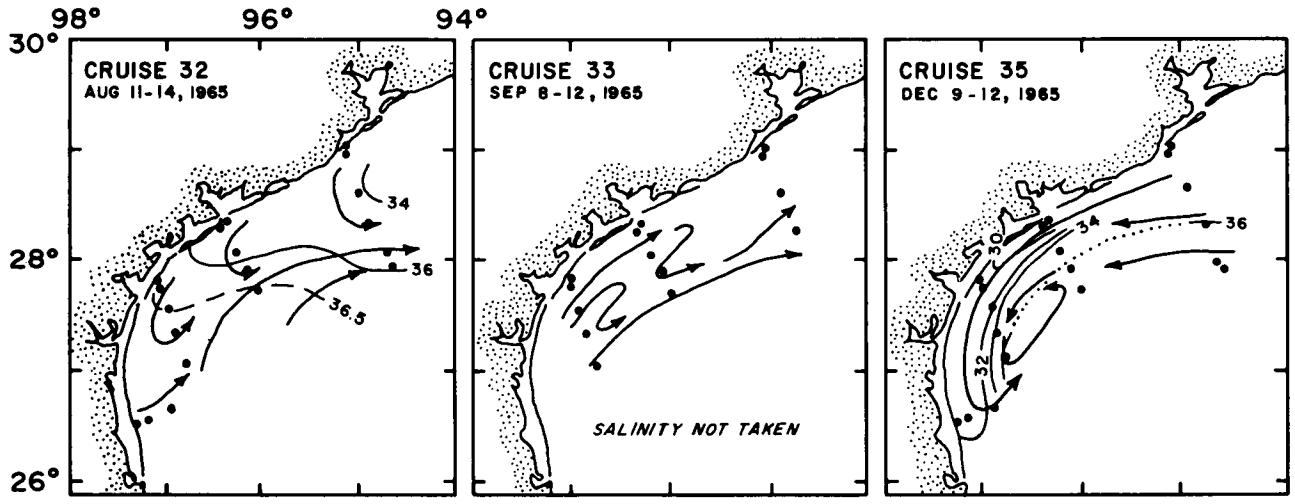

Figure 42. Surface salinity and inferred shelf water circulation for GUS III cruises, August 11-December 12, 1965. Salinity in °/oo.

As in the case of the drifter studies, the GUS III data indicate distinct seasonal patterns. The circulation inferred from the hydrographic properties of the water agree well with the results of the drifter studies. The maps (figs. 39 through 42) indicate that over the outer shelf flow was to the north and east from mid-March through September, and to the west and south from October through February. In the southern area from Port Aransas to Port Isabel, the presence or absence of an eddy, apparently at irregular times, was the principal cause of flow. Such an eddy, which probably could develop during any season, appeared to be related to locally interacting flow patterns. A zone of convergence developed in the waters of the inner and middle shelf and was most pronounced in the spring. The nature of the convergence zone was similar to that indicated by the 1970 to 1973 drifter studies in that the nearshore location of the convergence shifted up the coast during spring through early summer. The GUS III observations suggest that the convergence developed because of contrasting flows of nearshore and offshore water: the nearshore flow was westward while the offshore, as well as all waters in the southern part of the area studied, moved north and east. The zone of convergence was absent from October through February because the flow was to the west and south throughout the area.

Oil spill centroid trajectories

A series of trajectories indicating possible directions of oil drift under specified conditions on the water surface of the South Texas OCS have been prepared using computer analysis of existing data and numerical modeling. Steady-state currents computed for the shelf waters were derived

through the equations of motion. These currents correspond to a forcing function representing a steady field of wind stress that neglects field acceleration and lateral friction. The fluid is assumed to have a homogeneous density and a constant value of the vertical exchange coefficient. The equations used represent the classical Ekman problem expanded to include the slope terms of the geostrophic relationship. The complete formulae used in the trajectories computation are given in Angelovic and others (1976).

In preparing the trajectories, a suite of representative cases were selected which correspond to prevailing seasonal wind patterns over the South Texas OCS. Constant and uniform winds were assumed as forcing functions for the prototype. Two speeds, 5 and 10 m/sec, and 4 directions, east, southeast, south-southeast, and northwest, were programmed, and each of the 8 cases were run on the computer to the point judged to be dynamic equilibrium. Surface water velocity components from each run were combined with the Stokes drift vector to provide a total velocity. Seven source locations were picked in the region and trajectory plots were made for the centroid of the oil spill in each case. The investigators who made the trajectories analyses stressed that the system applies to the South Texas OCS only when the model assumptions are approximated and:

1. a steady-state wind field exists over the area for a period of at least a week;
2. no other currents are operative;
3. the Stokes drift introduced by wave action can be approximated by the addition of 3 percent of the wind speed; and
4. the trajectories are not extended within 10 km of the shoreline.

The trajectories indexed in terms of elapsed time in hours along the path are shown by figures 43 to 46. Under the assumption and limitations of the model, a significant difference does seem to exist between winds of 5 m/sec and those with a velocity of 10 m/sec. Because of the strong geostrophic regime set up along the coastline, the movement of the oil spill centroids toward the coast as in the 5 m/sec case is augmented by a long sequence parallel to the coast. Northwest winds (fig. 46) will not generate a threat to the U.S. coastline following a spill. South-southeasterly winds (fig. 45) will bring the oil spill centroids to the immediate coastline in light winds. However, stronger wind speeds indicate movement toward the Texas coast north of the South Texas OCS from sites on the outer continental shelf. Southeasterly winds can be expected to move spilled oil along trajectories which, for the greater part, will approach the shoreline in the local area.

Obviously, the oil spill centroid trajectories must be viewed within the idealized and theoretical constraints built into the model. Furthermore, the model can in no way consider either the volume of oil that might be spilled or the size of the surface patch it might create nor can it account for changes in wind speed and direction during transit. These are important factors in estimating the possible damage to a proximal coastline from an offshore spill. The travel-time lapse calculated for the stations farthest offshore is as much as 6 days. The degree to which a spill of some size might be dissipated during a passage time of 5 to 6 days will be directly related to the constancy of conditions on the sea surface. Consequently, deviations from the idealized trajectories will be most marked during those seasons when wind patterns are subject to

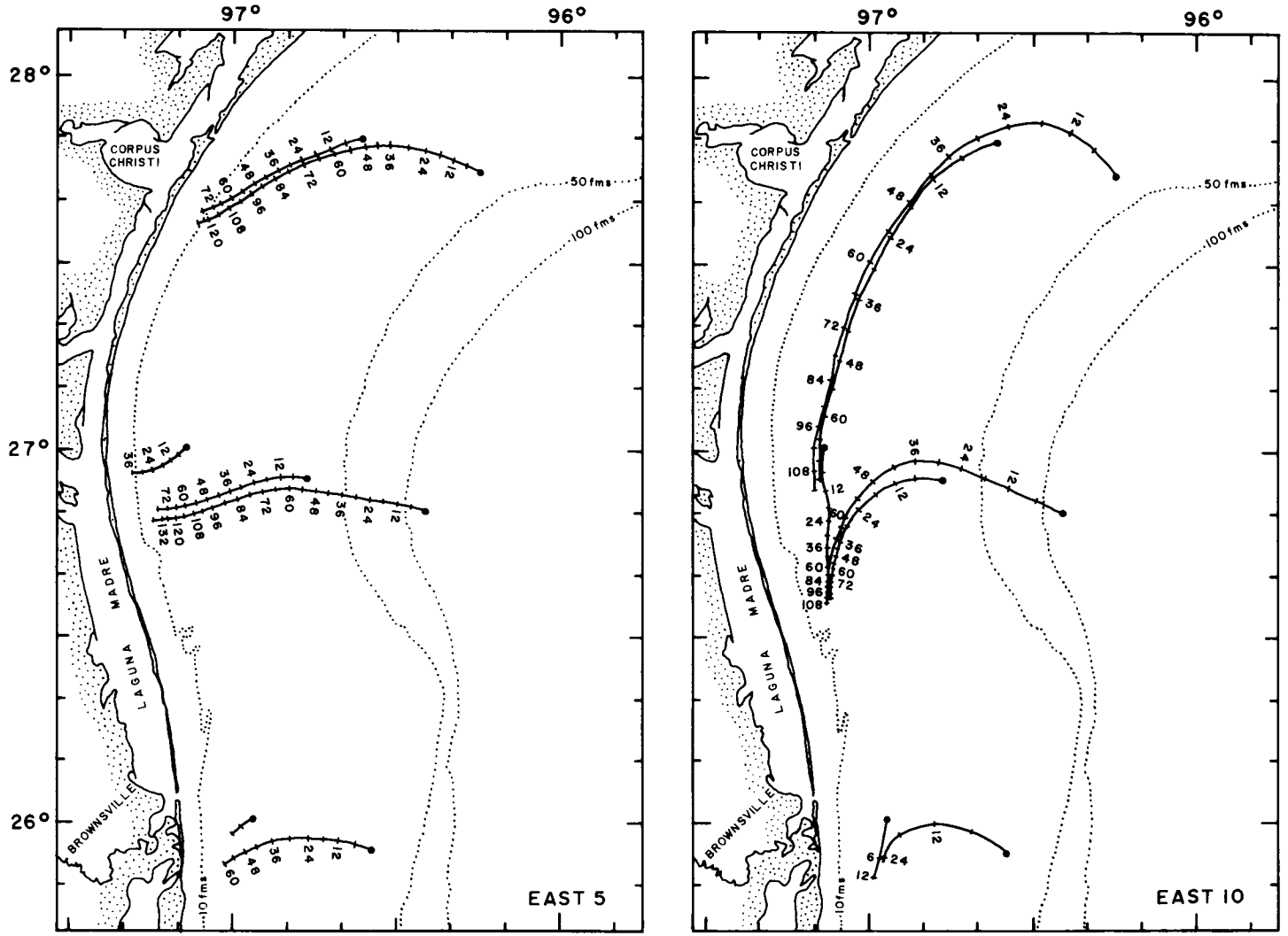

Figure 43. Centroid trajectories for east winds of 5 and 10 m/sec. Time in hours.

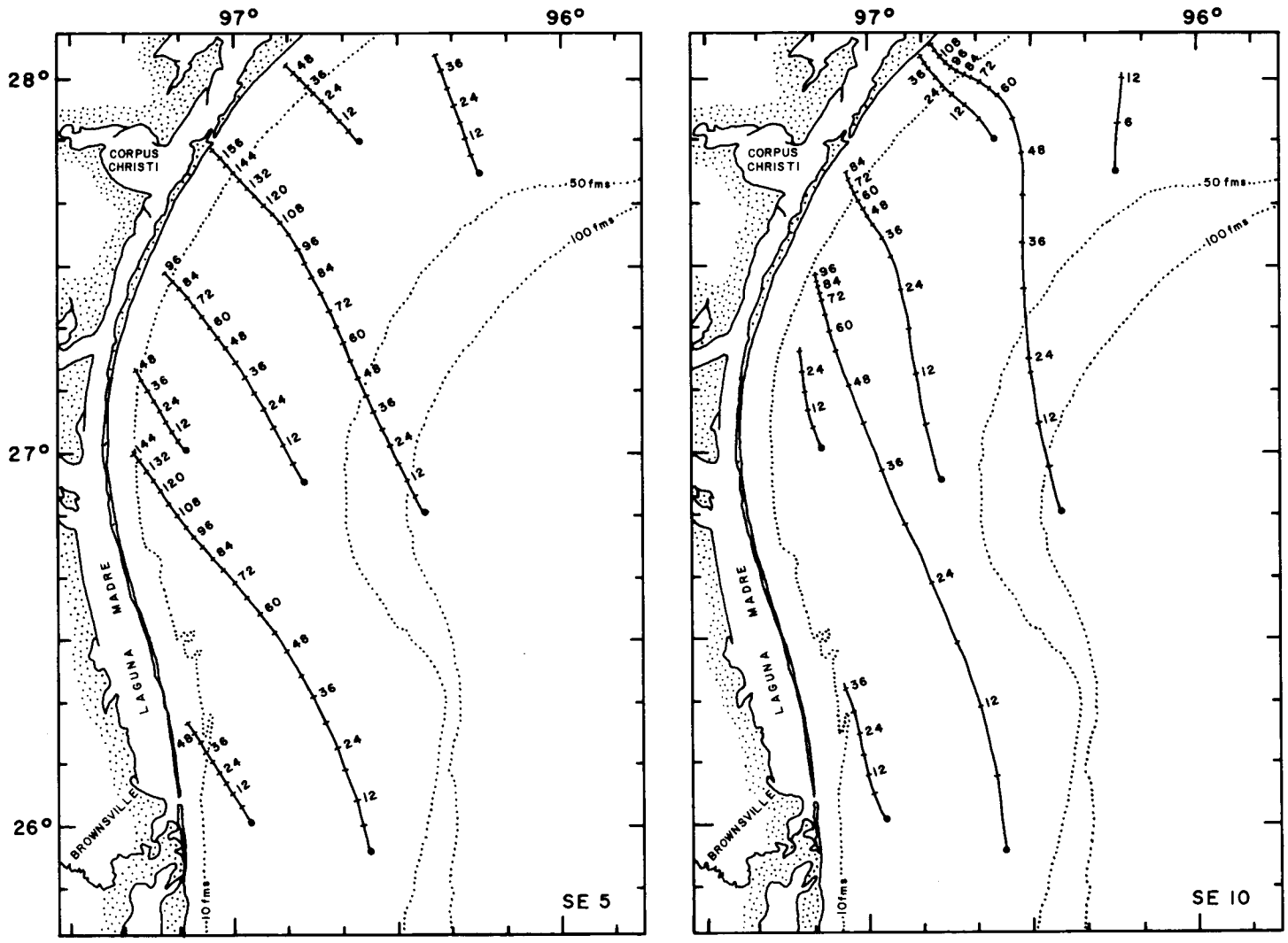

Figure 44. Centroid trajectories for southeast winds of 5 and 10 m/sec. Time in hours.

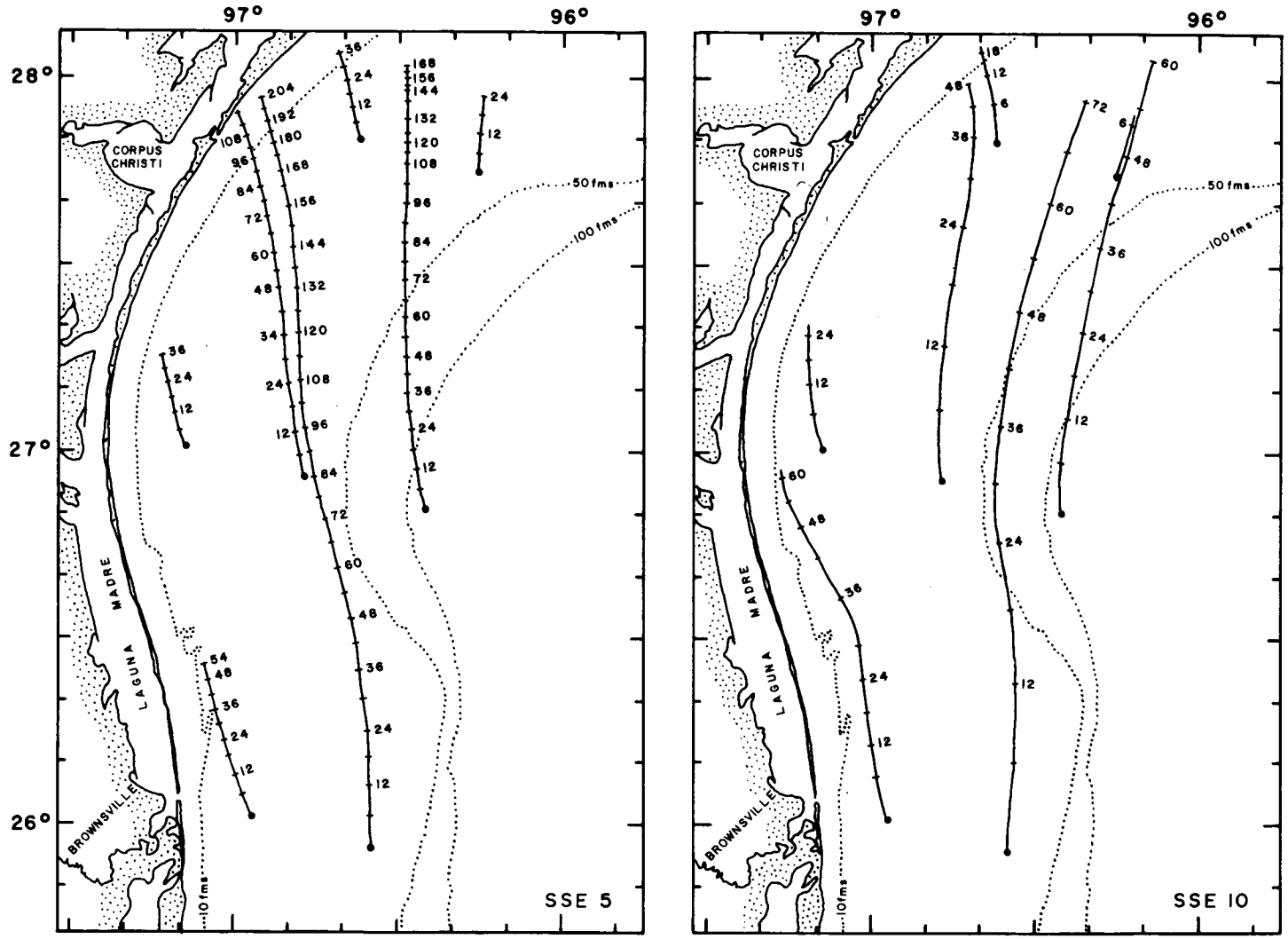

Figure 45. Centroid trajectories for south-southeast winds of 5 and 10 m/~~sec~~. Time in hours.

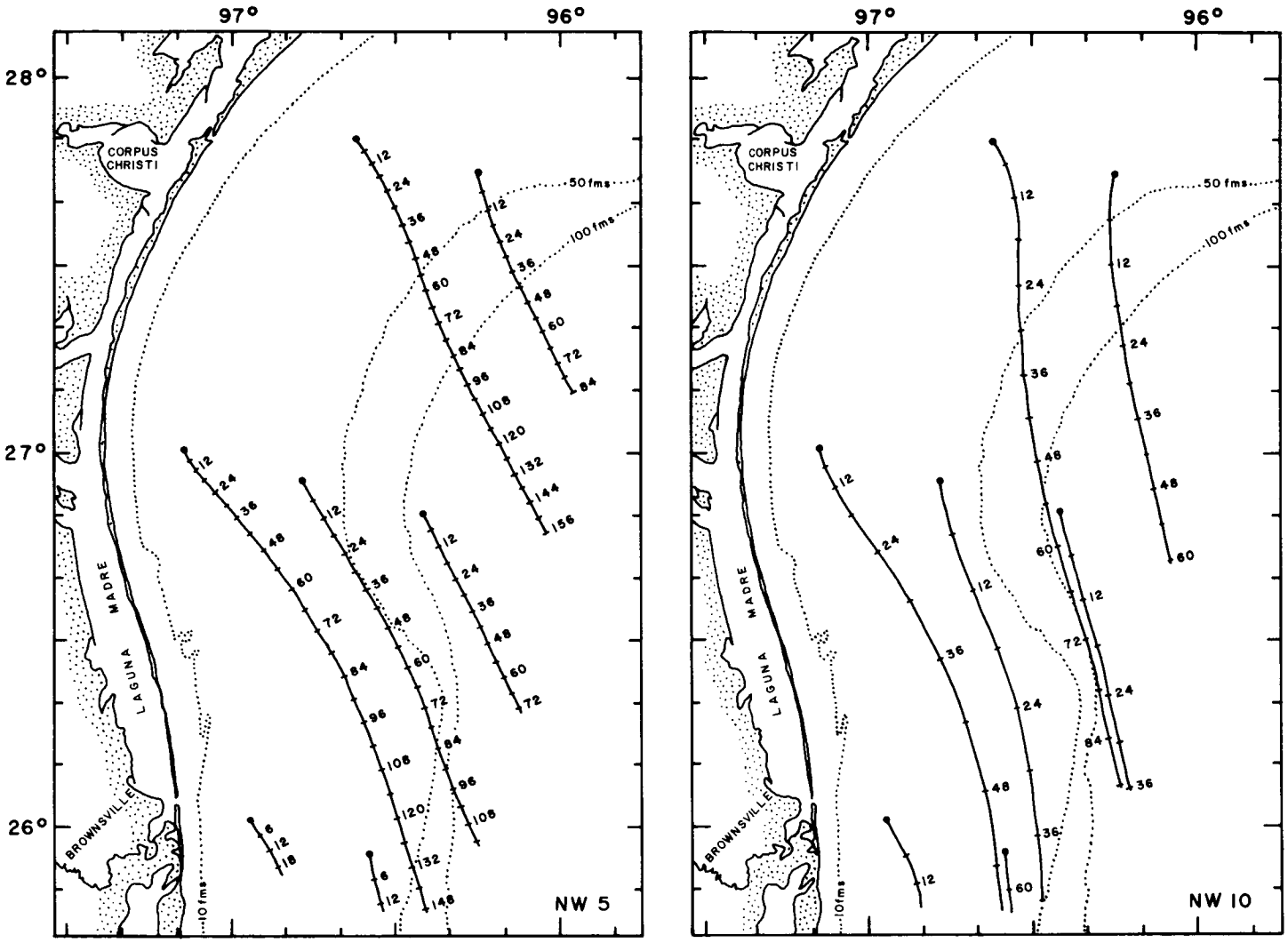

Figure 46. Centroid trajectories for northwest winds of 5 and 10 m/sec. Time in hours.

changes in direction over relatively short periods of time, as during the winter months and to some extent, during the spring and fall months.

Summary of Regional Characteristics

The physical oceanographic and hydrographic characteristics of the South Texas OCS, as indicated by the data described, can be summarized as follows:

1. Patterns of water movement and temperature/salinity variations through the water column are decidedly seasonal in nature.
2. Surface movement, except during hurricanes, is most strongly influenced by the prevailing direction of the wind, which varies through the year in response to seasonal changes in the atmospheric regime: net surface drift is southerly during the winter, northerly during the summer and geographically variable from north to south in the spring and fall when atmospheric conditions are transitory. During the periods of seasonal change in the spring and fall, drift tends to be southerly over the northern part of the region and northerly to westerly over the southern part.
3. Net bottom drift on an annual basis is southerly throughout the region but seasonal deviations occur: northerly during the summer over the northern half and westerly during the winter over the northern half.
4. Surface temperatures throughout the South Texas OCS closely parallel air temperatures, but over the outer shelf temperatures below the surface have a distinctly different seasonality. Fluctuations in surface temperature correlate either with monthly mean air temperatures or with daily averages. Seasonal cooling of the surface water moderates offshore and down the coast to the southwest.

5. Subsurface water temperatures over the shelf at depths greater than 27 m are highest in fall and lowest in spring from the time of the spring minimum; bottom temperatures increase gradually through the summer until overturning resulting from surface cooling makes the water column almost isothermal and raises bottom temperatures to their annual maximum. Further cooling through the winter tends to decrease temperatures through the water column in unison, but continued cooling of the bottom waters offshore in the spring apparently results from annually recurring upwelling. Persistence of the upwelling through August each year is suggested by more gradually increasing temperatures at the bottom than at the surface. In some years the upwelling may extend well onto the inner shelf.
6. The principal periods of decreased surface salinity seem to be governed mainly by the discharge of the Mississippi River with a time lag of about one and a half months offshore. The degree of spring freshening of water from year to year seems to correspond to the magnitude of outflow from the Mississippi River.
7. Subsurface salinities in offshore waters remained high (about 36.5 $^{o}/_{oo}$) throughout the period of study (3 years) while surface salinities were lowest in the spring.

SUSPENDED SEDIMENTS

General Statement

As noted in the resumé of field sampling in the Introduction, samples were obtained by NISKIN cast at three depths in the water. The depths were near surface, at either the thermocline or roughly mid-water depth if the

thermocline was absent, and near bottom. Because of the time spread of more than a month in the sampling period, the data as a whole are not time synoptic; however, data for some stations collected over shorter time intervals of a few days for individual transects and of about a week for adjacent transects are quasi-synoptic.

As the overall sampling was not time synoptic, only the relative amounts at a specific station or along a single transect have reliable scientific significance. A total of 65 samples were analyzed for sediment concentration and particle size.

Analytical Methods and Techniques

Particle Counts and Grain Size

The approximate concentration and grain size of the suspended sediments were determined by COULTER COUNTER analyses. Concentrations were determined in terms of total particle counts per standard unit volume. Employing a 30 μm aperture tube, total particle counts per 0.05 cc were determined for sediments within the 0.63-16 μm size range. A replicate count was made on each sample, and the average of the two values was used as the total particle count. Counts were obtained in an unagitated state. Supplemental concentration data also were obtained while stirring the sample suspension at a constant speed just below the threshold of creating a vortex in the liquid.

Grain-size analyses were made according to the following procedures:

1. The water samples were brought to room temperature and aerated in darkness to liberate dissolved gases and minimize organic growth.
2. The entire 250 ml seawater sample was analyzed in its natural untreated state; however, in some instances, only smaller volumes were available for analysis.

3. Sample concentrations were maintained at a sufficiently low level to minimize coincidence error; if the original concentration exceeded this level, the sample was diluted with seawater electrolyte filtered through a 0.2 μm filter until less than 5 percent coincidence was achieved.
4. For each sample, combined 200 μm and 30 μm tube analyses were made, providing an analytical range from 0.63 μm (10.62 Ø) to 80.6 μm (3.62 Ø). For the purpose of deriving statistical parameters based on a 0.5 Ø interval, an extrapolated analytical range of 11.0 Ø to 3.5 Ø was utilized.

Mineralogy

For mineral determinations, a 1 to 3 l aliquot of seawater collected during the NISKIN casts was filtered aboard ship through a preweighed SELAS FLOTRONICS filter having a 0.45 μm nominal pore diameter. The material was washed with 100 ml of deionized water to remove the salts. The filter pads were frozen for transfer to the laboratory.

In the laboratory, the samples were thawed, dried, and weighed on a micro-balance. The mineralogy was determined by X-ray diffraction patterns using a sensitivity of 100 counts per second full scale and a scanning speed of 2 degrees 2 theta per minute. Three additional patterns were made for each sample: 1) after treatment with ethylene glycol; 2) after heating to 400°C; and 3) after heating to 550°C. Chlorinity was measured by titration of a single aliquot taken at the time of field sampling.

Trace Metals

On board ship, the filtration was accomplished by an adaptation of the in situ filters of Davey and Soper. The filters were made by heating 0.4

μm NUCLEPORE filter material to make bags 3.5 cm in diameter by 7 cm in length. The filter bags were encapsulated in polyethylene vials with entrance and exit tubes sealed at each end. The inline filter capsules were washed with 1 to 1 nitric acid and deionized water before use. The filters were attached to the polyethylene bottles containing the sample water to be filtered by means of polyethylene fittings sealed to the bottle caps. Ten liters of seawater were then passed through the filter. Once filtration was completed, the encapsulated filters were sealed in polyethylene bags for transfer to the laboratory.

In the laboratory, all analytical preparation was performed in an ENVIRCO clean bench which utilized a filtered air flow to isolate the interior of the bench from the remainder of the laboratory. The samples were thawed, the filter capsules opened and the bags removed. A jet of deionized water was directed onto the exposed filter surface. The water and dislodged particulate material were collected in a 100 ml beaker; 70 to 100 ml of deionized water was used in this step. This suspension was then filtered under vacuum on a 25 mm diameter, 0.4 μm pore-size NUCLEPORE filter which had been acid washed, dried over anhydrous magnesium perchlorate and weighed. The filters with sample material were then placed in a desicator over anhydrous magnesium perchlorate for 24 hours and reweighed. All weighings were made on a PERKIN ELMER AD-2 autobalance (readable to 1.0 μg) placed in the clean bench. Only deionized water and redistilled nitric acid were used in the analytical preparation. All labware was washed with 1 to 1 nitric acid and deionized water before use.

After reweighing, the filter and sample were placed in a 50 ml teflon beaker. Two ml of concentrated nitric acid were added and the samples were

dried under infrared lamps at a temperature of 80°C. One ml of concentrated nitric acid was then pipetted onto the dry sample. The sample and acid were allowed to equilibrate for half an hour and were then transferred to an acid-washed lucite sample cup. This solution was used for analysis by atomic absorption spectroscopy. All analyses were made by a PERKIN ELMER model 303 atomic absorption spectrophotometer using a model 2100 HGA graphite furnace. For all metals the amounts were determined in the deionized water and the redistilled nitric acid. A procedural blank was then determined by taking one of the original acid-washed filter capsules through the entire procedure as if it were a sample. Four blanks were run. The blank value thus determined was used in all calculations.

The sample size, 0.1 to 15 mg total weight, made contamination a problem in analysis. Every effort was made to control all possible types of contamination, including analysis of ship's paint, use of clean bench, use of carefully selected reagents, and careful washing of all labware in 1 to 1 nitric acid.

Sediment Concentrations

Sediment concentrations among all the stations sampled ranged from a minimum of 5,746 counts at station 10 to a maximum of 237,297 counts at station 156. The particle counts by station for each of the three water depths sampled are listed in table 8. The composite patterns of geographic distribution for each of the three water depths is shown by the maps on figure 47. Profiles were constructed to show the concentration gradients through the water (figs. 48 and 49).

Comparison of the data displayed on the three figures and listed in the table shows that the amounts of suspended sediment relative to depth

Table 8. Suspended sediment concentrations in particle counts per unit volume by station at three depths: T-surface; M-mid depth; B-near bottom.

Station Number	(30 μm tube analysis/0.05 cc)	(200 μm tube analysis/2cc)
10WT	5,746	31,057
10WM	15,638	12,958
10WB	12,598	57,014
24WT	97,917	12,148
24WM	177,001	17,255
24WB	46,495	1,946
32WT	39,513	15,362
32WM	46,864	1,238
32WB	95,050	24,936
60WT	10,869	2,001
60WM	16,444	981
60WB	156,651	80,378
70WT	78,704	18,294
70WM	94,344	2,479
70WB	97,620	29,667
73WT	13,763	2,058
73WM	14,395	721
73WB	23,947	10,441
85WT	24,000	1,429
85WM	24,241	383
85WB	127,724	81,381
88WT	19,656	519
88WM	38,123	957
88WB	186,788	22,839
95WT	11,720	2,381
95WM	16,087	2,002
95WB	9,179	2,810
110WT	24,176	529
110WM	29,419	494
110WB	81,807	68,090
114WT	27,441	827
114WM	9,216	116
114WB	116,353	201

Table 8. Suspended sediment concentrations in particle counts per unit volume by station at three depths: T-surface; M-mid depth; B-near bottom--Continued

Station Number	(30 μm tube analysis/0.05 cc)	(200 μm tube analysis/2 cc)
115WT	26,611	383
115WM	21,664	218
115WB	99,388	85,588
155WT	21,558	677
155WM	11,480	142
155WB	160,252	1,787
156WT	32,817	650
156WM	18,615	154
156WB	237,297	85,173
157WT	28,838	1,027
157WM	18,824	222
157WB	57,946	11,840
160WT	25,493	249
160WM	22,260	1,077
160WB	46,423	343
164WT	27,213	815
164WM	43,612	740
164WB	21,950	1,661
165WT	42,070	435
165WM	19,385	907
165WB	16,669	3,488
238WT	24,560	5,010
235WM	96,485	21,787
236WT	44,643	2,891
236WB	49,482	66,765
241WT	30,344	648
241WM	7,176	344
241WB	16,893	1,338
243WT	29,423	6,857
243WM	21,243	2,992
243WB	35,095	6,883
245WT	67,308	9,102
245WM	141,335	1,878
245WB	68,699	7,879

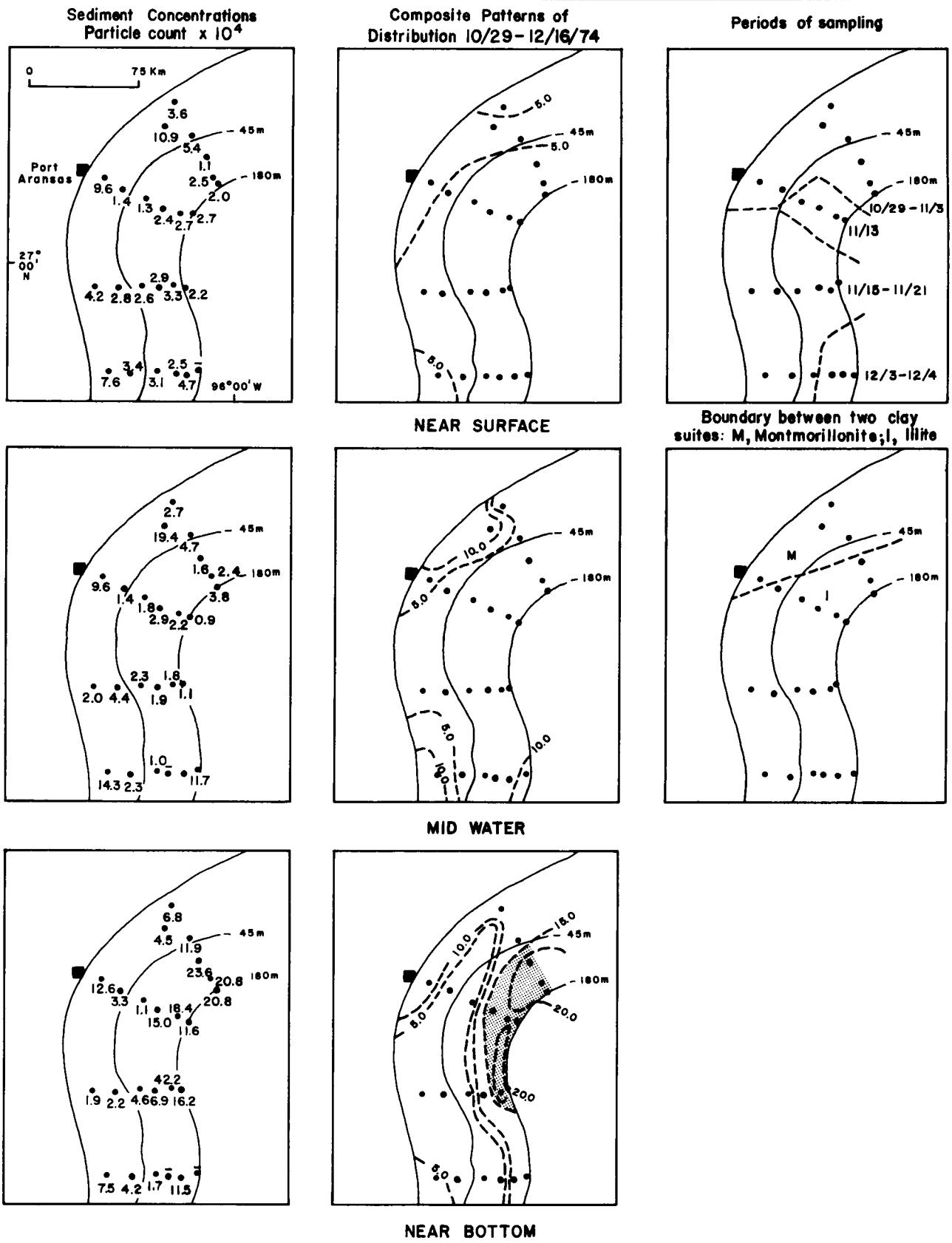

Figure 47. Distribution of suspended sediments by number of particles. Dot indicates location of sample station. Broken lines are inferred isopleths. Shading indicates relatively higher concentrations.

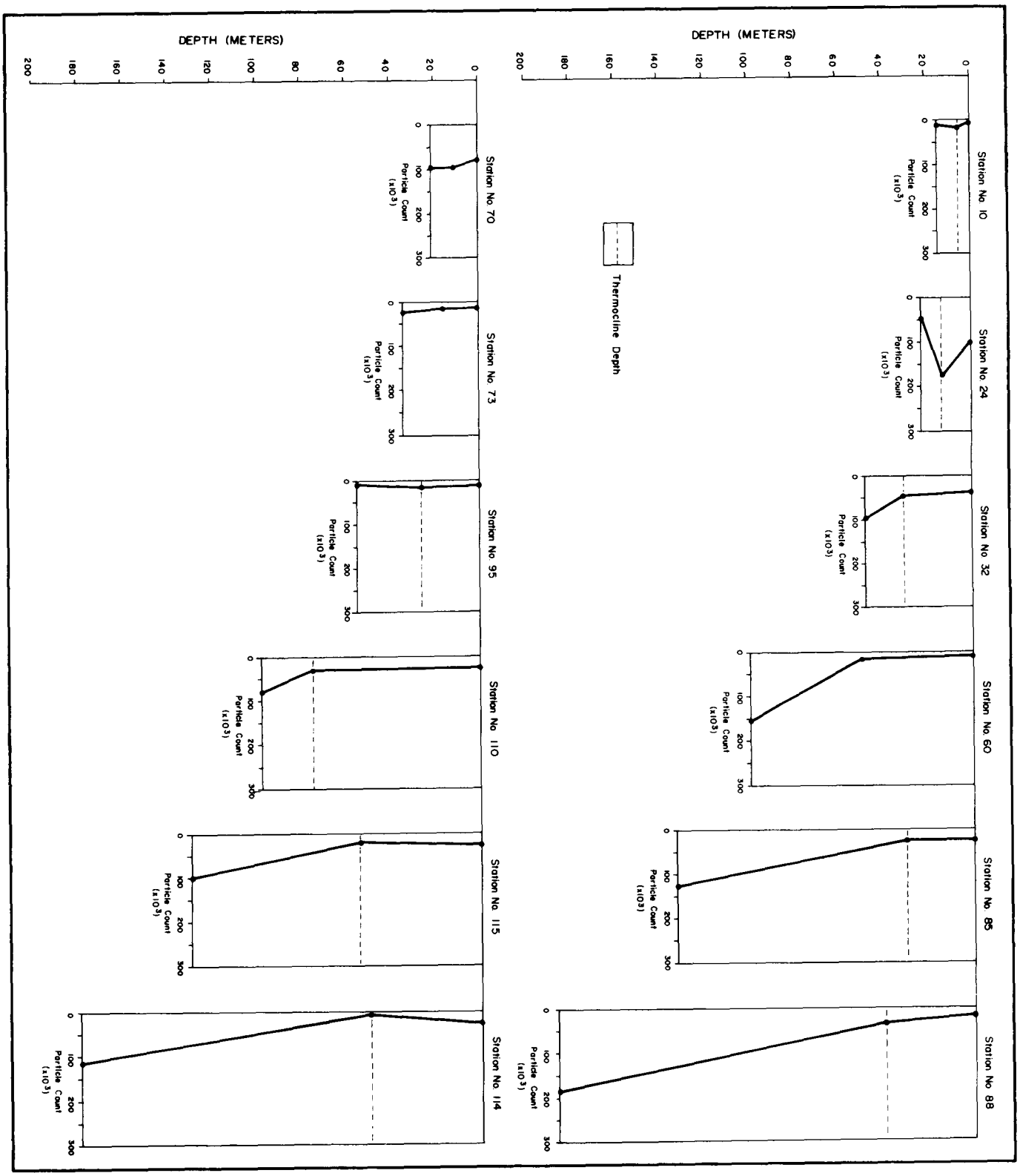

Figure 48. Variations in amount of suspended sediment by depth, 0.63 μm size fraction: stations 10-115. See figure 9 for location of stations.

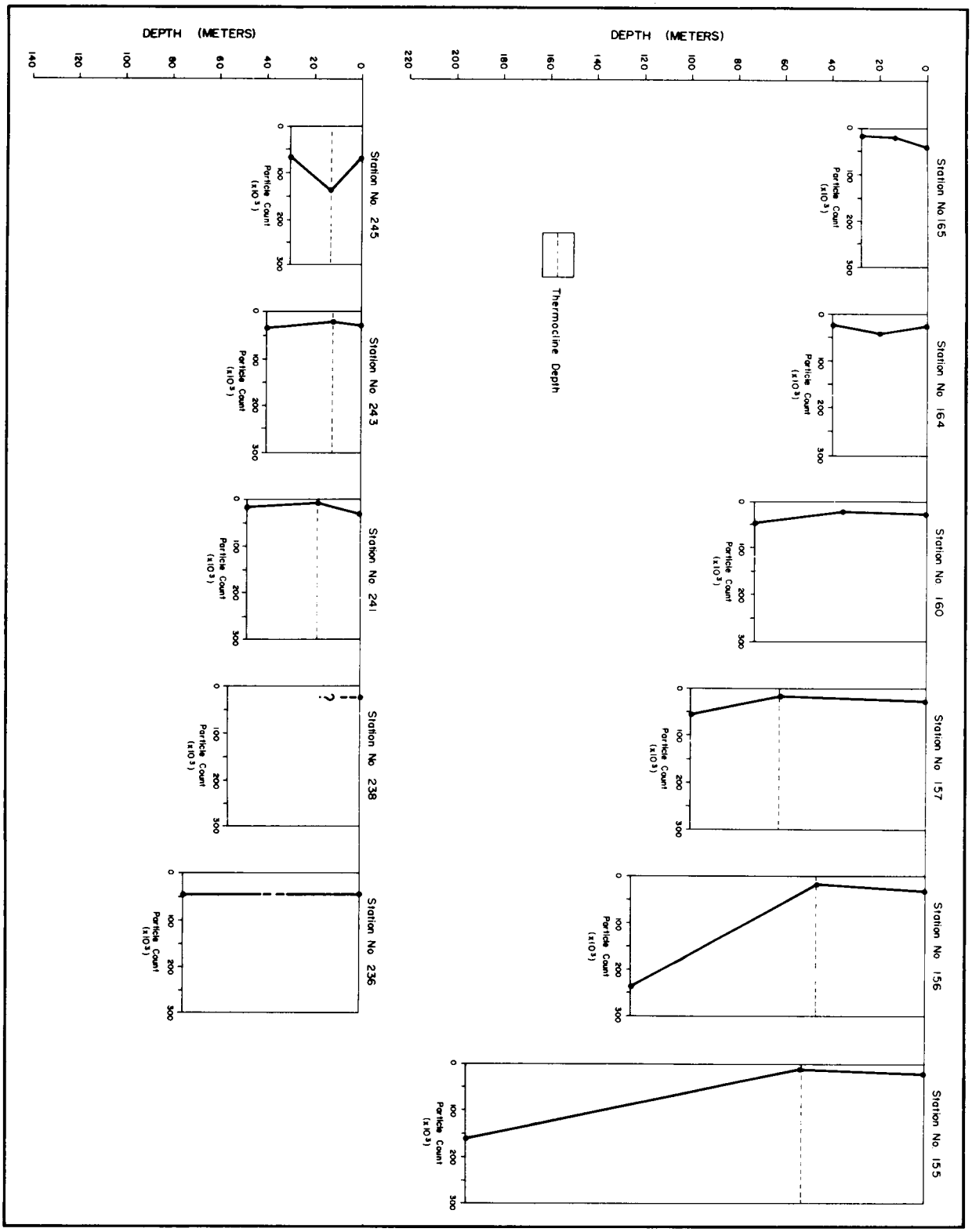

Figure 49. Variations in amount of suspended sediment by depth, 0.63 μm size fraction: stations 155-245. See figure 9 for location of stations.

varied considerably during the sampling period. Gradient reversals occurred at the majority of stations and the reversals were most frequently associated with the depth of the thermocline. The majority of stations showed a net increase in sediment concentration with depth (see map for near bottom samples, fig. 47); however, a net decrease was not uncommon at some of the shallower stations. Although the sampling was not time synoptic, the composite pattern of distribution for the inner shelf at all three depths is remarkably similar. Equally intriguing is the area of high suspended sediment concentration in the bottom waters of the outer shelf. Samples from the outer stations were collected over shorter time spreads and consequently are quasi-synoptic. The composite patterns suggest two "systems" of suspended sediments during the 1974 sampling period: one on the inner shelf at surface and mid-water depths, and another in bottom water of the outer shelf.

Grain Size

The suspended sediments have a wide range in grain size, and in most samples, the size of grains has a complex polymodal distribution. The individual modes reflect a mixture of organic particulate subpopulations (nannoplankton, microplankton) and the inorganic particulates, clay and silt. The only individual size aspect evaluated during the study is the mean diameter (first moments) variability at each sample station. This particular aspect was selected because it provides a good general characterization of the overall particulate system. The mean grain-size variability as a function of depth is shown by the series of graphs in figures 50 and 51. The profiles for stations 10 to 115 are on figure 50 and those for

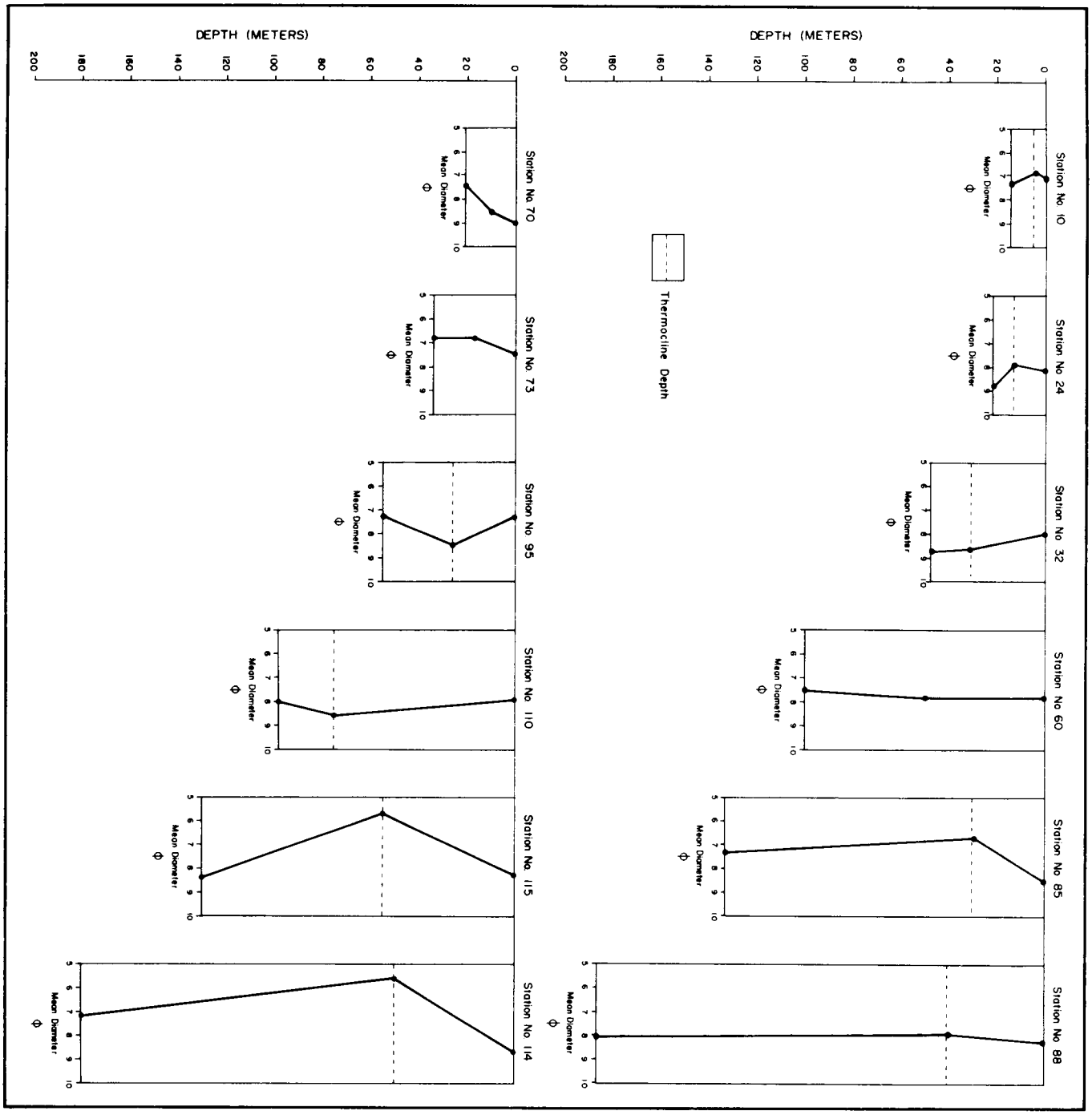

Figure 50. Variations in mean grain size of suspended sediment by depth: stations 10-115. See figure 9 for location of stations.

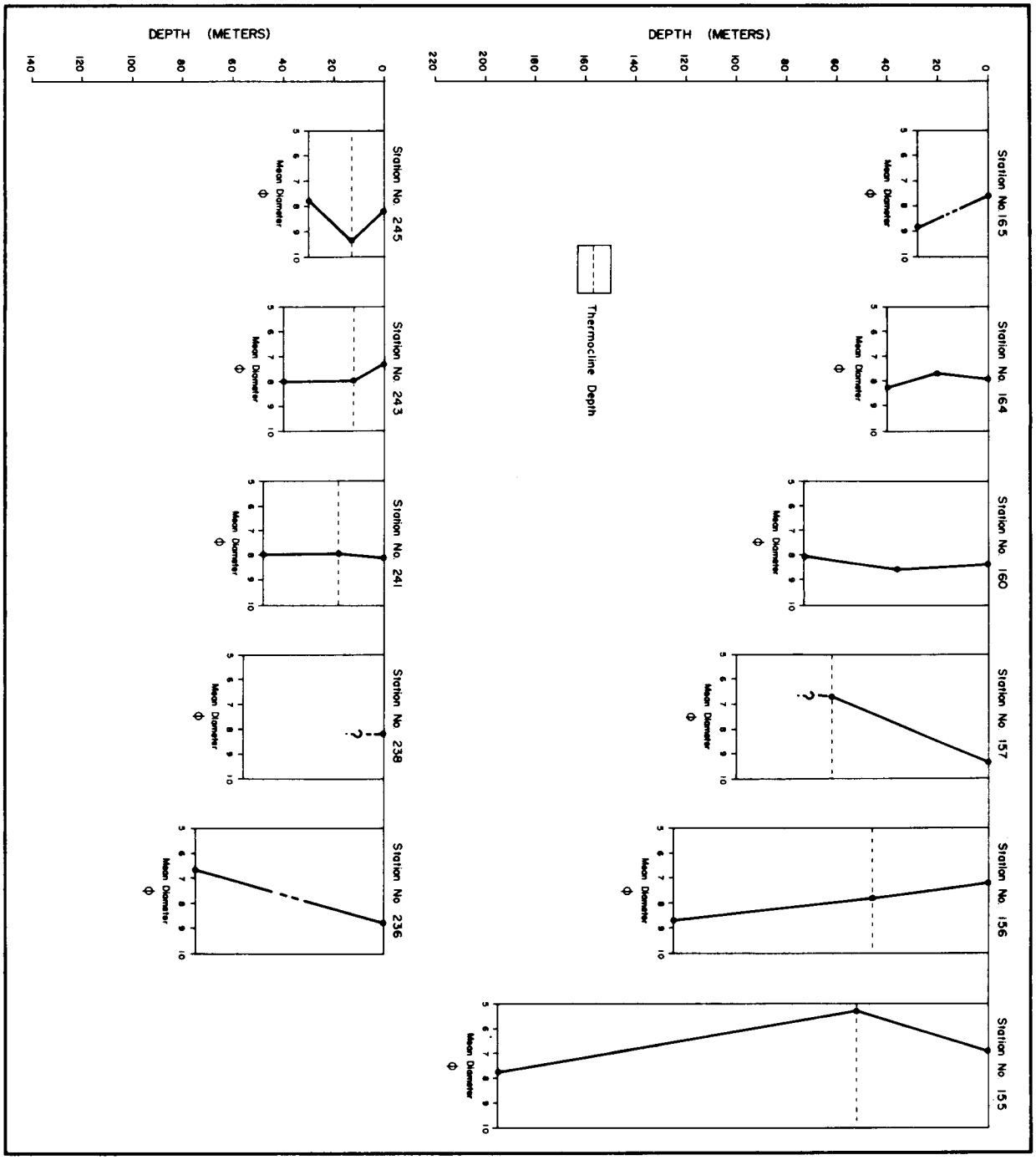

Figure 51. Variations in mean grain size of suspended sediment by depth: stations 155-245. See figure 9 for location of stations.

stations 155 to 245 are on figure 51. The grain-size data are summarized by the composite patterns on the maps in figure 52.

The overall range of mean grain size for all stations was from a minimum of 9.37 Ø (clay) at station 245 to a maximum of 5.3 Ø (medium silt) at station 155 (larger Ø values indicate smaller grain sizes). The majority of analyses indicate mean diameters larger than 3.9 μm (8.0 Ø) or within the classification range of silt. The coarsest material was in the water over the outer shelf. The composite patterns for mean grain size, as did those for the concentrations of sediment, suggest two "modes" of distribution: one for the inner shelf where grain size was generally small, and one for the outer shelf where the material was coarser. The coarser material on the outer shelf reflects the greater abundance of microzooplankton there.

Mineralogy

The X-ray analysis showed that the detrital suspended material was made up primarily of clay minerals with only trace amounts of quartz and other material. The mineralogical data, though not time synoptic, do define two distinct water masses in terms of clay-mineral content: a montmorillonite-rich water mass over the northwesternmost part of the OCS; and an illitic-rich water mass over the remainder of the shelf. The distribution of the two water masses is shown by figure 47.

The areal distribution of the two water masses followed roughly the same pattern of distribution as the chlorinity, indicating that the montmorillonite probably is characteristic of the less saline inflowing river water. The low content of montmorillonitic material in the bottom water over most of the area during the sampling period suggests that the

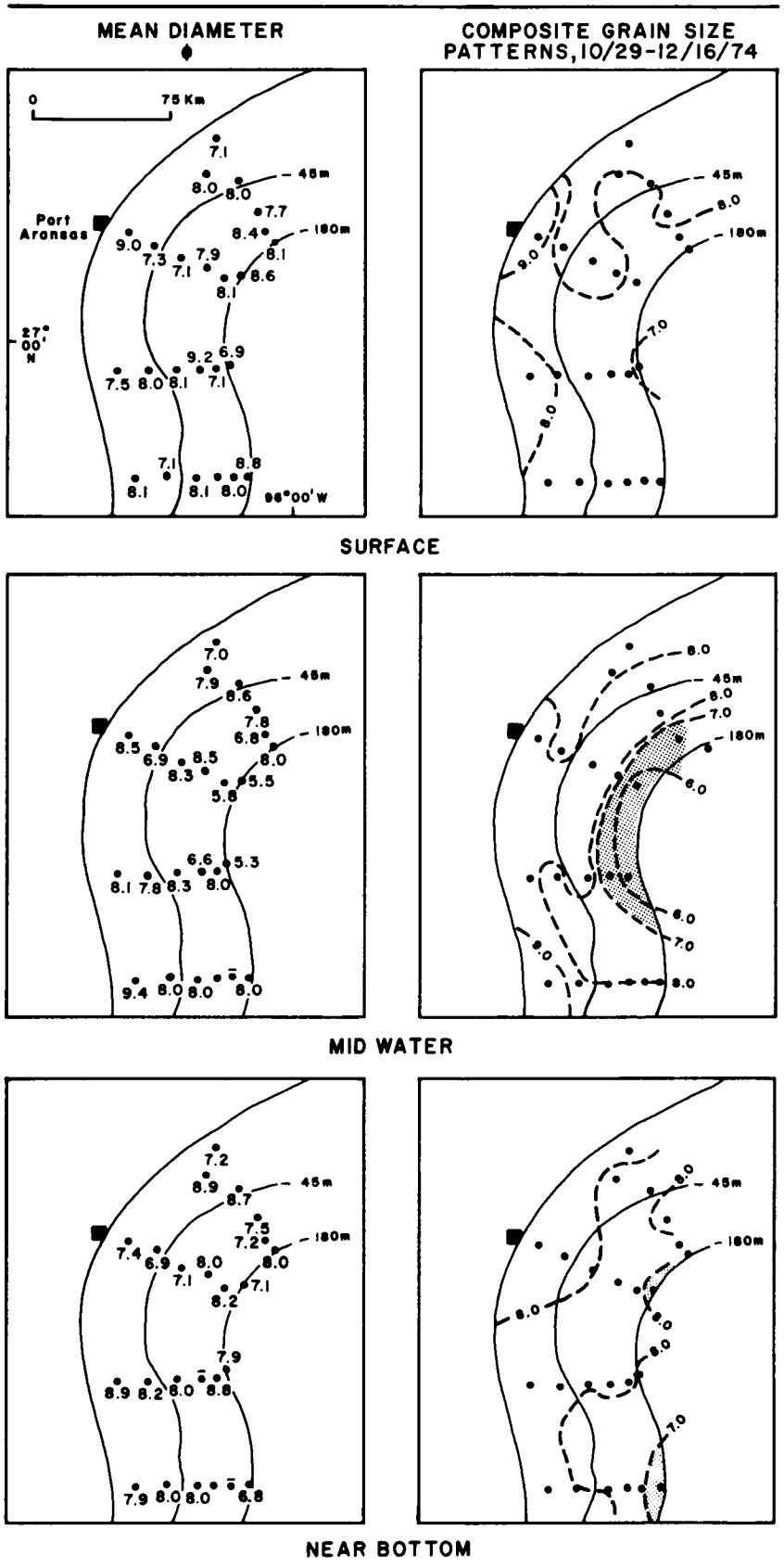

Figure 52. Mean diameters of grains for suspended sediments and composite regional patterns of distribution by grain size. Dot indicates location of sample station. Broken lines are isopleths inferred from the analyses. Shading indicates areas having mean diameters coarser than fine silt. The 8.0 Ø (3.9 μm) isopleth is the boundary between clay (>8.0 Ø) and silt (<8.0 Ø). (Larger Ø values indicate smaller grain sizes.) See figure 47 for periods of sampling.

clay minerals in suspension were not being derived from the surficial bottom sediment, which are high in montmorillonitic clay.

Trace Metals

The non-synoptic nature of the suspended sediment data preclude any definitive conclusions regarding the trace metals content, except at specific stations and for a single transect. The composite patterns of distribution for the trace metals covering the entire sampling period are shown by figures 53, 54 and 55.

Keeping in mind the lack of a time synopsis in the data, except for increments of the area as indicated, several general characteristics of the trace metals in the suspended sediments are shown by the maps. The trace metals can be divided into two groups on the basis of regional distribution. Those in group one include cadmium, chromium, copper, nickel and lead, all of which have a similar pattern: a range in content in the surface and mid-water samples, and a possible bimodal character and minimal values in the bottom water. Group two includes manganese and vanadium, both of which have a unique pattern: maximum content in bottom water and minimum content at mid-water and surface. The patterns for iron and zinc are not so distinct because of the contamination problems encountered with the two elements during analysis. Nevertheless, iron does show some similarity to manganese and vanadium, and zinc appears to belong in group one.

In essence, the amounts of trace metals in the bottom samples differ distinctly from the amounts in most of the samples from surface and mid-water depths, suggesting at least two sources for the trace metals in the suspended sediments. Other studies have shown that patterns of occurrence

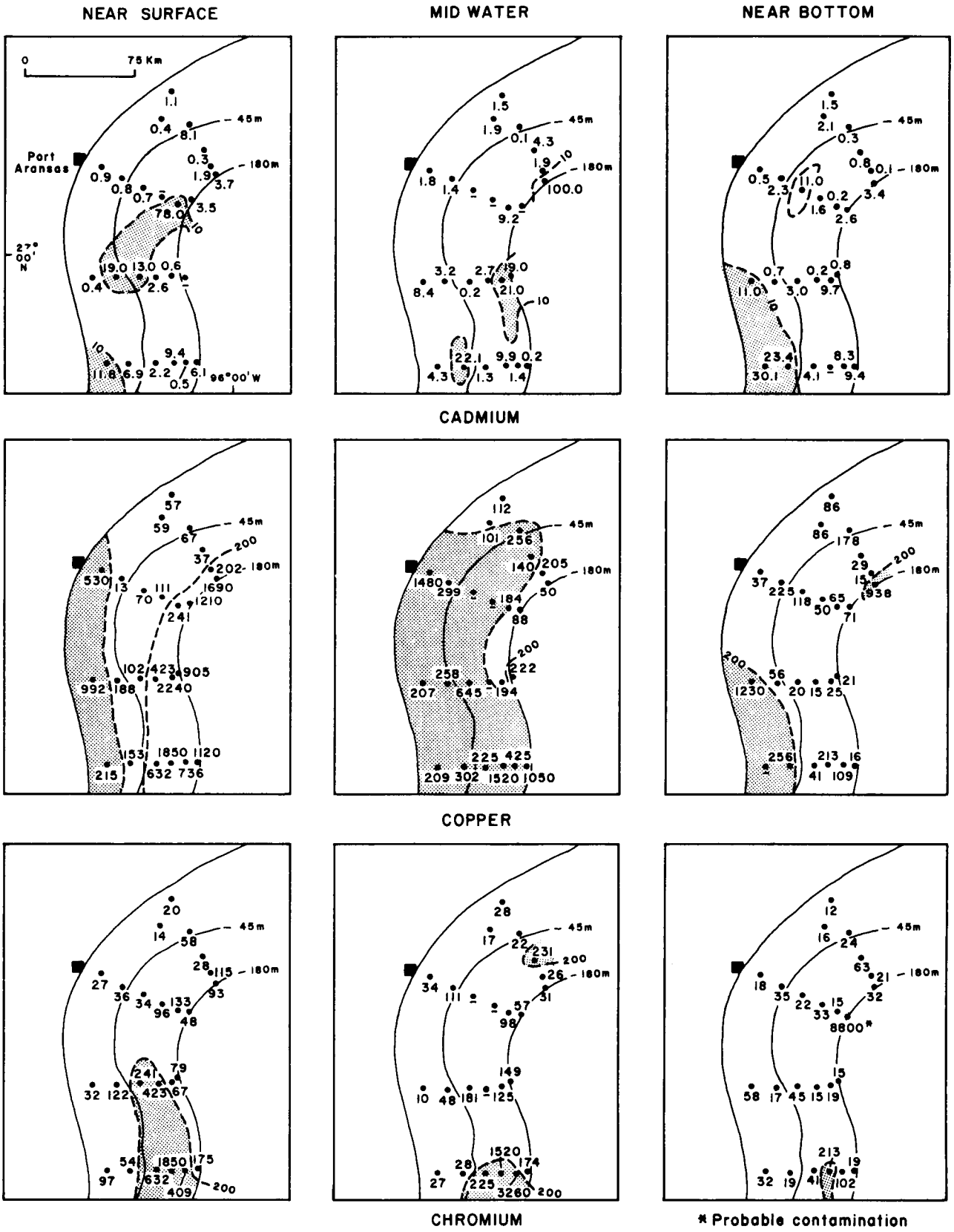

Figure 53. Distribution of trace metals in suspended sediments: Cd, Cu and Cr (in ppm unless otherwise indicated). The patterns are composites for October 29-December 16, 1974. Dot indicates location of sample station. Shading indicates amount above regional average. See figure 47 for periods of sampling along specific transects.

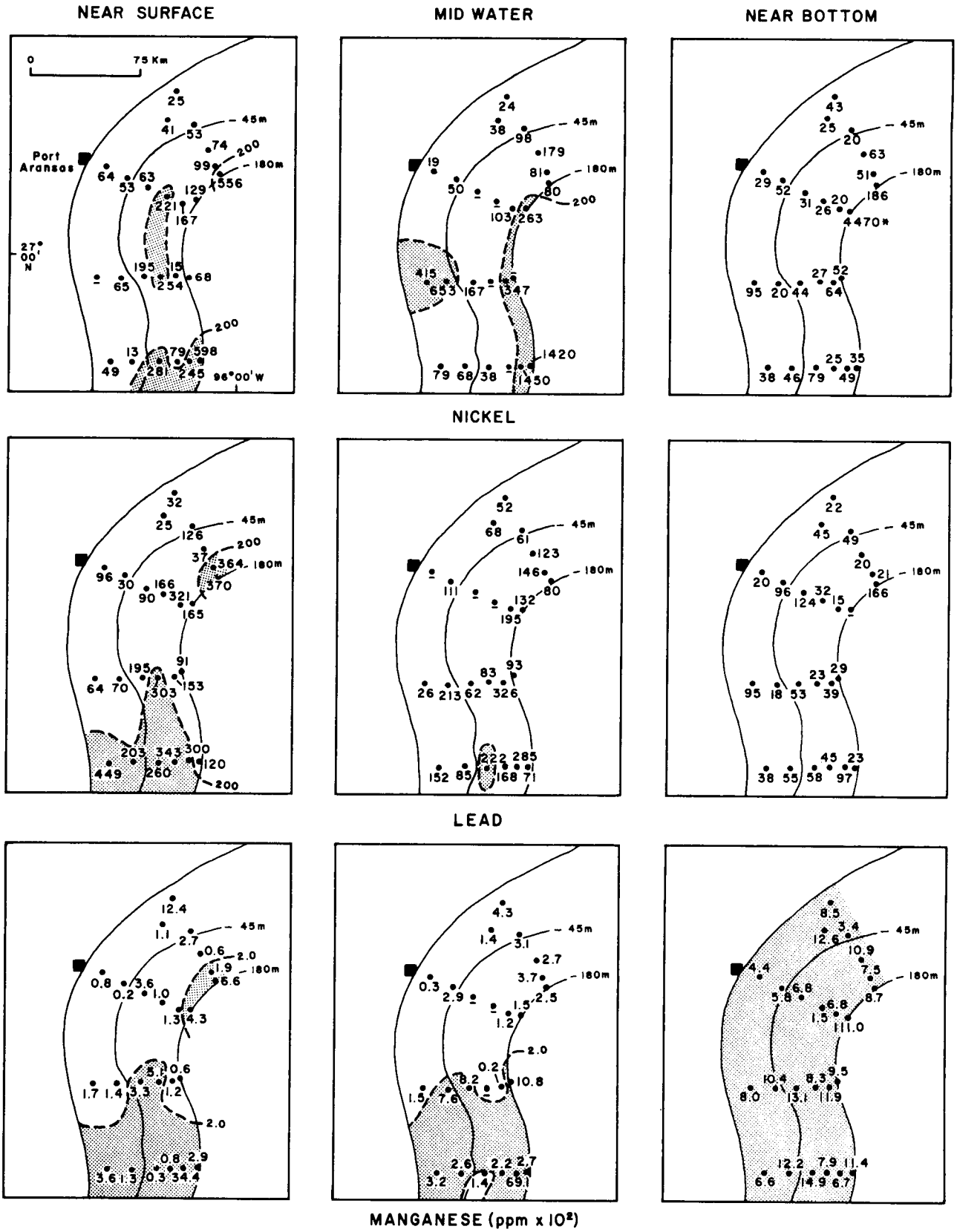

Figure 54. Distribution of trace metals in suspended sediments: Ni, Pb and Mn (in ppm unless otherwise indicated). The patterns are composites for October 29-December 16, 1974. Dot indicates location of sample station. Shading indicates amount above regional average. See figure 47 for periods of sampling along specific transects.

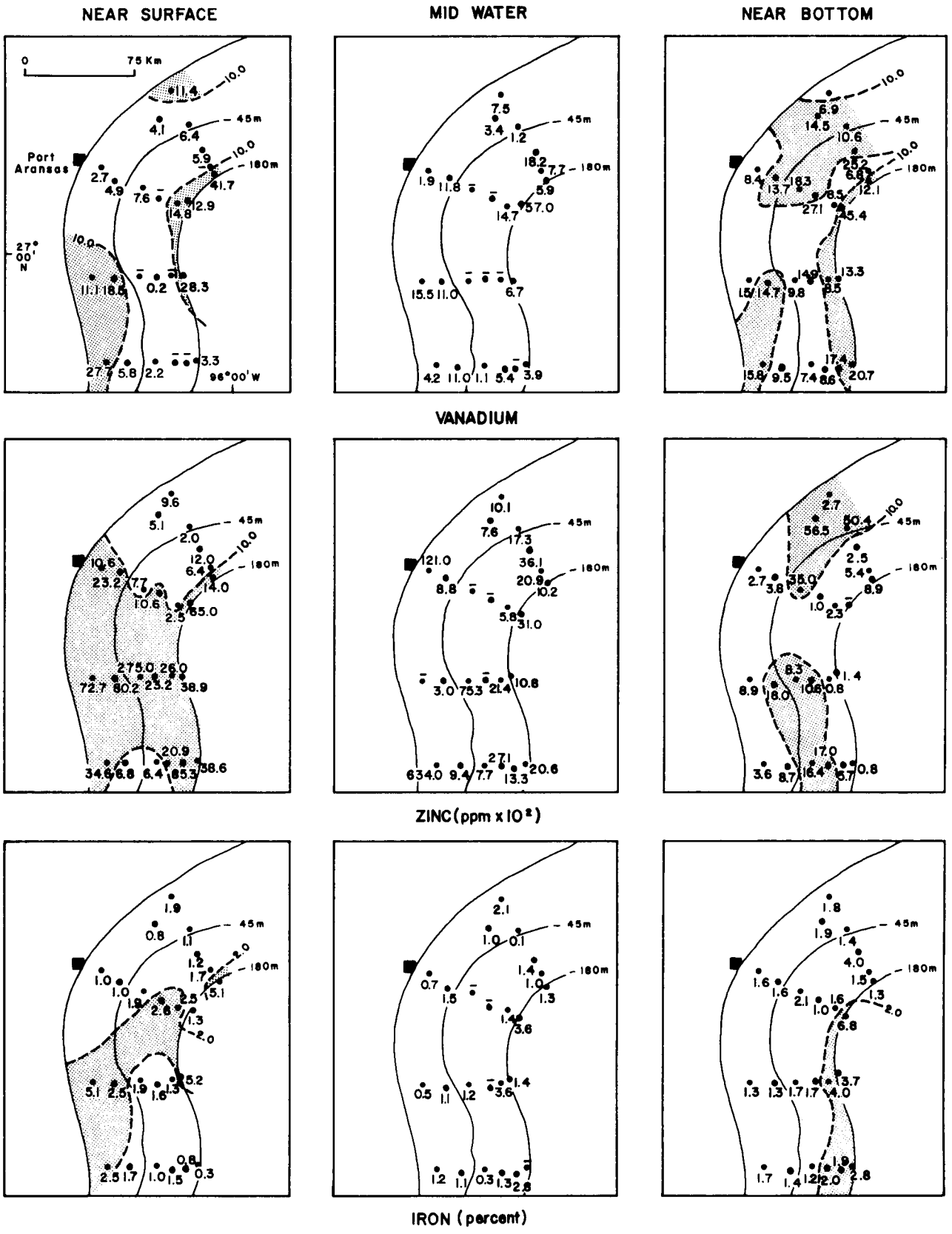

Figure 55. Distribution of trace metals in suspended sediments: V, Zn and Fe (in ppm unless otherwise indicated). The patterns are composites for October 29-December 16, 1974. Dot indicates location of sample station. Shading indicates amount above regional average. See figure 47 for periods of sampling along specific transects.

for trace metals in suspended matter may be related to the nature of the material: organic or inorganic. The metals Cr, Cu, Cd, Ni, Pb and Zn seem to be more abundant in planktonic organisms than in terrigenous detritus, but Fe, Mn and V seem to occur in the same proportions in both types of material. If this relationship is applicable generally, it suggests that the bottom suspended sediments analyzed from the South Texas OCS are more inorganic in nature, and the near-surface and mid-water material more organic.

When compared to the total concentrations of suspended sediments, very little if any correlation existed between the abundance of trace metals and the amount of total suspended particulate material during the sampling period (fig. 47). A possible exception is indicated for the outer edge of the shelf, particularly the northwestern part: in the bottom water increased amounts of Cd, Cu, Ni, Pb, V, Zn, Fe and Mn fall within the zone of increased suspended sediment.

Interrelationships

Regardless of the 2 months span of time involved in the sampling for suspended sediments, the data support the general statement that amounts of material in suspension throughout the sampling period were relatively large over most of the OCS. The large amounts of suspended material measured may have been caused by the weather conditions. Passage of strong cold fronts (northers) through the area began relatively early in the fall of 1974 and recurred frequently during the sampling period. Turbidity of the water caused by winds accompanying strong northers and heavy rainfall and runoff induced by the fronts along the northern Gulf coast may possibly

have been responsible for the large concentrations of suspended sediment encountered.

The predominance of montmorillonitic clay in suspended sediments of the northwestern part of the OCS is significant. The clays normally encountered on the shelf off south Texas are pervasively illitic. Consequently, the presence of montmorillonite indicates a distinct mass of water that was encroaching southward. The persistence and spread of this water mass during the spring of 1975 is indicated by the hydrographic data collected from January through April. As noted earlier, the encroaching water mass was attributed to Mississippi River runoff.

The coarse grain size of the suspended material over the outer shelf is misleading at first glance (fig. 52). As noted earlier, the seemingly anomalous situation probably is caused by large numbers of microzooplankton in the suspended material.

PRIMARY PRODUCTIVITY

Included in the discussion of primary productivity are the nutrients, chlorophyll a, adenosine triphosphate (ATP), and phytoplankton abundance. Also included are the hydrographic data, temperature and salinity, plus samples of water for measuring dissolved oxygen, all gathered at the same time as the samples for the primary productivity studies.

Nutrients

During the sampling for low-molecular-weight hydrocarbons, subsamples for determination of phosphate, nitrate, and silicate were taken in separate 6 ounce WHIRL-PAK plastic bags and frozen. The water samples

were collected by standard NISKIN and NANSEN hydrographic casts. The amount of nutrients available in water of the continental shelf is directly related to levels of biological productivity and changes in the patterns of nutrient distribution through time can complement other data in indicating patterns of water mass movement. In fact, the distribution of nutrients is so closely related to hydrographic conditions that the data for temperature and salinity collected in 1975 are discussed in the section on nutrients. Amounts of each nutrient were determined at three levels in the water column: surface, mid-depth and near bottom, for each of three seasons: winter, spring, and summer.

Phosphate

The amount of phosphate in the water varied both geographically and seasonally during 1975. In general, the content decreased systematically from winter to summer. Surface to bottom variations within a season were less pronounced than geographic and seasonal changes. The distribution of phosphate for the 3 periods of sampling is shown by figure 56.

During the winter, when phosphate content was highest, amounts were larger in the shallow waters of the inner shelf adjacent to land than in the surface and mid-depth waters. At the near-bottom level during winter, larger amounts of phosphate were localized in three areas: two on the inner shelf, and another on the outer shelf (fig. 56). During the spring sampling, the phosphate content was lower regionally than during the winter and was more evenly distributed at surface and mid-depth levels; the highest content during the spring was in the bottom water at the same locale on the outer shelf and in approximately the same amount as during

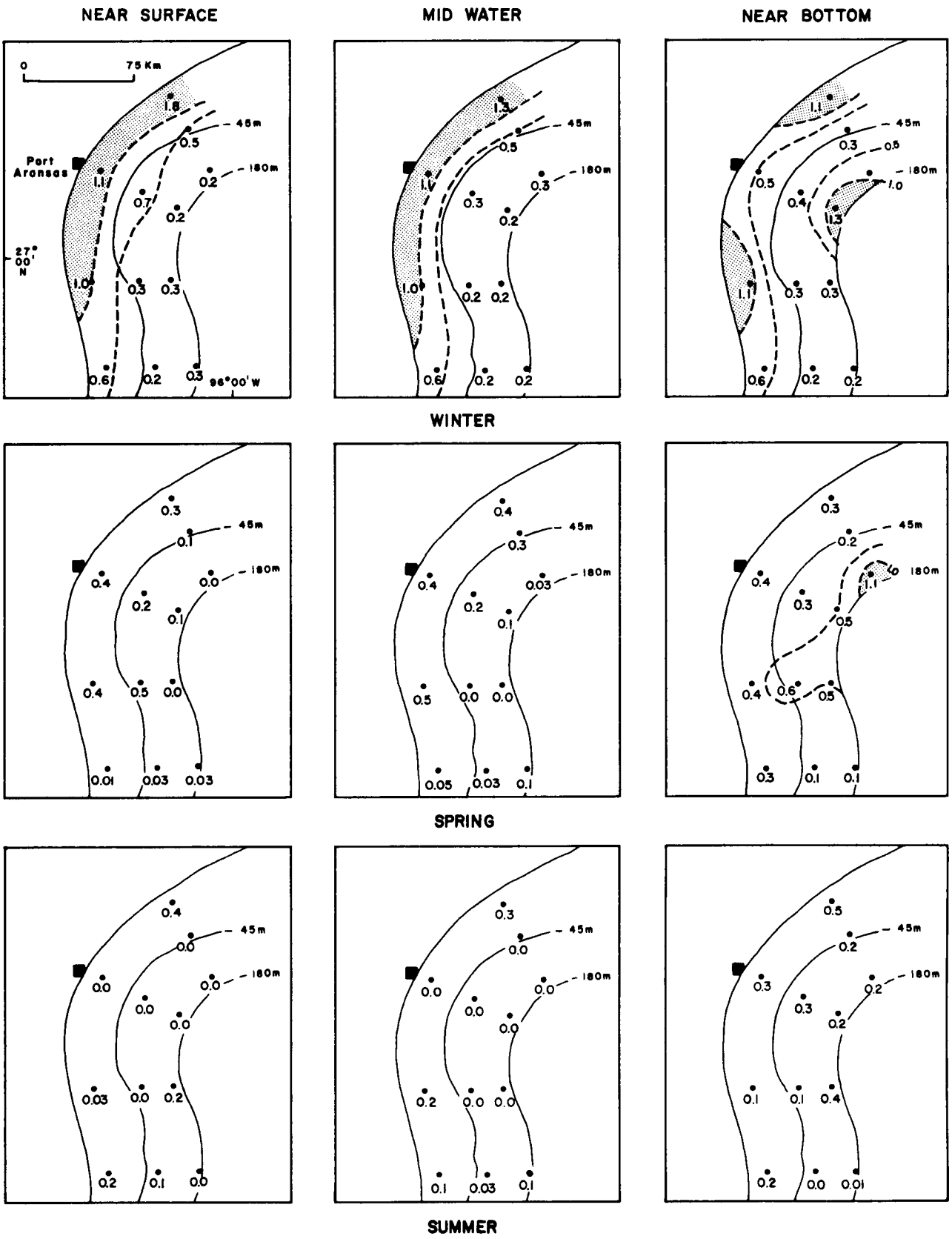

Figure 56. Seasonal distribution of phosphate in shelf water by depth (in µg-at/l). Dot indicates location of sample station. Broken lines are isopleths inferred from the analyses. Shading indicates amount above regional average.

the winter. In the summer, amounts had diminished still further. No phosphate was detected at some stations for surface and mid-depth levels, but amounts near the bottom were comparable to spring levels, although they were more uniformly distributed. The increased amount in bottom waters of one area on the outer shelf during the winter and spring had disappeared by the time of the summer sampling.

Nitrate

The nitrate content of water over the South Texas OCS is low, according to the samples collected during 1975. Amounts larger than 1.0 µg-at/l (micrograms per atom liter) were localized on the inner shelf adjacent to land and over the outer shelf in the northeast part of the South Texas OCS. The largest amounts during all three seasons were localized in the bottom water on the outer shelf while content was low, except for the spring, in bottom water of the inner shelf. At mid-depth and near-surface levels, amounts on the inner shelf generally were slightly more than shelf averages during all three seasons. The ranges in nitrate content in water of the South Texas OCS, illustrated to show variations by season and by depth, are recorded in figure 57.

The patterns of distribution for nitrate were similar to those for phosphate, except that nitrate content consistently was more than regional averages in bottom water over the outer shelf. At all water levels of the outer shelf, nitrate tended to be more evenly distributed than phosphate.

Silicate

During each of the three sampling periods, the amounts of silicate decreased seaward, as a regional pattern. The silicate content decreased

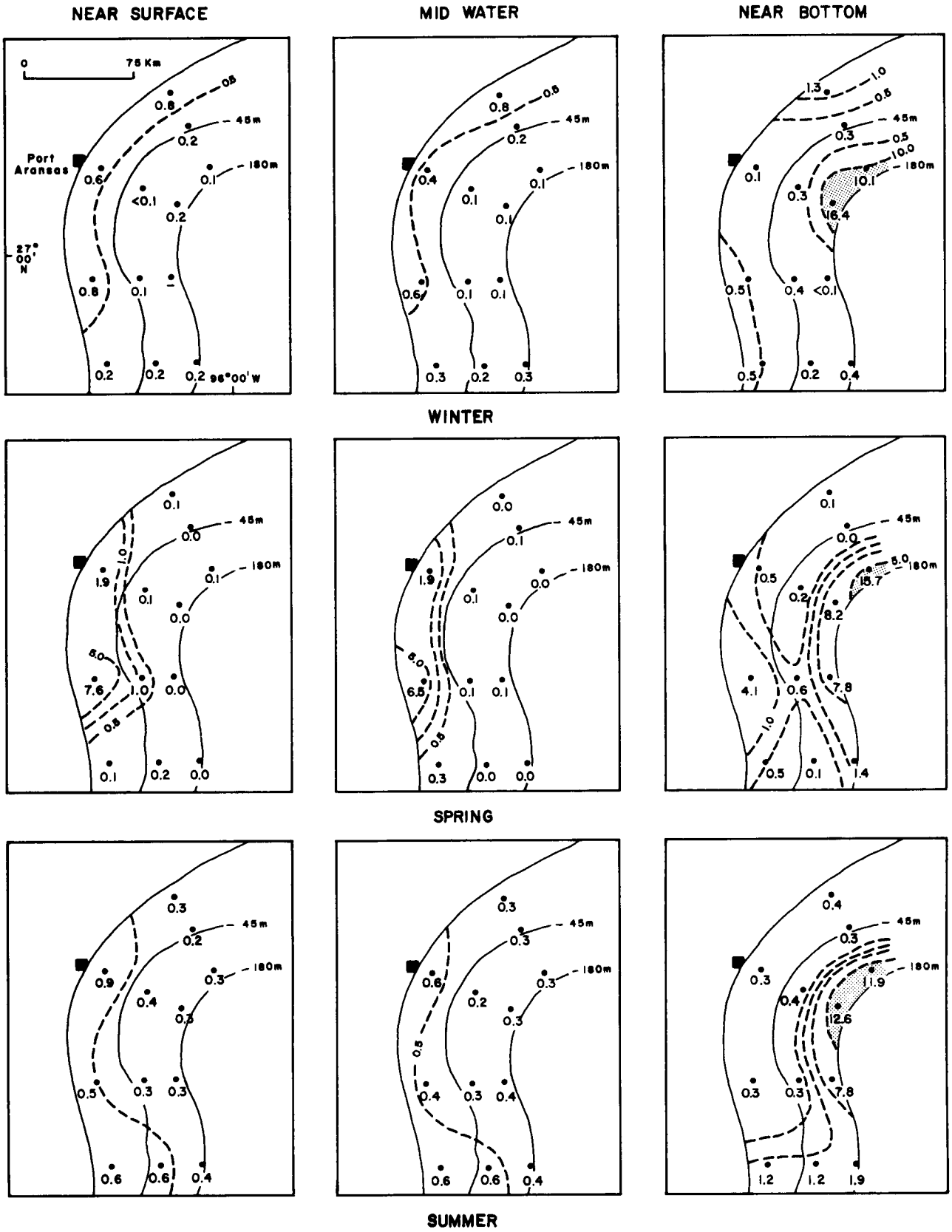

Figure 57. Seasonal distribution of nitrate in shelf water by depth (in µg-at/l). Dot indicates location of sample station. Broken lines are isopleths inferred from the analyses. Shading indicates amount above regional average.

uniformly in the near-surface water, but less uniformly at mid-depth. The content increased from mid to outer shelf in the bottom water. The distribution of silicate for 3 seasons and at 3 depths is shown by figure 58.

The largest amounts of silicate were at the northwesternmost station during the summer sampling period, where the content was significantly more than the regional average at all three water levels sampled. In fact, the analyses indicated almost identical amounts of silicate at all three levels. The patterns of distribution for silicate were similar to those for phosphate and nitrate except that the amount of silicate in the bottom water of the outer shelf was not as much above the regional average as was the amount of nitrate.

Chlorophyll a

The amount of the pigment chlorophyll a was calculated from the absorbance curves as recorded by a CARY-118C spectrophotometer operating in a scan range of 400 to 720 nm (nanometer).

The distribution of chlorophyll a by season and by water depth is shown by figures 59, 59a and 59b: near surface depth by 59; depth of approximately one half the photic zone by 59a; and below the photic zone by 59b. Two amounts were calculated for each absorbance curve: one using the equation of Parsons and Strickland and a second using the equation of Lorenzen. The amounts determined by the Parsons/Strickland equation consistently were slightly more than amounts determined by the Lorenzen formula. The amounts plotted on figures 59, 59a and 59b are averages of the two. By season the chlorophyll a content of the water was significantly more during the spring than during the winter and summer; amounts in winter and summer were comparable

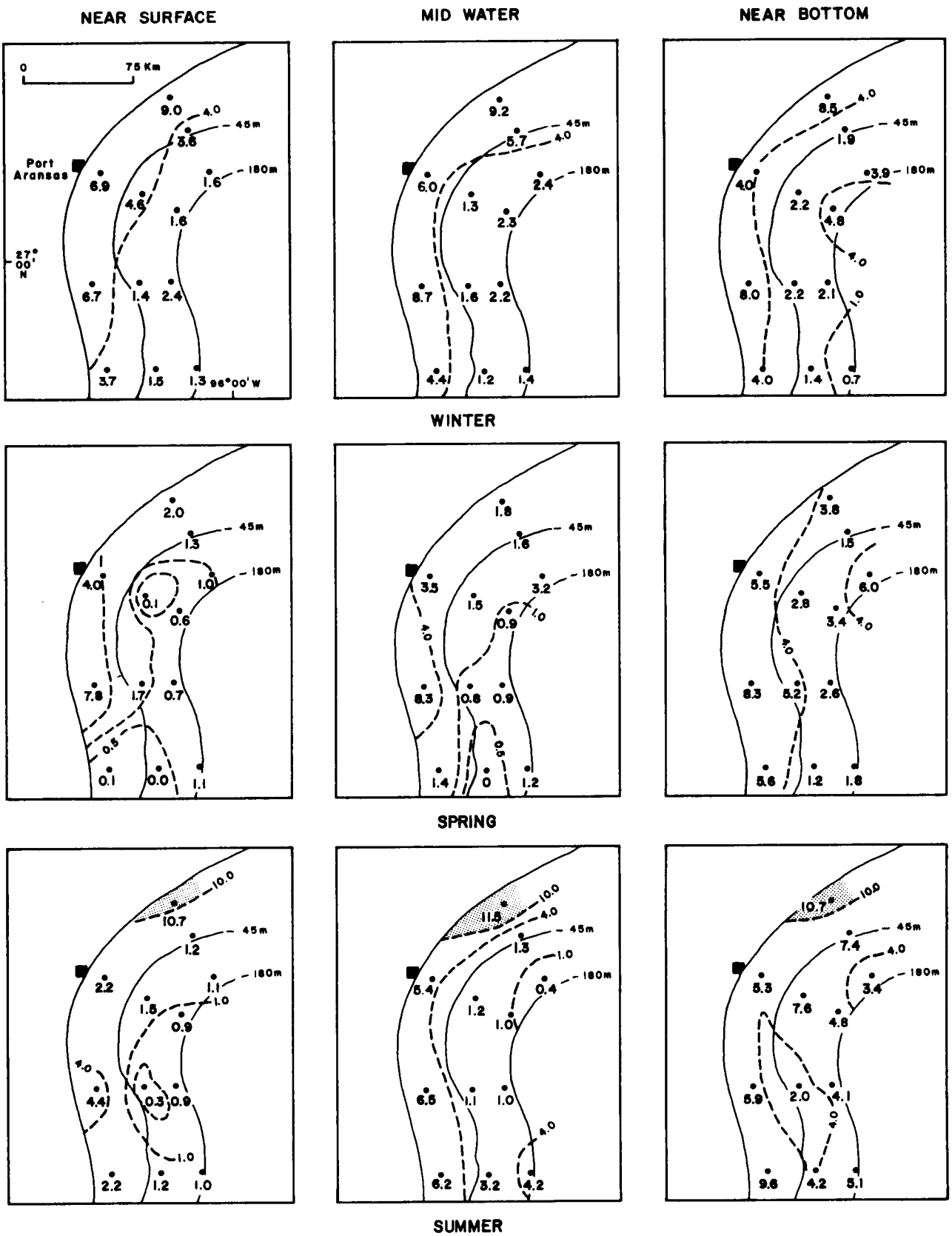

Figure 58. Seasonal distribution of silicate in shelf water by depth (in µg-at/l). Dot indicates location of sample station. Broken lines are isopleths inferred from the analyses. Shading indicates amount above regional average.

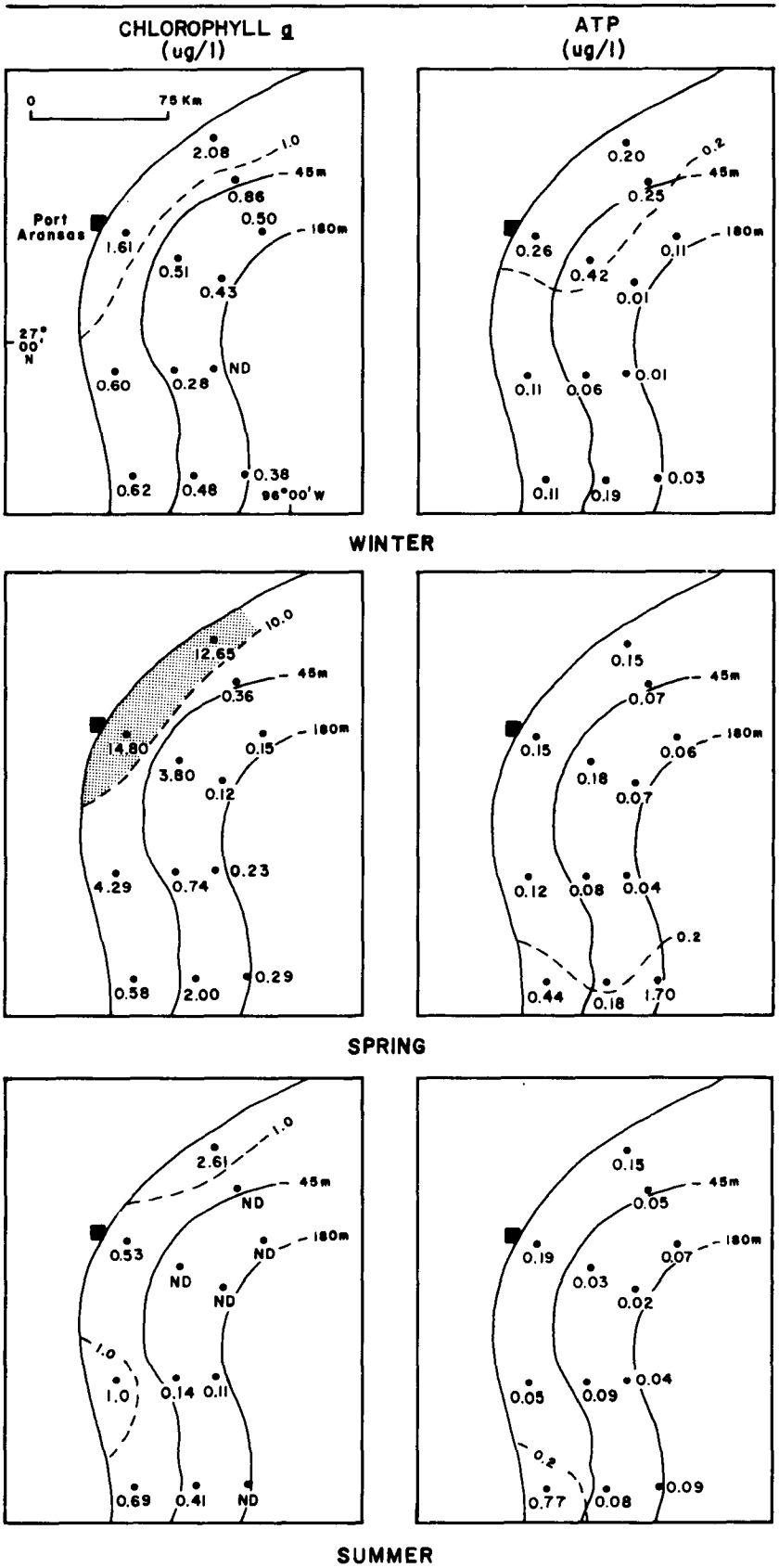

Figure 59. Seasonal distribution of chlorophyll a and adenosine triphosphate (ATP) in near-surface water at average depths of 1-4 m. Dot indicates location of sample station. Number is average of day/night sampling at the station. ND indicates amount was below limit of detection. Broken lines are isopleths inferred from the analyses. Shading indicates amount above regional average.

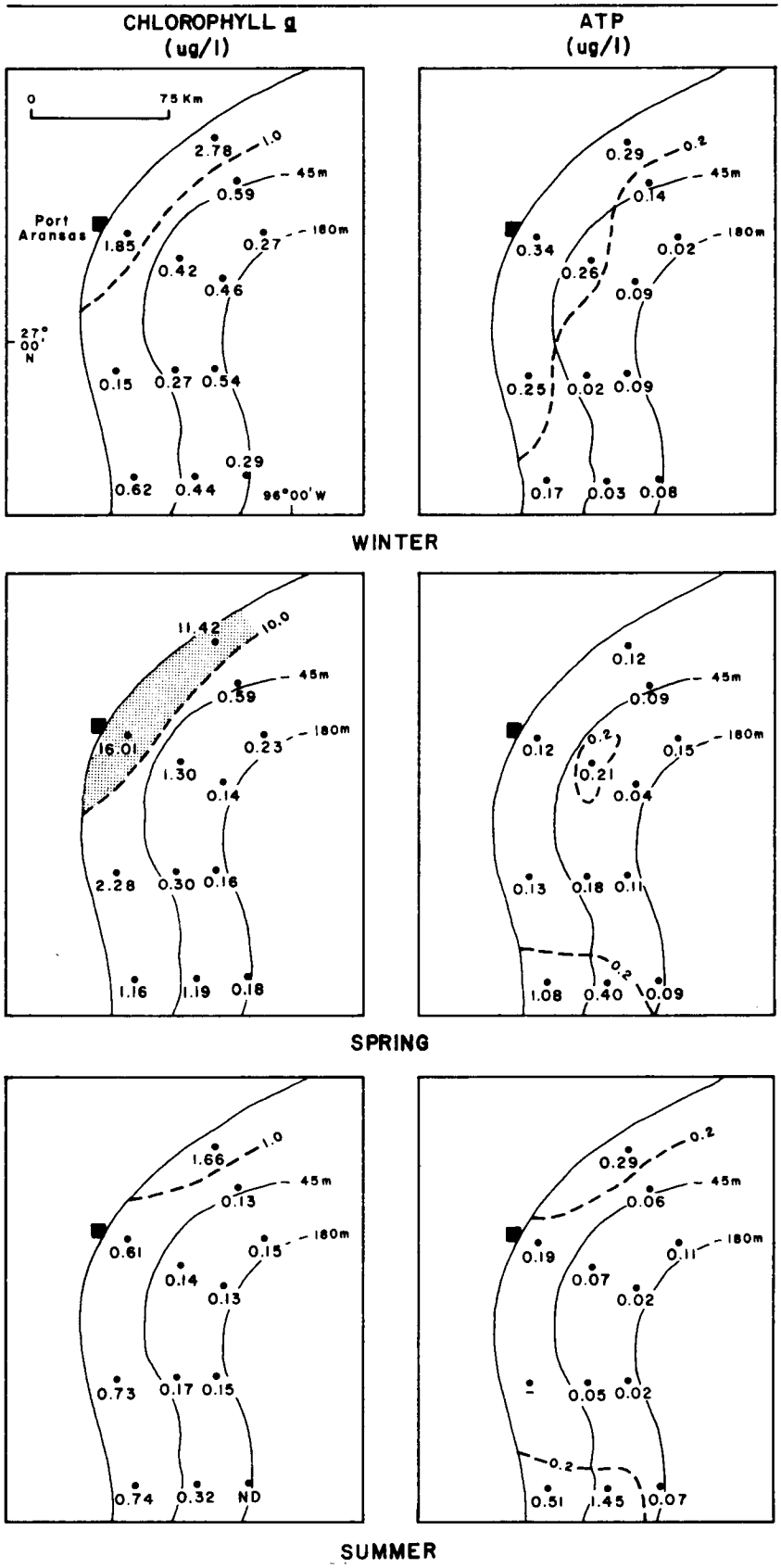

Figure 59a. Seasonal distribution of chlorophyll a and adenosine triphosphate (ATP) at water depths of approximately one half the photic zone (~10 m at inner shelf stations; ~25 m at mid and outer shelf stations). Dot indicates location of sample station. Number is average of day/night sampling at the station. ND indicates amount was below limit of detection. Dash indicates no analyses. Broken lines are isopleths inferred from the analyses. Shading indicates amount above regional average.

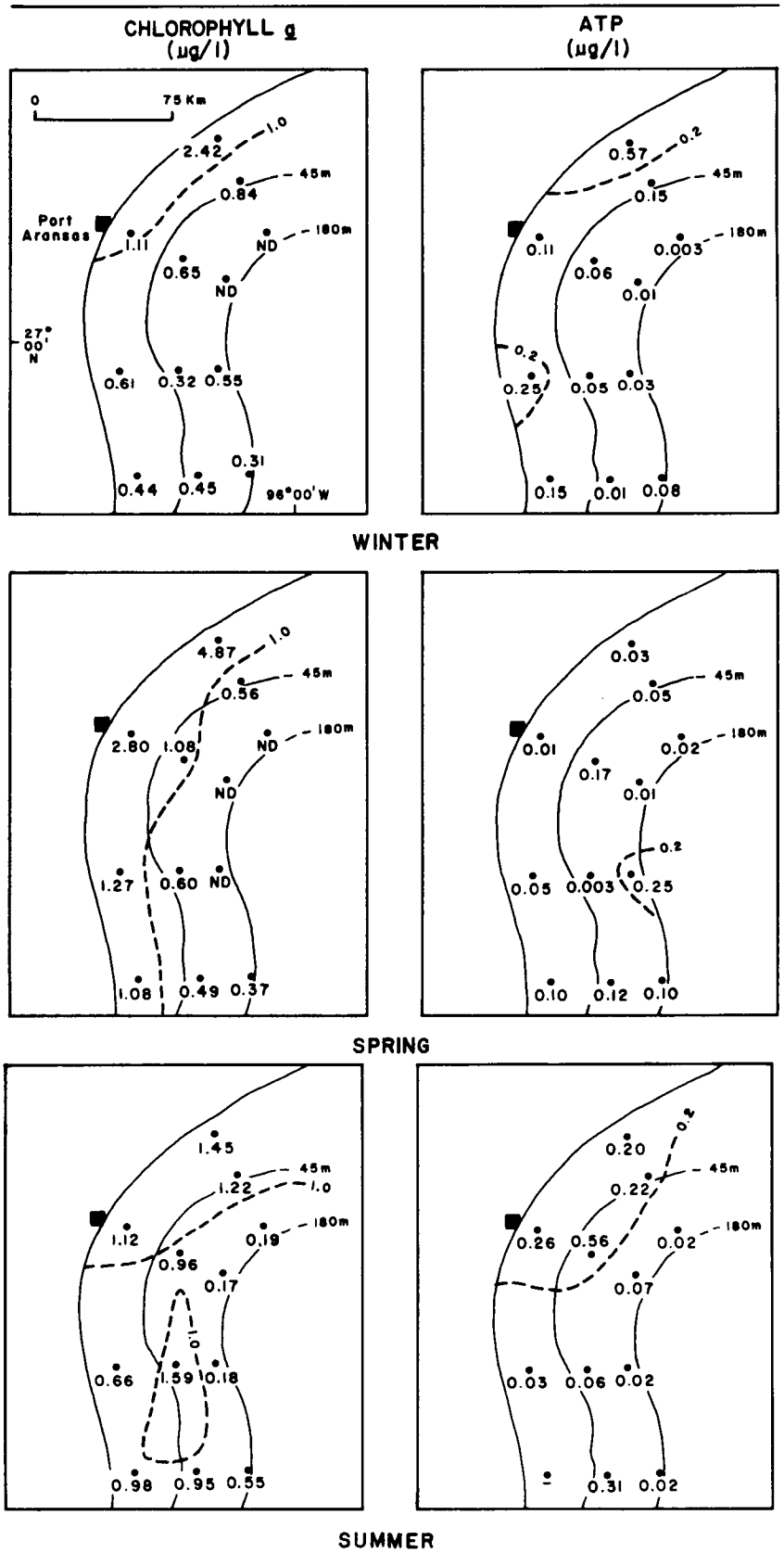

Figure 59b. Seasonal distribution of chlorophyll a and adenosine triphosphate (ATP) at water depths of approximately one half the photic zone (~10 m at inner shelf stations; ~25 m at mid and outer shelf stations). Dot indicates location of sample stations. Number is average of day/night sampling at the station. ND indicates amount was below limit of detection. Dash indicates no analysis. Broken lines are isopleths inferred from the analyses. Shading indicates amount above regional average.

and in all seasons amounts decreased sharply seaward. Geographically the chlorophyll a content at all four inner shelf stations generally was nearly double the amounts at the stations farther out with only one or two exceptions; content at the two northern inner shelf stations generally was more than at the two southern ones. The amount of chlorophyll a at the two inner shelf stations off Port Aransas and Pass Cavallo during the spring was 5 to 20 times more than elsewhere. By water depth, amounts in general were larger near the surface and at a depth of approximately one half the photic zone. However, amounts were more evenly distributed vertically at the nearshore stations. Below the photic zone, the amount of chlorophyll a was more evenly distributed geographically. This was most pronounced during the summer.

Adenosine Triphosphate (ATP)

ATP serves as the principal means of transfer of chemical energy in cells and is used here as an indicator of the biomass of micro-plants and micro-animals in the water column.

The amounts of ATP were calculated using the integrated area of the first 15-30 seconds of the recorded absorbance curves. This area was compared to one and occasionally two standards for every three samples run. The distribution of ATP is shown on figures 59, 59a and 59b. The ATP content was largest in the extreme southern part of the South Texas OCS during both spring and summer and at all three water depths sampled. The patterns of distribution for ATP were similar to those for chlorophyll a during the winter only.

Phytoplankton

Sample material for phytoplankton counts was prepared from the initial water sample as follows: an initial 20 l of water was passed through a 20 μm NITEX net. The net contents (net plankton) were washed off with 250 ml seawater into a 500 ml bottle to which 8 ml of buffered formalin was added. After a settling period of 3 to 7 days, the supernatant was decanted to 12 ml. An aliquot was counted under phase contrast at 200x in a SEDGEWICK-RAFTER counter, and species and numbers were recorded. Two liters of the filtrate (nannoplankton) from the 20 l originally passed through the 20 μm mesh net were passed through a 0.4 μm NUCLEPORE filter, which was washed with 10 ml of sea water and preserved in 0.25 ml of buffered formalin. Samples were mounted and the slides were examined under oil immersion at 1000x. Examination of slides was generally limited to scanning. However, qualitative recordings were made of those samples having a high incidence of identifiable microalgae.

The total phytoplankton counts for the three seasons are shown by the series of maps in figure 60. The larger numbers for the inner shelf stations on the two northern transects during the spring are the most conspicuous features of the phytoplankton; notably, the abundance decreases markedly both seaward and southward from the two stations. The abundance of phytoplankton during the spring also was greater in the extreme southern part of the South Texas OCS than in the adjacent central sector. The pattern of regional distribution for the summer followed that for the spring, but the numbers were much less in the summer. As a summary statement regarding patterns of regional distribution, the 1975 study indicated a primary area of high phytoplankton proliferation in the northwestern part of the OCS

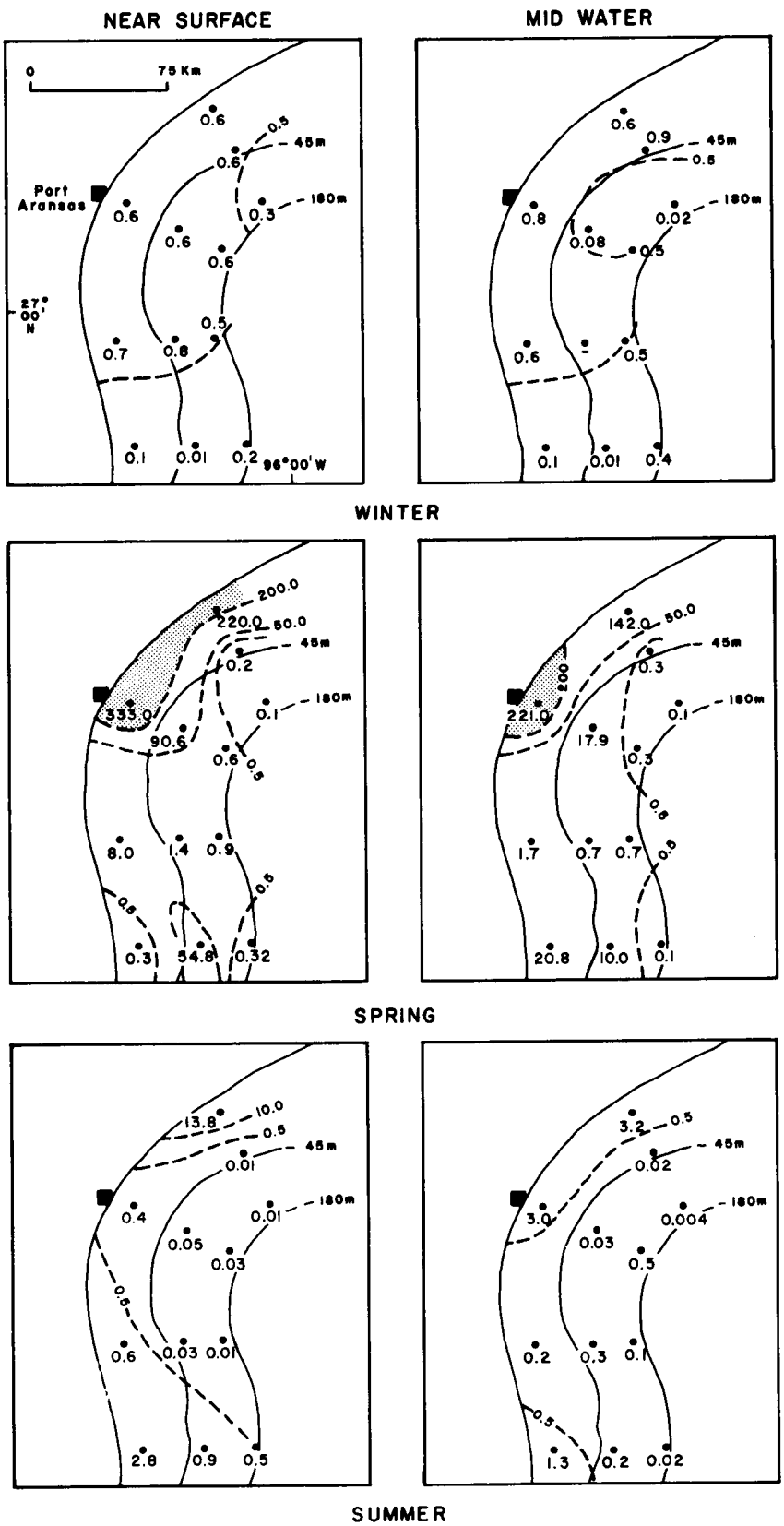

Figure 60. Seasonal distribution of phytoplankton by water depth. Mid water is ~ one half the photic zone. Dot indicates location of sample station. Number is number of cells x 10^4. Dash indicates no sample. Broken lines are isopleths inferred from the station counts. Shading indicates amount above regional average.

region and a secondary area in the southernmost part. In both areas, the abundance of phytoplankton during the spring was substantially larger than elsewhere.

The average abundance of phytoplankton along the 4 transects for all 3 seasons of sampling was 4.1×10^5 cells per liter at the inshore stations, 7.8×10^4 at the middle stations and 2.6×10^3 at the outer stations. The yearly averages were greatly affected by the very large numbers counted in the spring samples. The spring average for all stations and all depths was 4.7×10^5 cells per liter, for the summer 1.1×10^4 and for winter 4.9×10^3. The average for summer was somewhat weighted by the substantially larger counts at inner shelf stations; the summer average for more than half the stations (14) was less than 1,000 cells per liter. The winter counts were more consistent with little variation from inner to outer shelf.

The dominant species generally were the same common phytoplankters noted in other studies. Species common throughout the year were Thalassionema nitzschioides, Rhizosolenia alata, Bacteriastrum hyalinum, Chaetoceros curvisettus, C. decipiens, C. diversus, Nitzschia delicatissima and N. seriata. Forms dominant during the spring bloom but not significant during the winter and summer were Leptocylindrus minimus and Asterionella japonica. Skeletonema costatum, the most numerous organism during the spring (1.6×10^6 cells per liter at one station), also was common in the winter but was insignificant in the summer. Cerataulina bergoni followed much the same pattern. Rhizosolenia alata, Nitzschia delicatissima and several species of Chaetoceros were dominant in the summer. Thalassionema nitzschioides and Thalassiosira rotula were the most common phytoplankton in the winter but were not as dominant as other species in the spring and summer. Species

diversity was greatest in the winter. However, this observation might be attributed to the fact that smaller volumes of samples, because of greater numbers of cells per liter, were being counted in the spring samples.

For the net plankton, the diatoms greatly outnumbered any other group. If continuing studies bear out the results for the first year, Thalassionema nitzschioides, Rhizosolenia alata, Nitzschia delicatissima, Bacteriastrum hyalinum and Chaetoceros curvisettus might be considered as indicator species.

Within the nannoplankton, no microalgae could be identified with certainty. Nitzschia delicatissima, Pleurosigma spp. and Navicula spp. were the most common organisms, but they were not numerous and in all cases had been noted in the net plankton. The nannoplankton is mostly composed of delicate, naked flagellates and coccolithophorids that are destroyed by filtration through 0.45 μm filters and subsequent preservation with formalin. The procedure for collection and identification of the phytoplankton has been changed for the 1976 sampling effort.

Hydrographic Aspects

The hydrographic data gathered during the seasonal sampling in 1975 have been plotted in map form for three ranges in water depth: surface, mid and near bottom, for ease of comparison with the data on productivity. The solubility of nutrients, for example, is influenced by hydrographic factors. The areal patterns for temperature, salinity and dissolved oxygen in each of three seasons are shown by figures 61, 62 and 63. (See figs. 24 and 25 for vertical profiles.) Variations in amounts of all three aspects were distinctly seasonal.

Fluctuations in temperature were greatest over the inner shelf where the recordings were lowest in winter and highest in summer, as would be

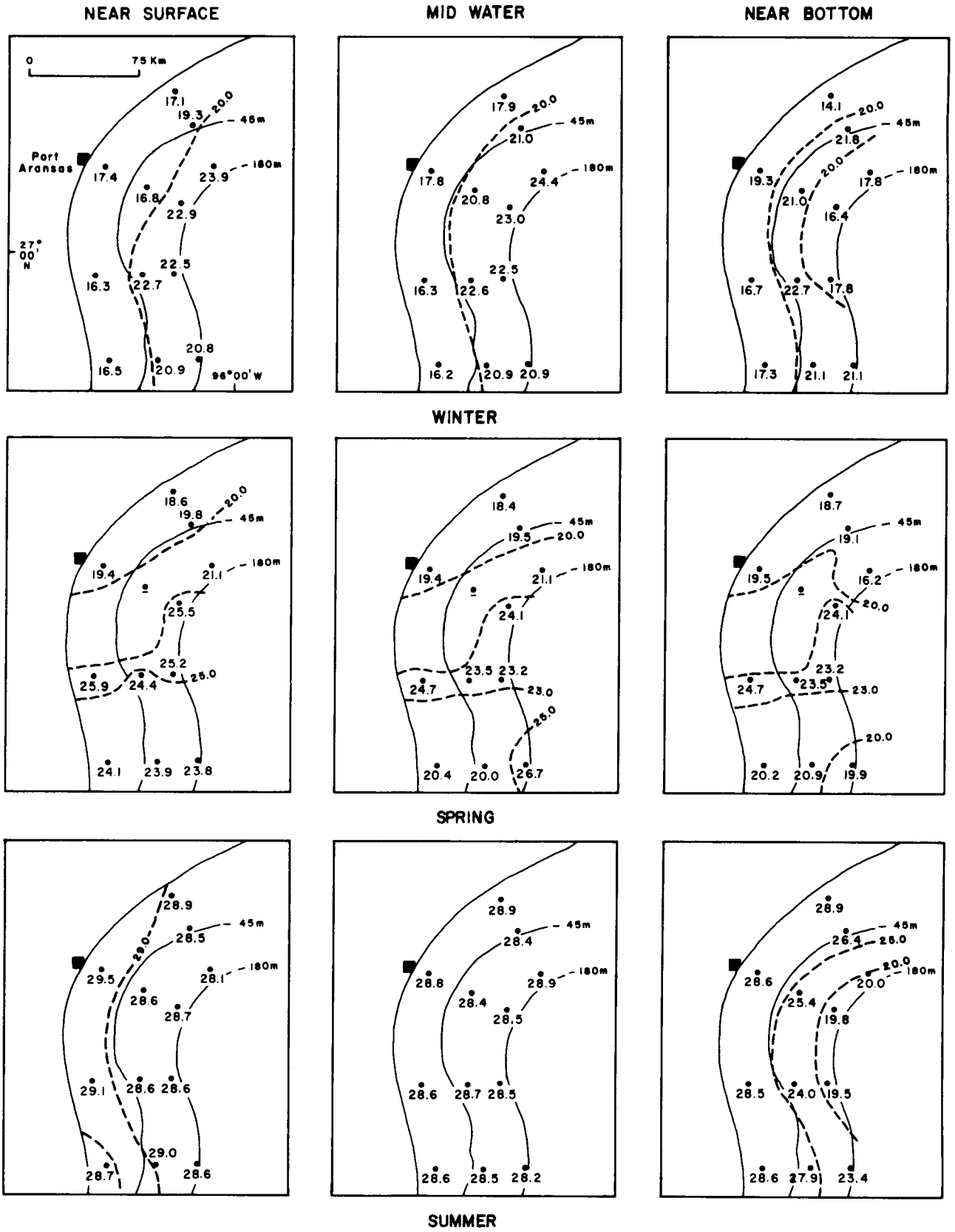

Figure 61. Seasonal temperature of shelf water by depth (in °C). Dot indicates location of sample station. Broken lines are isopleths inferred from temperature readings.

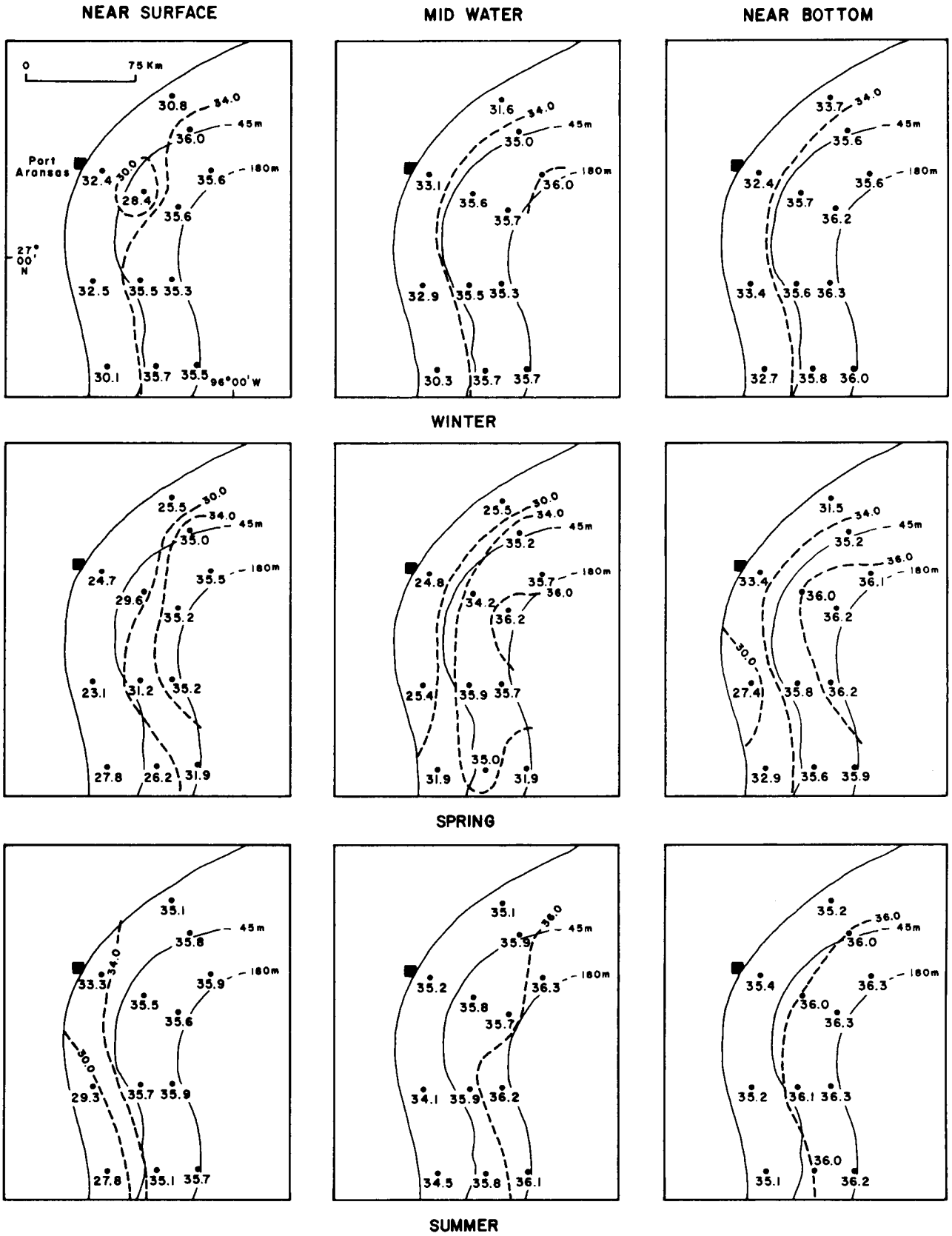

Figure 62. Seasonal salinity of shelf water by depth (in $^{o}/oo$). Dot indicates location of sample station. Broken lines are isopleths inferred from station readings.

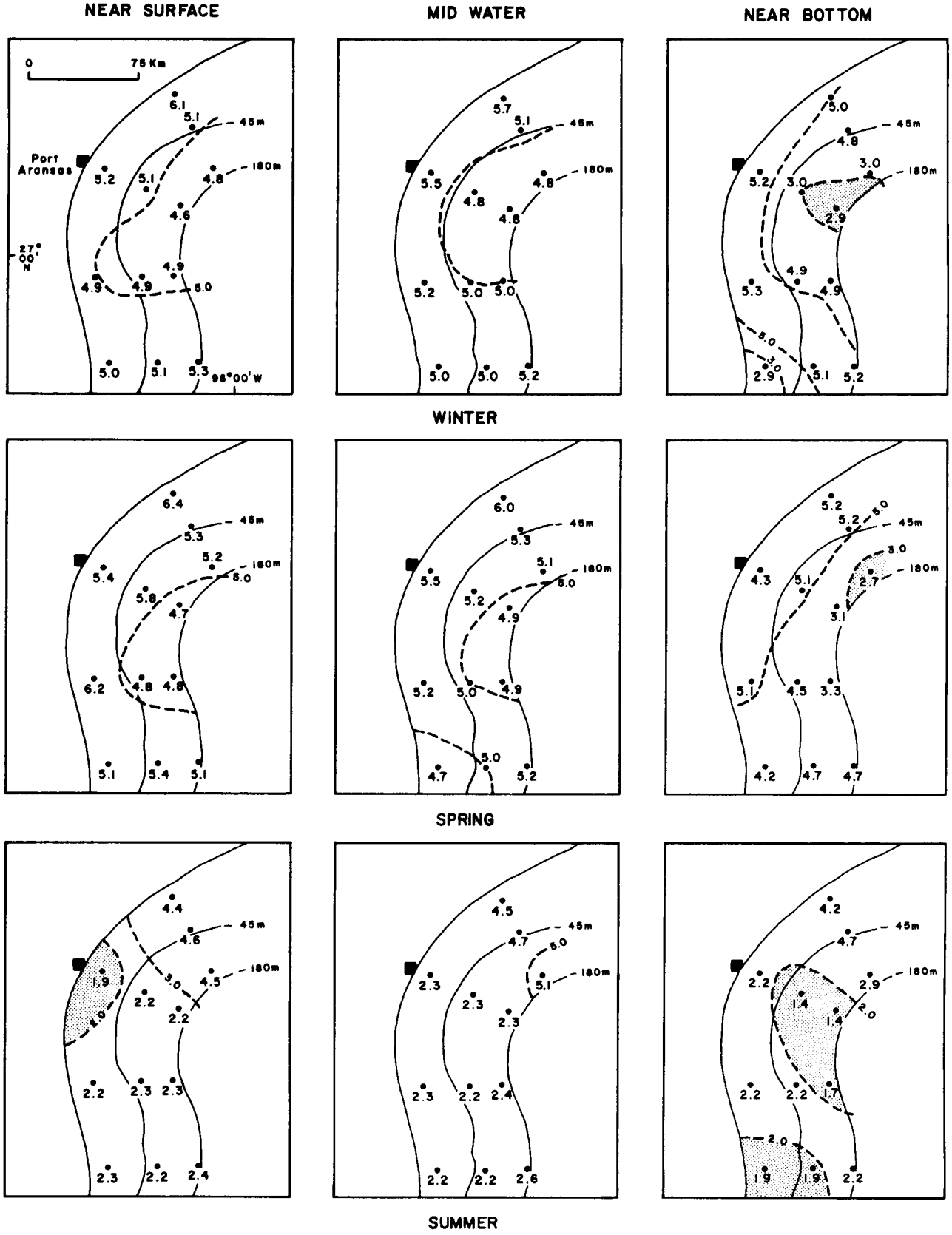

Figure 63. Seasonal distribution of dissolved oxygen in shelf water by depth (in ml/l). Dot indicates location of sample station. Broken lines are isopleths inferred from the analyses. Shading indicates amount below regional average.

expected. In winter, the temperature of surface to mid-depth water increased progressively seaward, but the same warming trend in the bottom water was reversed from mid shelf outward. In spring, the temperature increased from north to south rather than seaward. An anomalous feature of the spring was the set of higher temperatures along transect III. Whether the "ridge" of higher temperatures was actual or simply a manifestation of non-synoptic coverage is not known. Notably, the bottom temperature at the outer station on transect I was significantly lower than other bottom temperatures in the spring and also was lower than any inner shelf station. During the summer, in the surface through mid-depth range, temperatures were remarkably uniform; in the bottom water, temperature decreased seaward. The summer temperature of bottom water over the outer shelf was lower than during the spring, except for the extreme northeast station.

Water salinity increased seaward and with depth as a general pattern in all seasons. An exception was the anomalously low reading at station 2 on transect II in the surface water. When compared seasonally, the salinity was lowest in the spring along the inner shelf, both at the surface and at mid-water depth. Salinity was less than 30 $^{o}/oo$ at the two inner shelf stations south of the 27° parallel during the summer. The highest salinities (>36.0 $^{o}/oo$) were in the bottom water at all outer shelf stations in all three seasons with one exception: readings greater than 36.0 $^{o}/oo$ were recorded locally at mid-depth water depth over the outer shelf during both the spring and summer.

Regionally, dissolved oxygen content of the water was less variable within a season than was the nutrient content. Dissolved oxygen content

was greatest in winter and spring, and least during the summer; however, content at the northernmost three stations was greatest during the summer. The seaward decrease in all three seasons was most pronounced in the bottom water. The significantly low concentrations characteristic of the outer shelf in the summer extended up slope to one mid-shelf station.

Interpretation and Relationships

The data for primary productivity, nutrients and hydrography are strongly correlative. Furthermore, when compared on a regional basis, the data for nutrients are distinctly bimodal, suggesting two regimes relative to water influx: one over the inner shelf, and another over the outer shelf. The inner shelf regime is marked by the influence of continental runoff; the outer by the influence of water from the deeper Gulf.

Over the inner shelf, productivity, nutrients and hydrography show strong seasonal interrelationships; the inverse relation of the amount of productivity to the phosphate content is a typical characteristic. The amount of phosphate was largest for the shelf as a whole in the winter when phytoplankton activity was minimal. Conversely, when phytoplankton and associated by-products chlorophyll *a* and ATP were most abundant during the spring, and to a lesser extent during the summer, phosphate content was significantly reduced as a result of uptake by the phytoplankton. The reduced salinity of inner shelf water in the spring reflects the substantially increased continental runoff typical of the season. The increased runoff brings additional nutrients to the inner shelf which in turn sustain the phytoplankton bloom. Notably, nitrate did not show so close an inverse relationship to phytoplankton abundance as did phosphate. The nitrate

content, although lower than phosphate all along the inner shelf in the winter, was substantially higher than phosphate during the spring. However, the increase in nitrate was conspicuously localized at a single station on the south central inner shelf south of the area of greatest phytoplankton activity. An explanation is not readily apparent, considering the wide spacing of the data.

Over the outer edge of the shelf north of the 27° parallel, the amounts of nutrients generally are more than at mid shelf and a smaller seasonal variability in content relative to the inner shelf is indicated. This condition plus the persistence of much larger amounts of nitrate than those recorded on the inner shelf during three seasons and the presence of increased silicate in the winter seem to indicate that water from the deeper Gulf is the source and transporting agent. The manner in which the water moves onto the outer shelf and its relation to circulation in the deeper Gulf have not been determined.

HYDROCARBONS

Dissolved Low-Molecular-Weight Hydrocarbons

Methods

The analyses for low-molecular-weight hydrocarbons involved two methods. Methane was analyzed by the McAullife method, and C_2 and C_3 by a modification of the Swinnerton and Linnenbom method.

Samples for quantitative analysis by the Swinnerton and Linnenbom method were collected by standard NISKIN and NANSEN hydrographic casts. After retrieval, the sea water samples were transferred by gravity flow

into 1 liter glass bottles and were stoppered in a manner that would avoid entrapment of gas bubbles. Sodium azide was added to prevent bacterial alteration. Samples for the McAullife method were collected in 125 ml narrow-mouth bottles having screw-top caps. The bottles were stored inverted until analyzed.

Open ocean amounts of C_2 and C_3 hydrocarbons were determined quantitatively by the Swinnerton and Linnenbom method, which involves purging 1 liter of sea water with a hydrocarbon-free helium stream and collecting the light hydrocarbon in a cold trap. After collection, the trap is heated to inject the absorbed hydrocarbon into the chromatographic stream. The precision of the determination at the lower level of sensitivity (0.05 nl/l) is $\pm$10 percent (standard deviation of replicate determinations). The precision of the determination of methane at 50 nl/l is $\pm$2 percent, with sensitivity and precision increasing rapidly as hydrocarbon concentrations increase.

McAullife's method of multiple phase equilibrium involves equilibrating 25 ml of purified helium with 25 ml of sample water in a 50 ml syringe having a LUER-LOK stopcock. As 96^+ percent of the light aliphatic hydrocarbons partition into the gas phase, analysis is performed by injecting 1.76 ml of the equilibrated helium into the chromatographic stream by means of a sample injection valve. In determinations of open ocean concentrations of light hydrocarbons, this method is sufficiently sensitive for methane only.

Methane

According to Henry's Law, the equilibrium concentration of a dissolved gas in surface sea water is the product of its solubility coefficient and

its partial pressure in the atmosphere. For the low-molecular-weight hydrocarbons, only the partial pressure of methane, 1.4 ppmv for the atmosphere over the earth as a whole, is known with any degree of certainty. Using this number and reported solubility coefficients, the equilibrium concentrations of methane in nanoliters per liter (nl/l) as a function of salinity and temperature are shown by table 9.

Table 9. Equilibrium concentrations of methane in surface sea water as a function of temperature and salinity. Results in nanoliters per liter.

Temperature	Salinity (parts per thousand)			
°C	30	32	34	36
0	64.7	63.8	62.8	61.9
10	49.8	49.1	48.5	47.8
20	40.2	39.8	39.3	38.8
30	34.0	33.6	33.2	32.8

Comparison of the measured methane concentration, salinity and temperatures in the South Texas OCS with the amounts calculated in table 9 indicates a 10 to 200 percent supersaturation of methane in surface water for all profiles. Figure 64 shows the distribution of methane in water of the South Texas OCS; figures 61 and 62 show the temperature and salinity measurements made at the time samples were collected for methane determination. In examining the maps in the figures, keep in mind that sampling was not time-synoptic but was spread over periods of 2 to 3 weeks duration. Sampling along a given transect usually was completed within 2 days, and 2 adjacent transects usually were covered in less than a week.

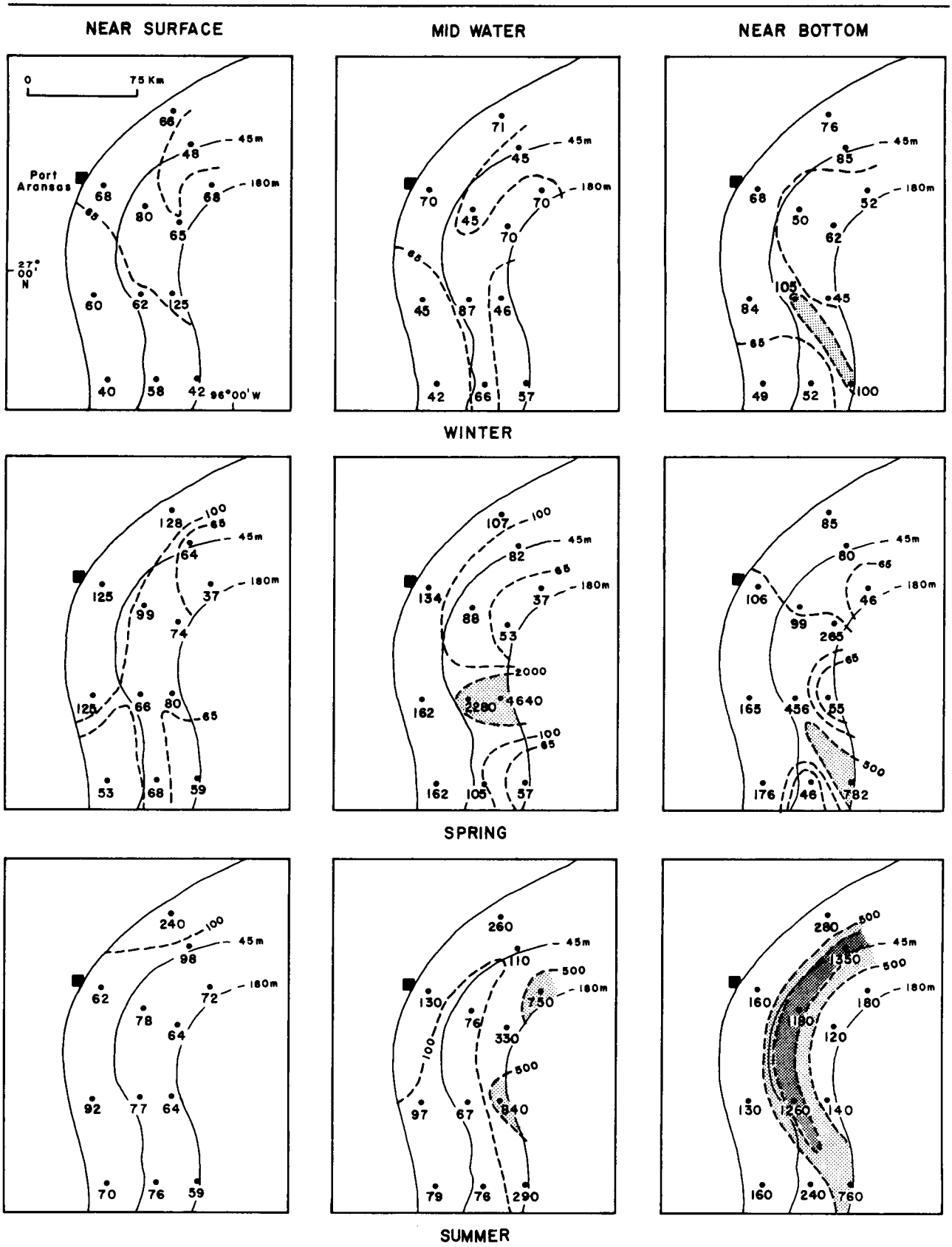

Figure 64. Seasonal distribution of methane in shelf water by depth (in nl/l). Dot indicates location of sample station. Broken lines are isopleths inferred from the analyses. Shading indicates amount above regional average.

Thus most transects taken individually are quasi-synoptic as are some adjacent transects as well. Consequently, the patterns shown are general guides to trends and must be used in that perspective.

The most obvious feature revealed by the maps is the large amount of methane at both mid-water and near-bottom depths from mid to outer shelf in the spring and summer, and to a lesser extent during the winter. The most anomalous maxima were at mid-water depth during the spring at the outer two stations on transect III. The 4640 nl/l measurement at III/3 is higher than amounts measured in samples from parts of the shelf off Louisiana known to be heavily contaminated by low-molecular-weight hydrocarbons. Because of these anomalies, several additional mid-depth samples were taken during the summer sampling. The additional samples also showed a very pronounced mid-depth maximum in the depth range of 50 to 80 m at all stations along the outer shelf. A similar increase was measured within a depth range of 40 to 50 m at all mid-shelf stations. Thus a very large mid-depth maximum was confirmed for both spring and summer.

The patterns of methane anomalies in deep waters may be the most intriguing. They differ significantly from the mid-depth patterns, suggesting the building and progression of a trend through the three seasons.

Other Saturated Low-Molecular-Weight Hydrocarbons

Without knowledge of either the global partial pressures of ethane, propane and higher hydrocarbons or their solubility coefficients, it is not possible to calculate their equilibrium concentrations in oceanic surface waters. Considerable work has indicated that near-equilibrium values are approximately 2 nl/l for ethane and 1 nl/l for propane. These

low concentrations are very difficult to measure. Poor performance of the gas chromatograph during the spring sampling did not permit separation and detection of ethane and ethene separately.

The amounts of ethane and propane measured in surface water off the South Texas OCS are similar to amounts for open ocean water reported in previous reports. The largest concentrations of surface propane were in the summer and the smallest were in the spring with a single exception at the mid-shelf station on transect II. The patterns of distribution for propane are shown by figure 65. No systematic decrease of either ethane or propane with depth is indicated and no geographic correlation of ethane with methane is apparent. However, a notable and significant correlation in the occurrence of propane relative to methane is seen in the amount of propane in bottom water during summer. The maximum amount of each was in bottom water during summer at mid shelf. The geographic area of the occurrence is virtually identical. (Compare figures 64 and 65.)

A significant feature of propane is that the average concentration for 35 samples is 3.1 nl/l, a factor of three higher than apparent equilibrium levels. Thus the high propane concentrations parallel those of methane as a regional characteristic. The ratios of methane to propane are shown on figure 66. The areas of low ratios have been shaded to emphasize the higher propane concentrations. The mapped ratios show that some parts of the OCS have higher propane concentrations, indicating possible petrogenetic sources for the dissolved gas.

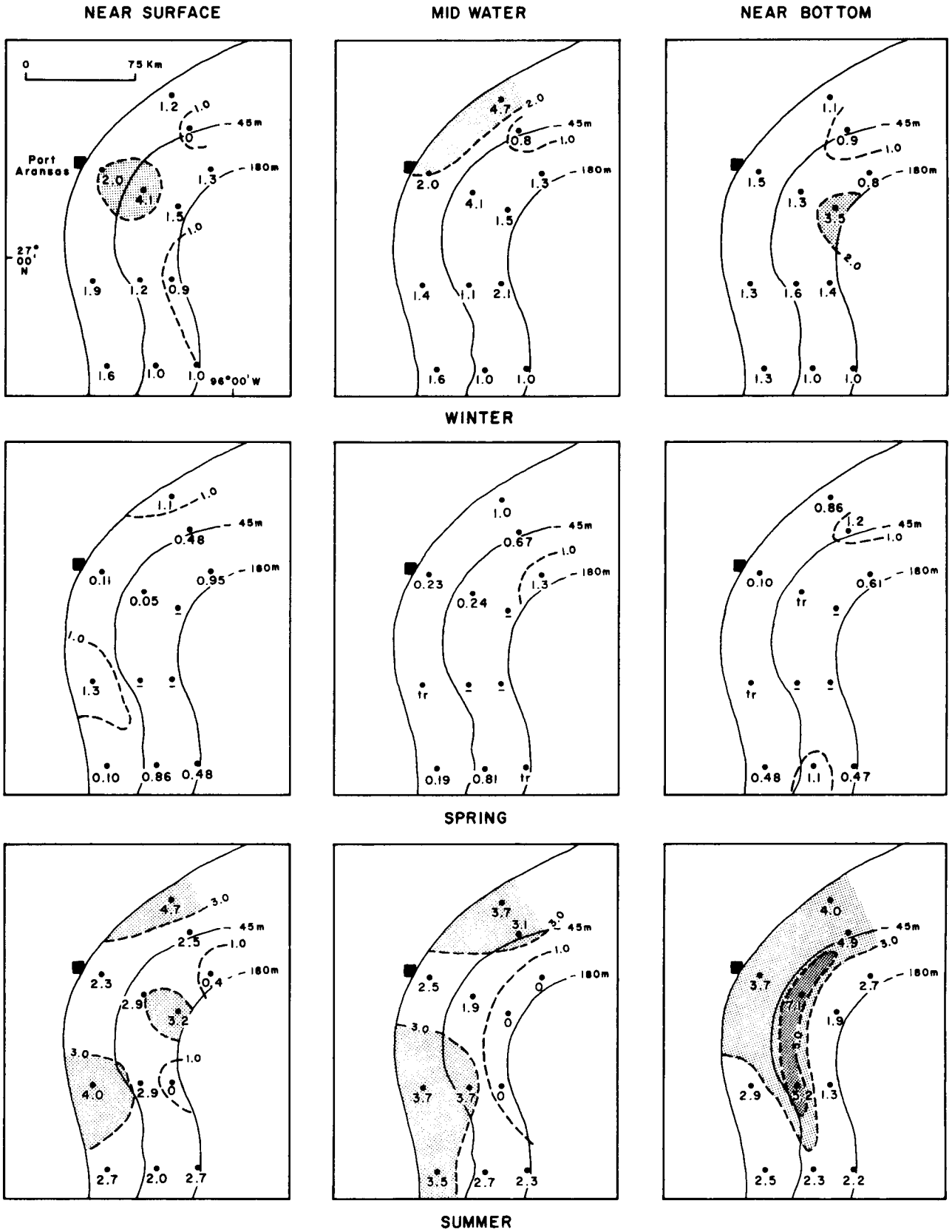

Figure 65. Seasonal distribution of propane in shelf water by depth (in nl/l). Dot indicates location of sample station. Broken lines are isopleths inferred from the analyses. Dash indicates no analysis; tr indicates trace only. Shading indicates amount above regional average.

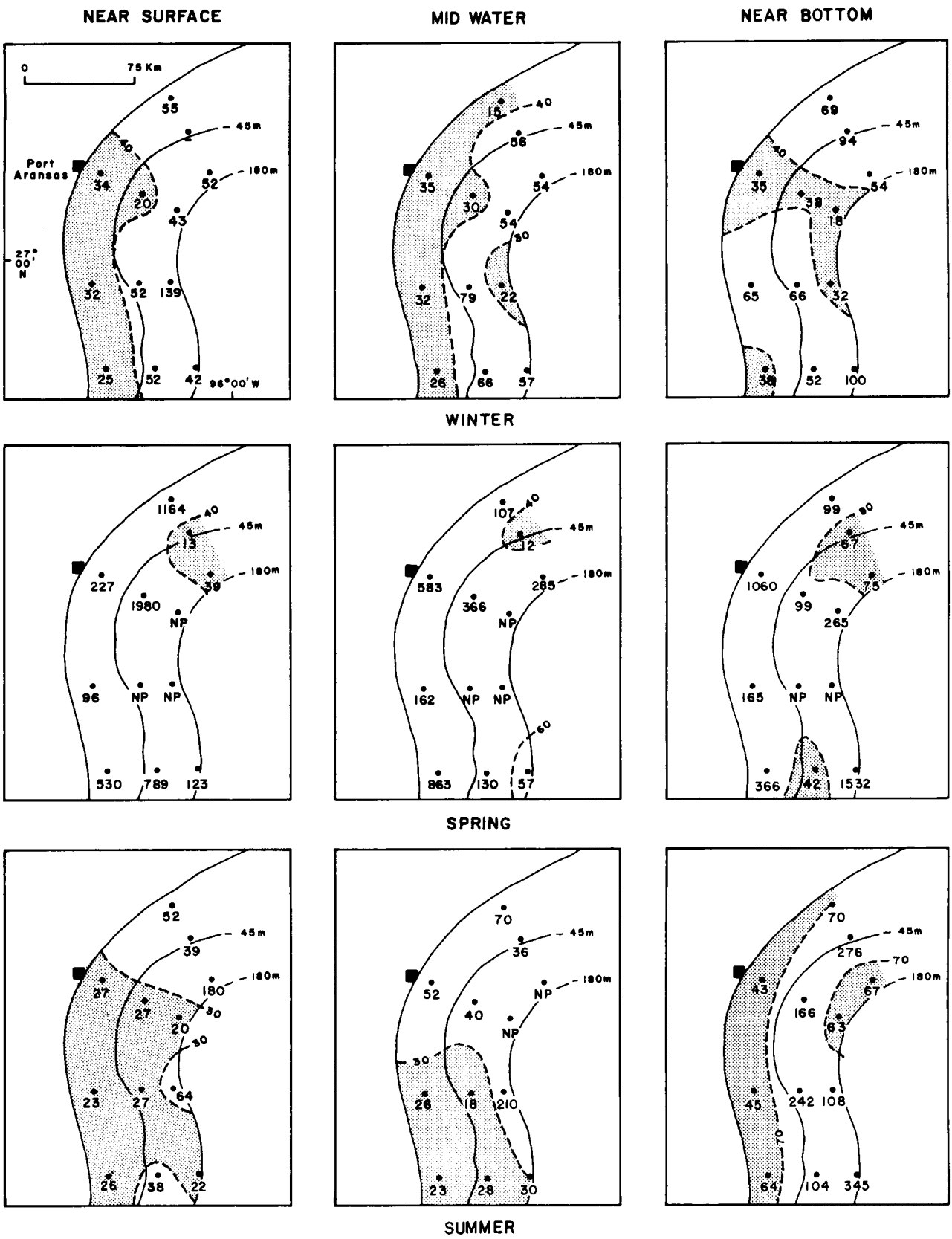

Figure 66. Seasonal ratios of methane to propane in shelf water by depth. Dot indicates location of sample station. Broken lines are isopleths inferred from the analyses. Dash indicates no analysis; NP indicates not present. Shading indicates lowest ratios to emphasize areas of increased propane.

High-Molecular-Weight Hydrocarbons

Methods

Water samples were collected at a depth of about 10 m in 19-l glass carboys. The carboy was held in a weighted stainless steel cage fitted with a tapered TEFLON plunger which sealed the mouth of the carboy. The carboy was lowered with a nylon rope and the plunger was then partially removed by an accessory rope. After the bottle had been filled, tension on the accessory rope was relaxed and the carboy was again sealed by the plunger.

Samples to be filtered were processed aboard ship soon after collection. GELMAN type A glass fiber filters, which previously had been extracted in boiling benzene, were used. The water was transferred through glass tubing and an all glass filter into another 19-l carboy in which the pressure had been reduced by means of an aspirator. The filters required for a given sample were placed in a 125 ml flask and frozen. The samples were poisoned with about 15 g of mercuric chloride and were stored subsequently in dim light at room temperature until extraction.

Extraction of hydrocarbons from seawater was carried out for 24 to 36 hours in all glass, continuous, liquid-liquid extractors using benzene as the solvent. Approximately 250 ml of benzene were used per sample. The extract was reduced to near dryness (0.1 to 0.2 ml) in a KUDERNA-DANISH concentrator on a steam bath. The sample was transferred in a total volume of about 1 ml of hexane to a micro-silica gel (WOELM, Activity I) column which had been packed in hexane. The column was eluted with 2 ml of hexane to remove saturates and then with 2 ml of benzene to remove the more polar compounds,

including aromatics. These fractions were concentrated to 50-100 µl with air filtered through silica gel. The samples were kept warm, about 40°C, on a hot plate during evaporation.

The hydrocarbons in particulate matter from seawater were extracted from filter pads on a hot plate with methanol (25 ml) and then with benzene (25 ml). The two extracts were combined in a separatory funnel, and about 5 ml of water was added. The mixture was shaken and allowed to separate. The benzene layer was evaporated to 1-2 ml; it was saponified for at least 2 hours with 10 ml of KOH in methanol (15 g; 500 ml). After addition of 5 ml of water, the mixture was extracted three times with benzene. The benzene extract was concentrated and fractionated on micro-columns of silica gel as described for water samples.

Several experiments were conducted as checks of the procedures. (See Parker and others, 1976.) The analytical method was gas chromatography using either a PERKIN-ELMER model 900 or a HEWLETT-PACKARD model 7620A. Routine analyses were conducted on 1/8 in x 6 ft stainless steel columns of 5 percent FFAP on 80/100 mesh GAS CHROM #Q (3 percent APIEZON L was used on a few samples collected during the winter). Combined gas chromatography-mass spectrometry (GC-MS) was carried out with a VARIAN 2700 chromatograph interfaced to a DUPONT 21-491 mass spectrometer. GC-MS analysis for identification and/or confirmation was done on more than 10 percent of the samples. Mass spectra obtained were compared with spectra published in the Registry of Mass Spectral Data (1974) and with mass spectra taken of known compounds. Some spectra were processed through the Mass Spectral Data Base of the Environmental Protection Agency and the National Institute of Health maintained on the "Cybernetics" time-sharing computer.

Results

The regional distribution of n-paraffins in the seawater by season is shown on figure 67. The distributions of pristane and C_{18} plus phytane, as a percent composition of the n-paraffins, also are shown on figure 67. The amounts indicated are averages of replicates run for each station. Duplication of results within relatively narrow limits was a continuing problem during analysis; considerable variation was encountered between several replicates. Despite continuing experimentation to provide closer duplication of replicate analyses, the problem persisted. However, considering the small amounts of material analyzed, the averages for a station probably are more meaningful than a single analysis would be.

For the "dissolved" hydrocarbons, three general trends are suggested by the distribution of n-paraffins: a seaward decrease, increased concentrations in the spring and relatively uniform regional distribution within a given season, except for the spring measurements at three stations. Seasonal averages of all stations are as follows: winter, 0.13 µg/1; spring, 0.64 µg/1; and summer, 0.23 µg/1. Comparison of patterns of distribution for the components pristane and C_{18} plus phytane, as percentages of total n-paraffins, indicates not only large variations and pronounced highs within a season but substantial variations from season to season as well. Furthermore, the similarity in trends for the two components within a season is obvious; high concentrations near mid shelf are characteristic of winter and spring, and localized high amounts at southern and northern nearshore stations are characteristic of summer.

The average concentration of n-paraffins in particulate matter in the water was determined for the summer samples only. Consequently, no

distribution maps were included. The data for the summer suggest a decrease seaward, but no consistent variation between transects is apparent.

Concerning the overall variations in percentage composition of the n-paraffins, some general differences did occur with season, as in the case of pristane and C_{18} plus phytane. Winter samples contained a higher percentage of hydrocarbons in the C_{15} to C_{20} range and lower in the C_{30} to C_{35} range than did spring and summer samples. The most abundant n-paraffin in the spring particulate samples was C_{22}; in summer C_{31} was generally the most abundant. No consistent change in percentage composition relative to either distance from shore or geography was apparent.

Analyses of benzene fractions from samples of water and particulate matter did not disclose the presence of representative petroleum derived aromatic compounds such as napthalenes or alkyl phenols. GC-MS analysis indicated that the most abundant compound in most of the water and particulate samples was diethylhexl phthalate ($C_{24}H_{38}O_4$). The origin of most of this phthalate probably was short lengths of TYGON tubing used to give flexibility to an otherwise inflexible glass filtration and extraction apparatus. Other compounds identified were $C_{19}H_{34}$ (C_{19}:3) and $C_{19}H_{36}$ (n_{19}:2).

Interpretation and Relationships

Low-Molecular-Weight Hydrocarbons

As significant amounts of methane are not known to be biologically produced in the water column, the most likely source for the methane causing the supersaturated conditions in waters over the South Texas OCS is the sea floor sediment, where the methane is generated by either bacterial or thermocatalytic processes. Numerous "plumes" recorded on analog seismic reflection

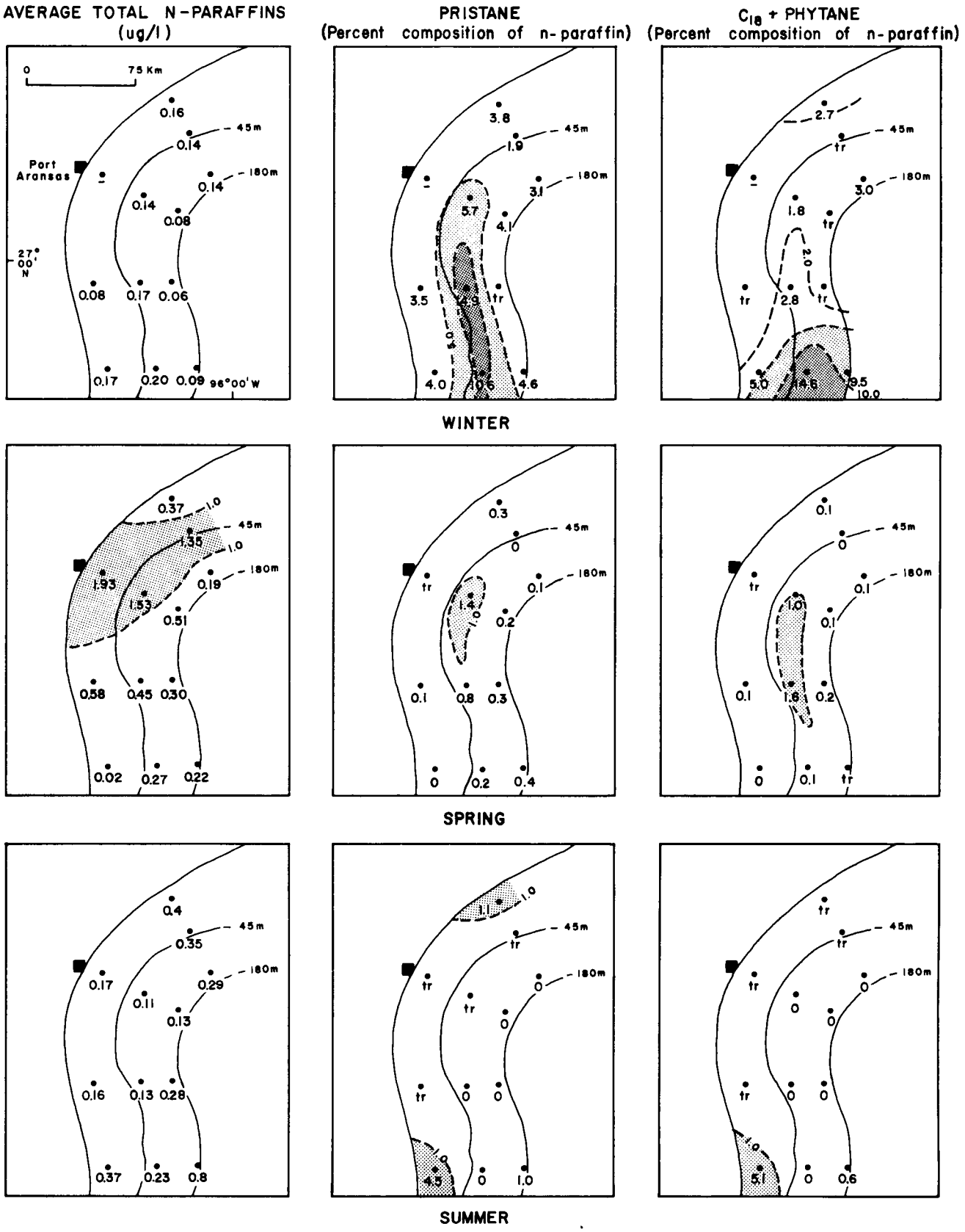

Figure 67. Seasonal distribution of high-molecular-weight hydrocarbons in shelf water. Distribution of n-paraffins by total average concentration (in µg/l); distribution of pristane and C_{18} plus phytane as percent composition of n-paraffins. Broken lines are isopleths inferred from the analyses. Dash indicates no analysis; tr indicates trace only. Shading indicates amount above regional average.

profiles above the water-sediment interface have been interpreted as probable natural gas seeps. No systematic survey for possible gas seeps was made, but a number of sound reflection signatures believed to be gas emanations were recorded during the geological/geophysical baseline studies. The general areas where the probable gas seeps were recorded are shown by figure 109, map F.

Although seepage of natural gas into the water of the South Texas OCS would seem to be the most likely source for the large amounts of methane measured, the patterns of distribution for methane in the bottom water do not show such a direct, simple relationship. In fact, greatest concentrations of methane do not coincide with the areas where the suspected gas seeps are most numerous. If the methane is coming from the sea floor, factors such as water circulation patterns and seasonal variations in temperature, both of the water and of the sediment, must govern the patterns in which it is distributed and becomes concentrated in shelf waters. The seasonal temperature fluctuations, particularly in the sea floor sediments, could affect the solubility of methane, causing the gas effluence to be periodic rather than continuous.

The origin of the propane is somewhat equivocal. The highest concentrations of propane for all three seasons are almost identical in area of occurrence with that for the highest concentrations of methane in the summer bottom water. When methane/propane ratios are compared, a bimodal distribution pattern is suggested: inner shelf and outer shelf. This pattern suggests two general sources for the gases: one related to the inner shelf and its processes, and another to the outer shelf and the gas seeps.

The narrow, crescent-shaped area conspicuously outlined by the highest concentrations of both methane and propane in the summer near the bottom

suggests a relationship to the series of dead carbonate reefs that lie along the sea floor just seaward of mid shelf. (See figure 5 for reef locations.) Gas "plumes" were recorded on seismic reflection profiles above several of the reefs in November and December 1974. The high concentrations of gas along the trend of the reefs during the summer suggest that the gas is biogenic. The restriction of the phenomenon to the summer is not readily explainable, but the relationship may have been a simple coincidence during the summer of 1975. Continuing studies may yield more conclusive evidence.

High-Molecular-Weight Hydrocarbons

The concentrations of n-paraffins in seawater measured during 1975 were similar to concentrations reported for earlier studies on the Texas and Louisiana coasts and in the Florida Straits. The high concentrations in the spring appear to reflect the high productivity during this season. Likewise, the trend toward high concentrations at inshore stations in all seasons presumably indicates the increased abundance of phytoplankton and zooplankton over the inner shelf.

The percent composition of n-paraffin in seawater did not show a significant systematic change with increased distance from shore and showed only slight changes with season. Percent composition in many samples reached a maximum at or near C_{22}. The hydrocarbon C_{22} is a major constituent in many marine substances such as zooplankton, fish and sediment.

The amounts and percent composition of hydrocarbons in particulate matter did show significant changes between spring and summer samples. The four samples taken in the spring had larger amounts (average 1.63 µg/l) with

a maximum at C_{21}; summer samples averaged 0.09 µg/l with a maximum at C_{31}. The larger amounts in spring are consistent with the greater abundance of phytoplankton and zooplankton in the spring. Smaller amounts in the summer could reflect decreased abundance of phytoplankton.

The results of the work during 1975 indicate a very low level of petroleum-type hydrocarbons over the South Texas OCS. This tentative conclusion implies that the samples collected were uncontaminated and that the area is suitable for meaningful monitoring of oil drilling and production in the future.

NEUSTON

Neuston is composed of the plants and animals that live on or just beneath the surface film of water. Sargassum was the most abundant plant collected in the neuston samples. The most abundant organisms collected are described below.

Methods

In the laboratory the samples were allowed to thaw and were placed in a graduated beaker where they were diluted from 200 to 800 ml, depending on the abundance of the organisms. From this concentration, both 1 to 4 ml and 20 ml aliquots were taken using a HENSEN-STEMPEL pipette. Aliquot size ranged from 1/800 to 1/10 and the number of organisms counted ranged from 27 to 523. Aliquots were placed in a WARD zooplankton counting wheel and were counted at 25x with a WILD M-5 dissecting microscope. Only the most abundant organisms were counted in the 1 to 4 ml aliquot; less abundant organisms in the first aliquot were counted in the 20 ml aliquot. Most of the organisms were damaged beyond species recognition by the freezing;

therefore, most identifications were made only as far as major groups of animals. As no flowmeter was used in the net during the collection of neuston, no quantitative counts were possible.

General Components

The total number of organisms collected from all stations for each season was winter - 769,293; spring - 581,410; and summer - 229,036. The patterns of distribution for total numbers of organisms in the neuston and for the two most abundant components, calanoid and cyclopoid copepods, are shown on figure 68. The distribution for the less abundant components, mollusc larvae, fish larvae and fish eggs, is shown on figure 69. Relative abundance of sargassum in the samples is also noted on figure 68.

No consistent pattern or trends for neuston organisms are indicated, either geographically or seasonally. The largest counts of organisms in winter were on the inner shelf off Port Aransas but abundance was relatively uniform along the inner shelf from Port Aransas to Port Isabel. The largest counts for all seasons were in the spring at mid shelf off Port Aransas. The copepods greatly outnumbered other organisms in all three seasons.

Trace Metal Content

The neuston samples were analyzed for six trace metals: Cu, Zn, Cd, Pb, Ni and Cr. When compared as a group, the patterns of distribution for the six elements are characterized by an almost total lack of correlative trends, either geographically or seasonally. The lack of trends and correlations is not surprising considering the rapid changes that often take place at the surface of the sea as a result of varying sea

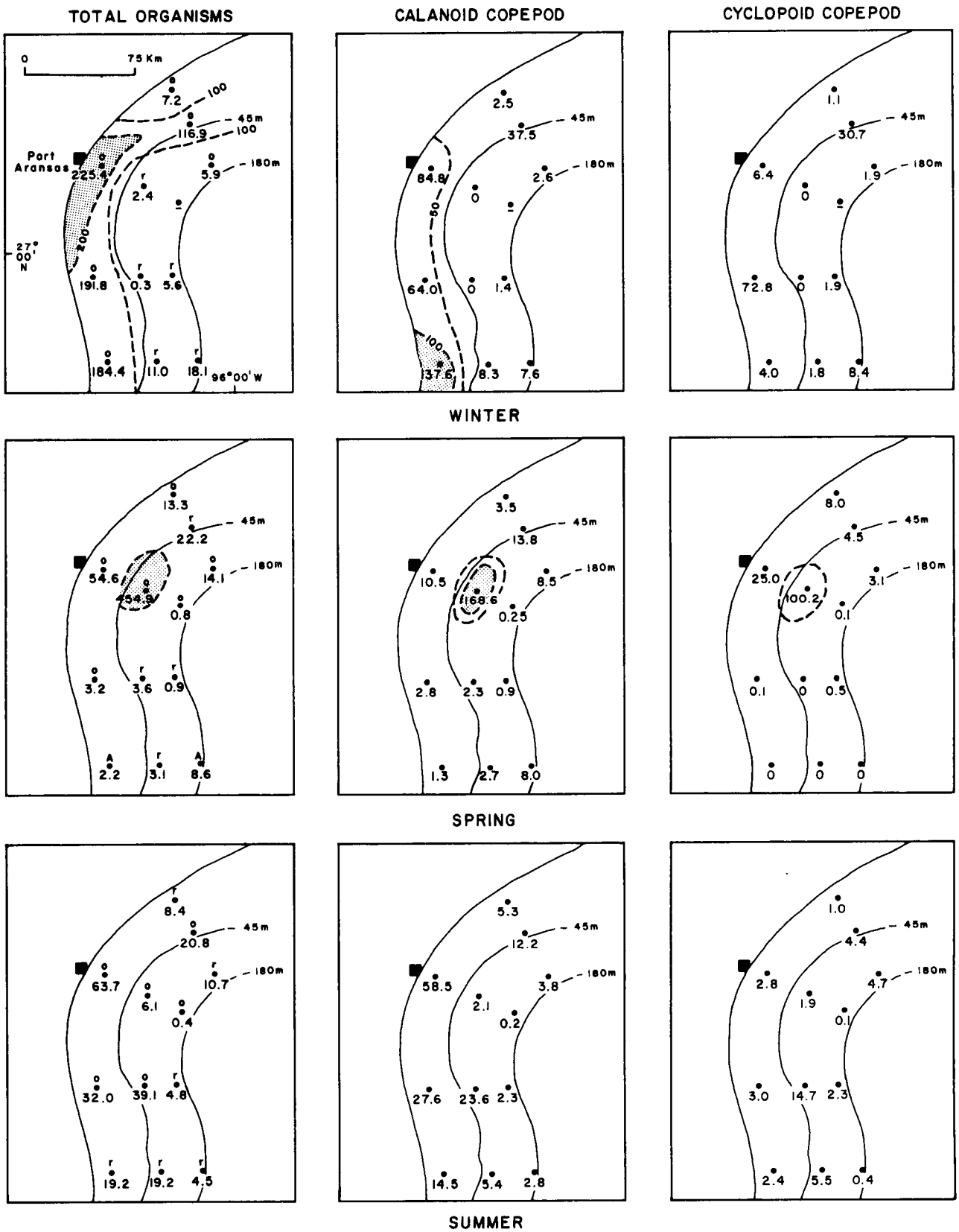

Figure 68. Seasonal distribution of biota in the neuston: total numbers of organisms, of calanoid copepods and of cyclopoid copepods. Numbers in thousands. Dash indicates no samples; large O indicates not present. Sargassum reported above dots indicating sample stations as follows: o, absent; r, reported; A, abundant. Broken lines are isopleths inferred from station counts. Shading indicates amount above regional average.

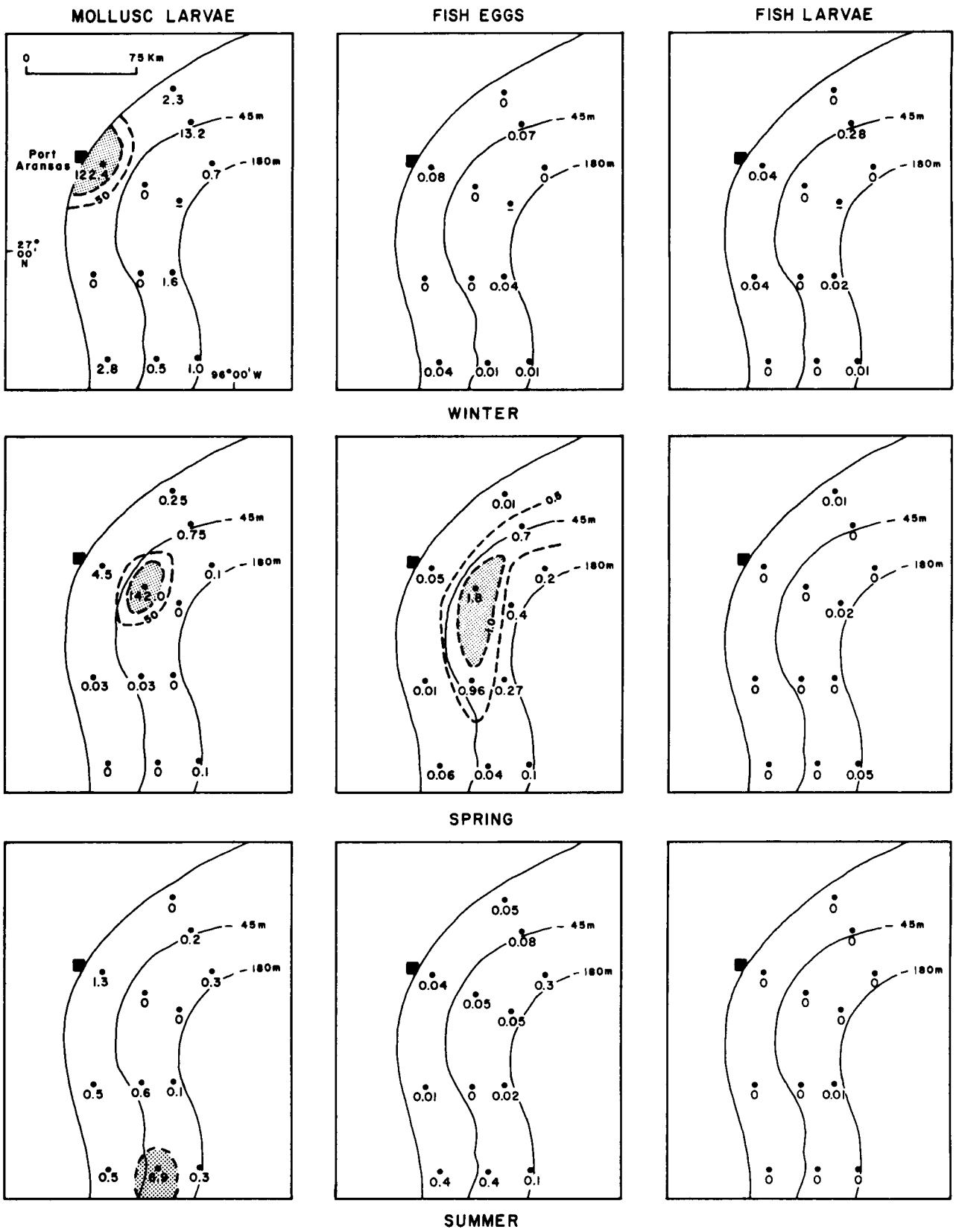

Figure 69. Seasonal distribution of biota in the neuston: mollusc larvae, fish larvae and fish eggs. Numbers in thousands. Dash indicates no samples; large 0 indicates not present. Dot indicates location of sample station. Broken lines are isopleths inferred from station counts. Shading indicates amount above regional average.

state conditions caused by changes in weather. These changes can affect concentrations and patterns of distribution in a matter of a few hours. The patterns of distribution for the trace metals are shown by figures 70 and 71.

In the winter and spring collections, many samples were almost pure sargassum and, not surprisingly, were fairly constant in chemical composition. The sargassum is much lower in Zn content, 30 to 40 ppm, than the samples of mixed sargassum and plankton which had 100 to 150 ppm Zn. The sargassum also is somewhat lower in Pb and Cu. Two samples had anomalously large amounts of Ni: 108 ppm in the spring sample from station 3, transect I; and 321 ppm in the summer sample from station 3, transect IV. The amount of Zn in the summer sample was correspondingly large. Neither sample was thought to have been contaminated and no explanation was evident for the anomalously larger amounts of Ni and Zn.

High-Molecular-Weight Hydrocarbons

Methods

The samples for analysis of high-molecular-weight hydrocarbons in the neuston were frozen aboard ship for transfer to the laboratory. In the laboratory, the samples were thawed by immersing the sample container in warm water. The particulate matter (zooplankton) was separated from the seawater by direct filtration into a precleaned, cellulose extraction thimble. Visible tar ball contaminants were removed; no attempt was made to remove microscopic-sized tar balls.

The samples were extracted with methanol in a SOXHLET extractor for at least 8 hours. The preliminary extraction removed the water and part of the

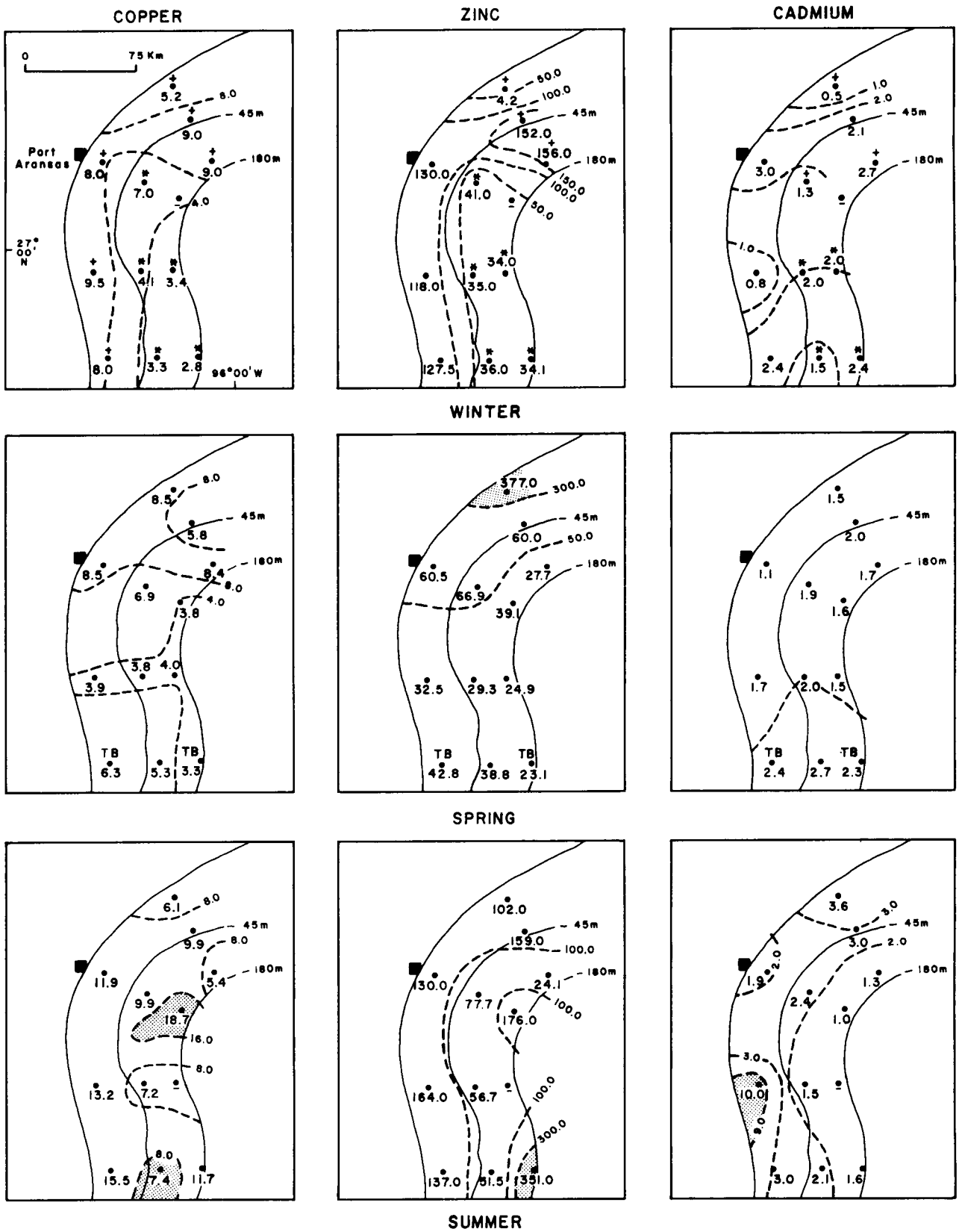

Figure 70. Seasonal distribution of trace metals in neuston (day): Cu, Zn and Cd (in ppm dry weight). Plus indicates analysis includes surface plankton plus sargassum; *indicates sargassum only; TB indicates presence of tar balls. Dot indicates location of sample station. Broken lines are isopleths inferred from the analyses. Shading indicates amount above regional average.

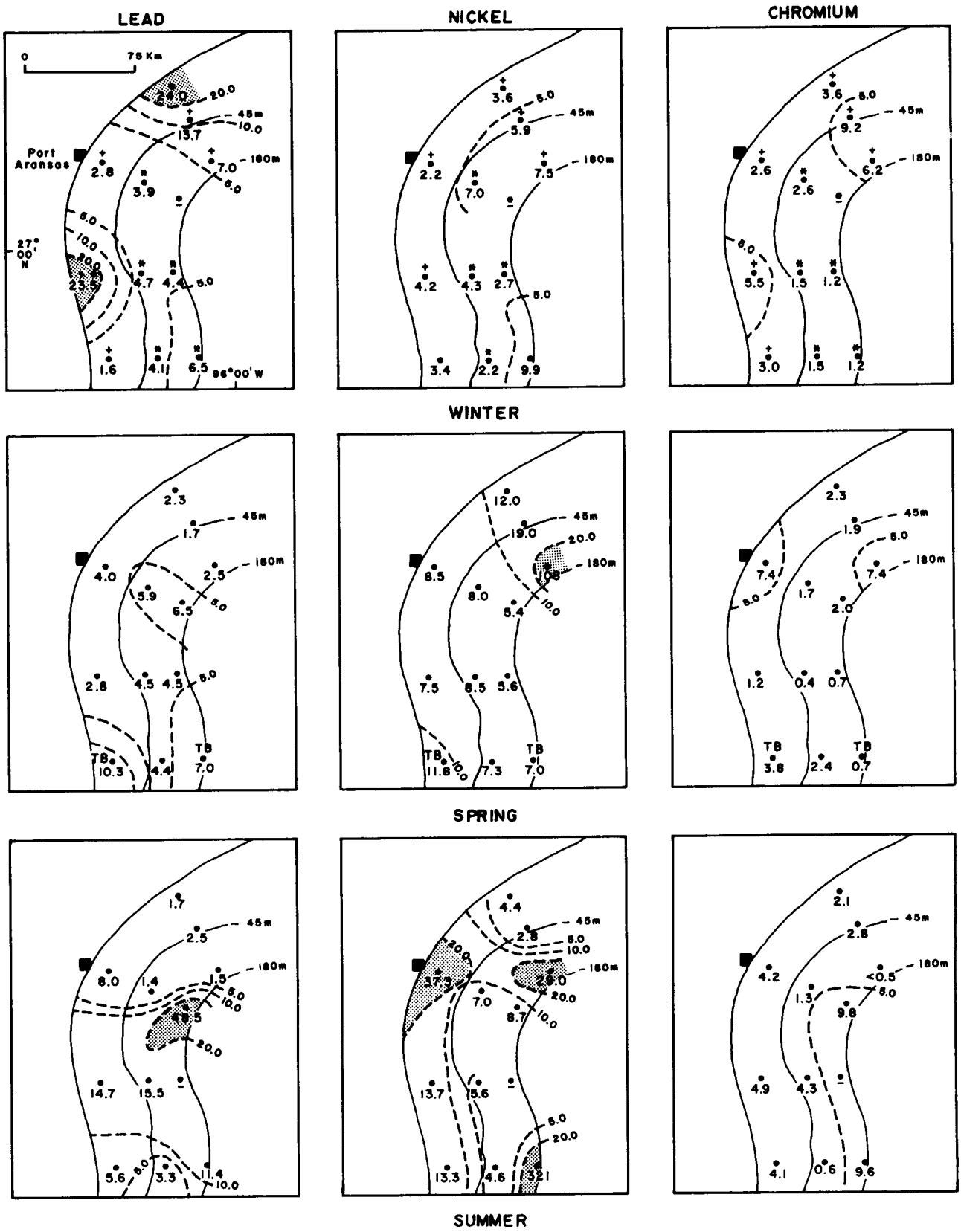

Figure 71. Seasonal distribution of trace metals in neuston (day): Pb, Ni and Cr (in ppm dry weight). Plus indicates analysis includes surface plankton plus sargassum; *indicates sargassum only; TB indicates presence of tar balls. Dot indicates location of sample station. Broken lines are isopleths inferred from the analyses. Shading indicates amount above regional average.

hydrocarbons. The remaining hydrocarbons then were extracted from the sample for at least 8 hours using benzene as the solvent. This technique was tested using re-extraction and was found to remove essentially all of the hydrocarbons. A chromatogram was made of the recovered saturate hydrocarbons. After re-extraction with benzene, a second chromatogram was run. Based on the areas beneath the known peaks, no more than an additional 2 percent of these materials were removed by the second extraction. The extracts also contained many nonhydrocarbons.

The extracts were recovered from the solvents by evaporation under partial vacuum on a flash evaporator at 45°C. Approximately 50 ml of a solution of potassium hydroxide in methanol (30 g KOH per 1 CH_3OH) were added for saponification. The mixture was refluxed on a steam bath for 4 to 15 hours.

Distilled deionized water was added to the saponified mixture and the nonsaponifiable hydrocarbons were extracted into hexane using a separatory funnel with gentle mixing to avoid emulsion formation. The hexane was evaporated from the hydrocarbons under a nitrogen "blanket" at 40°C and the "total hydrocarbon" was recovered and weighed.

The "total hydrocarbon" sample was separated by column chromatography into two fractions. A column 20 cm long by 1 cm in diameter was packed with silica gel and prewashed with purified hexane. The total nonsaponifiable organic extract was washed onto a column with 1 ml of hexane and the "saturate" hydrocarbons were eluted from the column with 50 ml of hexane (3 to 4 volumes). Hexane insoluble material not previously added to the column was washed onto the column with 1 ml benzene and the column was eluted of nonsaturate hydrocarbons with 50 ml of benzene.

The eluting solvents were evaporated from the saturate and nonsaturate hydrocarbons with a nitrogen stream at 40°C. The two fractions were weighed and diluted with 0.2 ml of hexane for gas chromatographic analysis. Gas chromatographic methods for the analyis of saturate and nonsaturate fractions were identical to those outlined for the analysis of heavy hydrocarbons in water.

Results

Two main types of saturate hydrocarbons were identified in the neuston samples: 1) those that resemble zooplankton in having major peaks at C_{17} and pristane, and smaller peaks at C_{15}, C_{19} and C_{22}; and 2) those that apparently were contaminated with petroleumlike alkanes having a full suite of n-alkanes from nC_{15} to nC_{35}. Twenty samples were of type 1 and 12 of type 2. The content and distribution of total heavy hydrocarbons in the neuston samples and a classification of the saturates at each station as either petroleumlike or zooplanktonlike are shown by figure 72.

Of those neuston saturate analyses that resembled zooplankton, only two did not have a "hump" of unresolved hydrocarbons in the gas chromatograms. In this respect, the chromatograms are more complex than those for zooplankton. Most of the samples having a petroleumlike distribution of n-alkanes also had a "hump" of unresolved peaks. Many of these petroleumlike saturates still showed some of the zooplankton characteristics by having relatively high nC_{17}, pristane and nC_{22}. This suggests possible contamination of zooplankton-type samples with petroleumlike organic matter, probably tar balls of unknown origin.

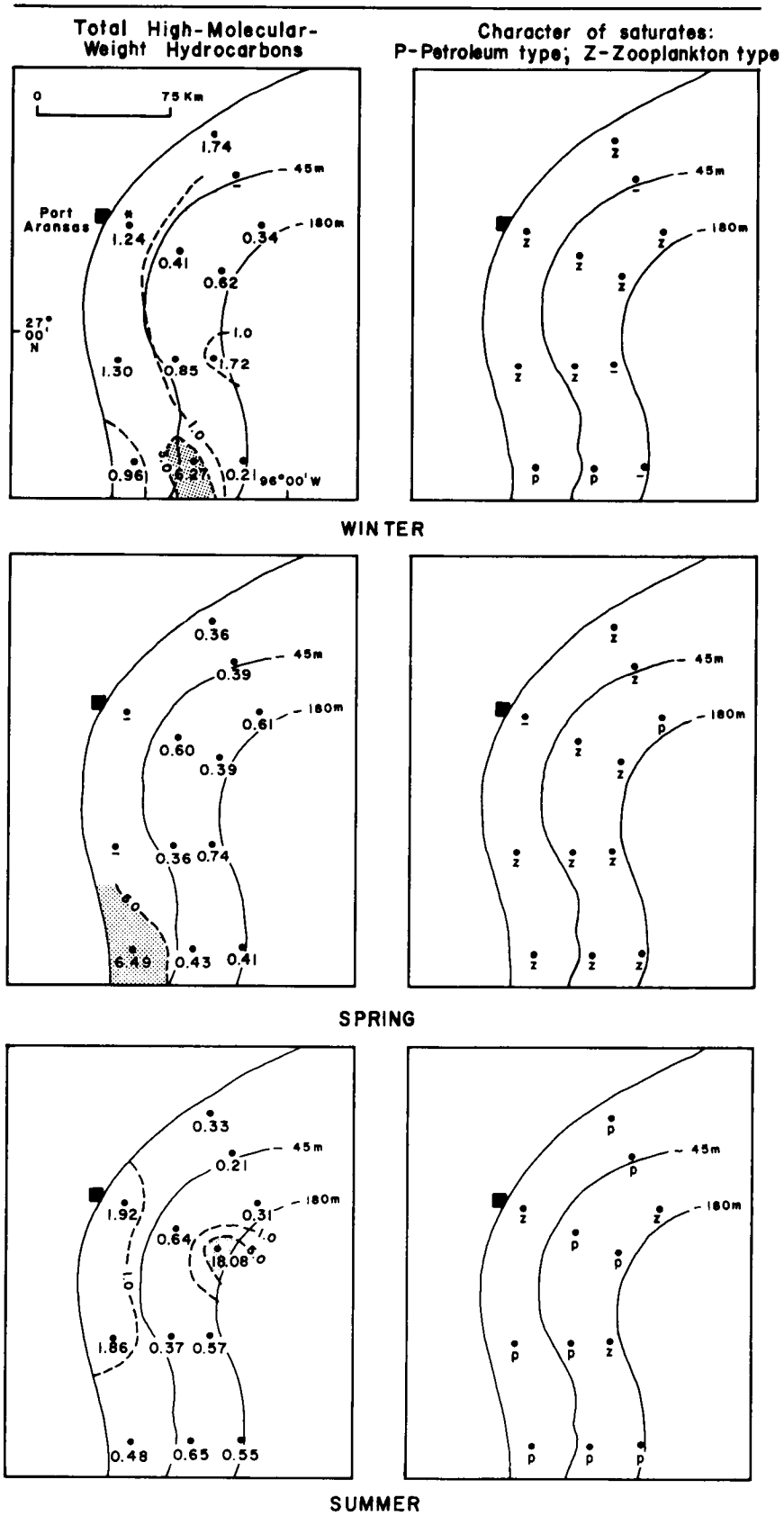

Figure 72. Seasonal distribution of total high-molecular-weight hydrocarbons in neuston (in mg/gm dry weight) and classification of analyses by hydrocarbon type: petroleum or zooplankton. Dot indicates location of sample station. Asterisk indicates probable sample contamination. Broken lines are isopleths inferred from the analyses. Shading indicates amount above regional average.

The petroleumlike saturates were more prevalent in summer samples and the zooplankton type in the spring. Other aspects of the hydrocarbons, such as pristane/phytane ratio, pristane/C_{17} ratio and C_{17}/C_{18} ratio showed no areal trends.

ZOOPLANKTON

Microzooplankton

Methods

The samples for the shelled microzooplankton studies were taken from a daytime vertical tow of a 30 cm NANSEN net (76 μm mesh), were preserved in buffered formalin and were stained with rose Bengal. Additional samples from specific water depths were taken as follows, using 30-l NISKIN bottles: at stations 1 and 2 of each transect, 10 m and one half the photic zone; at station 3 of each transect, 10 m, one half the photic zone, photic zone, between the bottom of the photic zone and the sea floor, and near the sea floor. One l of each sample was preserved unfiltered; the remainder of the sample was filtered through a 38 μm stainless steel tube screen, stained and preserved with buffered formalin.

Sediment (benthic) samples were taken from a bottom grab using a plexiglass tube to sample the surface layer. These samples were stained with rose Bengal and were preserved with buffered formalin. The sediment samples were washed through a 62 μm screen and the large fraction was saved and dried for counting and identification.

The plankton were treated with rose Bengal so that living and dead ratios could be determined by use of inverted and reflected-light microscopes.

The NANSEN net samples were split with a FOLSOM plankton splitter and one half of each sample was counted. The filters from the NISKIN bottles were washed into a plankton counting tray and an aliquot counted for the common planktonic groups.

Planktonic Foraminifera and Radiolaria

The benthic foraminifera recovered in the plankton tows appear to be largely a result of stirring of the water which caused the bottom dwellers to be swept up into the nets. However, the persistence and abundance of at least one species, Bolivina lowmani, in the plankton samples suggest that certain foraminifera known to be benthic in the adult stage are planktonic at an immature stage. Therefore, live species of foraminifera that were recovered consistently from the water column were counted as planktonic forms in the statistical results even though they may be considered strictly benthic forms in the adult stage.

The distribution of live planktonic foraminifera varied seasonally and geographically both in number of individuals and number of species. In the winter, the number of individuals counted and the number of species represented were overwhelmingly largest at the extreme northeastern edge of the OCS area and at the extreme south central part. In the spring, the number of individuals was largest in the inner shelf in the extreme northwestern part of the region; the number of species represented remained largest over the outer shelf but were reduced generally. In summer, abundance of individuals again was largest over the northern part of the shelf and the numerical distribution of species remained the same as in the spring. The abundance and diversity of live planktonic foraminifera are shown by figure 73. In summary, the

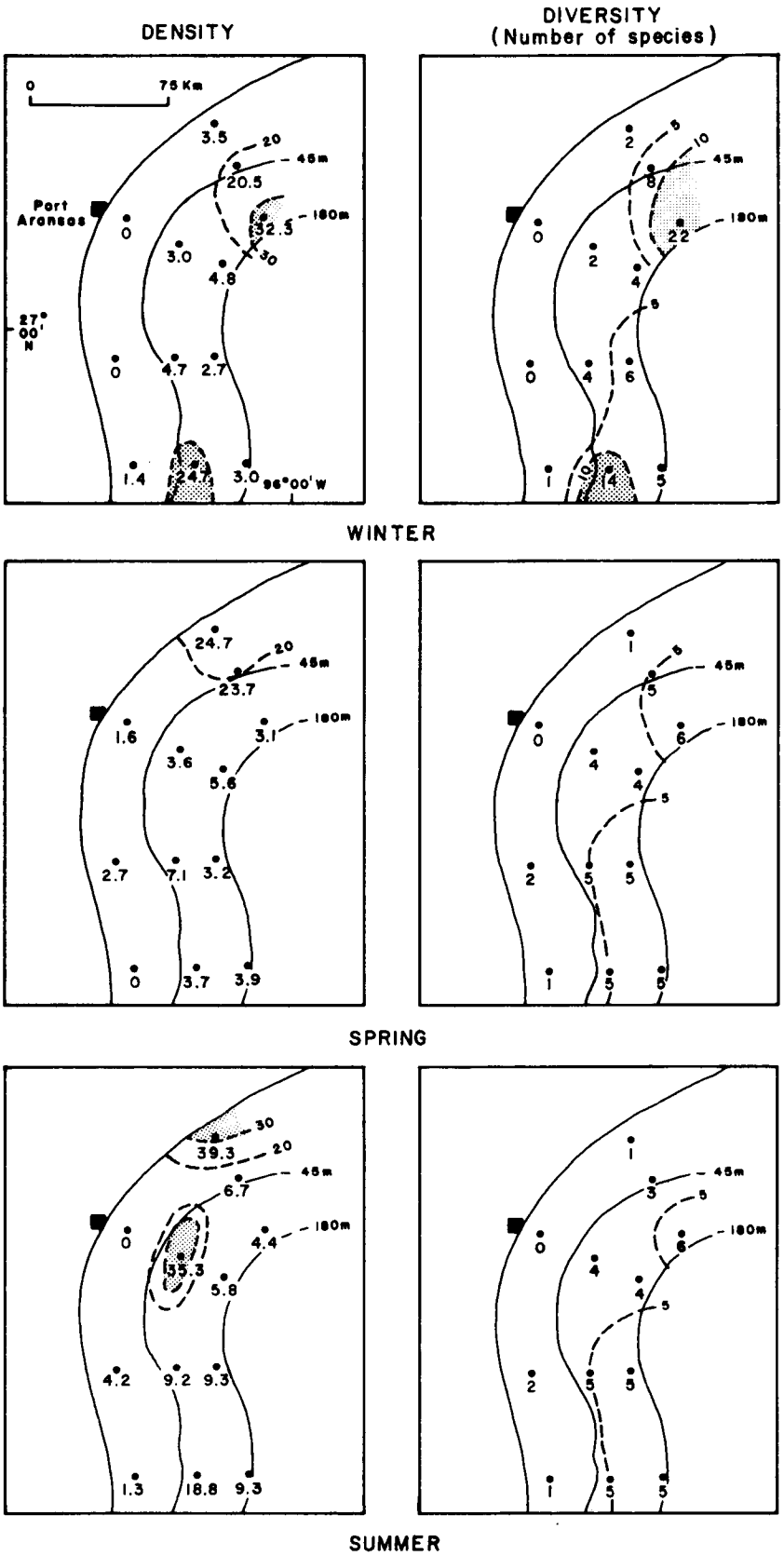

Figure 73. Seasonal abundance and diversity of live planktonic foraminifera. Density in number per m^3; diversity by number of species per net tow. Dot indicates location of sample station. Broken lines are inferred isopleths. Shading indicates amount above regional average.

abundance of patterns for live foraminifera indicated localized high concentrations that varied geographically from season to season. The greatest proliferation was in the summer on the inner shelf; the greatest diversity of species was on the outer shelf in all seasons. Distinct winter and summer foraminiferan assemblages were identified by using the clusters from an R-mode dendrogram as a guide. The winter assemblage was dominated by Globigerina falconensis and G. quinqueloba and the summer assemblage by G. bulloides and Globigerinoides ruber. The spring sampling indicated a transitional period between winter and summer; Globigerina quinqueloba was the dominant species.

The live radiolaria characteristically were most abundant and most diverse over the outer part of the OCS, but both abundance and diversity varied seasonally. The abundance was greatest in the summer at station 2 of transect II on the mid shelf; diversity, though lower than in spring and winter, remained greatest on the outer shelf. Of note is the coincidence of greatest abundance for both the radiolaria and the planktonic foraminifera at mid-shelf station 2 in the summer. The abundance and diversity of live radiolaria is shown by figure 74. The isopleths on the maps were drawn by the principal investigator responsible for the microzooplankton studies.

Distinct winter and summer assemblages also were indicated by the radiolaria. The winter assemblage was dominated by a Theopilium tricostatum-Spriocyrtis scalaris fauna and the summer by a Lamprocyclas maritalis-Euchitonia elegans fauna. The spring assemblage appears to show no real dominance; however, the Acantharian-? Acanthocyrtidium ophiurensis fauna might be considered dominant.

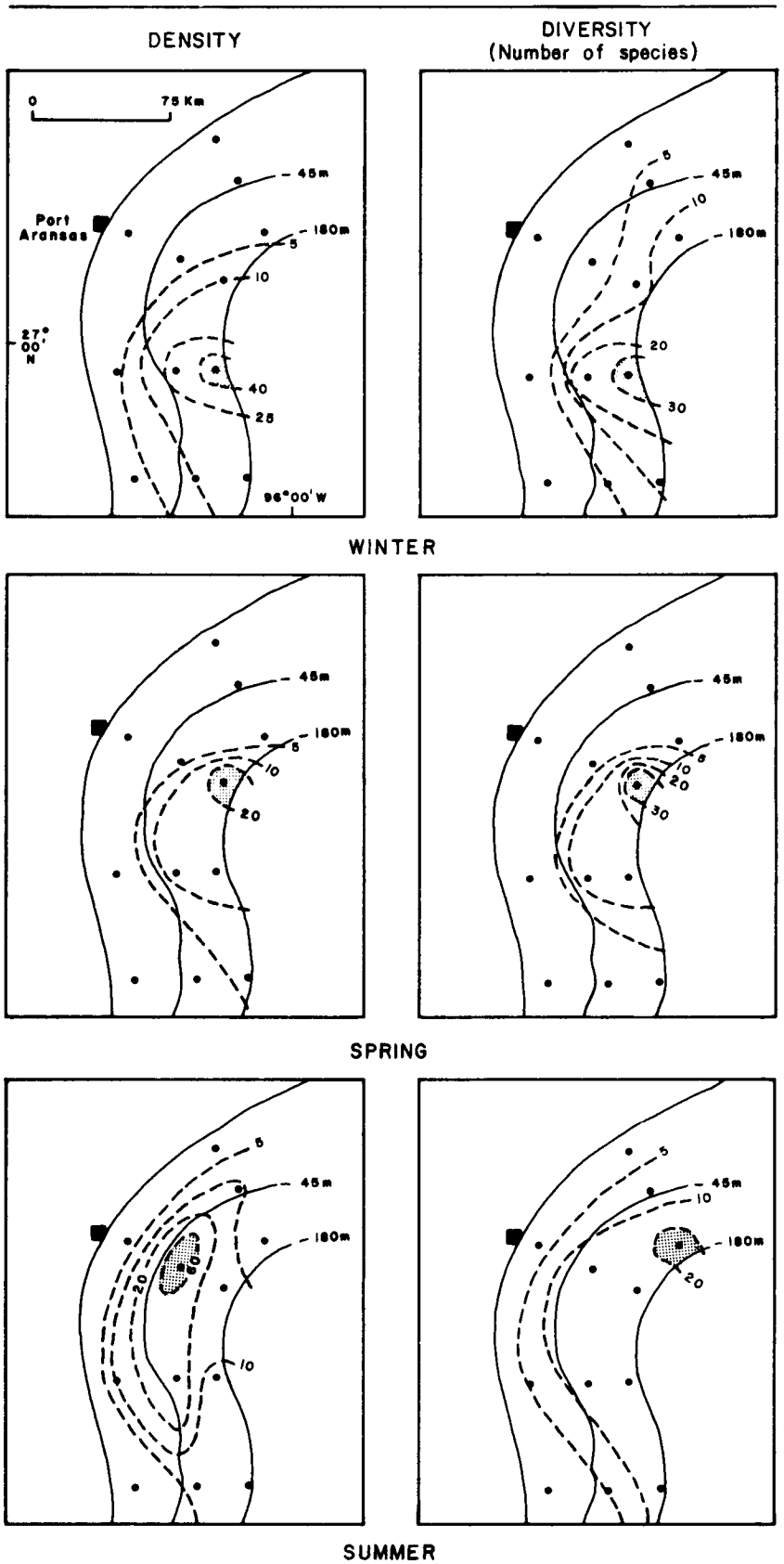

Figure 74. Seasonal abundance and diversity of live radiolaria. Density in number per m^3; diversity by number of species per net tow. Dot indicates location of sample stations. Broken lines are inferred isopleths. Shading indicates amount above regional average.

Benthic Foraminifera

Foraminifera recovered in plankton tows but considered to be benthic in the adult stage were not included in statistical summaries of benthic foraminiferal populations. Only those living species found in sediment samples were included.

As the data for the summer sampling were not available for this report, the discussion of benthic foraminifera is limited to the winter and spring. The benthic foraminifera were more uniformly distributed both in abundance and diversity than either the planktonic foraminifera or the radiolaria. The number of individuals tended to be slightly larger at mid shelf during winter and on the outer shelf during spring. No benthic forms were in the sample collected in the spring at outer shelf station 3, transect I. The benthic foraminifera were considerably more abundant than the planktonic foraminifera. The abundance and diversity of the benthic foraminifera are shown by figure 75.

In terms of species dominance, a seasonal variation was indicated. Nonionella basioloba and Brizalina lowmani were dominant winter types whereas B. spinata and species of Buliminella, Cibicides, and Fursenkoina were dominant spring types. Geographic variation also was evident. Ammonia beccarii and Brizalina lowmani were dominant in the shallower stations (18 to 26 m) in the north. Nonionella basiloba and species of Buliminella were dominant to the south. Faunal changes with depth were consistent with previous studies. R-mode cluster analysis indicated distinct inner and outer shelf assemblages and a mixed fauna at mid shelf.

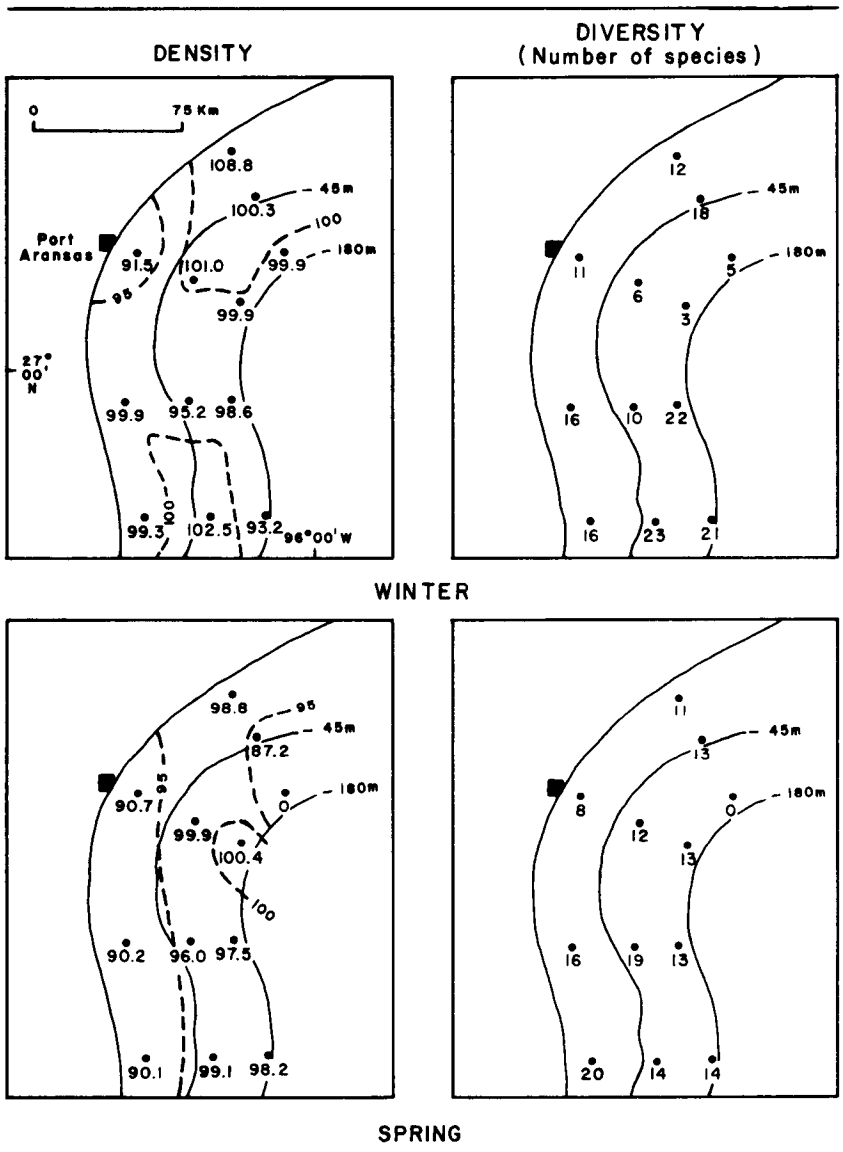

Figure 75. Seasonal abundance and diversity of live benthic foraminifera. Density in number per m^3; diversity by number of species per net tow. Dot indicates location of sample station. Broken lines are inferred isopleths. No data are available for summer samples.

Mesozooplankton

Methods

The samples for the mesozooplankton studies were collected by tows of standard 1 m NITEX nets of 233 μm mesh employing a digital flowmeter in the mouth to determine the volume of water filtered in each tow. Each station was occupied twice: once during the day and once at night. Two samples were taken during each occupation yielding four samples per station for each sampling period. The entire water column was sampled from near bottom to surface by oblique tows of about 15 minutes duration. A time-depth recorder was used to determine the maximum depth of sampling. The contents of the cod end were drained through a 100 μm NITEX net, were transferred to a jar and were preserved in buffered formalin.

In the laboratory, the samples were passed through a FOLSOM plankton splitter to achieve adequate subsamples for analysis and archiving. The subsample for biomass determination was adjusted to the capacity of a 50 ml crucible. As the samples varied in size, the subsample used for biomass ranged from a 1/64 to a 1/4 aliquot, depending on the original size of the sample.

Determinations of volume were made after large organisms were removed. The large organisms then were returned for determination of dry weight and dry organic weight. During vacuum filtration, a constant pressure of about 15 in mercury generally was maintained until water droplets ceased to form on the side of the filtration crucible. After measuring the displacement volume by filling up the filtration crucible with fresh water, the subsample was drained again by vacuum filtration and dried in the same crucible to

a constant weight at 55°C. After determining the dry weight, the subsample was ashed in a muffle furnace at 550°C to obtain the ash weight.

The size of subsample examined for species and abundance varied from 1/4096 to 1/64; the number of zooplankters in the subsamples varied from 660 to 5405. Each subsample was sorted into major taxonomic components which were placed in separate dishes for further taxonomic and quantitative analysis. The copepods were most intensively studied. They were first separated into three suborders (Calanoida, Cyclopoida and Harpacticoida) and then each suborder was separated into adult females, males and immature forms. All adult female copepods were identified to the species level and their numbers recorded for each species. In addition to the subsamples noted above, a large part of the remaining sample, usually about half of the original sample, was examined in a BOGOROV plankton sorting tray for copepod species that were not represented in the subsample.

Abundance and Composition

The biomass in all transects increased consistently from the deep to shallow stations. The increase was particularly steep in the spring and summer months when the mesozooplankton population was greatly increased at the shallow stations. Averaged over the three periods of sampling, the biomass was largest at station 1 of transect I, and of the four transects, transect III had the smallest biomass.

The number of mesozooplankters per m^3 of filtered water was closely proportional to the biomass and varied from 166 to 10,840. As in the biomass, numerical abundance increased markedly from deep to shallow stations. The increase was most pronounced along transect I during the spring sampling

when the population at station 1 was extremely large. The abundance and distribution of the mesozooplankters are shown by figures 76 and 77. The daytime counts are shown by figure 76 and the nighttime counts, by figure 77. The numerical abundances shown by the figures are broken down into three categories: total organisms, copepods and other. The other category includes Ostracoda, Mollusca (mainly veliger larvae), Chaetognatha and Larvacea.

In all samples, the Copepoda were the most abundant group, making up approximately 70 percent of the mesozooplankton by number. Although the numbers of copepods increased markedly from deep to shallow water as a consistent pattern, differences from north to south also were apparent. In the winter, copepod population decreased from south to north; in the spring and summer numbers were substantially larger in the northwestern part of the OCS. A total of 182 species of copepods were identified, including 118 species of calanoids, 57 species of cyclopoids and 7 species of harpacticoids. Contrary to the population trend indicated by numbers of individuals, the number of species increased considerably from shallow to deep water.

The most abundant species of copepods were Paracalanus indicus, P. quasimoto and Clausocalanus furcatus. The first two species listed increased shoreward in abundance; the third increased seaward in abundance. Acartia tonsa, an estuarine or nearshore species, was an important component at the shallow stations. The greatest abundance of mesozooplankton recorded during the 1975 study (station 1, transect I) was due mainly to the increase of Acartia tonsa.

Of the other types of organisms, Mollusca, made up mainly of veliger larvae, were most abundant at the shallow stations. The Chaetognatha and

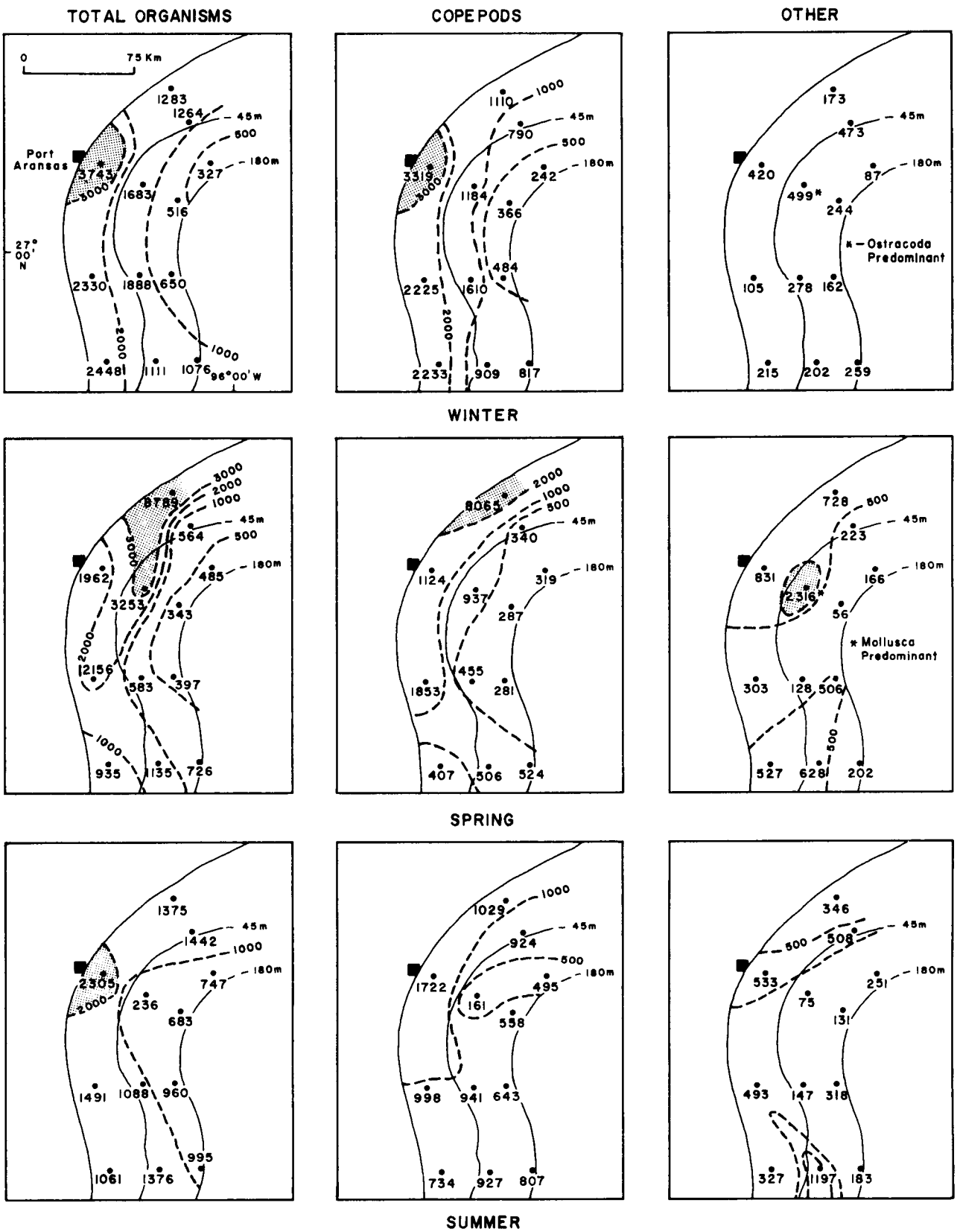

Figure 76. Seasonal abundance and distribution of mesozooplankton during day tows (in number per m^3). Number is average of replicate samples for each station. Tows were oblique, bottom to surface. Dot indicates location of sample station. Broken lines are inferred isopleths. Shading indicates amount above regional average.

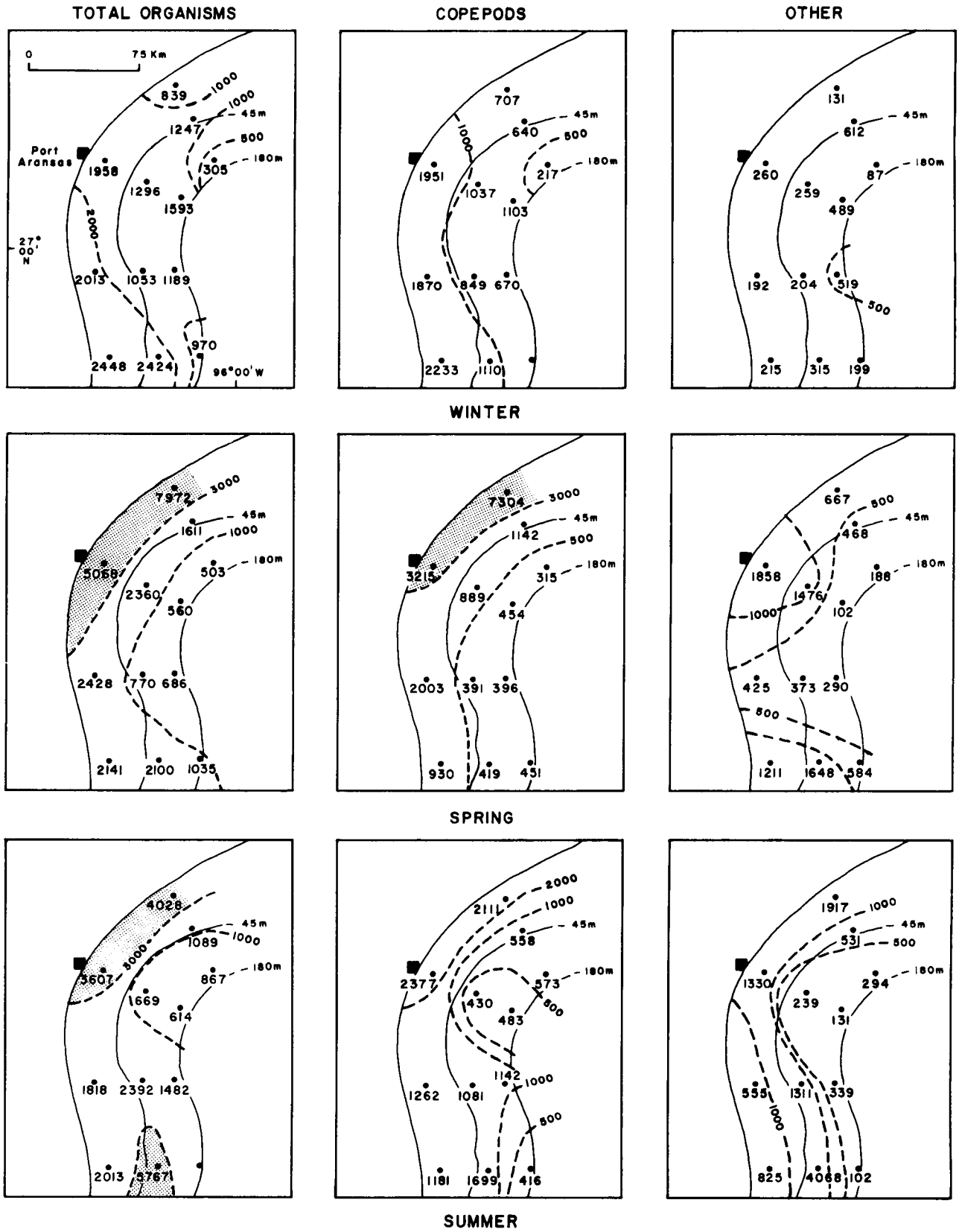

Figure 77. Seasonal abundance and distribution of mesozooplankton during night tows (in number per m^3). Number is average of replicate samples for each station. Tows were oblique, bottom to surface Dot indicates location of sample station. Broken lines are inferred isopleths. Shading indicates amount above regional average.

Larvacea were persistent throughout the OCS in all sampling periods and did not show any conspicuous variations either in geographic or seasonal distribution. The Ostracoda, however, showed a highly regionalized spatial distribution: the largest numbers consistently were at the stations of intermediate depth and abundance shifted southward as the seasons progressed from winter to late summer. Taking into consideration all 12 stations, station 2 of transect IV had the largest number of Ostracoda. The Ostracoda all belonged to the species Euconchoecia chierchiae.

Historical Mesozooplankton

The historical samples for mesozooplankton were collected by the Bureau of Commercial Fisheries (now NMFS) over the 3 year period 1963 to 1965. The sample coverage was limited to four stations along a single transect running south-southeast from Port Aransas (fig. 78, map A).

The samples were processed for analysis using the same procedures and employing the same techniques that were used for the baseline samples collected in 1975. As in the case of the baseline samples, the copepods were studied most intensively.

The number of mesozooplankters in the historical samples varied considerably from month to month. The range in abundance at each of the four stations during the 3 year period is as follows:

Total Mesozooplankton Organisms

Station	Range
W24	259-6288
W23	507-4268
W22	165-5028
W58	136-4435

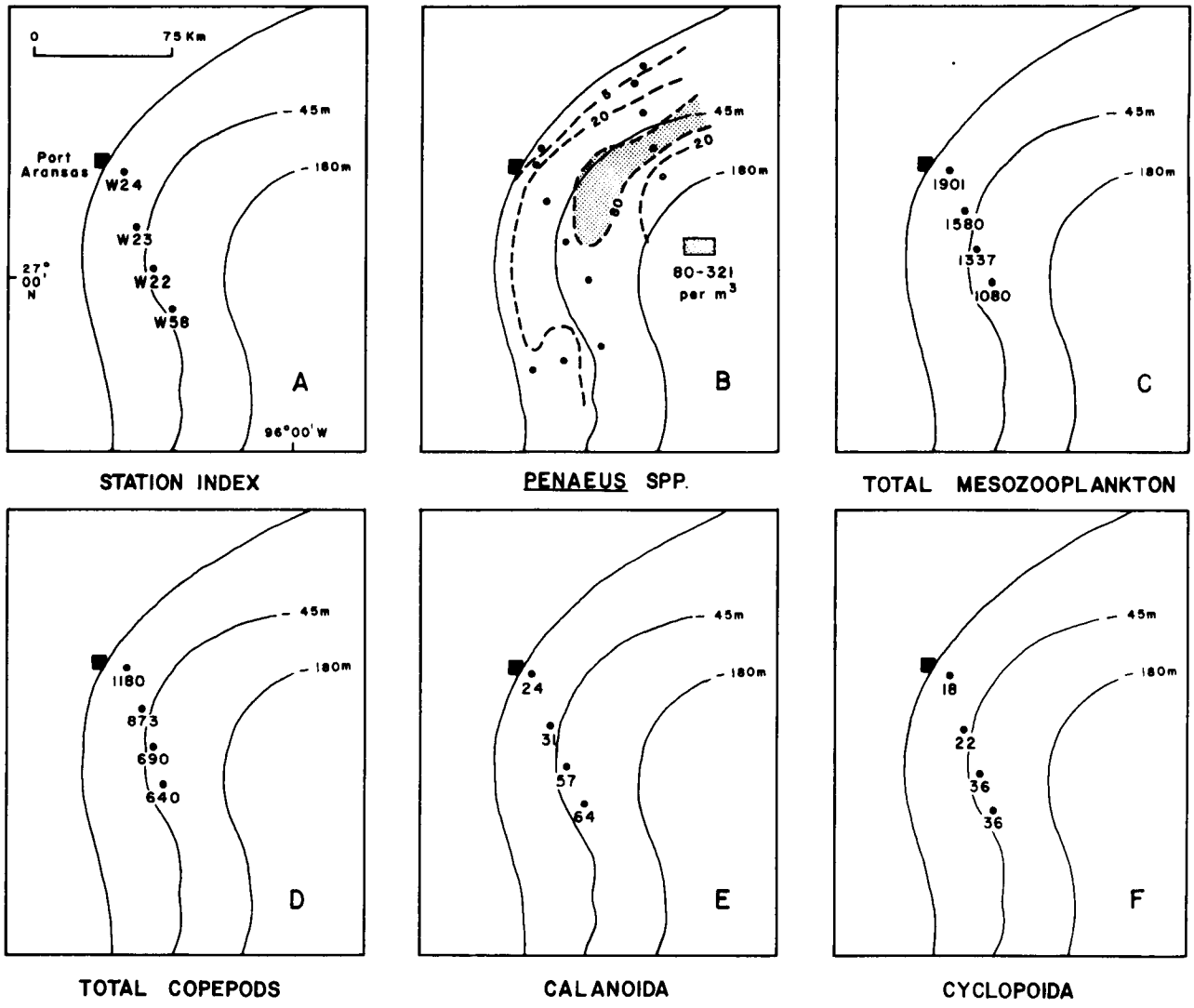

Figure 78. Average abundance of mesozooplankton and of the shrimp larvae (Penaeus spp.) for the period 1963-1965. Abundance (in number per m^3) based on monthly catches. Dot indicates location of sample station. Broken lines are inferred isopleths. Shading indicates area of greatest abundance.

The averages for the 3 years at each station are on figure 78, map C. The averages show a gradual decrease of mesozooplankton from the shallow to deep stations and thus indicate the same trend as shown by the data for 1975. The historical data show no definable seasonal pattern at any station. The largest temporal fluctuation was at the shallowest station (W24), and the three offshore stations were more or less similar in the magnitude of fluctuations. At station W24, peaks of abundance were in the summer-fall period during the first 2 years, 1963-1964, and at the three offshore stations, peaks were recorded more often in the spring (April-May) than in any other season. At all the stations, peaks commonly were followed by a sudden drop, which was in turn succeeded by an abrupt increase, giving a picture of short-term, irregular fluctuations.

The proportions and abundance of the several components comprising the mesozooplankters in the historical data are comparable to the 1975 data. Copepods make up about 70 percent of the total organisms. The other relatively abundant groups were the Ostracoda, Larvacea, Mollusca and Chaetognatha; all of them showed extensive and irregular temporal variations. The Larvacea and Chaetognatha occurred regularly in large numbers and showed no obvious variation in abundance among stations. However, the Ostracoda were abundant only at the two deeper stations and the Mollusca were abundant only at the two shallower stations. The Ostracoda consisted mainly of the species Euconchoecia chierchiae and the Mollusca were mainly veliger larvae.

The trend of temporal variation for most copepods was similar to that for the total mesozooplankton at all stations. The range in numbers per m^3 over the 3 year period was as follows:

Copepod Abundance

Station	Range
W24	118-4385
W23	312-2095
W22	82-1640
W58	94-2379

The average numbers at each station for the 3 year period are shown by figure 78, map D. The averages for the copepods showed the same decrease from shallow to deep stations as did the total mesozooplankton. The most abundant suborder of copepods was the Calanoida. The Cyclopoida were second in abundance.

The number of copepod species identified at each station are as follows:

Number of Copepod Species

Station	Calanoida	Cyclopoida	Harpacticoida	Total
W24	24	18	2	44
W23	31	22	3	56
W22	57	36	7	100
W58	64	36	4	104

The areal distributions of mesozooplankton by station are shown by figure 78. Contrary to the trend of numerical abundance, the number of copepod species increased considerably from shallow to deep water. The most abundant species at all the stations were Paracalanus indicus and P. quasimoto. The species Clausocalanus furcatus and Oithona plumifera were most abundant at the deeper stations; the species Acartia tonsa, Paracalanus crassirostris and Oithona nana were most abundant at the shallowest station.

The general trends of overall abundance, numbers of species and seasonal variations, shown by the 1963 to 1965 data, are similar to those shown by the

1975 data. The two sets of data are strongly complementary in indicating the regional depth characteristics of the mesozooplankton.

Historical Larval Shrimp (*Penaeus* spp.)

Between February 1962 and December 1965, monthly sampling for the three species of penaeids, white (*Penaeus setiferus*), brown (*P. aztecus*), and pink (*P. duorarum*) was conducted by the Bureau of Commercial Fisheries (NMFS) at the 13 stations shown on figure 78, map B. The regional range in average abundance of *Penaeus* spp. for the 1962 to 1965 period also is shown.

The characteristics of distribution for *Penaeus* spp. summarized by the map can be related to specific water depths and to seasons. In the depth range of 7 to 14 m, the larvae occurred between April and October, with spring and fall peaks in abundance apparently following the spawning seasons for the white shrimp. At the intermediate depths of 23 to 82 m, the larvae generally occurred throughout the year with peaks of abundance in the spring and late fall to early winter. Larval abundance was greatest in the fall/early winter peak, occurring slightly later as depth increased. Based on knowledge of the bathymetric range of adult shrimp of the genus *Penaeus*, the larval abundance at intermediate depth appear to reflect spawning of the brown shrimp. During the winter at depths of about 110 m, the trend in larval abundance was poorly defined because of small catches, but the trend did approximate the one indicated at the intermediate depth.

Comparison of catches of *Penaeus* spp. larvae by depth zones over the 4 year period indicated that the largest numbers were in water depths of about 46 m. Smallest catches were in the deepest water. *Penaeus* spp. larvae

occurred throughout the area but were most abundant geographically over the middle of the continental shelf (fig. 78B).

Ichthyoplankton

Methods

The method of collection for the fish eggs and larvae was similar to that for the mesozooplankton. The plankton in the cod end of the net were drained through a 100 µm mesh screen and were transferred immediately to a jar containing about 7 percent buffered formalin in seawater.

All aliquots used for the ichthyoplankton study consisted of one half of the total sample, except for the day and night samples for cruise 1 at station 3, transect I, where one quarter of the sample was used. The numbers noted in the discussion that follows have been converted to represent the whole sample. Fish eggs and larvae were counted, measured and classified to the lowest possible taxon. Most of the fish eggs could not be specifically identified although some were identified to family.

Abundance and Composition

During the 1975 study, a total of 78,378 fish larvae and 57,816 eggs were collected. Abundance of both was greatest in the summer sampling period when 44 percent of the total larvae and 40 percent of the total eggs were collected. Numbers of eggs were smallest in the spring and numbers of larvae were smallest during the winter. The majority of eggs (60 percent) and larvae (71 percent) were collected at night. The statistics indicate that abundance of both larvae and eggs followed a seasonal pattern and that

abundance was greatest in the night samples. The seasonal patterns of abundance for fish eggs are shown by figure 79 and those for the fish larvae, by figure 80.

The maps show distinct patterns for fish eggs and fish larvae both seasonally and for day and night, but differences are evident. In the winter and spring, abundances of fish eggs were markedly localized. The largest number of fish eggs were counted in the spring off Port Aransas. In the summer, the fish eggs were not only more uniformly abundant, but day and night patterns were similar, both showing a rapid and uniform decrease in abundance seaward. The summer distribution probably indicates the primary fish spawning season.

The overall patterns of abundance for the fish larvae are notably different from those of the fish eggs and day/night patterns are distinctly different. In winter larval abundance was significantly low at inner shelf stations. In the spring, numbers generally were largest along the inner shelf and in summer the pattern was similar, but overall abundance was greater. The seaward decrease in numbers of larvae was less abrupt than for fish eggs.

The numbers for the seven most dominant and widely distributed families represented by the fish larvae have been plotted to demonstrate diversity characteristics as well as seasonal and geographic variations. The families are anchovies (Engraulidae), sea basses (Serranidae), mackerel and tuna (Scombridae), drums (Sciaenidae), flounder (Bothidae), herring (Clupeidae) and codlets (Bregmacerotidae). The abundance and distribution of larvae for the seven families, by season and by day versus night, are shown by the series of maps on figures 81 through 87. The patterns of distribution are

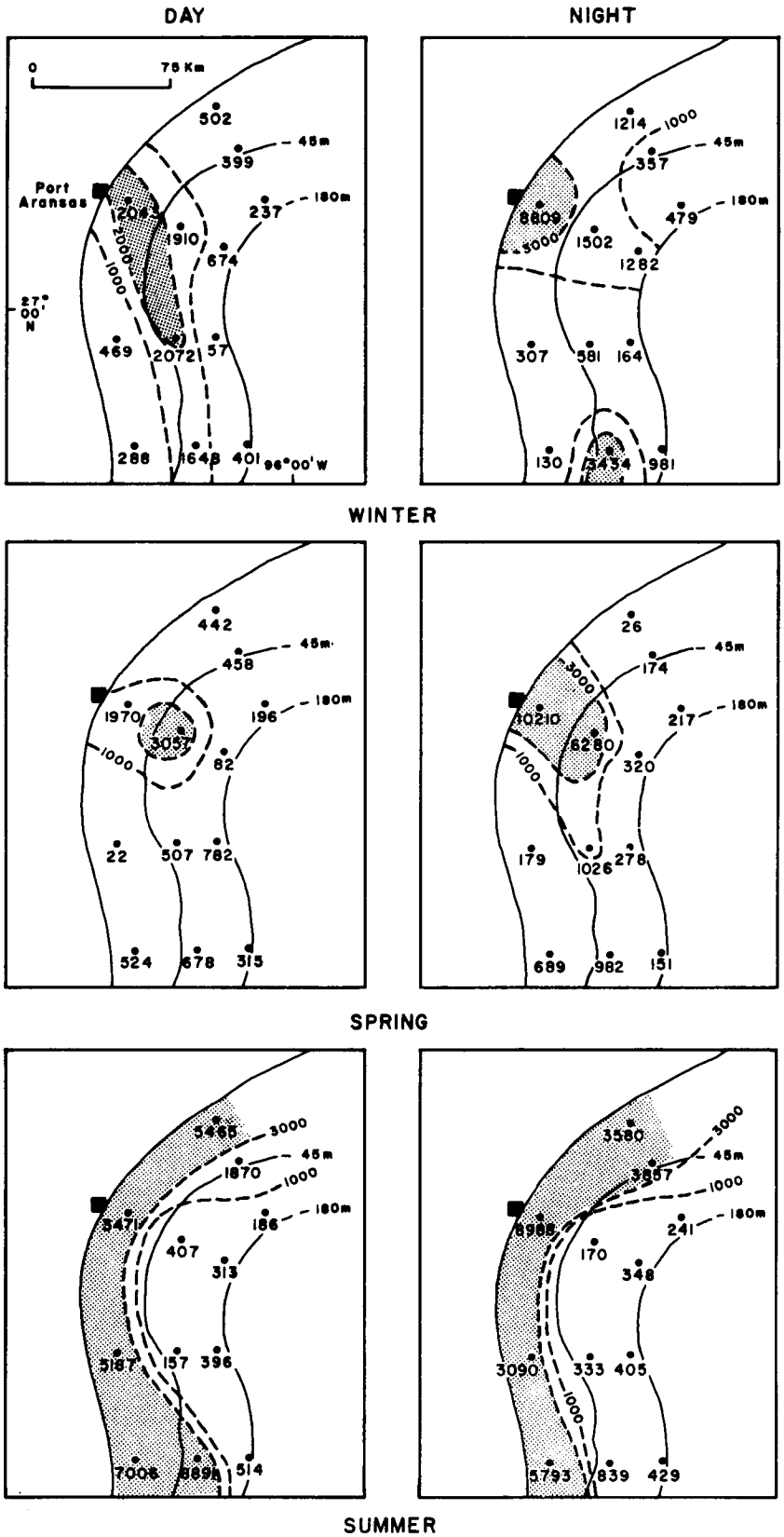

Figure 79. Seasonal abundance and distribution of fish eggs (in number per 1000 m^3; by day and night). Dot indicates location of sample station. Broken lines are inferred isopleths. Shading indicates amount above regional average.

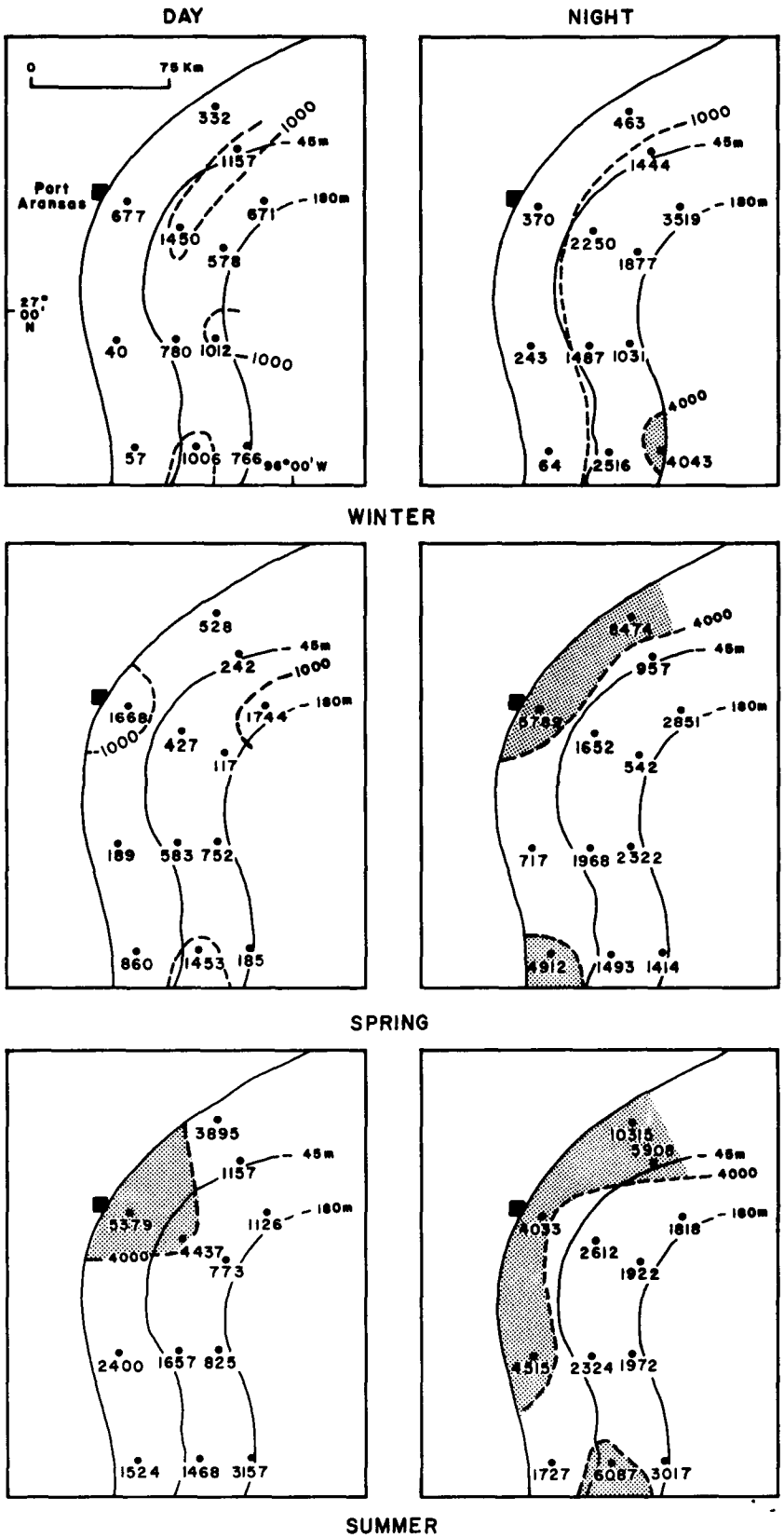

Figure 80. Seasonal abundance and distribution of fish larvae (in number per m^3; by day and night). Dot indicates location of sample station. Broken lines are inferred isopleths. Shading indicates amount above regional average.

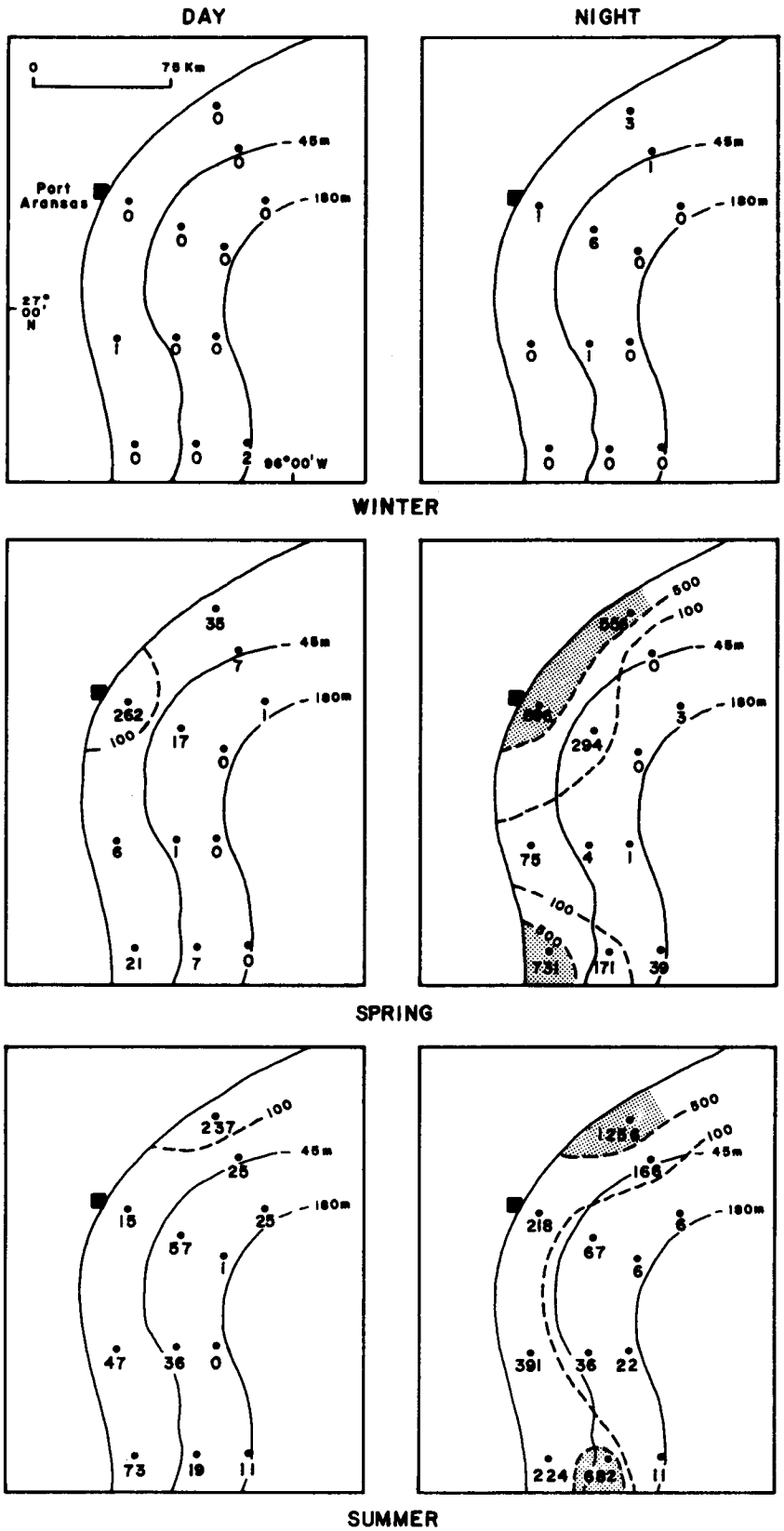

Figure 81. Seasonal abundance and distribution of larvae of the fish Family Engraulidae (in number per 1000 m^3; by day and night). Dot indicates location of sample station. Broken lines are inferred isopleths. Shading indicates amount above regional average.

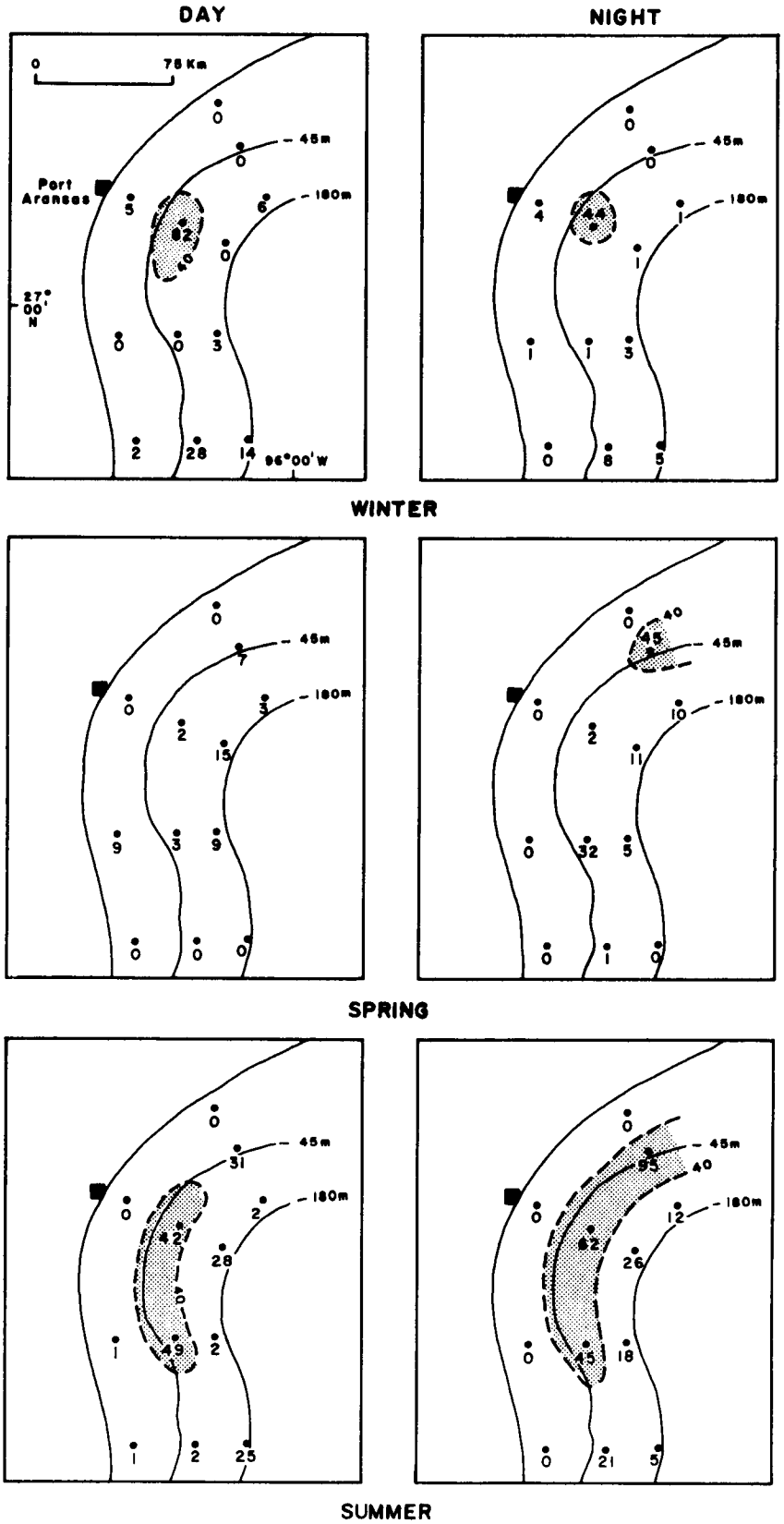

Figure 82. Seasonal abundance and distribution of larvae of the fish Family Serranidae (in number per 1000 m^3; by day and night). Dot indicates location of sample station. Broken lines are inferred isopleths. Shading indicates amount above regional average.

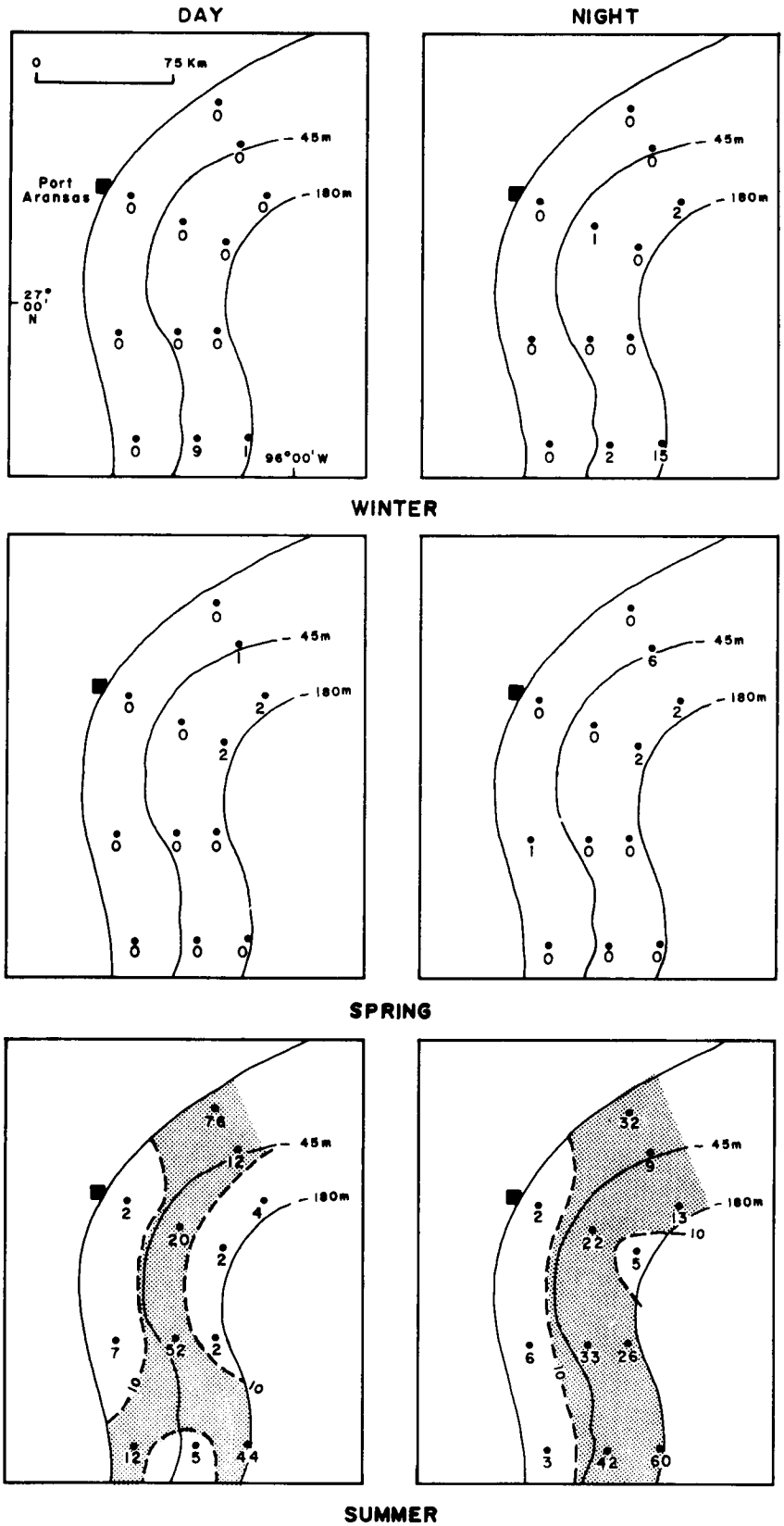

Figure 83. Seasonal abundance and distribution of larvae of the fish Family Scombridae (in number per 1000 m^3; by day and night). Dot indicates location of sample station. Broken lines are inferred isopleths. Shading indicates amount above regional average.

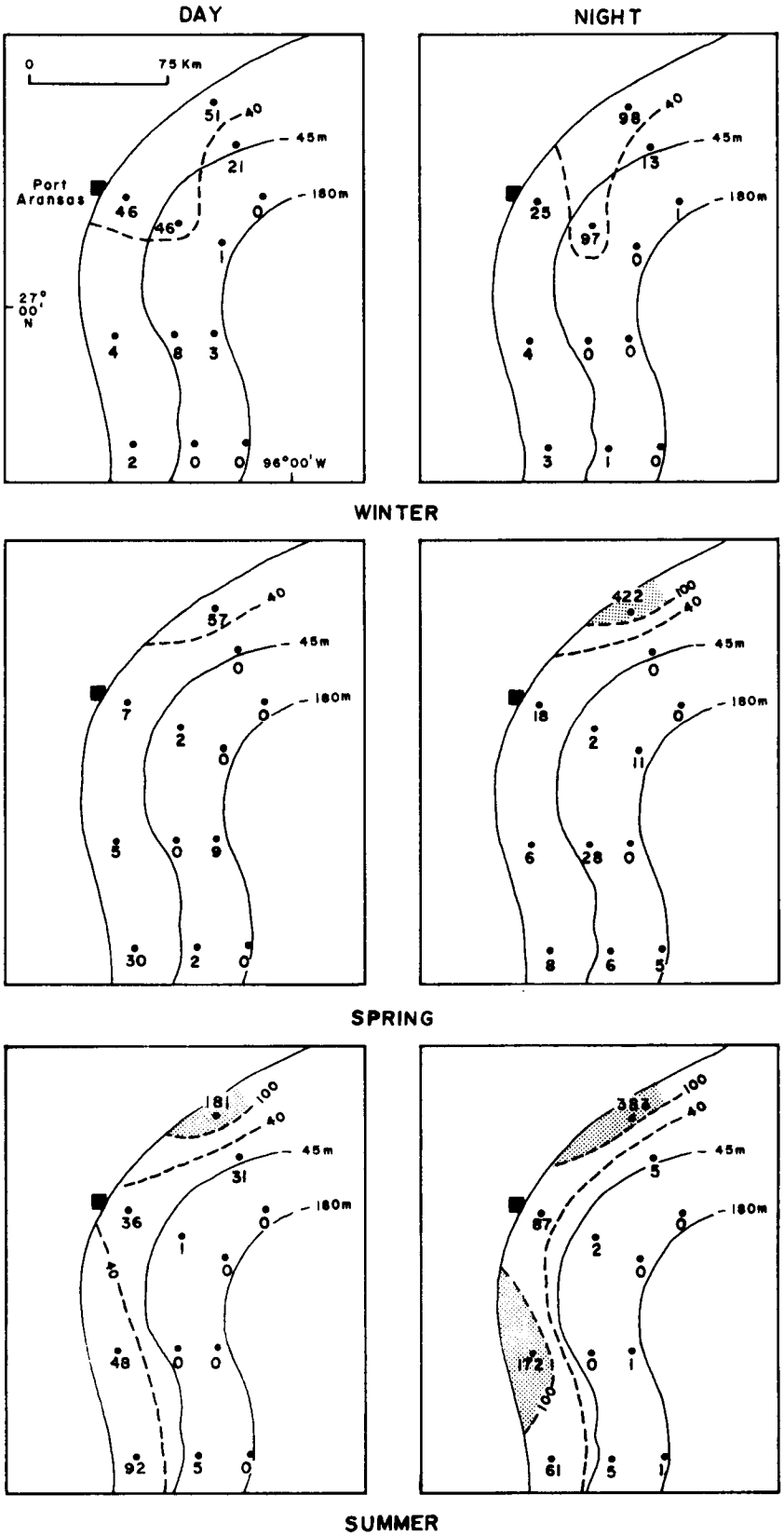

Figure 84. Seasonal abundance and distribution of larvae of the fish Family Sciaenidae (in number per 1000 m^3; by day and night). Dot indicates location of sample station. Broken lines are inferred isopleths. Shading indicates amount above regional average.

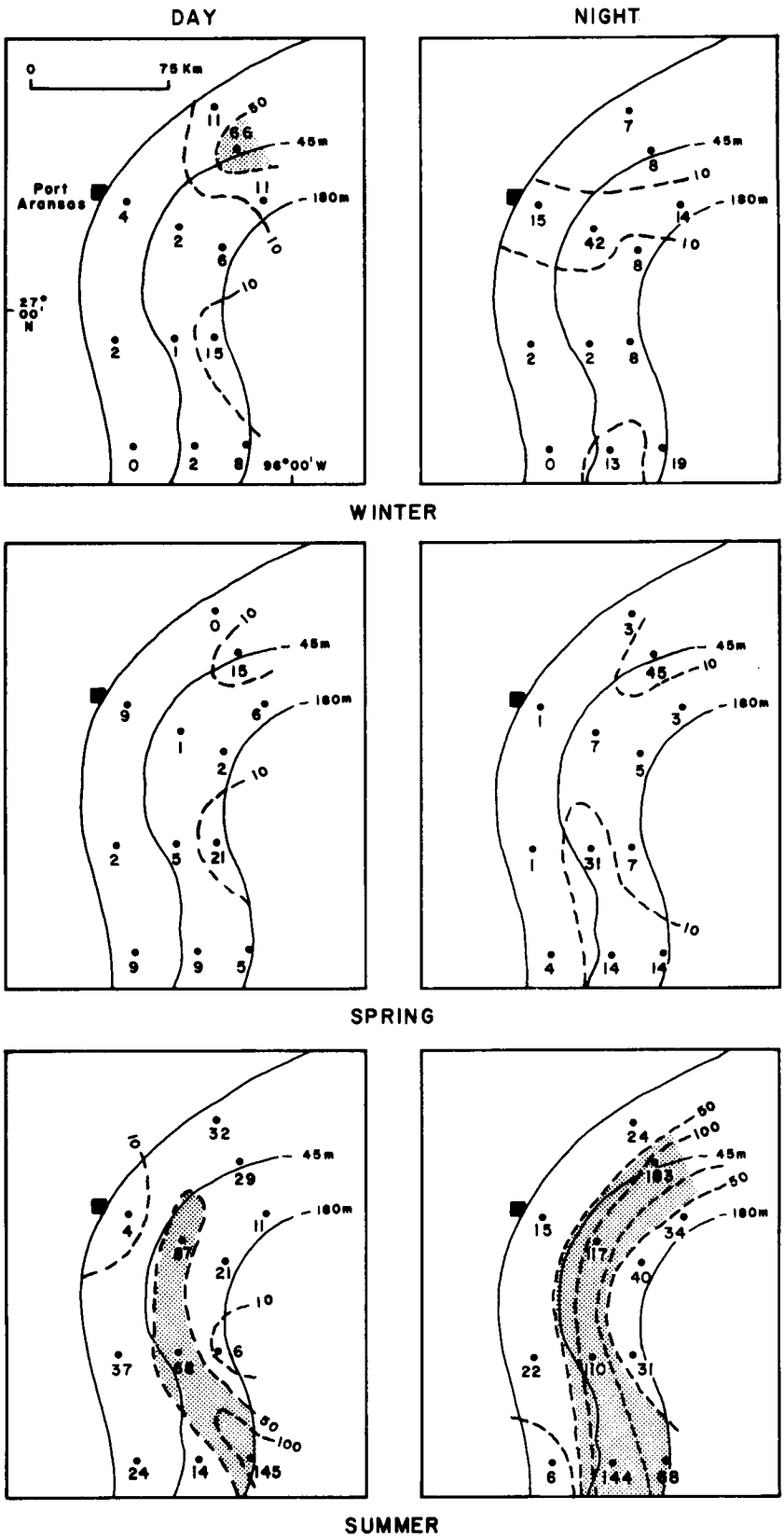

Figure 85. Seasonal abundance and distribution of larvae of the fish Family Bothidae (in number per 1000 m^3; by day and night). Dot indicates location of sample station. Broken lines are inferred isopleths. Shading indicates amount above regional average.

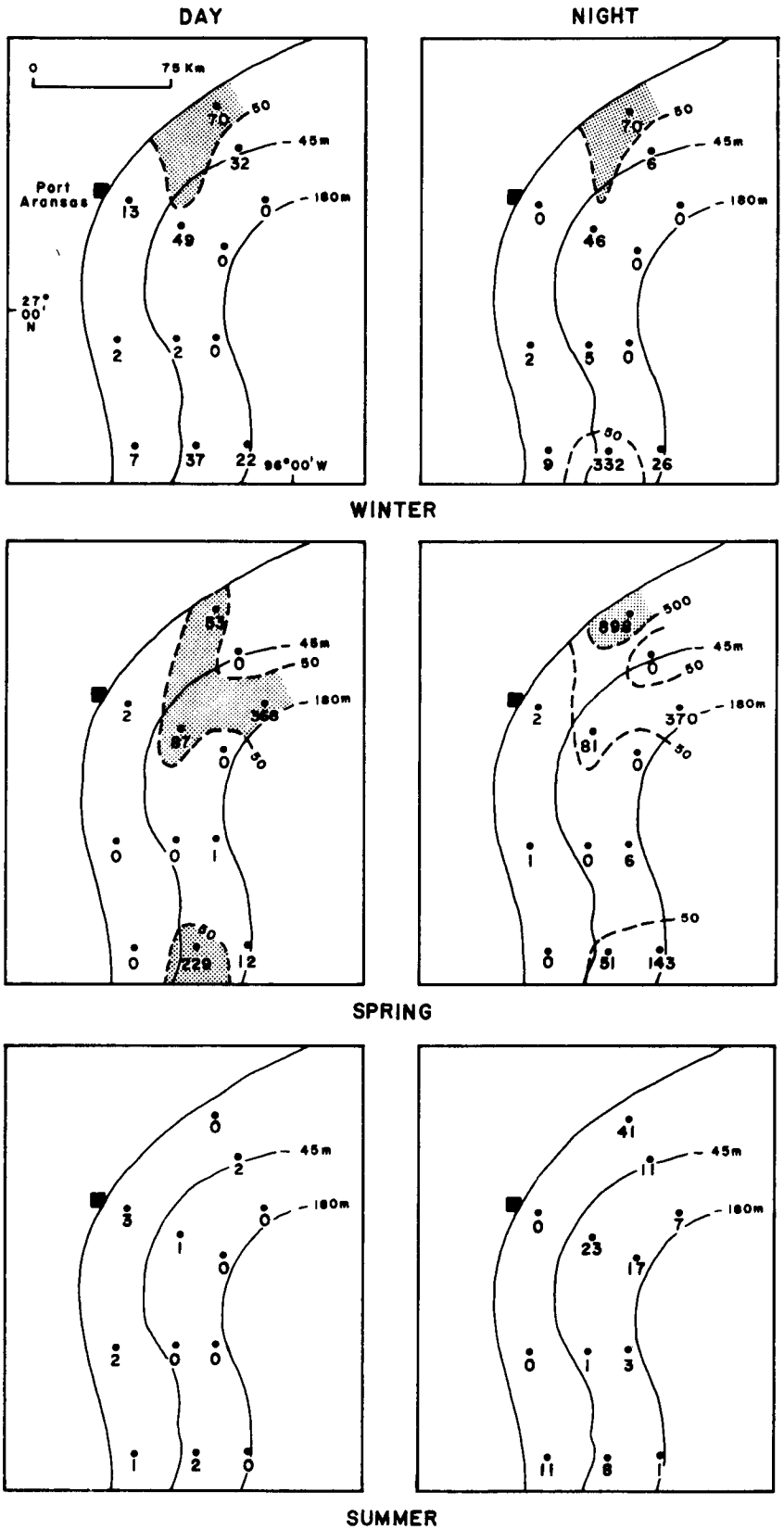

Figure 86. Seasonal abundance and distribution of larvae of the fish Family Clupeidae (in number per 1000 m^3; by day and night). Dot indicates location of sample station. Broken lines are inferred isopleths. Shading indicates amount above regional average.

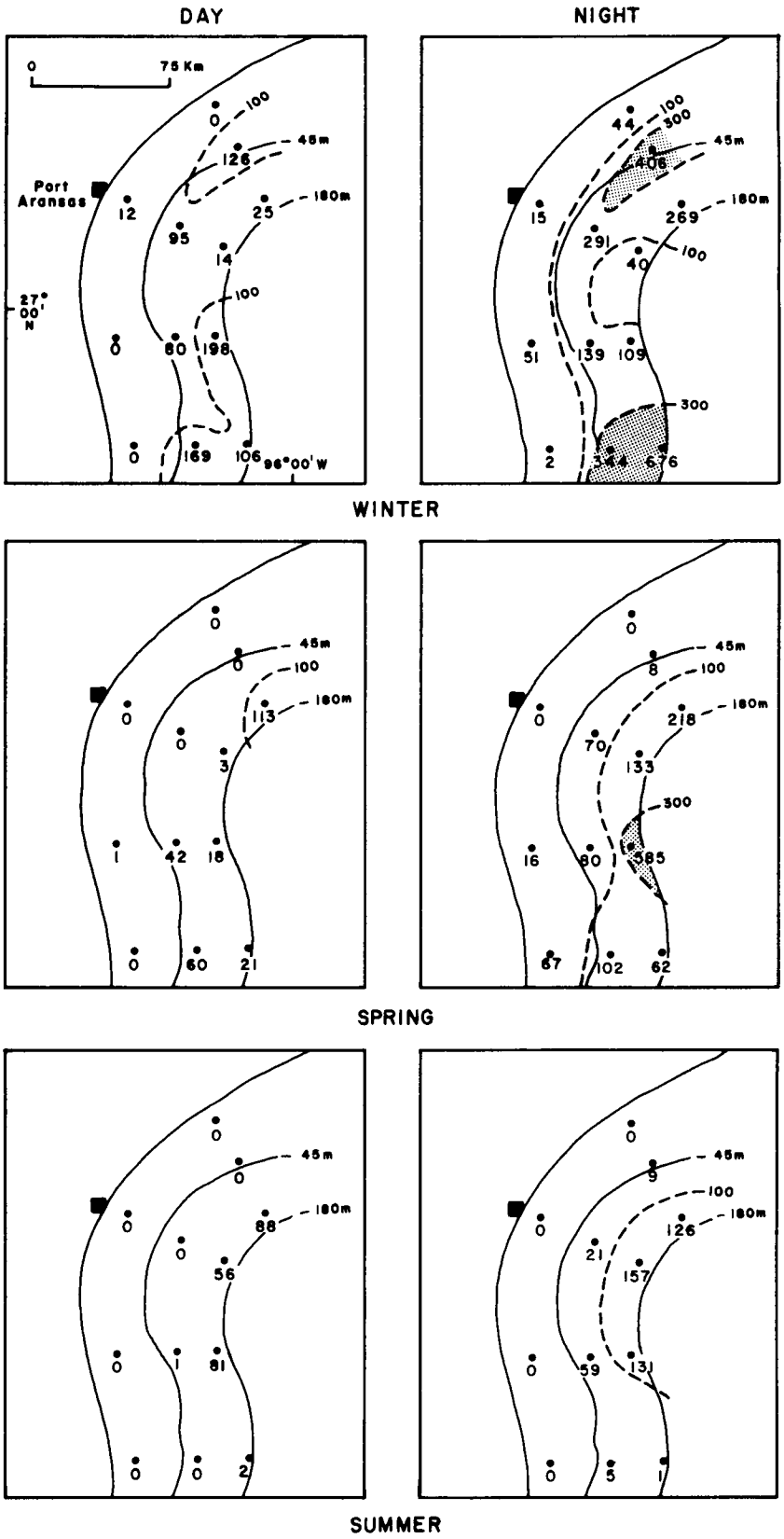

Figure 87. Seasonal abundance and distribution of larvae of the fish Family Bregmacerotidae (in number per 1000 m^3; by day and night). Dot indicates location of sample station. Broken lines are inferred isopleths. Shading indicates amount above regional average.

self-explanatory. Very distinct regional seasonal and diurnal characteristics are evident.

A separate study of the abundance and distribution of the King mackerel and Spanish mackerel larvae that included five sampling periods was made by the National Marine Fisheries Service, Galveston. The study covered the central sector of the South Texas OCS off Port Aransas. A total of 199 larvae were collected during the five sampling periods. The King mackerel larvae were by far the most abundant. The abundance and distribution of the King mackerel (Scomberomorus cavalla) larvae are shown by figure 88. Of the 32 Spanish mackerel larvae (S. maculatus) collected, most were from the two sets of stations nearest shore and seasonal distribution was relatively uniform.

Trace Metals in Mesozooplankton

Methods

In the laboratory, the mesozooplankton samples were thawed and poured onto a 200 μm NITEX nylon screen which had been laid over a series of paper towels. The samples were then gently squeezed with the flat side of a stainless steel spatula to remove as much moisture as possible.

The wet samples were placed in preweighed polypropylene beakers and weighed to determine the wet sample weight. They were then placed in a freeze drier for periods of 24 to 96 hours to remove all moisture. After removal from the freeze drier, the samples were reweighed to determine weight loss, and the percentage of moisture in each sample was calculated. The samples were then ground to a fine powder by a combination of an initial grinding and homogenization with two porcelain beads in a porcelain container

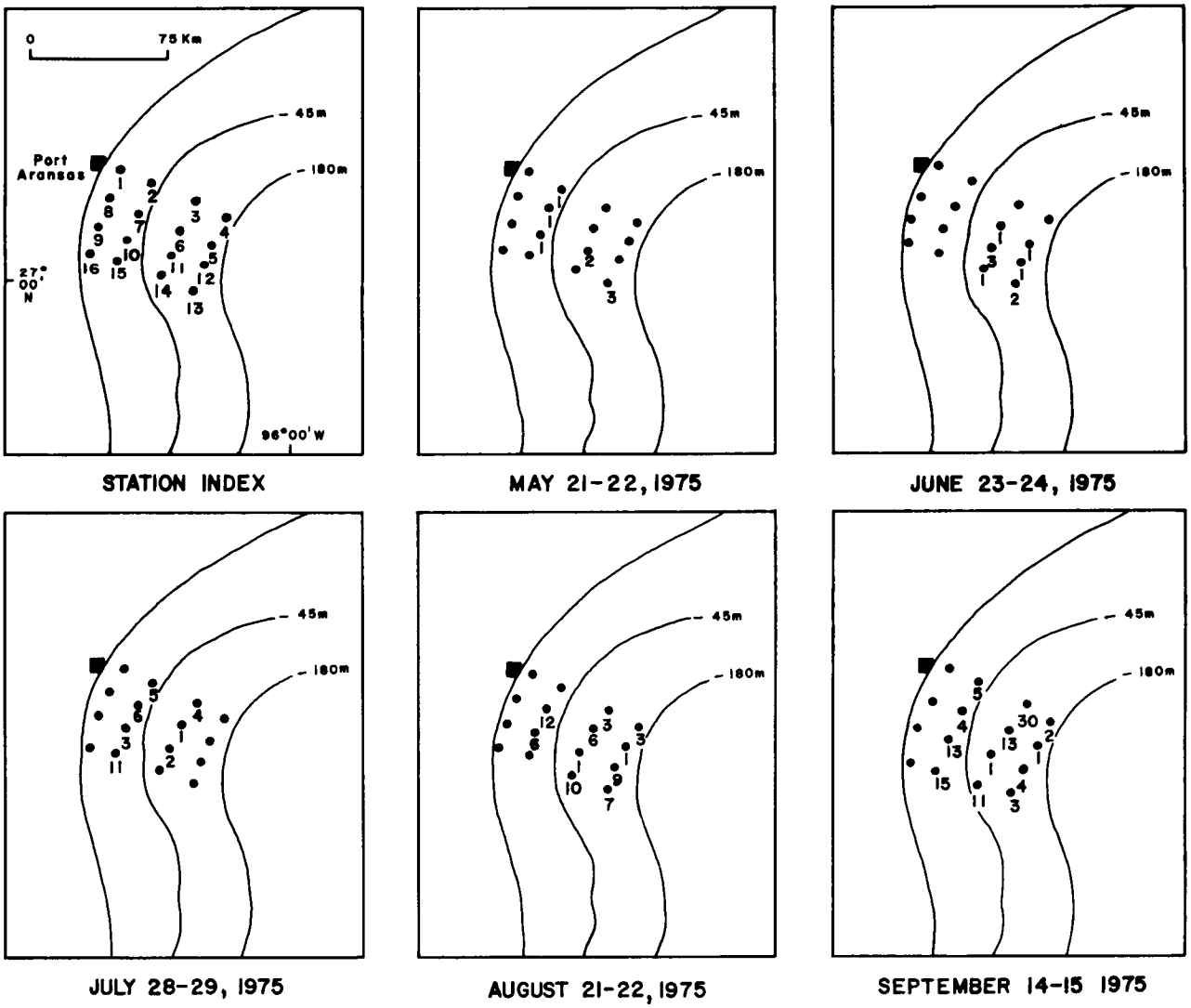

Figure 88. Abundance and distribution of King Mackerel larvae (Scomberomorus cavalla) over the central sector of the South Texas OCS. Dot indicates location of sample station. Absence of a number at a station indicates no larvae in the sample.

placed in a SPEX mixmill. The dried and homogenized samples were then stored in plastic vials inside a dessicator until they could be analyzed.

A 1 gm sample aliquot was weighed in a 200 ml tall-form beaker and was placed on a hot plate; 10 ml of a 3 to 1 concentrated HNO_3:$HClO_4$ mixture per gram of sample was added by automatic pipette and a watch glass was placed on top of the beaker. The beakers were heated at moderate temperatures and the solutions were allowed to reflux until nearly dry, generally a period of 2 to 3 hours. The residues in the beakers were washed into sample containers through WHATMAN number 40 filter paper with two or more 2 ml aliquots of water. The solutions were increased to a 10 ml volume with water. Blanks were prepared for each set of samples digested by adding 20 ml of the 3 to 1 HNO_3:$HClO_4$ mixture to tall-form beakers following the same procedure as that used for the samples.

The solutions were run on a JARRELL-ASH 810 atomic absorption spectrophotometer. Mixed standard metal solutions were prepared by diluting concentrated FISHER atomic absorption or TITRASOL standards. Because of the large quantities of interfering elements in the samples, notably calcium and sodium, background corrections were necessary to provide accurate results. This was accomplished by using a non-absorbing line for each of the sought metals. This method seems quite accurate, as indicated by similar results obtained in replicate sample aliquots that had undergone liquid-liquid extraction to remove the major cations. In addition, the results obtained on two National Bureau of Standards biological standards, Bovine Liver and Orchard Leaves, also indicated that the method was within acceptable limits of accuracy.

Amount and Distribution

The amounts of trace metals in the mesozooplankton, as a general characteristic, varied widely both geographically and seasonally. The patterns for day and night were related for some elements but not for others. The amounts and distributions of the six trace metals (Cu, Zn, Cd, Pb, Ni and Cr) are shown by figures 89 through 92.

The amounts of Cu averaged almost exactly the amounts reported in previous studies, but the winter and summer content had a wider range than previously reported. The variation was less in the summer than in winter and spring. Variations in amounts of Cu between day and night were relatively large but no geographic consistency was evident. Of note was the increased amount of Cu in those samples suspected of being contaminated by Pb.

The average Zn content also closely approximated amounts reported in previous studies. The amounts of Zn generally were less variable than amounts of Cu, especially in spring and summer. Unlike Cu, the day/night variations for Zn were more consistent geographically. Some of the variability in Zn content during winter may have been the result of contamination, though this was not proven. Three of the stations had values suspiciously above the regional average for winter.

The amounts of Cd seem to have been typical of uncontaminated samples from other places with few analyses indicating more than 5 ppm. Furthermore, the analyses for all three seasons fell within a narrow range. The Cd increased seaward as a regional trend during each season and day/night variations were more consistent geographically than those for most other elements.

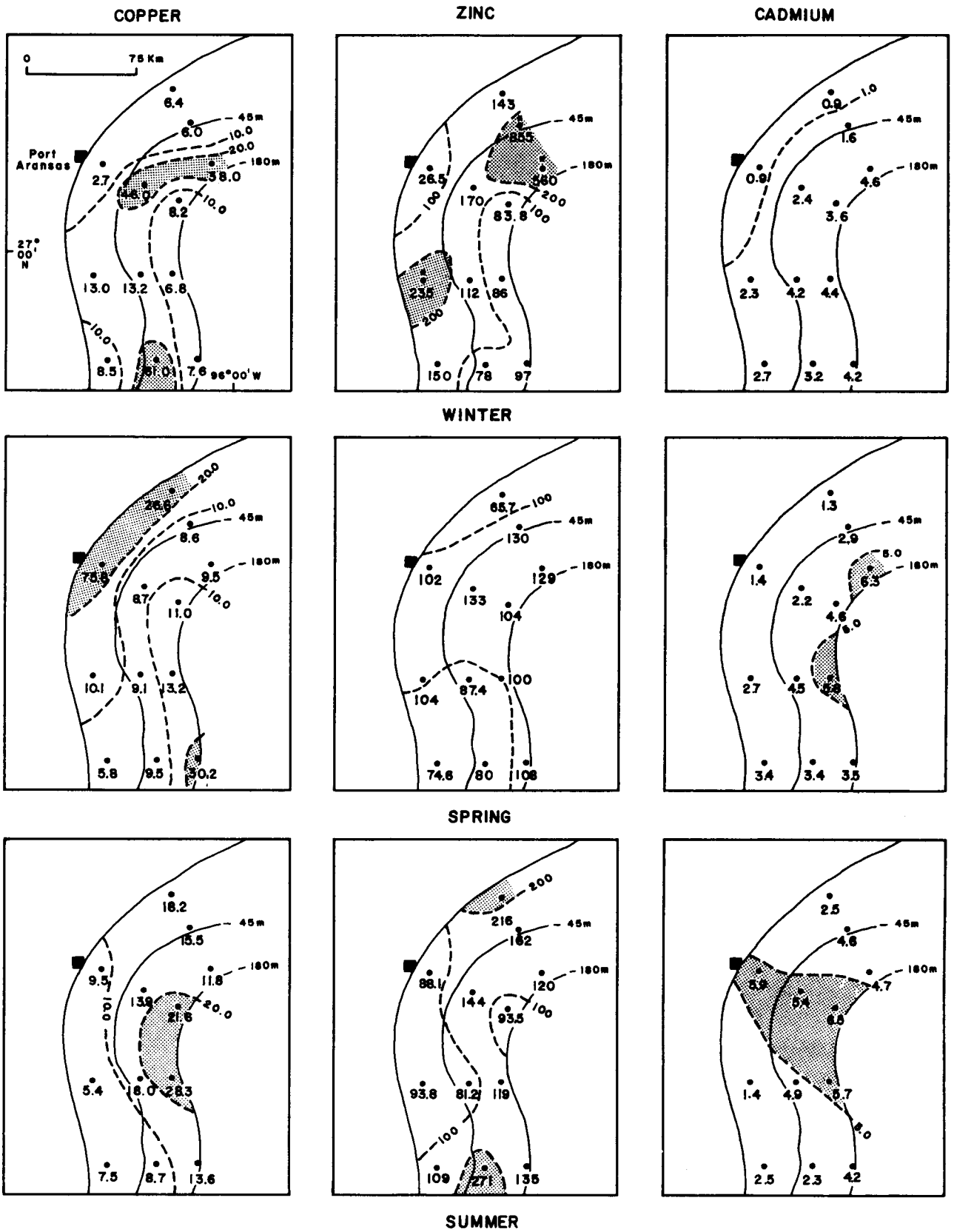

Figure 89. Seasonal distribution of trace metals in mesozooplankton (day): Cu, Zn and Cd (in ppm dry weight). Dot indicates location of sample station. Asterisk indicates probable sample contamination. Broken lines are inferred isopleths. Shading indicates amount above regional average.

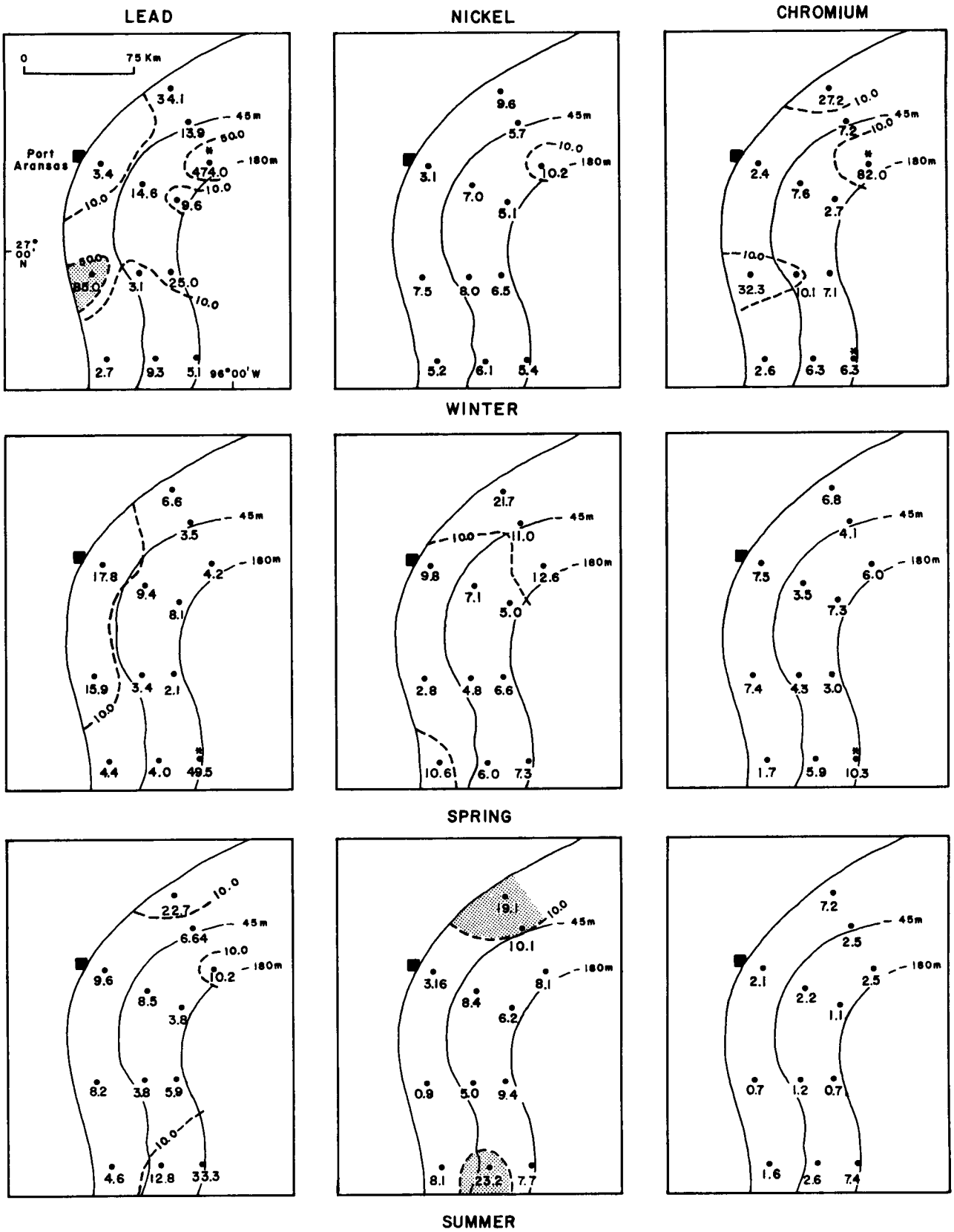

Figure 90. Seasonal distribution of trace metals in mesozooplankton (day): Pb, Ni and Cr (in ppm dry weight). Dot indicates location of sample station. Asterisk indicates probable sample contamination. Broken lines are inferred isopleths. Shading indicates amount above regional average.

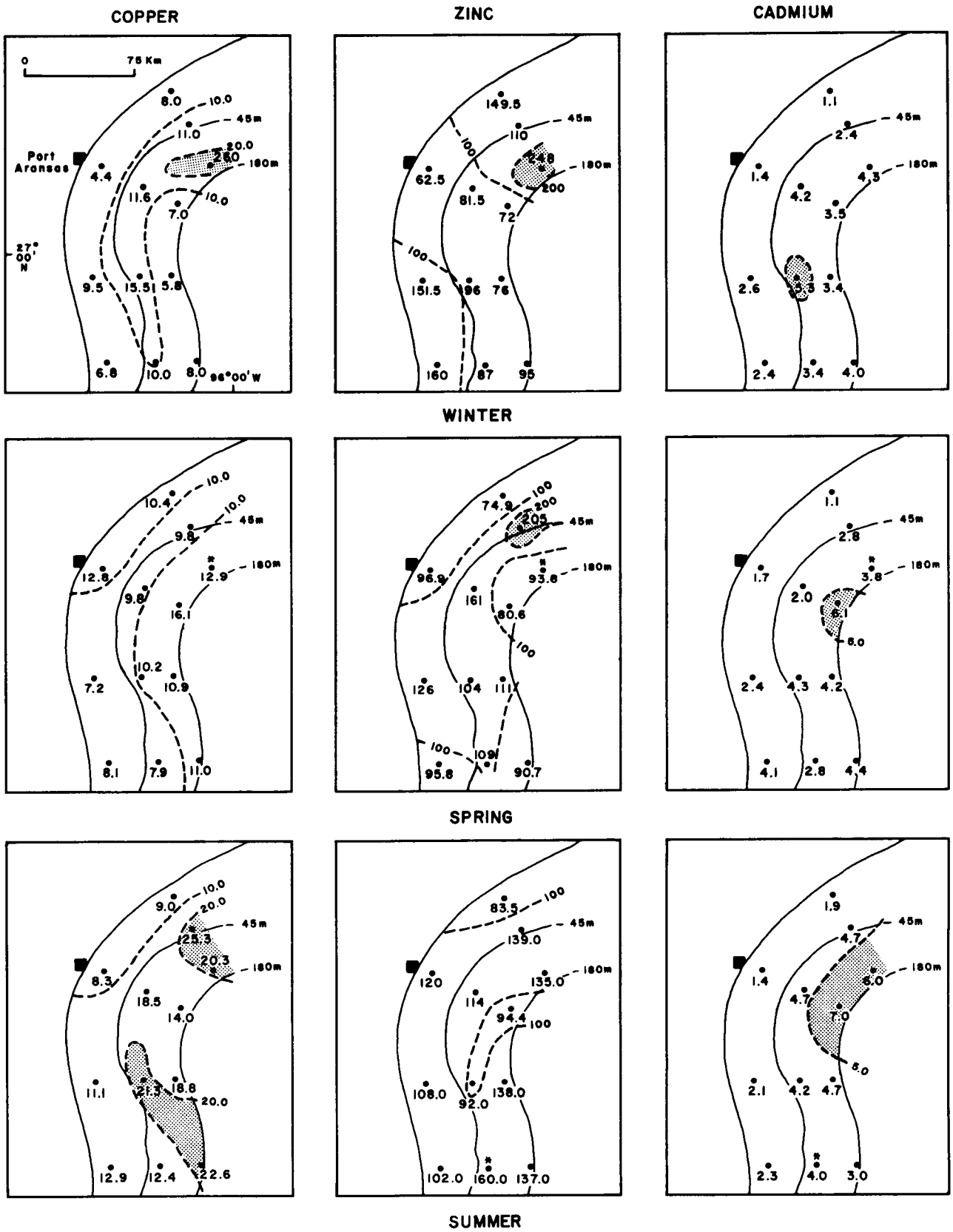

Figure 91. Seasonal distribution of trace metals in mesozooplankton (night): Cu, Zn and Cd (in ppm dry weight). Dot indicates location of sample station. Asterisk indicates probable sample contamination. Broken lines are inferred isopleths. Shading indicates amount above regional average.

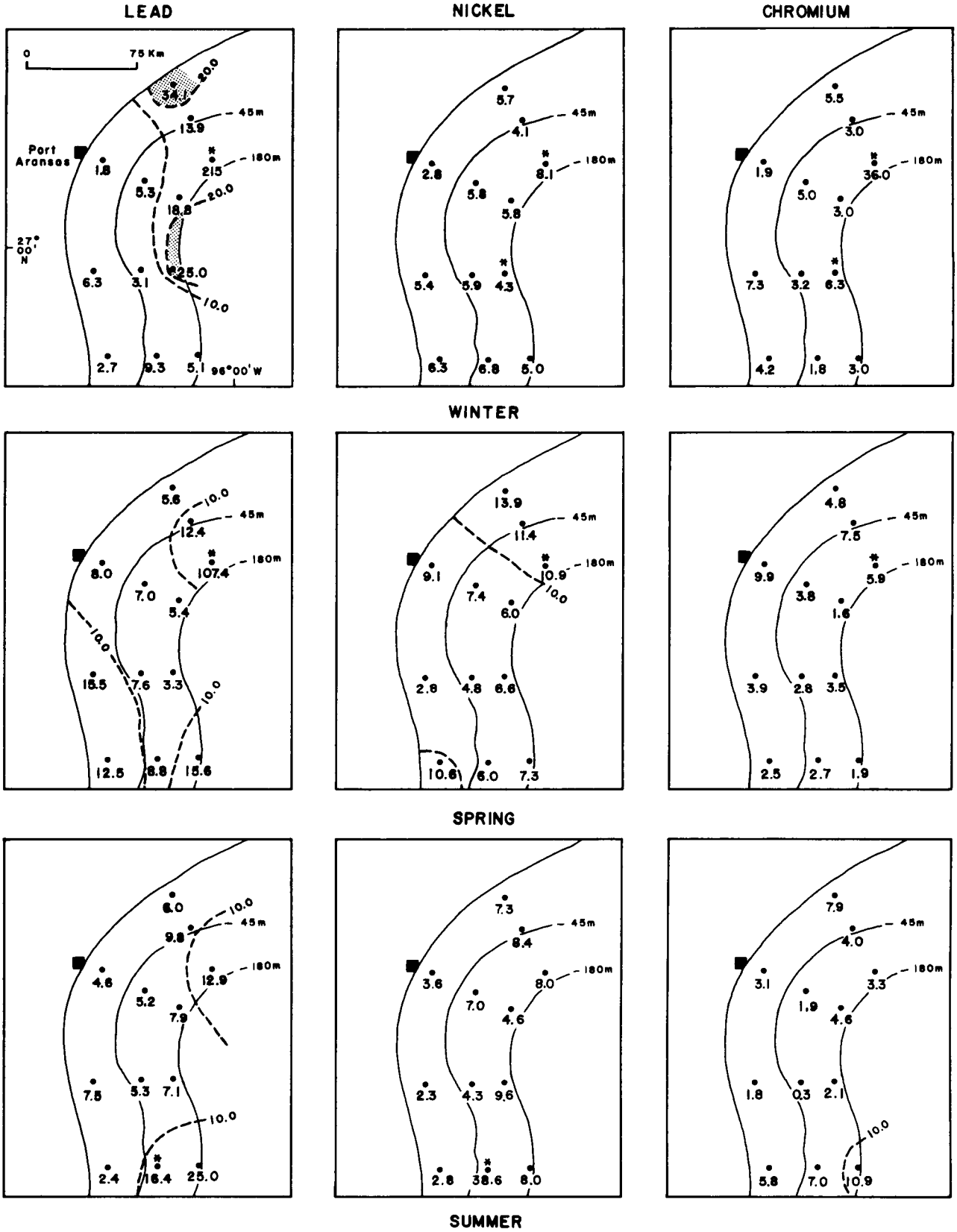

Figure 92. Seasonal distribution of trace metals in mesozooplankton (night): Pb, Ni and Cr (in ppm dry weight). Dot indicates location of sample station. Asterisk indicates probable sample contamination. Broken lines are inferred isopleths. Shading indicates amount above regional average.

The Pb content varied widely and the averages for the South Texas OCS were typical of those reported in other shelf areas. As previously noted, some of the variability seems to have been a result of contamination, but an agent for the contamination was not identified. For the region, fluctuations in amounts of Zn were smaller in the southernmost part, both seasonally and from day to night.

The amounts of Cr generally were larger than in a few analyses reported in the literature; largest amounts were collected in the day samples during the winter. Cr was correspondingly abundant in some of the samples suspected of Pb contamination.

The Ni content generally was similar to amounts reported in other studies. However, the amounts in the spring and at one station during the summer were larger than reported averages. Seasonal fluctuations were greatest in the northern and southern part of the OCS; Ni content along the two transects in the central sector remained relatively constant.

High-Molecular-Weight Hydrocarbons in Mesozooplankton

The processing of mesozooplankton material for analysis followed the same procedures and analytical techniques as those used for the neuston samples. Reference should be made to the neuston section for a resumé of procedures used.

In overall makeup, the high-molecular-weight hydrocarbons identified in the mesozooplankton samples were characterized by pristane, a nineteen carbon isoprenoid, and n-heptadecane as the two most prominent components. The predominance and prevalence of pristane were confirmed by GC-MS. Other hydrocarbons frequently identified were: nC_{15}, nC_{19}, nC_{22}, a phytadiene and

singly unsaturated C_{19}. Gas chromatograms of the saturate and nonsaturate hydrocarbons generally were not complex. That is, relatively few prominent hydrocarbon peaks were observed with a low background of unresolved hydrocarbons. Of the 69 samples analyzed, 1 showed no hydrocarbons, 9 showed a "hump" of unresolved hydrocarbons and 59 had either no "hump" or a small one. Amounts of the nonsaturates averaged less than 0.5 percent of the total hydrocarbons for all three seasons. No trends were apparent except that the 0.47 average for spring was higher than for either winter or summer. However, even that trend is misleading as the spring average was raised appreciably by the 6.92 percent measured at station 2 of transect I. The amounts measured at the same station in winter and spring were 0.007 and 0.03 percent respectively.

For only six mesozooplankton samples did the distribution of n-alkanes extend appreciably beyond nC_{22} and even those did not contain a full suite of n-alkanes from nC_{15} to nC_{35} as is usually associated with petroleum contamination. The alkanes nC_{15}, nC_{17} and nC_{22} are predominant in the six samples as they are in the other mesozooplankton samples. As the ratio of n-alkanes having odd numbers of carbon atoms to those having even numbers of carbons in the range of C_{25} to C_{35} is frequently cited as a measure of petroleumlike character of saturated hydrocarbons, OEP (odd-even predominance) curves were plotted for the six samples. Each of the curves shows a minimum at C_{22} and a maximum or upward trend at C_{17}, indicative of the predominance of the two hydrocarbons in the n-alkane distribution. For these mesozooplankton, the OEP curves fail as indicators of hydrocarbon contamination, as they do not cover the range of petroleum alkanes C_{15} to C_{35}. They do show the general character of OEP curves which may be attributed to "zooplankton

character". Perhaps significantly, five of the six samples were collected from the innermost stations during the summer sampling season.

The distribution of total heavy hydrocarbons in the mesozooplankton varied considerably both from day to night and seasonally. Regional averages were largest in winter and spring and the largest amounts at individual stations were in the spring. Day/night variations also were large during the winter and spring but were not geographically consistent. The distribution during summer was relatively more uniform but day/night changes showed no geographic consistency. The patterns of distribution for total heavy hydrocarbons, seasonally and for day and night are shown by figure 93. Also shown on the figure is the location of stations where n-alkanes having a molecular size in excess of C_{22} were recorded.

Interpretation and Relationships

Abundance

The components of the zooplankton showed distinct and characteristic patterns of abundance and distribution, both singularly and in relation to the other environmental factors: the seasonal distribution of the microzooplankton seemed to be related primarily to seasonal hydrographic conditions and secondarily to productivity; that for the mesozooplankton primarily to nutrients and secondarily to productivity; that for the ichthyoplankton equally to hydrographic conditions and productivity. The overall abundance of shrimp larvae probably is not related to patterns of distribution of other zooplankton; however, the regional coverage of data for the shrimp larvae is too sparse to permit definitive comparison.

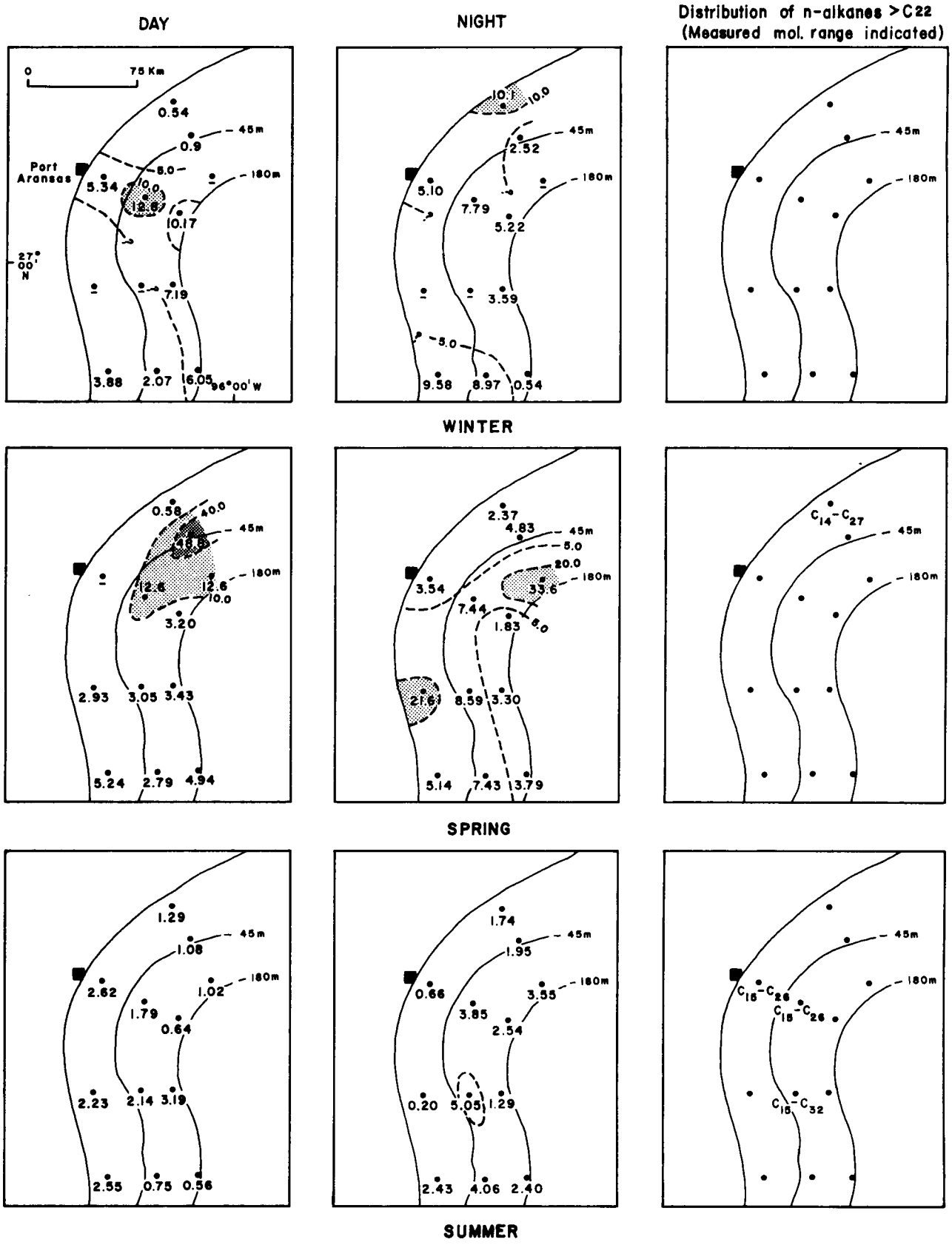

Figure 93. Seasonal distribution of total high-molecular-weight hydrocarbons in mesozooplankton (in percent). Dot indicates location of sample station. Dash indicates amount below level of detection. Broken lines are inferred isopleths. Shading indicates amount above regional average.

Within the microzooplankton group, the radiolaria seem to have the most clear cut relationship to hydrography. The patterns of abundance for the radiolaria on the outer shelf complement those for the nutrients nitrate and phosphate and those for temperature and salinity as indicators of a marginal movement of open Gulf water onto the outer OCS. The patterns for planktonic and benthic foraminifera are less distinct; in the spring and summer the planktonic forams are most abundant in areas of increased productivity, but in a somewhat localized sense. The greatly increased but isolated abundance of planktonic forams in the summer at mid-shelf station 2, transect II is noteworthy because mesozooplankton also were conspicuously abundant at this station in the spring, as were the ichthyoplankton. The condition responsible for such localized proliferation that affected different organisms in different seasons is not known. The increased abundance of planktonic forams along the mid shelf in the summer corresponds to greatly increased amounts of low-molecular-weight hydrocarbons in the same area.

The interrelationship between the mesozooplankton and other environmental aspects was examined in some detail. The seasonal abundance of mesozooplankton was notably related to amounts of chlorophyll a and to the temperature and salinity of the water. The changes that most markedly demonstrate the close interrelationships were those from winter to spring. The 3 fold increase in chlorophyll a coincided with a 1.7 fold increase in mesozooplankton biomass in terms of ash-free dry weight and a 1.4 fold increase in the number of mesozooplankters. An increase of the estuarine copepod Acartia tonsa by 27.6 times during the same period accompanied a decrease in salinity. This relationship was most pronounced at the innermost stations of transects I and II. On the other hand, the copepod Clausocalanus furcatus, a typically

oceanic species, showed a marked decline. Decrease in chlorophyll a and increase in salinity were coincident during the summer with declines in mesozooplankton biomass and number; Acartia tonsa was almost totally absent in the summer. Linear regression analysis indicated that changes in ash-free weight, number of mesozooplankters and number of copepods correlate better with salinity than with chlorophyll a. The greatest fluctuation in salinity was at station 1, transect I. During the spring, the inner shelf water is diluted by nutrient-rich land runoff which supports phytoplankton blooms that in turn provide a base for many food webs in the mesozooplankton.

The abundance of ichthyoplankton remained relatively constant from season to season. Both fish eggs and fish larvae were most abundant along the inner shelf where plankton likewise were most numerous and productivity was highest. However, the two components had different patterns of distribution and numbers of both eggs and larvae were consistently larger at night. The conspicuous localization of each at different stations along the shelf during the three seasons probably reflects the general feeding and spawning habits of the fish and very likely reflects the wide spacing of the sample stations. Eggs tended to be most numerous in the general area off Port Aransas. Larvae were most widely distributed at station 1, transect IV in terms of overall numbers, but the greatest numbers were at station 1, transect I in spring and summer, and on the outer shelf during winter. The increased numbers over the outer shelf during winter probably reflect the higher nutrient content of the water over the outer shelf during that season.

Trace Metals in Mesozooplankton

In general, little correlation is evident between amounts of trace metals and the total numbers of mesozooplankton. Of the six metals measured, only Cu correlated well with abundance of mesozooplankton in all three seasons and in both day and night samples. Areas of increased Cu corresponded very closely to areas of increased mesozooplankton. Amounts of Cr correlated reasonably well with the daytime abundance of mesozooplankton, especially at station 2, transect IV and station 1, transect II, but amounts of Cr in samples of mesozooplankton collected at night did not relate well to the abundance of mesozooplankton at the same stations.

Comparison of the amounts of trace metals to the abundance of mesozooplankton suggests that two factors are primarily responsible for the relationships noted. In the case of Cu, the close correlation of metal content and abundance of organisms is not surprising considering both the strong role of Cu in the life process and its high solubility in sea water. The same statement can be made for Cr, but to a lesser extent. For the other metals, which do not correlate well with numerical abundance but which in some cases seem to be in higher amounts where the number of organisms was below the regional average, a problem of analytical precision may have been involved. As the size of the sample decreases, the results become progressively less precise and any contamination, either from natural sources or otherwise, is magnified. However, a more definitive interpretation must await comparison of the 1975 data with the second year's results.

High-Molecular-Weight Hydrocarbons in Mesozooplankton

The distribution of amounts of total high-molecular-weight hydrocarbon relative to abundance of mesozooplankton shows a reasonable correlation for the spring. The largest amounts of total heavy hydrocarbon were measured in the spring when plankton abundance was greatest. The increases in the amount of high-molecular-weight hydrocarbon in the mesozooplankton also corresponds to the increases in the amount of heavy hydrocarbon dissolved in sea water during the spring. Thus the spring increase in heavy hydrocarbons in the mesozooplankton seems correlative to the general increase in spring productivity.

Although a generally direct relationship is suggested by comparison of the patterns of distribution for the two sets of data during the spring, a deviation is evident as well. The mesozooplankton population in the spring is largest at the innermost stations; the largest amounts of total heavy hydrocarbon are farther seaward. The reason for the offset in the two sets of patterns when overlaid is not readily apparent, but it may be due to the characteristics of the life cycle of individual components of the mesozooplankton and to the productivity factors involved in their proliferation. Again, a more refined interpretation must await the synthesis of several years of comparative data.

SHRIMP (Penaeidae)

Surveys for abundance and distribution of shrimp were not included in the general baseline studies to which this integrated report is principally addressed. Because of the high commercial value of shrimp in the western Gulf of Mexico, the historical data compiled by the Bureau of Commercial Fisheries plus data on commercial shrimp catches are summarized.

Two sets of data were included in the NMFS historical compilation: one for 1961-62 covering three transects (north, central, south) of six stations each across the South Texas OCS area; and another for 1963-65 covering two transects, one of five stations in the northern part and one of three stations in the southern part.

The results of the historical surveys, in terms of relative abundance, are relegated to three contiguous subareas or statistical zones of the South Texas OCS as follows: zone 21 from the border with Mexico to the 27° parallel; zone 20 from the 27° parallel to the 28° parallel; and zone 19 from the 28° parallel to the 29° parallel. Approximately the southern one-third of zone 19 is in the South Texas OCS.

The geometric and arithmetic mean catches per hour by statistical area are shown in table 10.

Table 10. Geometric (G) and arithmetic (A) mean catches of shrimp (Penaeidae) in number of individuals per hour by statistical area

Statistical area	Number of tows	G	A
19	114	54.3	164.4
20	387	49.7	175.4
21	131	42.7	158.6

By statistical area, the catch rate was highest in 19 and lowest in 21. By water depth for all species of Penaeidae, the catch rates were highest in the 23 and 28 m depths. By year, the catch rate for all species was highest in 1961 in area 19 and lowest in 1962 north of the South Texas OCS. By month, the catch rate for all species was highest in January and lowest in August.

Of the 11 species taken during the overall survey period, numbers of brown shrimp exceeded all others but were least abundant in area 19. On the contrary, white shrimp, second in abundance to brown shrimp overall, were most abundant in area 19.

A summary of the commercial catches of shrimp by species for the years 1970 through 1974 is shown by table 11. In the table "inshore" refers to lagoons and bays; "offshore", to the continental shelf. Again, the northern two-thirds of statistical area 19 lies north of the South Texas OCS; however, no statistical breakdown is available for only that part of area 19 included in the South Texas OCS.

The statistics in the table indicate that for the 4 year period, yearly catches were largest in area 19, followed by area 20. The catches each year in each area were dominated by the brown shrimp. The general abundance, as indicated by the commercial catches, in terms of species and geographic location correspond to the data on shrimp larvae described previously in the section on zooplankton. (See figure 78, map B). The southern end of the great shrimp fishing grounds of the northwestern Gulf of Mexico extends into the South Texas OCS.

FINFISH

Abundance as Based on Commercial Landings of Finfish and Shellfish

Over the 10 year period from 1965 through 1974, total commercial landings of finfish, blue crabs and squid from the waters off south Texas fluctuated between 0.8 and 1.5 million pounds. The finfish, represented by 13 species, made up the bulk of the harvest.

Table 11. Yearly commercial shrimp catches by statistical area and by species, 1970 through 1974 (in millions of pounds). Inshore indicates bay and lagoon; offshore denotes continental shelf.

Statistical area		Brown Shrimp	White Shrimp	Pink Shrimp
		1970		
	Offshore	13,501,560	3,364,992	2,065
19	Inshore	384,031	2,605,868	-
	Offshore	7,738,469	373,277	3,423
20	Inshore	86,300	134,300	-
	Offshore	7,244,012	257,721	33,102
21	Inshore	-	-	-
		1971		
	Offshore	14,637,968	2,269,283	2,335
19	Inshore	342,113	1,238,741	-
	Offshore	6,187,231	233,239	980
20	Inshore	12,000	54,600	-
	Offshore	4,292,696	179,093	785
21	Inshore	-	-	-
		1972		
	Offshore	17,434,436	2,929,785	5,063
19	Inshore	290,300	2,159,735	-
	Offshore	10,133,341	562,913	25
20	Inshore	33,200	257,787	-
	Offshore	4,745,720	135,312	-
21	Inshore	-	-	-
		1973		
	Offshore	5,834,492	3,269,298	-
19	Inshore	1,495,278	3,115,167	-
	Offshore	8,549,667	1,032,545	775
20	Inshore	481,300	581,400	-
	Offshore	6,993,975	254,207	-
21	Inshore	-	-	-
		1974		
	Offshore	4,779,471	2,301,099	-
19	Inshore	464,484	1,909,295	-
	Offshore	7,938,888	801,981	3,137
20	Inshore	96,200	208,000	-
	Offshore	5,502,797	155,011	-
21	Inshore	-	-	-

Of the finfish, the most valuable was the red snapper, despite a progressive decrease of approximately 50 percent in numbers of pounds taken between 1965 and 1974. In contrast, landings of redfish, flounder and spotted sea trout increased markedly over the 10 year period. Only minimal amounts of crab and squid were harvested.

Near-Surface Pelagic Fishes

Large populations of pelagic fish species exist in both nearshore and offshore parts of the South Texas OCS from Port Aransas south to Port Isabel. Species groups especially abundant during at least parts of the year are: sharks, tarpon, ladyfish, herrings, anchovies, needlefish, silversides, mullets, barracudas, mackerels, jacks, cutlassfish, bluefish, dolphin, and billfish.

An attempt was made to collect baseline data on the near-surface pelagic fish by use of gill nets placed at seven stations along a single transect extending in a southeasterly direction across the shelf beginning at Port Aransas. The sampling areas ranged in depths of water from 5 m at station 1 to 108 m at station 6 on the outer shelf.

Each gill net was 197 m long and 3.3 m deep, and consisted of six 32.8 m long panels of #208 monofilament nylon webbing. Each panel in each net was of a different mesh size and the panels were located randomly within each float and leadline frame. Stretched mesh sizes were 5.1, 6.3, 7.6, 8.9, 10.2 and 11.4 cm. From one to four nets were set at each station on different dates between 1600-1700 hr and retrieved between 0600-0900 hr the following day.

The four nets were set at the surface in water depths of 7 to 16 m at station 1 on June 12, 1975. During the night, 345 individuals comprising 14 species were caught. The catch per net ranged from 25 to 192 individuals. The suite consisted of a distinctly different species complex when compared with those obtained by trawling. The ten most abundant species represented in the catch were: Atlantic thread herring (99); Gulf menhaden (63); Atlantic sharpnose shark (39); blue runner (27); Atlantic bumper (25); sand sea trout (24); scaled sardine (24); Spanish mackerel (24); bluefish (10); and greater amberjack (9). Some 60 percent of the equipment was either lost or destroyed during high winds on June 13.

The second phase of the gill net survey included placing of nets at stations 2 through 6 during the period of September 19-27, 1975. The size of the catch was disappointing and plans for further use of the gill nets in the deep water as a baseline sampling tool were abandoned. The remainder of the sampling was done from early October to early November at a nearshore station, about 2 miles north of Port Aransas. During this period, 8 species of prey animals and 13 species of predator animals, mostly pelagic, were caught.

Historical Ichthyofauna Survey, 1962 to 1964

From January 1962 through December 1964, the Bureau of Commercial Fisheries carried out a comprehensive fishing survey over the continental shelf from the Mississippi River to the Rio Grande. Samples were taken monthly using flat trawl nets 14 m wide that were towed for 1 hour in each station area. The fish were identified to species and each species in a subsample was counted and weighed.

As available information indicated that the fauna could be adequately described by analysis of data for a relatively limited number of species that made up most (98 to 99 percent) of the fauna, this approach was taken with data collected in the 7 to 82 m depth range to reduce the enormous mass of numbers to a manageable quantity. The summation that follows covers data gathered over the South Texas OCS during the 1962 to 1964 survey in the depth range of 7 to 82 m.

The most abundant species for the overall survey period were in order: Stenotomus caprinus (16 percent); Syacium gunteri (8 percent); Cynoscion nothus (7 percent); and Micropogon undulatus (6 percent). By weight the species ranking was: Stenotomus caprinus (12 percent); Synodus foetens (10 percent); Micropogon undulatus (6 percent); Cynoscion nothus (6 percent); Syacium gunteri (6 percent); and Cynoscion arenarius (5 percent). The composition of the dominant fish fauna by number, weight and season is shown by table 12, and the composition by number, weight and water depth is shown by table 13.

Within the South Texas OCS, 14 families made up about 97 percent of the biomass and 96 percent of the number of species. In the depth range of 1 to 27 m, or within what is typically defined as the white shrimp grounds, changes in overall composition by season were small compared to drastic changes with depth. The fish community within the depth range defined was dominated by species of the Family Sciaenidae (drums). The offshore, 27 to 90 m depth, so-called brown shrimp grounds were dominated by the Family Sparidae (porgies).

The ichthyofauna at the depth of 110 m was extremely diverse, although species richness decreased off south Texas. The dominant taxa in the 100 m

Table 12. Composition of the dominant fish fauna by number and weight according to season.

Number per season by percent of total

Species	Winter	Spring	Summer	Fall
Inshore lizardfish	-	6	5	-
Blackear bass	-	-	6	-
Longspine porgy	16	13	17	17
Sand sea trout	8	-	-	-
Silver sea trout	9	10	-	8
Atlantic croaker	-	-	10	6
Star drum	5	-	-	-
Mexican searobin	5	-	5	-
Shoal flounder	9	8	6	11

Weight per season by percent of total

Inshore lizardfish	8	13	11	8
Rock sea bass	-	5	-	-
Longspine porgy	14	11	12	13
Sand sea trout	9	-	-	6
Silver sea trout	5	9	-	7
Southern kingfish	9	-	-	-
Atlantic croaker	-	-	10	8
Shoal flounder	5	6	-	6

Table 13. Composition of the dominant fish fauna by number and weight according to water depth.

Species	7	14	27	46	64	73	82
Number in percent of total by depth in meters							
Inshore lizardfish	-	-	5	7	9	9	6
Sea catfish	6	-	-	-	-	-	-
Rock sea bass	-	-	-	-	5	-	-
Blackear bass	-	-	-	9	-	7	5
Wenchman	-	-	-	-	-	-	7
Pinfish	5	-	-	-	-	-	-
Longspine porgy	-	-	10	22	34	38	28
Sand sea trout	-	6	6	-	-	-	-
Silver sea trout	15	18	10	-	-	-	-
Spot	6	-	-	-	-	-	-
Southern kingfish	8	6	-	-	-	-	-
Atlantic croaker	12	13	-	-	-	-	-
Star drum	7	8	-	-	-	-	-
Dwarf goatfish	-	-	-	-	-	6	-
Mexican searobin	-	-	-	-	10	6	13
Shoal flounder	-	7	28	8	-	-	-
Weight in percent of total							
Inshore lizardfish	-	-	-	17	17	18	14
Sea catfish	7	-	-	-	-	-	-
Rock sea bass	-	-	-	7	7	8	7
Wenchman	-	-	-	-	-	-	12
Longspine porgy	-	-	6	17	30	35	23
Sand sea trout	-	6	-	6	-	-	-
Silver sea trout	10	12	-	-	-	-	-
Spot	8	-	-	-	-	-	-
Southern kingfish	14	13	-	-	-	-	-
Atlantic croaker	10	13	6	5	-	-	-
Star drum	-	6	-	-	-	-	-
Mexican searobin	-	-	-	-	6	-	9
Shoal flounder	-	-	10	-	-	-	-

range were the Families Sparidae (porgies), Lutjanidae (snapper), Triglidae (searobins) and Serranidae (sea basses) with the longspine porgy, wenchman, Mexican searobin and blackear bass being the most numerous species in these families. Faunal compositions by percentage were very similar along the 110 m depth contour from the Mississippi River delta to the Rio Grande except for large changes in the abundance of longspine porgy, wenchman and blackear bass. The longspine porgy made up 30 to 35 percent of the faunal biomass and numbers outside the South Texas OCS, but only 10 to 12 percent within it. The wenchman and blackear bass increased greatly westward, apparently replacing the longspine porgy off south Texas.

THE SEA FLOOR

SEDIMENTS

Physical Characteristics

Grain Size

A total of 291 samples of surficial sea floor sediments were analyzed for grain size: 263 bottom grab samples, and 28 box core samples used as replicates for determining within-station variability of grain size. The locations of the grab sample stations are shown by figure 7. The grain size analyses were used to classify the uppermost sediments on the sea floor according to textural variability.

The sample used for grain size analysis actually was a composite of approximately the upper 10 cm of surficial sediments. The sample was obtained by inserting a plastic tube 10 cm long and 3.75 cm in diameter vertically into the undisturbed grab sample aboard ship. The tubes were capped and sealed for transfer to the laboratory.

Standard laboratory procedure involving six processing steps was used in preparing the sediment samples for analysis. Organic matter was removed by oxidation in a 30 percent hydrogen peroxide solution. After disaggregation and dispersion, the samples were wet-sieved to determine relative percentages of the size components: gravel, >2 mm; sand, 63 μm to 2 mm; and mud, <63 μm. As used in this report, the term mud covers the combined silt and clay-sized fractions of the sediment.

The amounts of the silt and clay fractions (<63 μm) were determined electronically at a half-phi interval by a 16 channel TA COULTER COUNTER.

By conducting duplicate analyses with 200 μm and 30 μm tube apertures, the instrument effectively analyzed the 0.63 to 63 μm size range. The electrolyte consisted of a 4 percent CALGON solution prefiltered through a 0.2 μm filter.

The size distribution of the sand fraction was determined by use of a Rapid Sediment Analyzer (RSA). The instrument consists of a settling tube of 1 m length and 8 cm internal diameter, and a pressure column tube of equal length adjoined to the settling column through a highly sensitive pressure transducer valve. Accessory equipment includes a HEWLETT-PACKARD amplifier (model 321) and a HEATH-SCHUMBERGER strip-chart recorder (model EU-205-11). Sediment particle fall times were converted to phi-size cumulative percentages at a 0.5 Ø interval.

The results of the grain size analyses were synthesized to demonstrate four types of textural interrelationships: 1) single component percentages - gravel, sand, silt, clay; 2) two component ratios - sand/mud, silt/clay; 3) composite classification based on mixed percentages of sand-silt-clay; and 4) statistical grain-size parameters - moment measures of mean diameter, standard deviation, skewness, kurtosis and modal diameters. The resumé of sediment properties given here is restricted to those aspects that most clearly demonstrate the regional patterns of sediment distribution and that most closely relate as controlling factors to other environmental aspects, such as distribution of epifauna and infauna, and chemistry of the sediments. The two aspects most applicable are the distribution of sand (fig. 94A) and the ratio of sand to mud (fig. 94B).

Gravel, or detritus of greater than 2 mm size, is a minor constituent largely restricted to the southern part of the South Texas OCS within the areas of >50 percent sand in figure 94A. The gravel is largely biogenic shell detritus with minor amounts of lithic fragments.

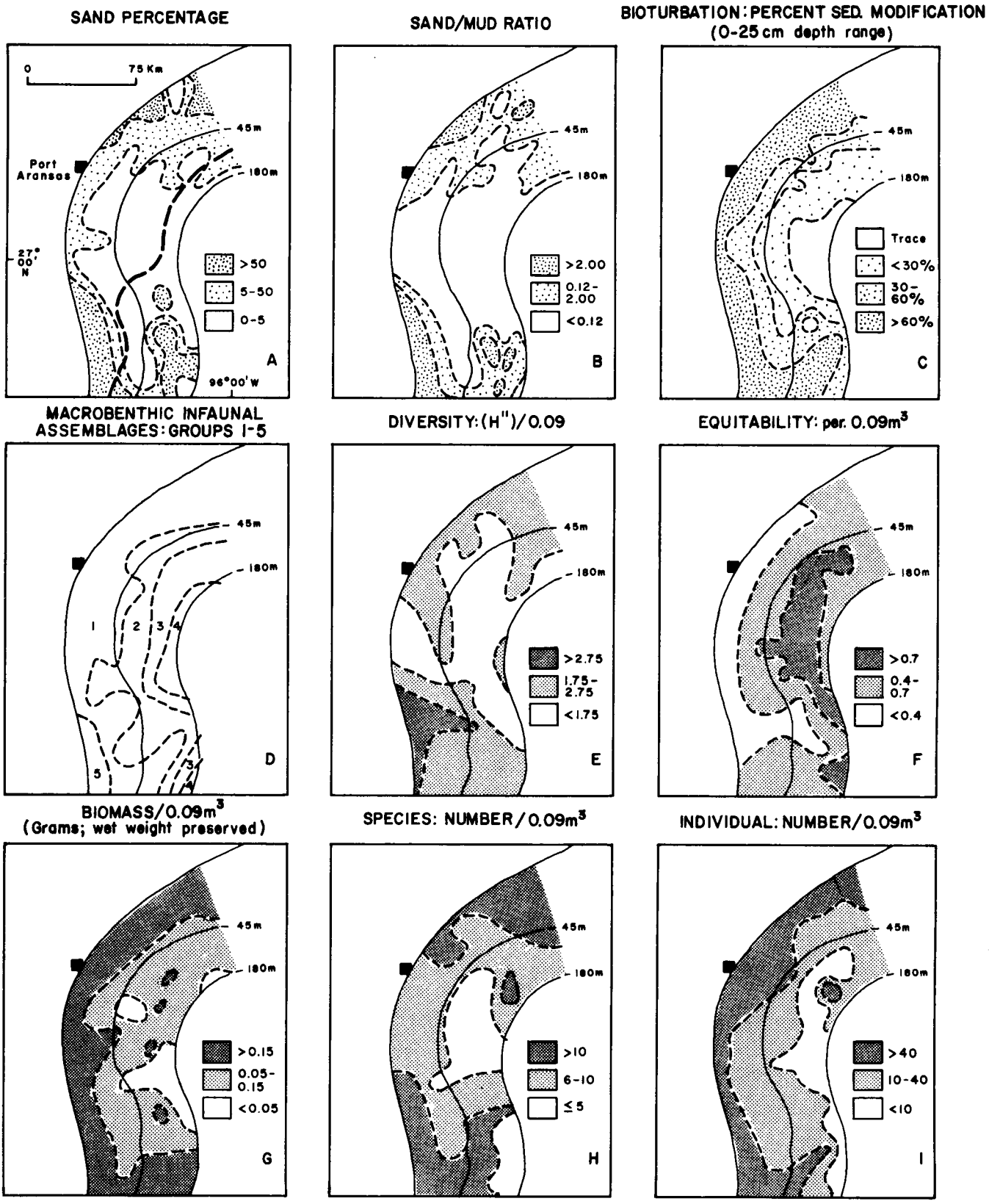

Figure 94. Distribution of surficial bottom sediments by grain size and general infaunal characteristics relative to the textural pattern of the sediments. The heavy broken line in map A is the approximate seaward extent of discrete sand layers in the sediments.

The sand-sized fraction is largely terrigenous, but does contain biogenic detritus. In regional perspective, the sand is most abundant in the northern and southern parts of the OCS; local large concentrations of sand are on the outer part of the ancestral Rio Grande delta.

The silt-sized detritus (3.9 to 63 μm) is a predominant constituent of bottom sediments throughout most of the South Texas OCS, especially in the central sector. Within the central sector, the amount of silt decreases toward the outer edge of the shelf.

The clay-sized fraction (<63 μm) of the sediments has a regional pattern of distribution that is the inverse of that for sand. The clay detritus is restricted largely to the central sector of the OCS and more specifically to the outer part of the shelf in the central sector. The clay-sized fraction is abundant locally in a few places, such as seaward of the outlet for Matagorda Bay in the northwestern part of the OCS.

Most of the South Texas OCS is characterized by sand/mud ratios of less than 0.25; the only areas where sand exceeds mud (>1.0) are on the two ancestral deltas at the northern and southern extremities of the region and along the western margin of the inner shelf. The ratio distribution map (fig. 94B) reinforces the trend indicated by the sand percentage map.

Clay Minerals

The wet-sieved fraction from 73 samples, selected from the 264 bottom stations so as to give an even regional representation, was analyzed for clay minerals identification. The samples were prepared in the laboratory following standard procedures and were scanned for clay mineral identification in a PICKER X-ray diffractometer within the scanning range of 2 degrees 2 theta to 35 degrees 2 theta.

The results of the X-ray diffraction analysis of the 3.0 to 0.45 μm fraction showed that the predominant clay mineral was of the expandable variety, probably calcium montmorillonite. The second most common clay was illite; only trace amounts of a chlorite-type mineral were identified. The expandable clay defined as montmorillonite plus the mixed-layer clay ranged from 38.9 to 90 percent in the 3.0 to 0.45 μm size range.

As a regional pattern of distribution, the amount of expandable clay decreased from north to south; however, two prominent salients low in expandable clays encroach onto the shelf from the east in the northern half of the OCS area. A third large salient low in expandable clays extends eastward across the shelf from the vicinity of the Rio Grande.

Stratigraphy of Shallow Subsurface Sediments

The stratigraphic relation of sand to mud at subsurface depths of up to 2.5 m below the sediment-water interface were determined from the 74 pipe cores whose locations are shown by figure 8. In the laboratory, the cores first were X-rayed at a 1 to 1 scale and then were described by megascopic examination and by use of the X-ray film strip. The descriptive log for each core was coded as to: 1) number of discrete sand layers; 2) types of sedimentary structures; 3) types and intensity of biogenic structures; 4) degree of sediment modification by bioturbation; 5) types of faunal remains; and 6) estimated total percentage of sand. During study of the cores, primary attention was given to the depositional aspects of the sediments most likely to yield significant and quantitative information on the directions and magnitude of transport over the continental shelf as a function of water mass movement. These depositional aspects were:

1) number and thickness of discrete sand layers; 2) the areal extent of discrete sand layers that seem to be correlative from core to core; 3) amount of sand relative to finer grained sediments; 4) presence and extent of ripple or cross laminae in the sands that indicate the extent to which moving water or relatively high energy has been involved in sediment transport; 5) features such as sharp boundaries between sediment types, erosional or scour contact at the base of the sand layers; and 6) vertical changes in types of sediments that record significant and progressive long-term changes in patterns of sediment movement during latest Holocene time.

The relative proportions of sand and mud in the cores indicate a composite pattern of sand distribution that is similar to the pattern for the surficial sediments as shown by figure 94A. However, when the cores were examined in 30 cm increments from top to bottom, the relative percentages of sand and mud in the cores at depths of 30 cm or greater indicate a somewhat more restricted area of mud and more extensive sand in the central sector of the shelf. The seaward extent of the sand increases with depth in the cores.

The number of discrete sand layers increased shoreward as would be expected from the regional ratios of sand to mud. Also, in the central sector of the shelf where mud is the predominant type of sediment, the number of sand layers decreased upward. The seaward extent of discrete sand layers is indicated by the heavy broken line on figure 94A. No discrete sands were in the cores taken east of the line shown. Note that the line lies well west of the areas of sand that lie on the outer shelf in the southern part of the OCS. The sand in these areas represents relict shoreline and associated deposits of the ancestral Rio Grande delta, laid down

under an earlier sedimentary regime. The broken line has been drawn in reference to conditions that have existed during the Holocene shelf transgression of sea level. A representative set of diagrammed logs showing the typical stratigraphic relations of sand and mud across the shelf are shown by figure 95 (See fig. 8 for location of the cores.)

The most common depositional structures in the sands are interlaminations of irregular pattern that range in form from very crude ripple to small-scale foreset, and cut and fill; cross laminae are not common, are of very small scale and, where noted, are in cores from the inner half of the shelf. Graded bedding or upward decrease in grain size is apparent in many of the sand layers. The discrete sands typically have a sharp basal contact with underlying mud. The depositional structures described, though not uniformly distributed either vertically in a core or between cores, were noted at one place or another over all of the shelf that lies west of the broken line shown in figure 94A.

Animal-Sediment Relations

An understanding of benthic biological processes is essential to making useful sedimentological, paleoecological and related environmental interpretations because bioturbation commonly modifies both grain size relations and depositional structures to a marked degree in some depositional environments. The modifications apparently take place very soon after the sediments are deposited. Also, understanding biologic processes is important in defining depositional environments. The chronology of biogenic sedimentary structures helps to define the depositional history, gives quantitative information on rates of deposition or erosion and helps to define more precisely key marker

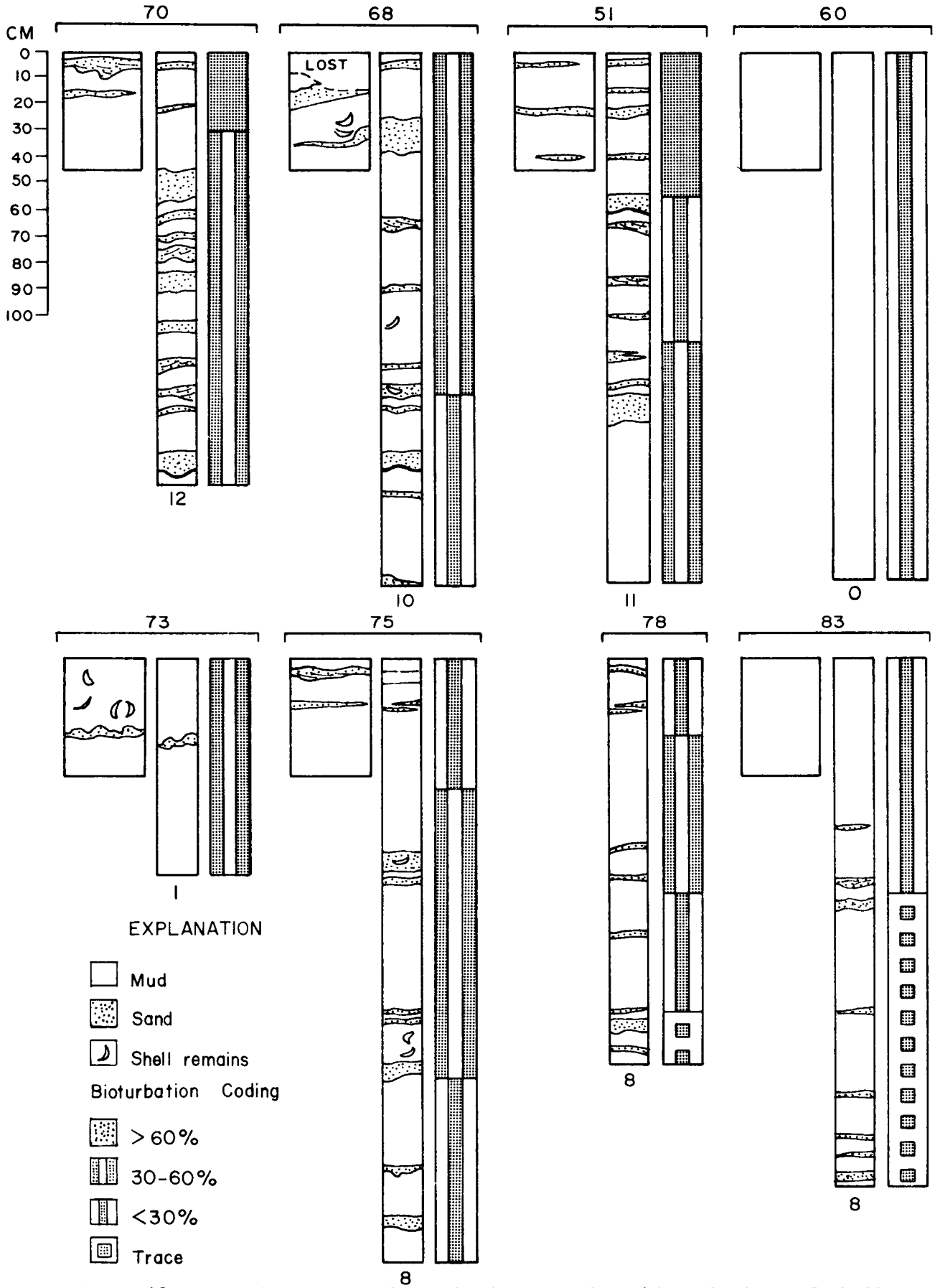

Figure 95. Descriptive core logs showing stratigraphic relations of shallow subsurface sediments seaward across the shelf and amount of bioturbation. Left block is box core; center column is pipe core; right hand column indicates degree of sediment modification by bioturbation. For location of stations see figure 8. Number at bottom of pipe core column is number of discrete sand layers.

beds, such as sand layers deposited during major storms. Recognizing certain biological functions, as revealed by the structures of biogenic origin in the sediments, simplifies the interpretation of other aspects of the environment such as aeration of water and sediment, substrate coherence, and stability and provinciality. Knowledge of the overall extent and intensity of biogenic activity, both laterally and vertically, is a key to predicting the impact of contaminants introduced on and into benthic sediments.

The samples used for the biogeologic studies came from the 81 bottom grab stations shown on figure 7a. Aboard ship the sediment remaining in the grab sampler after the subsamples to be used for the physical and chemical analysis had been removed, was washed through a large (46 cm) diameter aluminum funnel having a 0.5 mm SARAN bag acting as a screen at the terminal end. After washing, the biological material caught in the fine mesh bags was placed in jars containing 5 percent buffered formalin. In the laboratory each sample was transferred to a 45 percent isopropyl alcohol solution to await counting, sorting and identification.

Synthesis of the biological material included determination and compilation of biomass, major macrobenthic assemblages, numbers of species, numbers of individuals, species diversity and species equitability. The extent of bioturbation and types of biogenic structures were determined by use of the 1 to 1 X-ray film strips of the pipe and box cores. The results of the biogeologic studies are shown by the series of maps in figure 94. The regional patterns for the several aspects of the biogeologic data are so strikingly similar to those indicated by grain-size distributions in the sediments that little further elaboration is necessary. The two primary factors that control the zonation and other characteristics of the infaunal

communities obviously are the grain size of the sediment and the depth of water. Examples of the variations in the extent of bioturbation, both laterally across the shelf and with depth in the sediments, are shown by figure 95. The coded columns beside the core logs indicate the degree to which the sediments have been modified by the burrowing organisms.

Carbonate Reefs

A series of so-called topographic highs lies along the outer part of the South Texas OCS at water depths of approximately 80 to 90 meters. The location and trend are shown by figure 5. These features are dead carbonate reefs that grew along the ancient shoreline during the last low stand of the sea during Pleistocene time. The inferred paleogeography and probable position of the shoreline at the time the reefs formed are shown by figure 109, map C.

Radiocarbon dates for samples taken from two of the reefs were 18,000 yrs BP and 10,950 yrs BP, respectively. The reefs are relict bottom features of the South Texas OCS that are being progressively covered by Holocene shelf sedimentation. As a separate study under the sponsorship of the BLM, the biology and geology of the carbonates have been reported on by Bright, Rezak and others (1976).

Interpretation and Relationships

Using the distribution of the sand-sized fraction as the key indicator, several summary statements can be made regarding the most recent directions of sediment transport and deposition. From the high energy zone of the innermost shelf, sand is being transported seaward over the shelf (fig. 94A). The presence of thin discrete sand layers in the subsurface sediments to a

distance of at least 30 miles from shore strongly suggests that the seaward transport of sand is temporarily but nevertheless markedly increased by short-lived events. The most obvious mechanism is hurricane or major storm activity. The encroachment of sand onto the shelf from the north indicates a regional southward movement of sediment. The central sector of the OCS seems to be acting as a depocenter for fine-grained sediments.

Superimposed on the net regional southward movement is a westward encroachment or spreading of the mud or fine-grained sediment of the central sector. This trend is indicated by the relative upward decrease in the number of discrete sand layers in the cores from the central sector of the shelf. The westward encroachment of the fine sediments reflects the transgressive rise in sea level during the Holocene. The rate of sediment deposition in the central sector of the OCS, as suggested by age dating of the carbonate reef material and undisturbed articulated shell material in the sediment, may have averaged a half a meter or more per thousand years during the Holocene. The relatively high rates of sedimentation suggested by the studies in 1975 must be considered tentative and preliminary until results of the continuing studies are completed.

Chemical Characteristics

Carbonate and Organic Carbon

Methods

In the laboratory, the 264 subsamples (see fig. 7 for location) for organic carbon and carbonate analyses were thawed and removed from the plastic tubes. The samples were homogenized, air dried, ground to a fine powder and were analyzed.

The method of analysis for the carbonate was as follows. From 0.2 to 1.0 g of sample material was placed in a digestion tube and 2 ml of 5 percent $FeSO_4$ was added. After the system was closed to the atmosphere, 3 ml of 2N HCL was introduced into the digestion tube by gravity feed and pressurized O_2 was also introduced at a flow rate of 0.5 l/minute. Heat was applied to the digestion tube after effervescence ceased to assure complete digestion. When digestion was complete, the O_2 pressure was increased to 1.0 l/minute to sweep the evolved CO_2 into the burette of a LECO carbon analyzer. All gases leaving the digestion assembly were passed through a concentrated H_2SO_4 scrubber to eliminate any water vapor, through a MnO_2 trap to remove any SO_2 present, and then through a catalyst furnace to convert CO to CO_2. Only the CO_2 from the digested sample and excess O_2 used to sweep completely the digestion assembly and purifying train enter the burette and replace a non-absorbing solution of approximately 0.6N H_2SO_4. Methyl red was added to the solution to facilitate leveling and reading. The gas mixture was passed from the burette by O_2 pressure into the absorption vessel containing 9N KOH where the CO_2 was absorbed in approximately one minute. Release of the pressure allowed the remaining O_2 to be returned to the original burette and the H_2SO_4 solution was then adjusted to atmospheric pressure. Inasmuch as the height of the liquid column above zero is equal to the volume of the absorbed CO_2, the percentage carbon per gram of sample weight could be read from the calibrated burette of the carbon analyzer. The final corrected reading was then converted to percent carbonate by the factor of 8.33, which related the carbon value to $CaCO_3$.

Organic carbon was determined by measuring the total carbon minus the carbonate carbon. The procedure for determining the total carbon was as

follows: a sample ranging from 0.2 to 1.0 g was weighed and placed in a carbon-free ceramic crucible, which then was placed in an induction furnace through which purified O_2 was passed. An iron chip accelerator and a strip of tin-coated Cu were added to start oxidation at a lower temperature. The sample was quickly fired at 1500°C so that all the carbon would be converted to CO_2 in approximately one minute. Any sulfur present was converted to SO_2, whereas Fe, Cu, silicon and associated elements remained as solid oxides. Most of the solid oxides were retained in the crucible, but some particles were carried along by the O_2 stream until caught by a dust trap. The SO_2 was absorbed in a MnO_2 trap. Beyond this point, the CO_2 and O_2 entered the calibrated burette. The remaining procedures were identical to those previously described for the $CaCO_3$. The samples were run in triplicate with an average variation of less than 5 percent for both Ca and CO_3.

Amount and distribution

The organic content of the shelf sediments ranged from 0.2 to 1.2 percent. The pattern of distribution shows that amounts of organic carbon were largest along the outer part of the shelf and smallest in the northern part. The range in amounts of organic carbon seems to relate principally to a combination of two factors: an area of probable gas seeps (fig. 109F) on the outer shelf and the grain size of the sediments. The sediments may trap and retain small amounts of organic carbon during seepage. The fine-grained sediments of the outer shelf, high in clay content and less subject to winnowing and aeration by rapidly moving water, hold and retain a larger percentage of entrapped organic carbon. Another probable factor accounting for the higher organic carbon content of shelf edge sediments is the high concentration of microzooplankton remains in the bottom sediments.

The carbonate content of the sediment ranges from <1 percent to 100 percent on the carbonate reefs. In sediments away from the reefs, the maximum content is 14 percent. Regionally, the carbonate content of the sediment is largest in two widely separated parts of the shelf: on the northeastern outer edge and on the south central inner shelf. The carbonate at the northeastern edge of the shelf is almost entirely microzooplankton tests, whereas that on the inner shelf is almost entirely shell debris associated with the ancestral Rio Grande delta.

The distribution of organic carbon and carbonate are shown by the maps in figure 96. For uniformity in comparing results to those for other environmental aspects of the region, the maps in the figure have been generalized to show the amounts only for the stations that correspond to the biological stations. The results, though somewhat generalized, do not basically change the patterns shown by the more detailed maps in the report of Berryhill and others (1976). This statement applies as well to the maps showing the physical and biogeologic characteristics on figure 94 and to the results for the trace metals analyses also shown on figures 96 and 97.

Trace Metals

Methods

The amounts of 10 trace metals in the 264 grab samples were determined by atomic absorption techniques. Triplicate subsamples from each of the 264 samples were analyzed; more than three analyses were run on randomly selected subsamples. The procedure of analysis was as follows: after removal from the sample container, the sample was placed in a porcelain dish, was mixed and dried at 100°C under infrared lamps. The sample then was ground in a

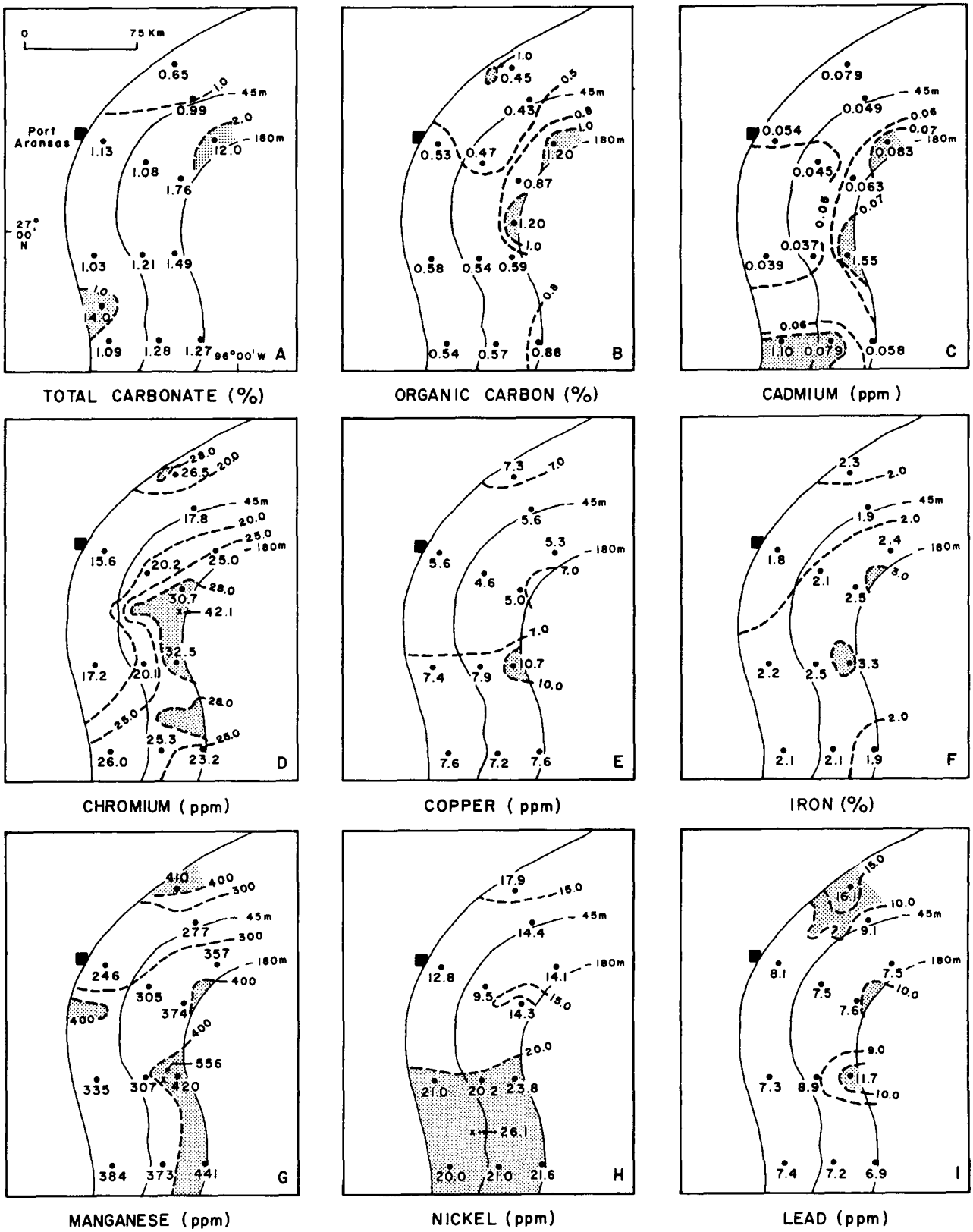

Figure 96. Distribution of carbonate, organic carbon and the trace elements Cd, Cr, Cu, Fe, Mn, Ni and Pb in bottom sediments. Dot indicates location of sample station. Broken lines are inferred isopleths. Shading indicates amount above regional average. The maps are generalized from the geologic data which include analyses from 264 sample stations (see fig. 7); X indicates significantly larger amounts at a geologic station.

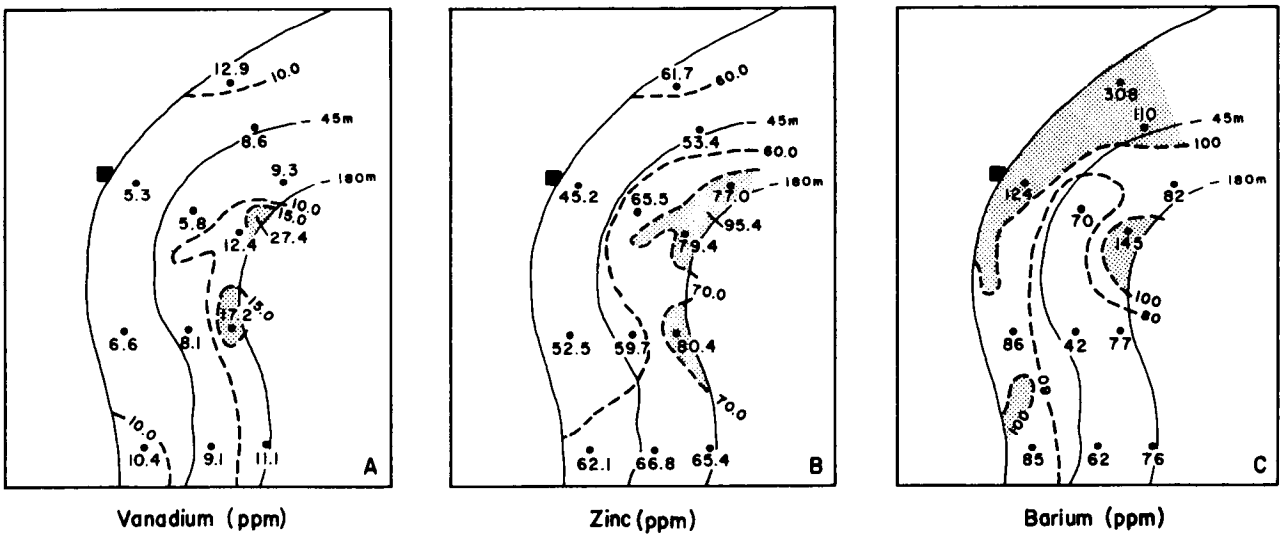

Figure 97. Distribution of the trace elements V, Zn and Ba in bottom sediments. Dot indicates location of sample station. Broken lines are inferred isopleths. Shading indicates amount above regional average. The maps are generalized from the geologic data which include analyses from 264 sample stations (see fig. 7).

porcelain mortar to a particle size sufficiently small to pass through a 200 mesh SPEX nylon screen. After homogenization, three subsamples were extracted, placed in a crucible and were heated to 450°C for 4 hours to ash the organic component of the sample. The sample was reweighed, transferred to an acid-washed culture tube and was leached with concentrated HNO_3 at 105°C until oxidation ceased. This method was used for all elements except Ba. Ba was brought into solution by a 1 to 1 mixture of concentrated HNO_3 and 30 percent H_2O_2. The resulting solution was analyzed by an atomic spectrophotometer. The specifications used in the analysis are shown by table 14.

Table 14. Instrument specifications and mode of analysis for trace elements in bottom sediments [303PE with an HG2100 graphite furnace]

Element	Wave Length	Dilution	Mode	Dry Temp.	Ashing Temp.	Atom. Temp.
Ba	2776	1:20(1:200)	Flameless	100°C	1200°C	2700°C
Cd	2293	1:10	Flameless	100°C	250°C	2100°C
Cu	3262	1:10	Flameless	100°C	900°C	2700°C
Cr	3589	1:100	Flameless	100°C	1200°C	2700°C
Fe	2483	1:1000	Flame	--	--	--
Mn	2801	1:1000	Flame	--	--	--
Ni	2330	1:10	Flameless	100°C	1200°C	2500°C
Pb	2842	1:10	Flameless	100°C	550°C	2000°C
V	3194	1:10	Flameless	100°C	1700°C	2700°C
Zn	2146	1:100	Flame	--	--	--

Amount and distribution

A statistical summary of the trace metals analyses for all 264 stations is shown by table 15. The patterns of distribution for the 10 trace metals are shown by the series of maps in figures 96 and 97. Summary statements regarding the patterns of distribution for each of the 10 elements follow table 15.

Table 15. Statistical summary of analyses for trace metals in bottom sediments at 264 stations. Data in parts per million.

Element	Mean	Standard Deviation
Ba	101.30	52.18
Cd	0.62	0.25
Cu	6.54	1.62
Cr	22.30	5.39
Fe	21869.40	3339.50
Mn	362.60	90.62
Ni	16.93	4.41
Pb	8.94	2.42
V	8.75	2.69
Zn	62.90	11.30

Cadmium (fig. 96C)--The amounts of Cd ranged from 0.2 to 1.55 ppm with an asymmetrical distribution skewed toward the higher end of the range from a strong dominant modal concentration of 0.5 ppm. The largest amounts (>1.0 ppm) are in separated areas: one at the shelf edge, and a second on the inner shelf seaward of the Rio Grande. The localized large amounts on

the outer shelf possibly can be attributed to emanating natural gas; those in sediments seaward of the Rio Grande possibly come from the river effluent which drains the intensively farmed Rio Grande valley where herbicides are used extensively.

Chromium (fig. 96D)--The Cr content of the sediments ranged from 4.9 to 42.1 ppm with a moderately skewed distribution from a modal value of 19 ppm. The pattern of distribution indicates three areas where content is greater than the regional average: south of the outlet of Matagorda Bay; a large westward trending salient on the central outer shelf; and the outer part of the ancestral Rio Grande delta. The largest amounts are on the central outer shelf in the suspected gas seep area.

Copper (fig. 96E)--The amount of Cu ranged from 2.6 to 10.7 ppm, symmetrically distributed around a modal value of 7 ppm. The significant features of the distributive pattern for Cu are the localized areas of increased content at the edge of the shelf and the abrupt increase south of a line that approximates the 27°15' N. parallel.

Iron (fig. 96F)--The amount of Fe ranged from 1.13 to 3.34 percent, distributed symmetrically around a dominant mode of 2.0 percent. Fe is widely distributed and differences in amount are not large. Somewhat larger amounts are in the suspected gas seep area at the shelf edge.

Manganese (fig. 96G)--The Mn content of the sediments ranged from 206 to 556 ppm, skewed asymmetrically toward the lower end of the range from a modal value of 375 ppm. Four separate areas have more Mn than other parts of the shelf: seaward from the outlet for Matagorda Bay; the suspected gas seep area on the outer shelf; a small area on the inner shelf south of Port Aransas; and the southern outer part of the shelf.

Nickel (fig. 96H)--Concentrations of Ni ranged from 3.5 to 26.1 ppm with a bimodal distribution around modes of 12 ppm and 20 ppm. Consequently, the pattern for Ni appears to consist of two populations: one characterized by the 12 ppm mode in the northern half of the OCS, and the other characterized by the 20 ppm mode in the southern part. The boundary between the two populations is the 27°15' N. parallel, which is also the boundary separating two modes of occurrences for Cu. The distributive pattern for Ni resembles that for Cr, particularly in the suspected gas seep areas.

Lead (fig. 96I)--The Pb content ranged from 2.2 to 16.5 ppm with a slightly asymmetrical distribution skewed toward the larger amounts. The largest amount of Pb is in sediments of the northwestern part of the OCS southeast of the outlet to Matagorda Bay. Pb content is greater than the regional average in two small areas at the edge of the shelf.

Vanadium (fig. 97A)--Amounts of V ranged from 4.1 to 27.4 ppm with distribution skewed asymmetrically toward the larger amounts from a modal value of 8.5 ppm. Highest V content is localized at the shelf edge within the suspected gas seep area and farther south in an area where organic carbon also is abundant.

Zinc (fig. 97B)--Concentrations of Zn ranged from 38.9 to 95.4 ppm with a broad and slightly asymmetrical distribution from a dominant mode of 60 ppm. The salient of increased Zn that extends westward from the area of suspected gas seeps approximates the same area where amounts of Cr, Cu and Ni also are increased.

Barium (fig. 97C)--The Ba content of the sediments ranged from 31 to 308 ppm. The distribution of the metal is asymmetrically skewed toward the larger concentrations with a dominant mode of 75 ppm. The pattern of distribution indicates three areas of significant Ba content. The largest amounts

The largest amounts are associated with oil fields where the Ba was most likely spilled onto the sea floor during the drilling of wells. For the entire OCS region, Ba content was highest over the northern half of the shelf; subareas there, having localized high Ba content, were in the extreme northwest and at the shelf edge.

Interpretation and relationships

The interpretive statements made in the preceding descriptive paragraphs can be summarized as follows: 1) sediments at the outer edge of the shelf had the largest amounts of Cd, Cr, Cu, Fe, Mn, V and Zn; 2) sediments seaward of the outlet to Matagorda Bay were highest in content of Pb and Ba and ranked second to the outer shelf in amounts of Cr, Mn and V; and 3) the southern half of the OCS contained Cu and Ni in amounts that averaged significantly larger than in the northern half.

The localized concentration of some of the trace metals in sediments along the edge of the shelf has been attributed in the descriptive statements to suspected natural gas seepage. The elements possibly are trapped in the sediments as the gas migrates upward to the sea floor surface. An alternative explanation is that the larger trace metal values in these areas simply are typical of fine-grained sediments that are characteristically rich in organic material and clay minerals. Trace metal content tends to be higher as a general rule in sediments of this type and in a setting where pelagic organic remains are a significant part of the fine-grained sediments. The salients in the distributive patterns for Cr, Ni, V and Zn suggest some net westward transport of the fine sediments, possibly by the movement of open Gulf water onto the outer shelf.

High-Molecular-Weight Hydrocarbons

Methods

Two basic techniques were used for extraction of the heavy hydrocarbons from the bottom sediments: SOXHLET extraction and ultrasonic dispersion. In both cases the samples were treated first with methanol to remove water and then with benzene to complete the extraction. In the SOXHLET extraction, each solvent was used for a minimum of 24 hours. For the ultrasonic extraction, the thawed sample was mixed with three sample volumes of solvent and sonicated for 10 minutes by a BRANSON model S-125 ultrasonic generator.

The sample was filtered under partial vacuum onto prewashed filter paper and re-extracted twice with each solvent. All extraction solvents were combined, reduced in volume, saponified, separated and analyzed in the same manner as described for the neuston.

Amount and distribution

High-molecular-weight hydrocarbons were extracted from sediments at each of the 12 stations, 3 seasons of the year. The nonsaponifiable extract averaged 0.02 percent of the total sample and ranged from 0.17 to 0.0001 percent. Analysis for the n-alkanes was successful for 34 of the 36 samples collected. Two samples contained few or no n-alkanes that could be resolved from a background "hump" of hydrocarbons.

The relative percentages of n-alkanes for each station by season and the inferred patterns of distribution are shown by the maps in figure 98. No trends are obvious, either areally or seasonally. The OEP values suggest

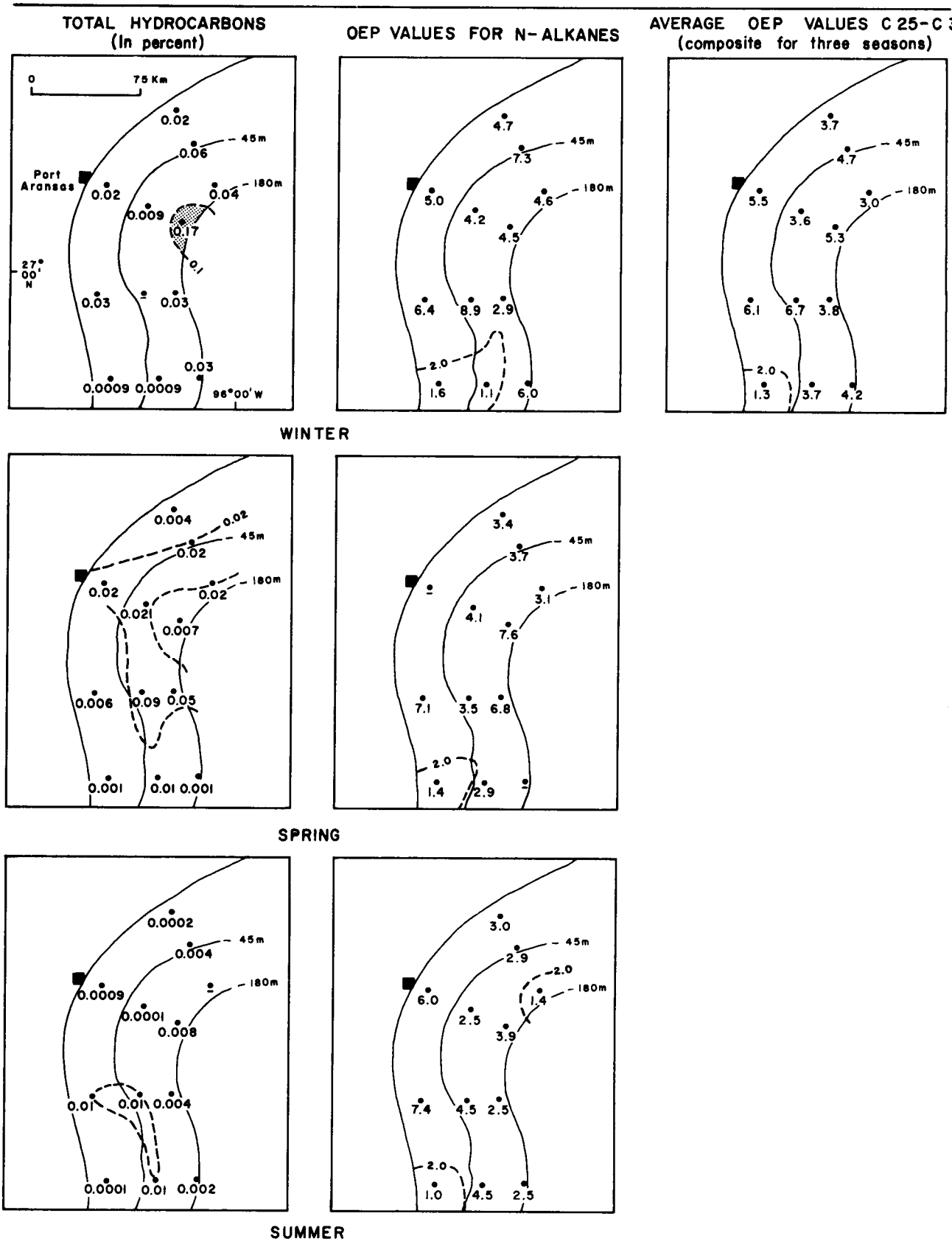

Figure 98. Seasonal distribution of total high-molecular-weight hydrocarbons (C_{15}-C_{35}) and odd-even preference (OEP) values for the n-alkanes in bottom sediments. Dot indicates location of sample station. Low ratios for OEP and high percentages of total hydrocarbons contoured. Broken lines are inferred isopleths.

a consistently small amount of n-alkanes for transect IV, station 1, possibly indicating an area contaminated with petroleumlike hydrocarbons, either from a seep or a spill.

In an effort to find a trend for the n-alkanes, the data for the four innermost stations were averaged and a smoothing factor was applied as a function of carbon number. The result is a general distribution envelope of n-alkanes with the usual odd predominance filtered out. Similar smooth weight percentages were calculated for the averages of other stations and transects. The outermost samples near the shelf edge appear to have larger relative amounts of the lower molecular size (C_{20} to C_{24}) n-alkanes. The lower n-alkanes may be contributed by more marinelike organisms and the higher n-alkanes by more terrestrial sources. No such trends were indicated when the data were averaged by transects.

The most prevalent compounds in the 5 samples of sediment analyzed by GC-MS were $C_{30}H_{50}$ (squalene), $C_{30}H_{50}O_2$ (betulin) and $C_{17}H_{34}O_2$ (methyl palmitate). The ratio of saturates to nonsaturates averaged 1.83 and ranged from 0.56 to 9.6. The averages by season were: winter, 1.4; spring, 1.8; and summer, 1.8. The summer average was weighted by a ratio of 9.6 at station 3, transect III.

BIOTA

Epifauna

Invertebrates

Epifaunal macroinvertebrate organisms were sampled by trawling both night and day at the 12 stations in figure 6. Because of the very soft mud bottom at some stations, the trawl at times netted significant amounts

of mud. When this happened, infaunal organisms became mixed with the epifauna, but the degree of mixing could not be quantitatively judged. The intermixing may explain some rather large variations in some types of organisms such as the Mollusca. Aboard ship, all invertebrates were preserved in a 5 percent formalin solution. In the laboratory, the preserved specimens were sorted, identified and enumerated by individuals and by species.

The benthic epifauna identified can be classified into two groups based on abundance and distribution: the first group consisted of a few species that were very common to nearly ubiquitous and were collected repeatedly during most of the year - Solenocera vioscai, Penaeus aztecus Trachypenaeus similis, Sicyonia dorsalis and Callinectes similis; the second group, common to uncommon species, included Amusium papyraceus, Squilla chydaea, Parapenaeus longirostris, Portunus spinicarpus, Astropecten duplicatus and Brissopsis alta. A large number of epifaunal species were collected very infrequently during the three periods of sampling. The seasonal distribution of the epifauna by number of individuals and by species is shown by figure 99.

The patterns of abundance shown by the maps indicate sizable seasonal and day/night variations in both numbers of individuals and numbers of species. Spring yields exceeded those for winter and summer significantly and night catches exceeded daytime catches in all three seasons, as a general regional trend. Nevertheless, at two individual stations, the day/night pattern was reversed. At station 1, transect I during the winter and at station 1, transect II during the spring, daytime totals substantially exceeded the night catches at the same station.

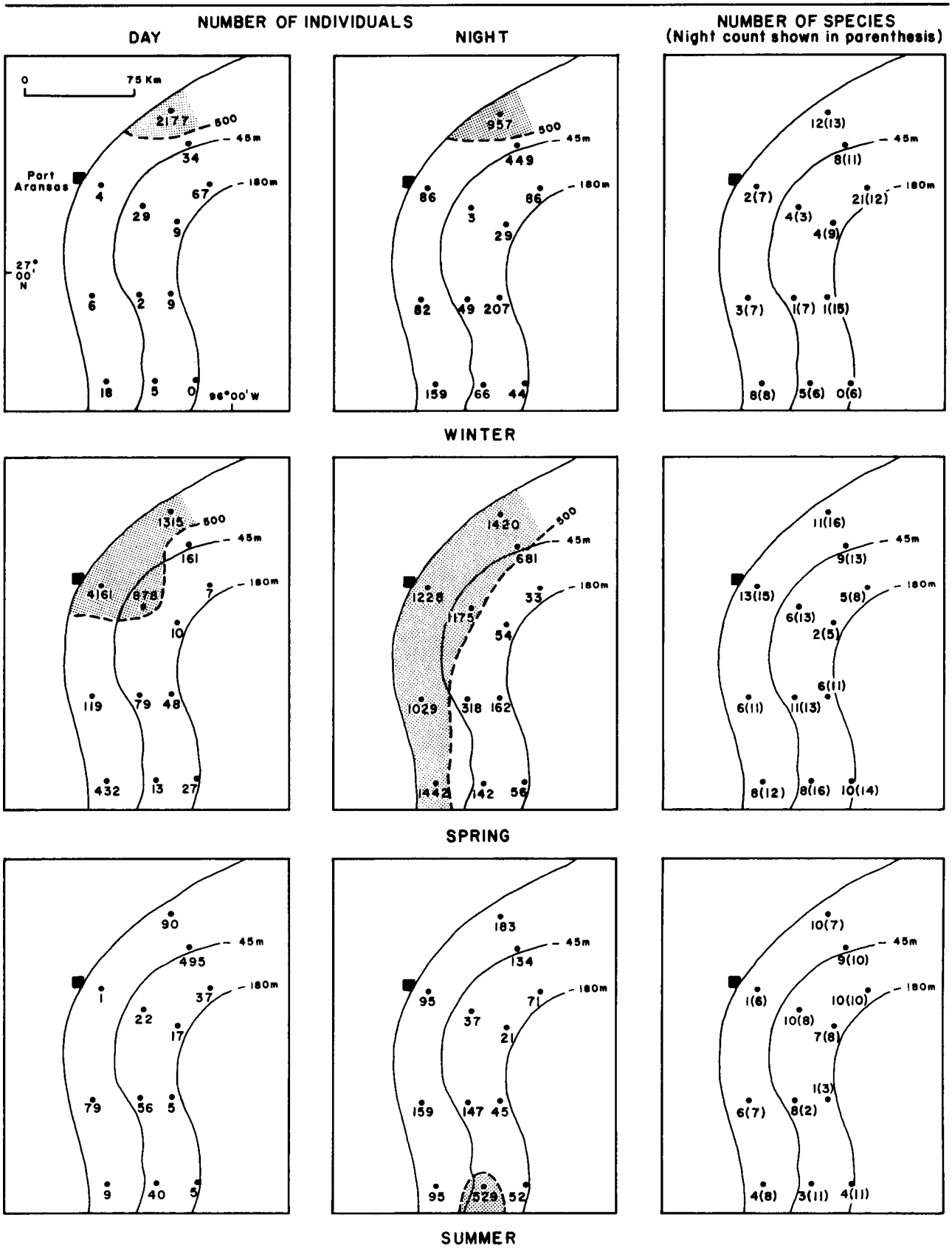

Figure 99. Seasonal distribution of epifaunal invertebrates by number of individuals and by number of species (day and night). Dot indicates location of sample station. Broken lines are inferred isopleths. Shading indicates amount above regional average.

In the winter, the total numbers at station 1, transect I exceeded the total numbers at the same station in the spring samples, but elsewhere numbers were small. In the spring, the organisms had increased greatly in number all along the inner shelf. Notably, the zone of greatest abundance in spring incorporated the mid-shelf stations on transects I and II but only the innermost stations of transects III and IV farther south. In summer, the numbers of individuals were greatly reduced below spring totals, but the numbers of species were not so drastically reduced. The greatest seasonal variation in numbers of both individuals and species for a single station was at the inner shelf station off Port Aransas.

No consistent patterns of species numbers or diversity are apparent in the epifauna. Individual species did exhibit some spatially limited distribution. Some congeneric species such as Portunus gibbesii and P. spinicarpus seem to have overlapping ranges; P. gibbesii is the dominant form at shallow stations and P. spinicarpus is dominant at the deeper stations. Several species, including Amusium papyraceus, Solenocera vioscai and Parapenaeus longirostris, were found only at the deep stations. Others, including Callinectes similis and Portunus gibbesii seem to be restricted to the shallower two stations on all four transects. Rossia tenera was limited to the mid-shelf station on all four transects and was found only in the spring samples. Large numbers of squid representing the species Loligo pealei, Lolliguncula brevis and Rossia tenera were caught during the daytime trawls but were virtually absent from the bottom at night. Consequently, the species of squid, though listed, were not used in the statistical calculations for the epifauna.

The epifauna are by nature motile and seem to wander widely. The patterns of distribution demonstrated in figure 99 show distinct seasonal

characteristics for winter and spring. Water depth seems to be a factor affecting distribution, but the increased food supply in the spring seems to be the controlling factor. The distributive pattern for the abundance of epifauna in the spring is very similar to those for nutrients and plankton in the same season.

Demersal Fish

As the specimens were preserved by freezing, wet weighing of the iced samples was done initially. Later, when the frozen fish were thawed, identified and weighed to the nearest 0.1 g, the total weights were summed so that a correction could be made for any weight losses of individual species due to dehydration. Fish from each sample were identified and weighed individually, and standard fork and total lengths were measured to the nearest millimeter. In all cases, the total numbers and weights of each species were determined. Statistics based on the numbers of individuals and species were derived for species diversity, probability of interspecific encounter (PIE) and equitability.

The seasonal distribution of the epifaunal fish by individuals and by species is shown by figure 100. In terms of greatest abundance, the patterns are similar to those for the epifaunal invertebrates; for the region as a whole, the fish are more uniformly distributed than are the invertebrates. Seasonal and diurnal differences are evident. The patterns suggest several significant characteristics: 1) substantially increased abundance in the spring; 2) consistently larger numbers of both individuals and species at the northwesternmost station; and 3) an increase in numbers of individuals at the southernmost stations in the summer. Day/night differences appear to be significant only at the shallow stations. These

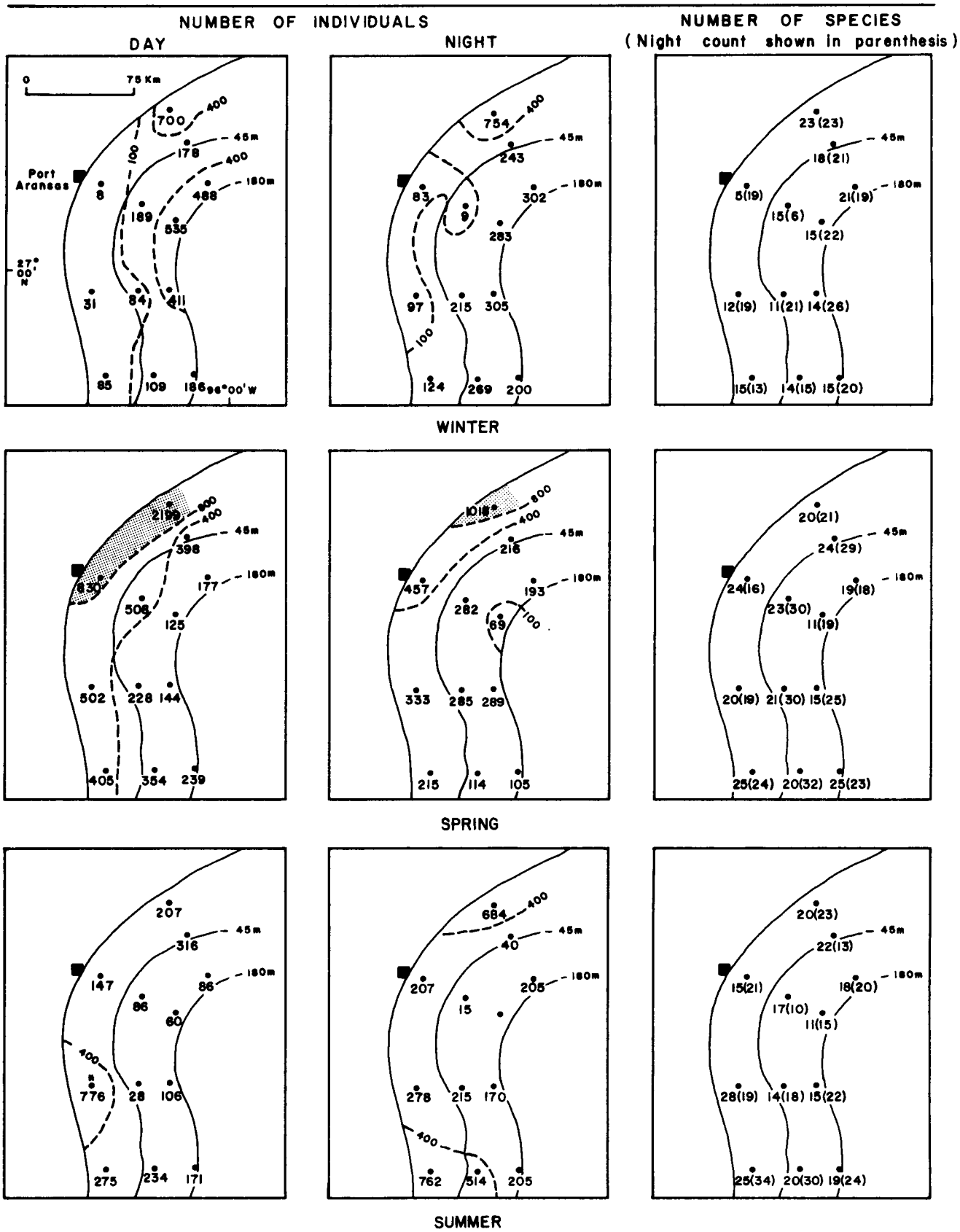

Figure 100. Seasonal distribution of epifaunal fish by number of individuals and by number of species. Asterisk on map for summer/day indicates largest single sample by weight for all three seasons (21,606.8 gms). Dot indicates location of sample station. Broken lines are inferred isopleths. Shading indicates amount above regional average.

differences are striking for all three major statistical components: individuals, biomass and species composition.

The statistical data on biomass were not plotted in map form but the daytime trawl in the summer at station 1, transect III, yielded 21.6 kg, the heaviest single catch for all three seasons. The statistics indicate that weight per fish increases with depth and that the greatest differences between catch numbers and weights seem to be at the inner shelf stations. The length-frequency tabulations show the expected increase in biomass from winter through summer; in most cases, the large, fast-growing fish were in the southern part of the OCS area.

The distributive patterns for epifaunal fish resemble those for nutrients and plankton. The increased food supply in the water seems to be the primary reason for the springtime proliferation.

Infauna

The samples for infauna were taken by a SMITH-MACINTYRE grab sampler whose capacity was 0.0125 m^3. Four samples were taken at each of the 12 stations, yielding about 0.05 m^3 of sediment for infaunal extraction at each station. One hundred and forty-four samples were collected and analyzed. Aboard ship, the sediment was washed through a 0.5 mm mesh screen and all invertebrates were preserved in a 5 percent formalin solution. Processing in the laboratory followed those steps used for the epifaunal invertebrates.

The results of the infaunal studies reported in this section are in part duplicative of those briefly reviewed in the section on bottom sediments. However, the two studies were made for different purposes. Those reported

with the sediment descriptions were biogeologic and related to infaunal activity as a modifier of sediment structure and texture. Those reported here are principally taxonomic. Furthermore, the taxonomic studies were based on four samples from each station rather than on a single sample.

The infauna collected are divisible into three groups of organisms based on abundance and distribution. The first group, consisting of a few species, were common to ubiquitous and were found at most sites during most of the year. The group included the polychaetes Paraprionospio pinnata, Nereis sp. and the amphipod Ampelisca agassizi. They were most common at the shallow stations and along transects I and IV. Some, such as Paraprionospio pinnata, were common at the deeper stations as well. A second group, generally less common and less widespread than group one, included Armandia maculata, Mediomastus californiensis, Tharyx setigera, Cossura delta and Ninoe nigripes. The third group, mostly species classified as rare, were found infrequently and in very small numbers. The infauna is dominated numerically and taxonomically by the polychaetous annelids. Molluscs were collected infrequently in the infaunal samples and were more abundant in the epifauna. The seasonal distribution of the infauna by numbers of individuals and by numbers of species is shown by figure 101.

The patterns of distribution for the infauna are very distinct. Both the numbers of individuals and the numbers of species decrease systematically with distance from shore. Several species were geographically restricted: the polychaete Paralacydonia paradoxa was collected only at the outermost station on each transect; Magelona sp., Nereis sp. and Diopatra cuprea were found primarily at stations 1 and 2 of each transect.

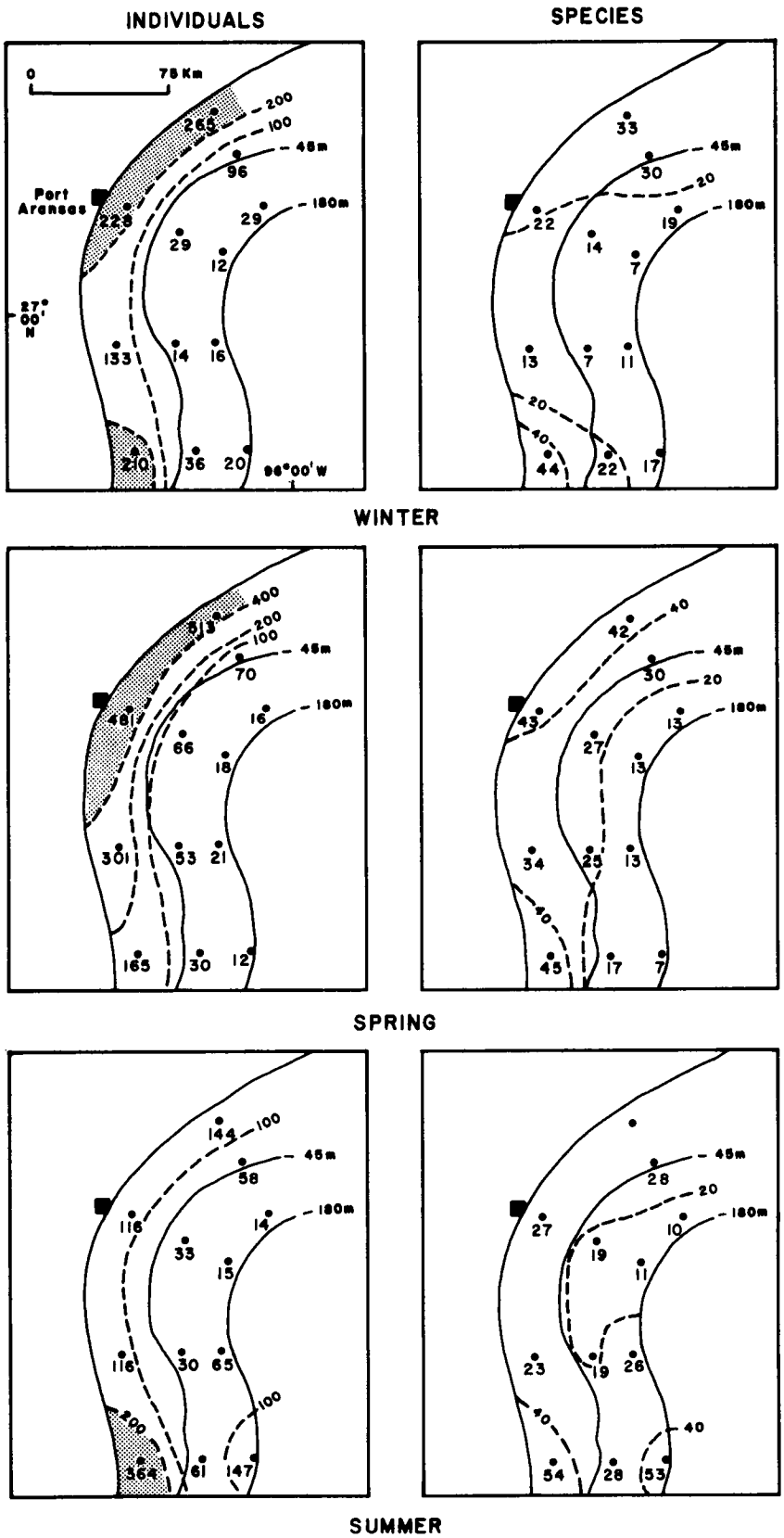

Figure 101. Seasonal distribution of infaunal organisms by number of individuals and by number of species. Dot indicates location of sample station. Broken lines are inferred isopleths. Shading indicates amount above regional average.

When compared seasonally, both numbers of individuals and numbers of species are largest in the spring. This trend follows the patterns for both epifaunal invertebrates and demersal fish. The infaunal abundance in the spring is another example of the regional biologic response to the increased nutrient supply that accompanies the spring runoff.

The spatial distribution of the infaunal invertebrates seems to be controlled primarily by the grain size of the bottom sediments. The infauna are most abundant along the inner shelf and over the ancestral Rio Grande where the sediments are coarse (sandy). This strong relationship also was borne out by the infaunal studies done in conjunction with the sediment studies. (Compare figure 101 to figure 94.) A secondary factor affecting spatial distribution may be water depth.

The diversity data for the taxonomic studies correspond to those for the biogeologic studies in some respects but not in others. Both indicated a consistently greater diversity and higher equitability at station 1, transect IV, which has a very shelly, sandy bottom. The taxonomic studies indicate an increase in diversity seaward along transects I, II and III, which is the reverse of the trend indicated by the biogeologic studies. The apparent contradiction may be due to the fact that four samples were taken at each station for the taxonomic studies, but only one sample was taken for the biogeologic studies. Moderate numbers of one or two very common species and a few individuals from a large group of uncommon or rare species are recovered from each inner-shelf sample. One grab sample probably collects approximately 30 percent of the species present at a given time at a specific inner shelf station; four grabs will recover slightly more than 60 percent. With each grab, the numbers of individuals of the ubiquitous to very common group

increase as do the numbers of common to rare species, although the latter increase at a lower rate. With four grabs, the domination of the sample by the ubiquitous to very common group is much greater, but the equitability and diversity are diminished. Consequently, the samples for taxonomy at the inner-shelf stations showed less diversity because of the dominance by a few species.

Trace Metals

Epifauna

The epifaunal organisms chosen for trace metals analysis were shrimp, squid and several species of demersal fish. These organisms were selected because of their ubiquitous occurrence in the samples collected and because of their mobility in the environment.

The samples were prepared for analysis as follows. The shrimp (Penaeus aztecus) were shelled, and the head, back vein and internal organs were removed so that only the flesh was sampled. Flesh samples from the squid (Loligo pealei) generally were taken from the mantle after it had been slit, and the chitinous pen and internal organs had been removed. The heads, fins and internal organs of the fish were removed prior to sampling. Where material was sufficient, the skin of the fish was removed and the flesh was separated from the bones. The processing procedure for analysis followed that described for the mesozooplankton, except that a 2 gm aliquot was used instead of 1 gm. The flesh was analyzed by atomic absorption spectrophotometry for amounts of Cu, Zn, Cd, Pb, Ni and Cr.

The results of the analyses by season for squid are shown by figures 102 and 103, and those for brown shrimp, by figures 104 and 105.

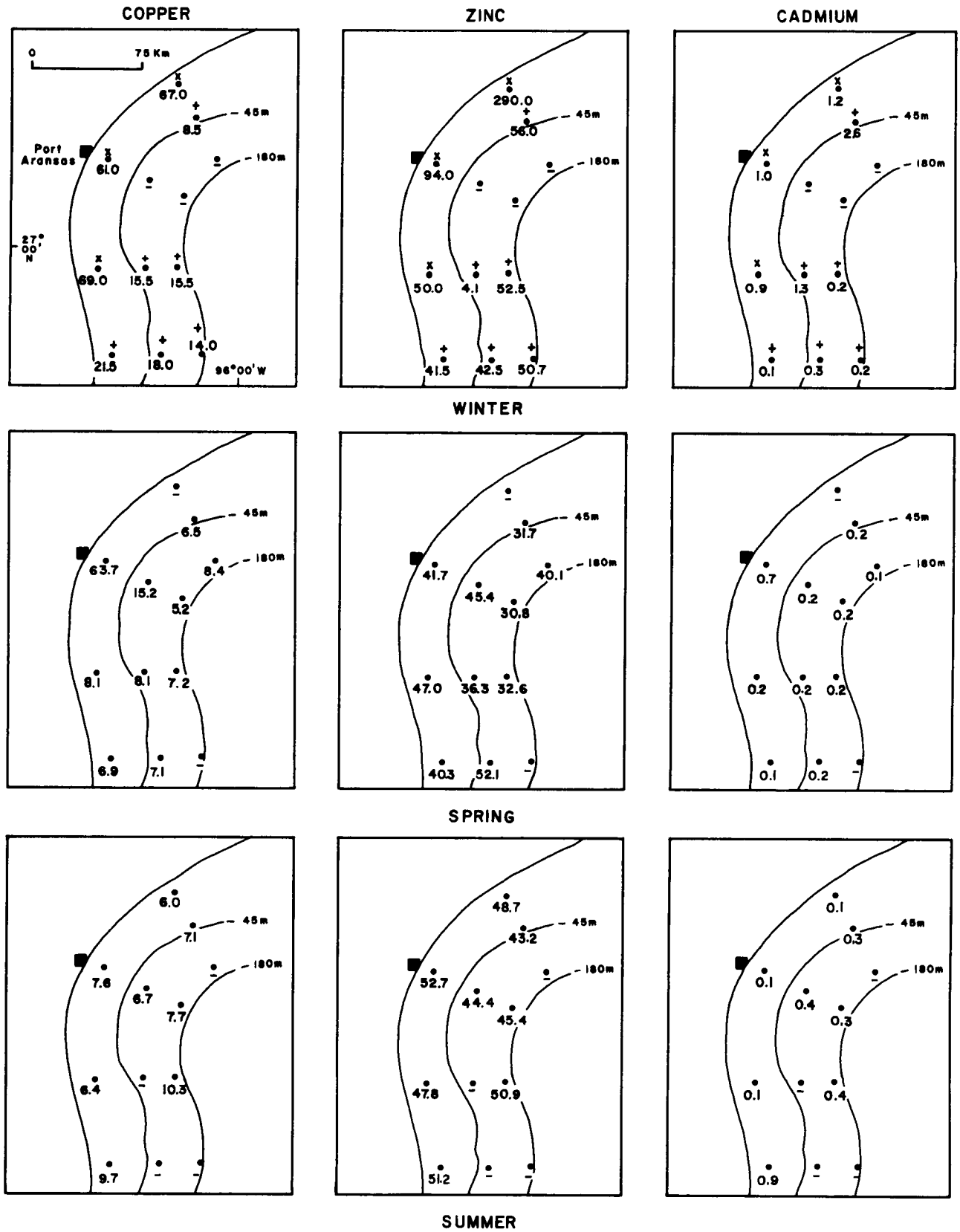

Figure 102. Seasonal distribution of Cu, Zn and Cd (ppm dry weight) in squid (Loligo peali) collected during the day. Blank indicates no squid in sample. For the winter analyses, the mantle tissue was used: X indicates analysis included skin; + indicates analysis excluded skin. For the spring and summer analyses, the muscle tissue was used. Dot indicates location of sample station.

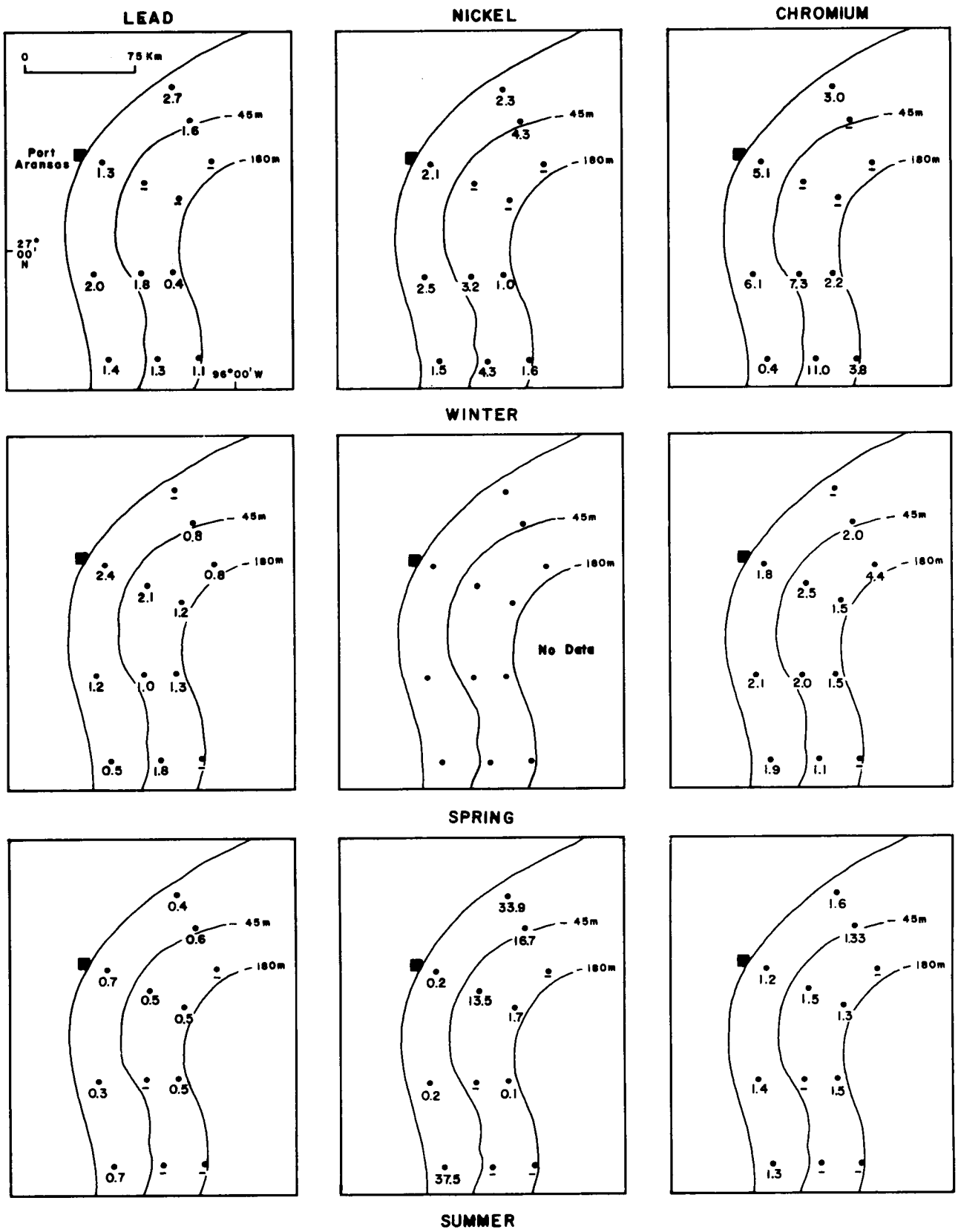

Figure 103. Seasonal distribution of Pb, Ni and Cr (ppm dry weight) in squid (Loligo peali) collected during the day. Blank indicates no squid in sample. Dot indicates location of sample station.

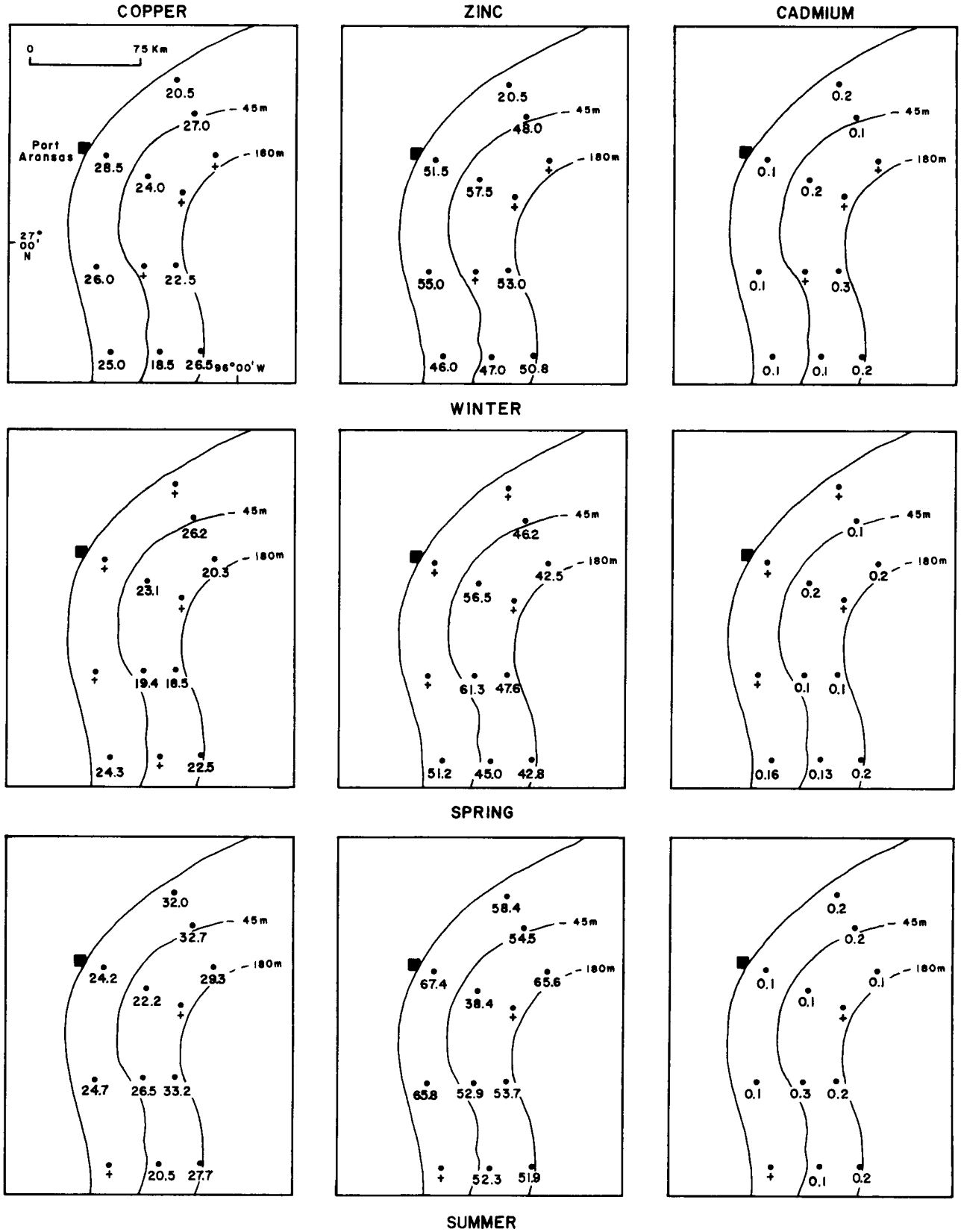

Figure 104. Seasonal distribution of Cu, Zn and Cd (ppm dry weight) in abdominal muscle of brown shrimp (Penaeus aztecus) collected during the day. Plus indicates no shrimp in sample. Dot indicates location of sample station.

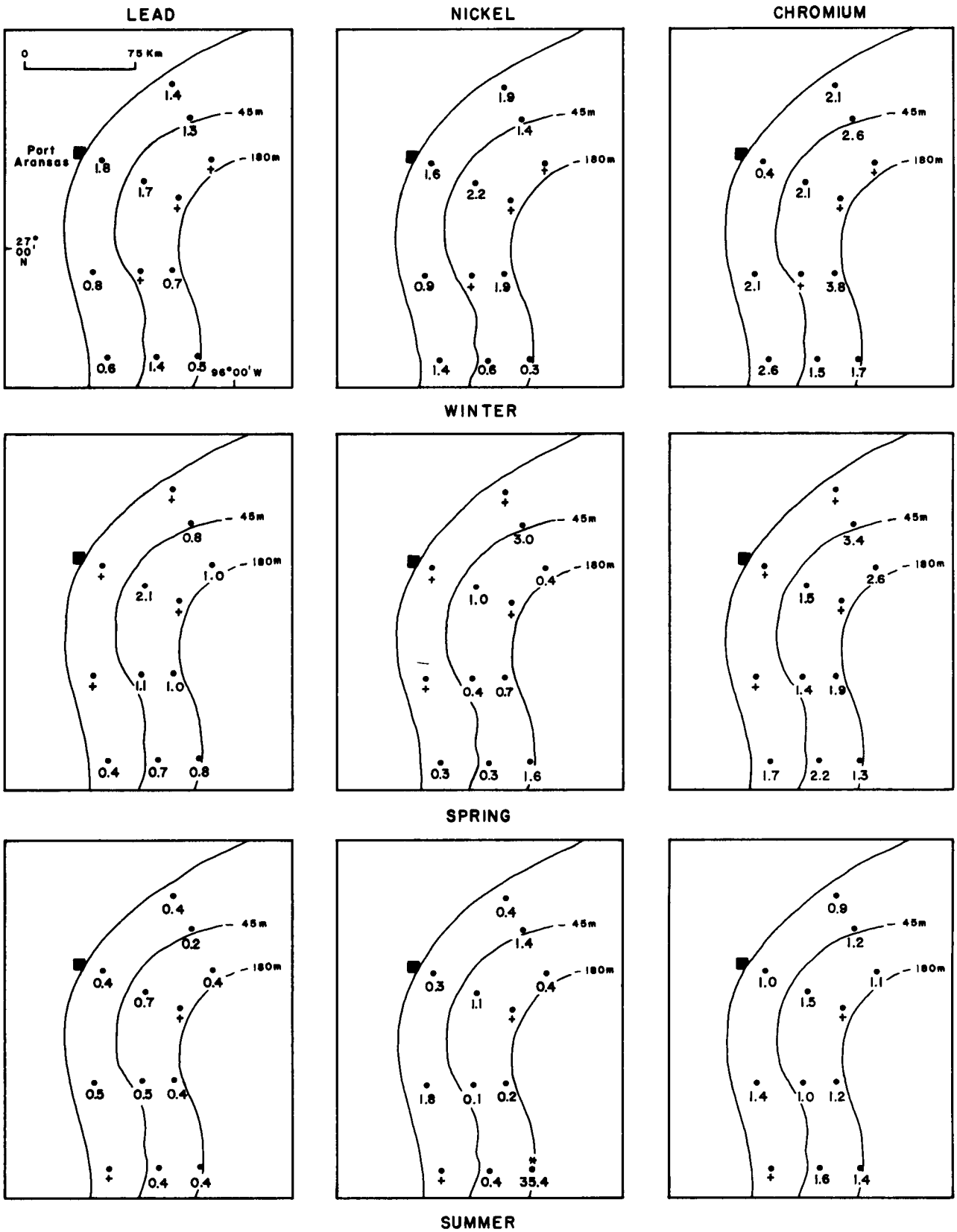

Figure 105. Seasonal distribution of Pb, Ni and Cr (ppm dry weight) in abdominal muscle of brown shrimp (Penaeus aztecus) collected during the day. Plus indicates no shrimp in sample. Asterisk indicates possible contamination. Dot indicates location of sample station.

For the squid, few trends are apparent. Regional comparisons were impossible because some analyses included the skin, but others did not; analyses incorporating the skin are uniformly more abundant in all six elements and are highly enriched in Cu and Zn. Disregarding the analyses containing skin, the distributions were essentially uniform over the region. Ni content was substantially higher at both ends of the OCS in summer: at station 1, transect I, and at station 1, transect IV. The amounts of Ni in the squid were similar to those reported in the literature.

The shrimp showed less chemical variability than fish or squid. Even the different species were similar, although the deep-water rock shrimp had less trace metals than the brown shrimp, which spends part of its life near-shore. The amounts of trace metals recorded were similar to those reported for other areas. No trends, either geographic or seasonal, were evident.

Demersal Fish

At least seven species of demersal fish were analyzed for trace metals content for each season of sampling. Variations in the species of fish caught from season to season precluded the use of the same seven species for all three sets of analyses. Consequently, regional trends in amounts of trace metals could not be established specifically and no distribution maps showing amounts of trace metals in demersal fish are included. At least 15 different species of demersal fish were analyzed during all three seasons. Even though a number of species were analyzed, amounts of trace metals in them remained fairly constant throughout the study. An exception was the larger amounts of Ni and Cr in the flatfish collected in the winter,

but the one or two analyses that increased the winter average were exceptionally high, possibly because of contamination. No obvious trends, either seasonal or geographic, were evident for the demersal fish or for the generally small amounts of trace metals concentrated in them. A total of 82 demersal fish samples were analyzed.

Interpretation and Relationships

Two concluding statements regarding the trace metals analyses of organisms are pertinent, not only to the epifauna and demersal fish but to other biota as well. They are enumerated as follows:

1) Almost all apparent seasonal variations results either from differences in the species composition or from one or two anomalous individual analyses;
2) The amounts of trace metals recorded in the biota either were similar to or were smaller than those reported for other areas in comparable types of samples, except for a few samples that may have been contaminated.

High-Molecular-Weight Hydrocarbons

Methods

The following types of benthic organisms were analyzed for high-molecular-weight hydrocarbon content: shrimp, wenchman, squid, flounder, rough scad, longspine porgy, sea robin, bass, sea trout, goatfish, flatfish, lizardfish, and 11 miscellaneous types of less than 3 specimens per species.

The samples, after defrosting for 1 to 2 hours, were transferred to preweighed 250 ml, round-bottom flasks. Small samples were used whole;

larger samples were cut into smaller pieces as needed for transfer to the flasks. After weighing, the samples were treated with potassium hydroxide (0.05 g/g tissue) and 50 ml of methanol. The samples were then heated under reflux for 2 hours. If digestion was not complete after 2 hours, heating was continued until no tissue remained. The methanolic hydrolysate then was transferred to a 250 ml separatory funnel. The extraction flask was rinsed with 50 ml of hexane, which was transferred to the separatory funnel. Approximately 100 ml of 5 percent NaCl in water was added to the funnel and the mixture was shaken. After allowing sufficient time for the separation of the hexane layer, the aqueous layer was decanted and the hexane was transferred to a KUDERNA-DANISH concentrator. The aqueous layer was extracted with two more 50 ml portions of hexane. The combined hexane extracts then were washed with salt water to remove the methanol and were concentrated to approximately 5 ml with steam.

Silica gel (WOELM, 70-230 mesh) was SOXHLET-washed with hexane and activated at 150°C for at least 24 hours before use. Ten g of the silica gel followed by 1 g anhydrous sodium sulfate were placed in a glass column (1.1 x 22 cm) containing hexane. The column was washed with 50 ml of hexane; care was taken to ensure sufficient solvent to just cover the solid absorbents. The hexane extract was then placed on the column and elution started. When the solvent miniscus reached the top of the column, the vial was rinsed with 5 ml of hexane, which was subsequently transferred to the column. The first 2 ml of eluate were discarded and a 23 ml hexane fraction was collected. A third fraction, containing the aromatic compounds, was collected using 50 ml of benzene. The column eluates then were concentrated as needed for gas chromatography using a stream of nitrogen.

A HEWLETT-PACKARD 5830 GC, equipped with dual flame ionization detectors, and a programmable integrator were used for the analyses. It was equipped with 6' x 1/8" stainless steel columns of 5 percent FFAP or 3 percent SE-30 on GAS CHROM Q 100/120. The injector was at 270° and the detector, at 350°. The column oven was programmed from 100° to 260° at 6°/minute. Columns of 1 percent SE-20 (6' x 1/8") and 5 percent FFAP (5' x 1/8") were used for the qualitative identification and quantification of the normal high-molecular-weight hydrocarbons. Quantification was performed with the aid of electronic integration, and calibration curves were established with standards made from nC_{18}, nC_{27}, nC_{32} and nC_{34} hydrocarbons obtained from Analabs.

Amount and Distribution

The species collected varied considerably between both sampling stations and sampling periods. Consequently, a meaningful statistical analysis of the analytical data was not possible. However, visual inspection of the results permit some general conclusions. No trends from station to station were evident; no petroleum contamination of the organisms was noted. The odd/even ratios were characteristic of biogenic hydrocarbons and very little phytane was detected. All samples yielded pristane in relatively large amounts. The most prevalent compounds in the 4 epifaunal samples analyzed by GC-MS were $C_{19}H_{40}$ (pristane), $C_{17}H_{34}O_2$ (methyl palmitate) and $C_{15}H_{32}$ (nC_{15}). GC-MS analysis attempts on 10 other epifaunal samples were not successful because of an inadequate amount of sample material.

Although the data indicated little variation of the high-molecular-weight hydrocarbon composition from station to station, valuable new

information was gained concerning concentration in several species of epifauna. Most of the organisms had relatively large amounts either of the C_{15} and C_{17} n-paraffins or of the C_{31} compound, or both. Shrimp, however, contained either none of the C_{15} and C_{17} paraffins or very small amounts. In squid, amounts of C_{17} were larger than amounts of C_{15} n-paraffin; in the fish C_{15} was dominant. All samples of wenchman had a large percentage of C_{15} and C_{17}. This occurrence is probably a result of their diet of algae since C_{15} and C_{17} are the major hydrocarbons in algae. The results of the analyses for squid, brown shrimp and wenchman are shown by figures 106, 107 and 108. The analyses for the other species were not amenable to map display because the representations varied considerably both between stations and between seasons. As a regional pattern, the analyses indicate that the shrimp and wenchman samples had less variation in aliphatic hydrocarbon distribution than did all other species, though both varied from one season to another. Of the species analyzed, these two would seem to be the most promising organisms for future monitoring of heavy hydrocarbon distribution and content against the 1975 baseline data. High-molecular-weight petroleum hydrocarbons of anthropogenic origin were not indicated in the 1974-1975 samples of epifauna from the South Texas OCS.

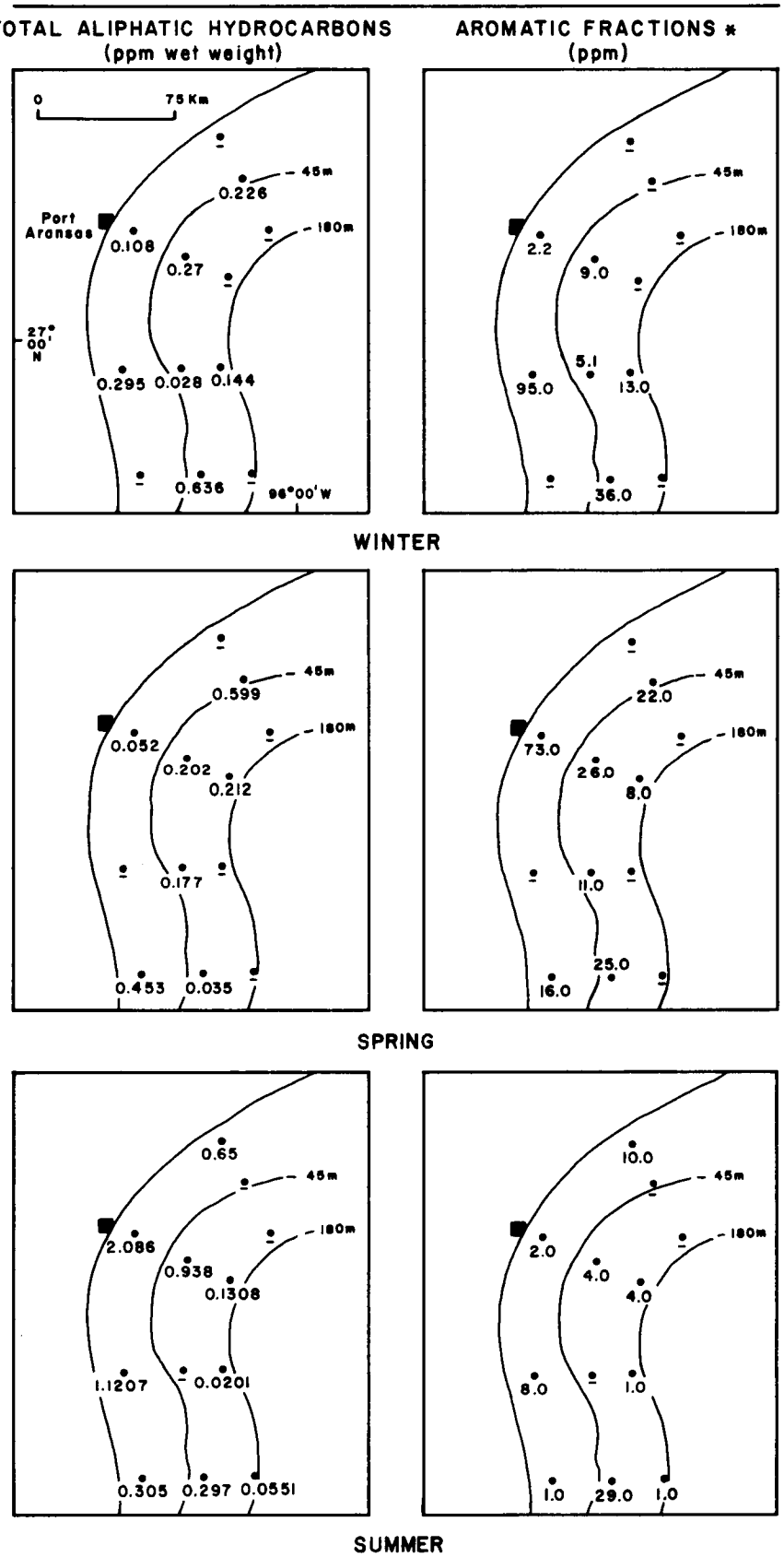

Figure 106. Seasonal distribution of total aliphatic hydrocarbons and of the aromatic fractions in squid. Blank indicates organism not present in sample. Dot indicates location of sample station.

*Aromatic fractions are the benzene solubles and include any organics that are soluble in benzene.

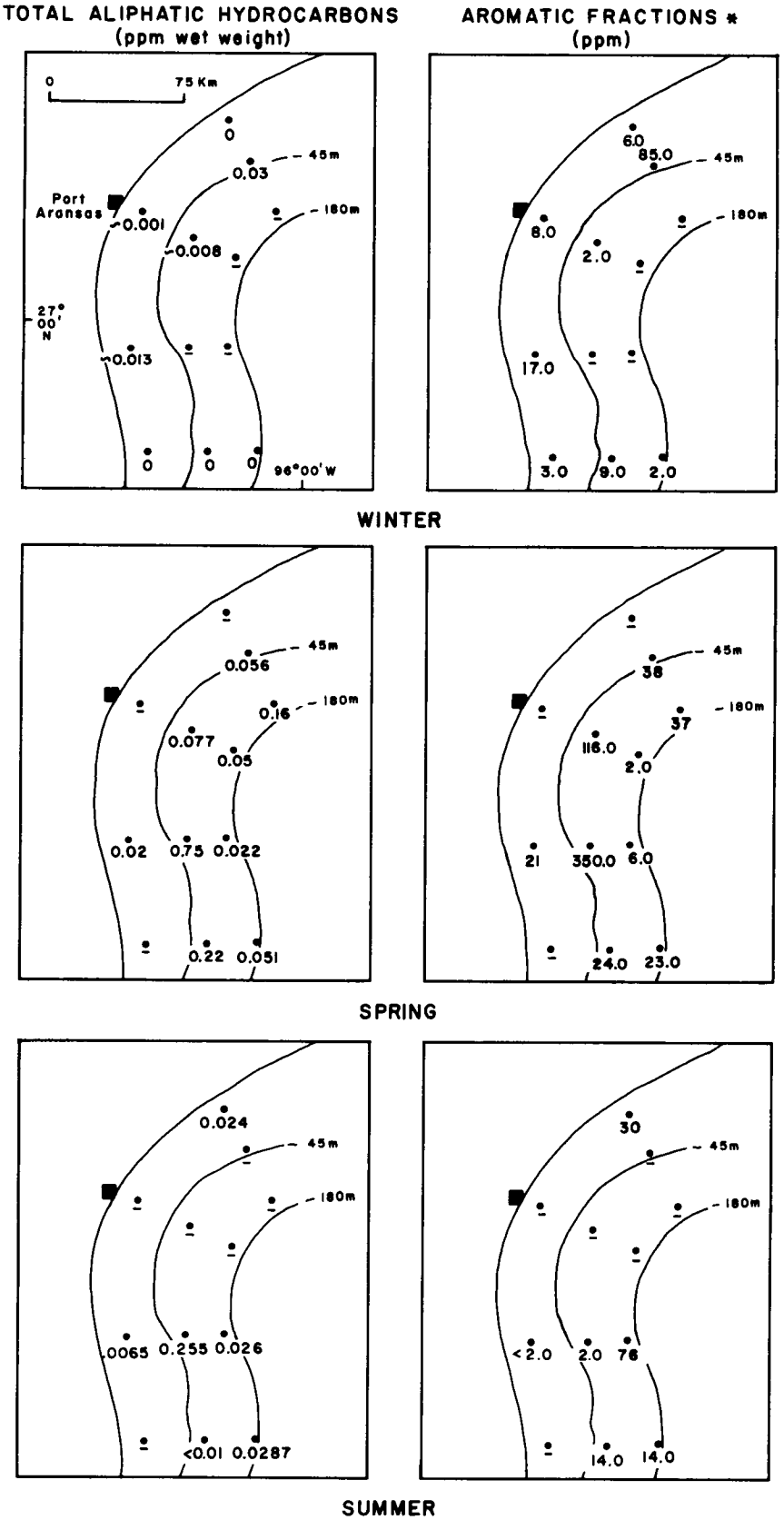

Figure 107. Seasonal distribution of total aliphatic hydrocarbons and of the aromatic fractions in brown shrimp. Blank indicates organism not present in sample; 0 indicates amount below level of detection. Dot indicates location of sample station.

*Aromatic fractions are the benzene solubles and include any organics that are soluble in benzene.

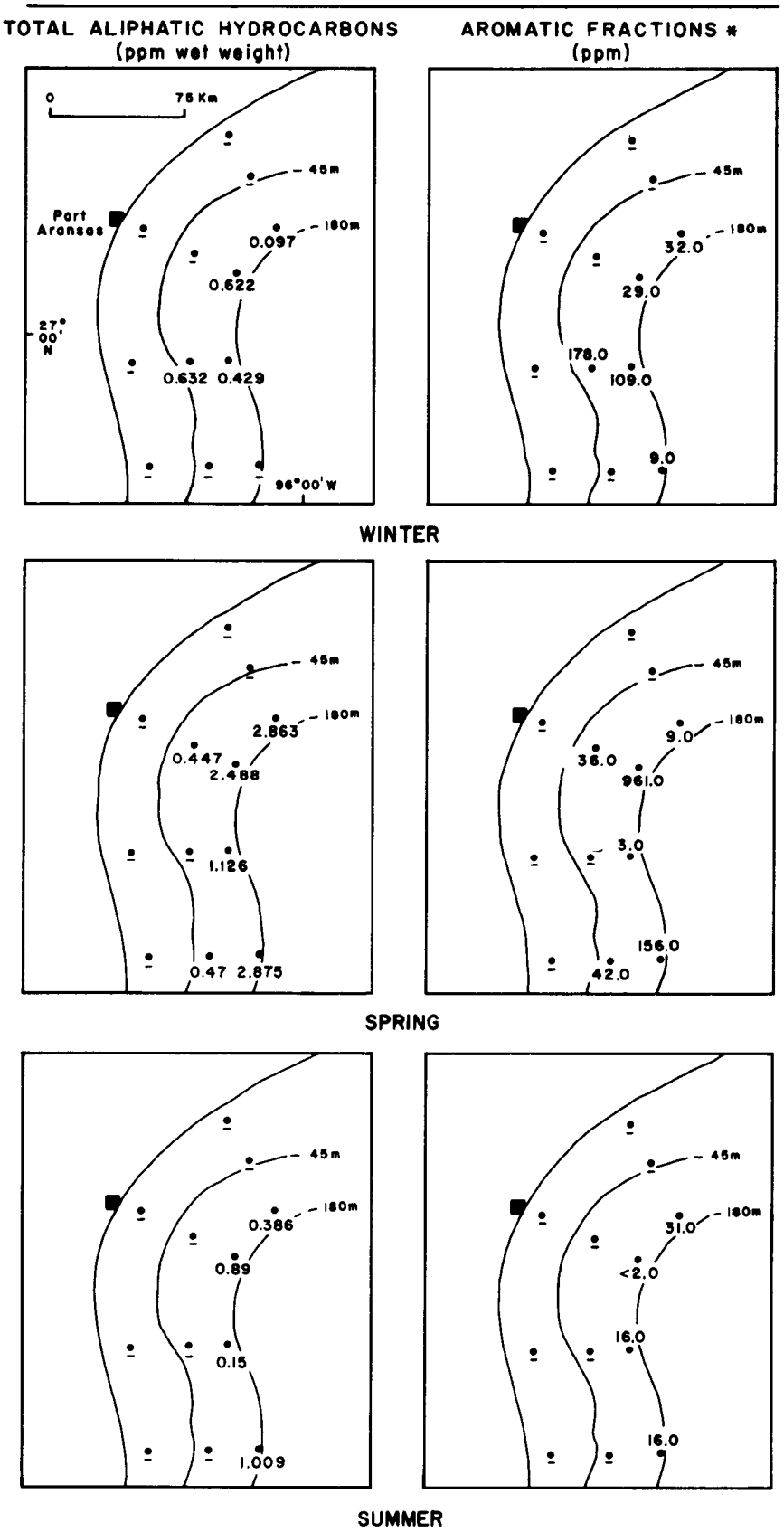

Figure 108. Seasonal distribution of total aliphatic hydrocarbons and of the aromatic fractions in the demersal fish, wenchman. Blank indicates organism not present in sample. Dot indicates location of sample station.

*Aromatic fractions are the benzene solubles and include any organics that are soluble in benzene.

GEOLOGIC STRUCTURE OF THE CONTINENTAL TERRACE

TECTONIC PATTERNS

Methods of Study

The basic data for interpretation of the geologic structure and framework were approximately 8,860 km of high resolution acoustic reflection profiles arranged in a traverse grid spacing of approximately 5 x 10 km. The systems used for collecting the geophysical data were: ACOUSTIPULSE transmitting 1000 joules and recorded at a sweep rate of 250 ms (0.25 sec); ANALOG REFLECTION sparker transmitting 900 joules and recorded at a sweep rate of 1000 ms (1 sec); sparker transmitting 10,000 joules and recorded at a sweep rate of 1000 ms (1 sec); and SUB-BOTTOM PROFILES transmitting 10 kw (3.5 kHz frequency) and recorded at a sweep rate of 500 ms (0.5 sec). The location of the acoustic profiles, coded as to the several types of acoustic reflection data obtained, are shown by figure 12. The navigation fixes taken at intervals of 305 m along most of the traverses and at 610 m intervals along others established the control points for plotting.

The tectonic patterns were determined by mapping all folds and faults and by preparing maps for two shallow key reflection horizons of regional extent to demonstrate amounts of deformation and sedimentation since late Pleistocene time. The subsurface maps indicate the spatial configuration of the horizons and the subsurface depth of the horizons beneath the sea floor surface.

Folds

Strata of the continental terrace display the undulating structure typical of folding. The strata have been gently buckled. A number of anticlinal crests were recorded on the 10,000 joule sparker analog profiles. The average depth from the sea floor to the crests is -200 ms or approximately -146 m. The location of the anticlinal crests is shown by figure 109, map A.

The anticlines have a general regional trend that varies from N30° to N45° E. The trend is parallel to shoreline over the northern half of the South Texas OCS, but is oblique to the shoreline over the southern part. The synclinal troughs between the anticlines are not well-defined within the penetration limits of the acoustic profiles. Consequently, the symmetry characteristics of the folds could not be determined.

Two domal structures probably formed by the diapiric movement of salt lie just seaward of the edge of the continental shelf. The domal structures are associated with branching anticlinal crests that lie along the juncture of the continental shelf and the continental slope.

Configuration of the Pleistocene/Holocene Contact

The extent to which the most recent deposits have been affected by the deforming movements within the continental terrace was examined by the construction of structure contour and thickness isopach maps for key subsurface horizons, as previously noted.

The younger of two very prominent reflecting surfaces of regional extent recorded on the profiles probably represents the base of the Holocene

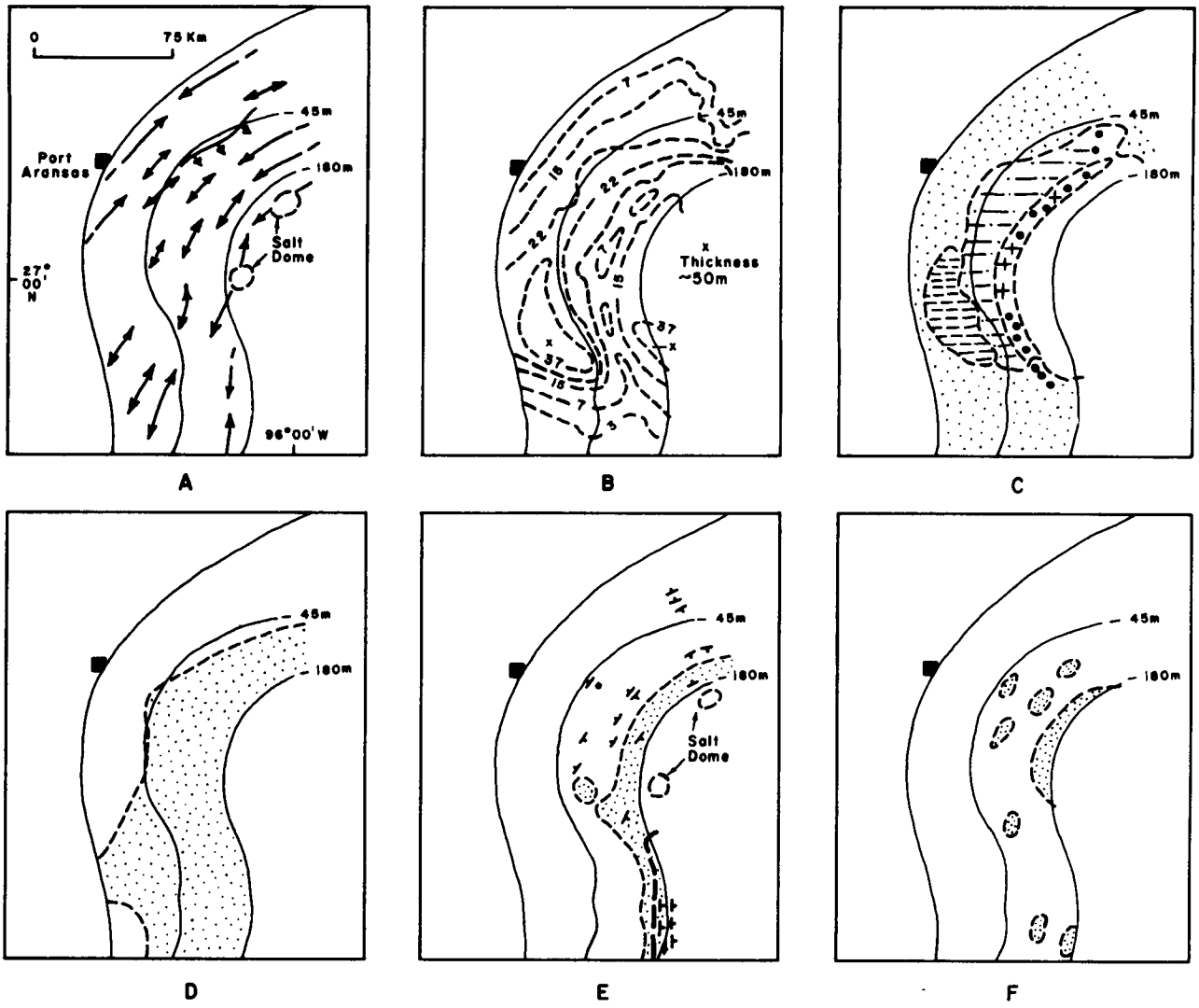

Figure 109. Geologic features of the South Texas OCS:

A. Location and trend of principal anticlinal folds. Arrows show direction of plunge.

B. Subseafloor depth (meters) of prominent acoustical reflecting surface believed to represent the Pleistocene/ Holocene boundary.

C. Nature of uppermost Pleistocene deposits and paleogeography of the South Texas OCS during the last low stand of sea level. Stippling indicates principally deltaic and fluvial deposits; bar and dot pattern indicates shallow lagoonal deposits; bars indicate probable organic-rich sediments deposited in a localized shallow depression characterized by poor circulation; plusses indicate probable shoreline deposits; large dots indicate the general locations of carbonate reefs.

D. Extent of late Pleistocene faulting. Stippling indicates area where late Pleistocene deposits are extensively offset by faults.

E. Extent of Holocene faulting. Stippling indicates area where Holocene deposits are extensively offset by faults. Perpendicular bar symbols indicate location of recent faults that extend to sea floor surface: short bar indicates dip direction of fault plane; long bar indicates strike direction. Heavy dashes enclose area of slumping.

F. Areas where seepage of natural gas is suspected.

sequence. As the age of the paleosurface has not been determined, it is designated "reflector A" for the purpose of discussion. Reflector A is defined as the surface that represents the lowest stand of the sea during the last glacial epoch. The interpretation is based solely on the geologic evidence as recorded on the acoustic profiles without qualifications as to whether or not the surface itself represents the Pleistocene/Holocene boundary or whether the boundary is more subtly concealed within the conformable sequence of sediments above reflector A.

Reflector A is coincident with the buried flanks of carbonate reefs of Pleistocene age whose tops have not been covered by sediments of Holocene age. Carbonate rocks dredged from two of the reefs have been dated by the radiocarbon (C^{14}) method: the indicated age for the material taken from Southern Reef is 18,990 years BP $\pm$370 years; that from Dream Reef, 10,580 years BP $\pm$155 years.

Reflector A is an uneven surface and the sediments above it are disconformable to those below. The configuration of reflector A and the thickness of sediments between it and the surface of the sea floor are shown by figure 109, map B. Although the sediments above the reflector have not been folded, the pattern of thickness for the overlying sediments suggests depositional control by the underlying folds in the outer part of the central sector of the OCS. (Compare maps A and B on fig. 109.) Maximum thickness of sediments above reflector A is about 51 m, indicating a relatively high rate of sedimentation on the South Texas OCS for at least the last 18,000 years. The most recent patterns of sediment deposition on the shelf are shown by figure 94, maps A and B. The types of deposits immediately beneath reflector A, as interpreted from the acoustic profiles, are shown by figure

109, map C. The map shows both the implied facies of deposits laid down during the last low stand of the sea and the inferred paleogeography of the time.

Faults

Every anticlinal crest shown on figure 109, map A is faulted. The faults are on both sides of the anticlinal crests and they tend to converge downward toward common depth points that usually lie beneath the depth limits of the sparker records. Along many of the faults, throw increases with depth, indicating progressive movement through time.

The several hundred faults noted on the acoustic profiles were plotted on maps to demonstrate the chronology of movement by faulting within the continental terrace since middle late-Pleistocene time. The upper terminus of each fault was plotted relative to stratigraphic position within the sediments and relative to two prominent subsurface reflectors: reflecting surface A, discussed previously, and a deeper-lying surface, B, thought to be of middle late-Pleistocene age. The faults that offset reflector B but not A are within the area shown on map D, figure 109. Those that offset reflector A, but not the sea floor surface, are within the area indicated by the stipple pattern on map E, figure 109. The locations of the scattered faults that extend to the surface of the sea floor also are indicated on map E.

The series of small faults along the outer edge of the continental shelf in the southern part of the OCS is associated with surficial slumping of unconsolidated sediments. The heavy broken line on map E indicates the general area of slumping. Most of the slumping is on the continental slope beyond the shelf.

Analog patterns recorded in the water column on the acoustic profiles are believed to represent natural gas that was seeping upward through the sea floor sediments and into the water above. The locations of areas where gas seepage is suspected are shown by figure 109, map F. Almost all of the suspected gas seeps were located above faults.

GEOLOGIC HAZARDS

The term "geologic hazards" is used here in a very broad sense for those geologic aspects of the South Texas OCS that should receive special attention when engineering development is being considered. The mission of the geologic studies conducted as a part of the environmental studies of the South Texas OCS was to identify in regional scope the features and the areas that should be subjected to detailed site-specific surveys when engineering projects are being planned.

Faulting

The South Texas OCS has no history of even moderate seismicity. The tectonic grain of the continental terrace indicates deforming movements that have been singularly of small scale but in aggregate continuous and progressive through time. Displacements of large magnitude have developed through time rather than as single events. Their nature can best be described as continuous creep rather than intermittent, abrupt rupture. The general mechanism involved is the gravity adjustments taking place between the thick sequence of rapidly deposited sediments in the continental terrace and the less dense, deep-lying salt that is being squeezed upward through the sediments. Faulting has occurred extensively along the outer shelf during Holocene time. The

direction of movement along these faults has been in part down-to-the-basin offset. However, the localized diapiric movement of salt just seaward of the shelf edge has caused additional fault offsets in the opposite direction. The faulting has been progressive as demonstrated by increased throw along most of the faults with depth. The historical pattern indicates that similar movements can be expected in the future. As noted previously, seepage of natural gas upward along some of the faults is suspected. The extent of the most recent faulting is shown by map E, figure 109.

Sea Floor Stability

The coherence of surficial and near-surface sediments over much of the OCS area is low. Variations in sediment coherence closely follow the textural patterns of the sediments, as shown by figure 94, maps A and B. The OCS area has been subdivided into six subareas on the basis of regional variations in the coherence of bottom sediments. (See fig. 110.)

Area A--General coherence is moderate to low: coherence increases landward as sand content increases. Although the sediments within area A are not sufficiently coherent to support a heavy structure founded at shallow depth, conditions are laterally uniform and abrupt lateral changes are not likely to be encountered.

Area B--General coherence is low, but abrupt changes occur laterally in the vicinity of the series of carbonate reefs. The flanks of the consolidated limestone reefs are buried by soft mud that becomes progressively thicker away from the reefs. Furthermore, the mud in the vicinity of the reefs contains varying amounts of reef rubble that impart varying coherency

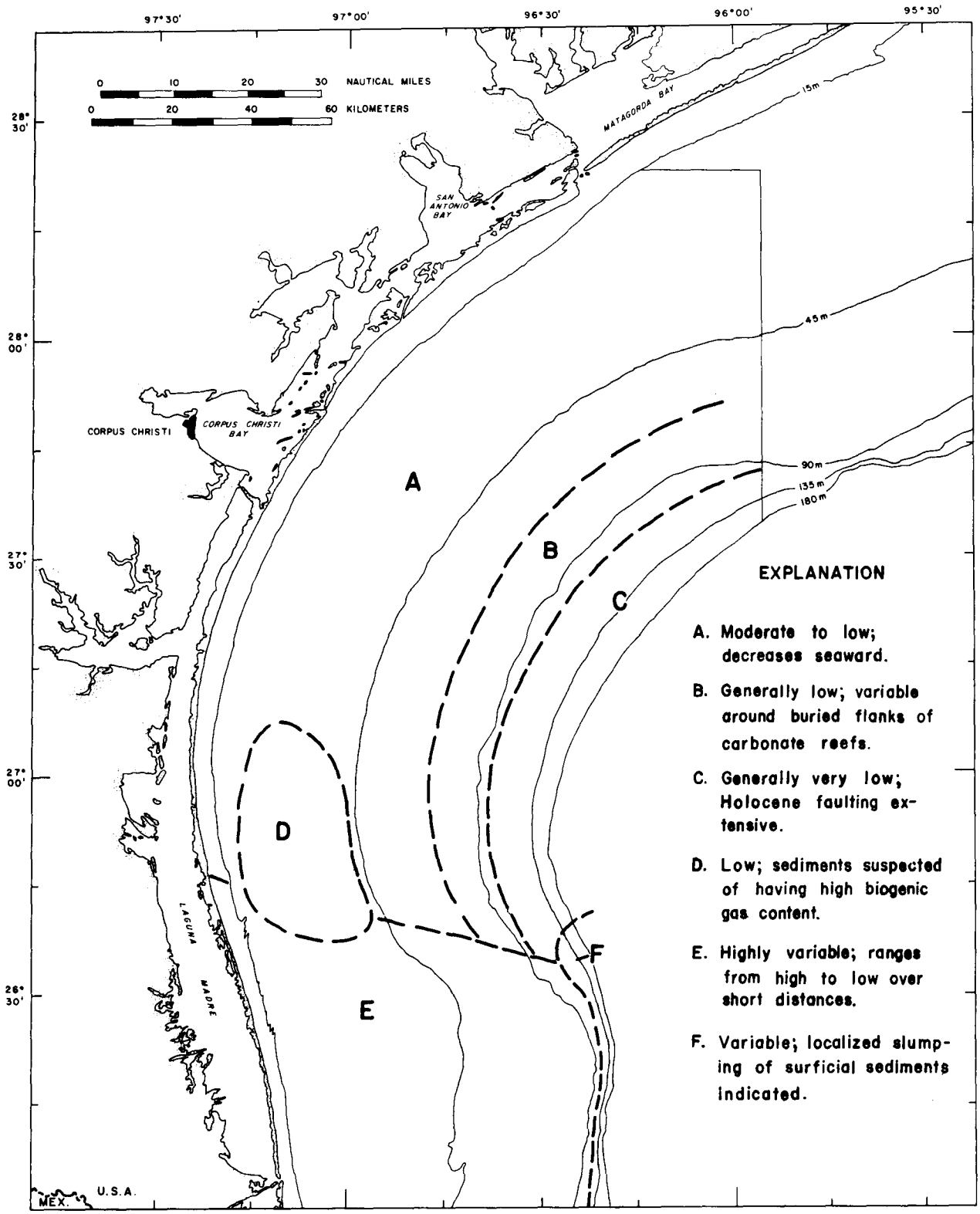

Figure 110. Classification of South Texas OCS according to coherence of shallow subsurface sediments.

to the sediments. The extent of the rubble is not known precisely, but cores indicate that the deposits of rubble are more extensive on the west side of the reefs. At Hospital-Aransas Reef (see fig. 5) the rubble in the muddy sediments extends approximately 305 m westward.

Area C--Coherence is very low; the finest grained sediments in the South Texas OCS are in area C and the clay mineral content of the sediments is large. The most extensive faulting during the Holocene has been in area C.

Area D--Coherence is low. A relatively large content of natural gas at shallow depths is strongly suspected on the basis of the analogs recorded on high resolution seismic profiles. The sediments within the general area outlined on figure 110 are acoustically incoherent; sound is effectively attenuated by the sediments at depths ranging up to a hundred m or more. The boundaries of the area are knife-sharp on the seismic profiles. The most likely causes for the condition seem to be either entrapped biogenic gas or unusually large amounts of organic material within the sediments.

Area E--Coherence is highly variable within subarea E. Where sands are exposed at the surface, the bottom is sufficiently firm to block penetration by a piston corer. Elsewhere mud of varying thickness overlies firm sand and gradients between sediments of different texture are steep, indicating abrupt lateral changes.

Area F--Coherence is variable as sands extend locally almost to the edge of the shelf. The distinctive feature of subarea F is the localized slumping of surficial sediments along the edge of the shelf. Although, as noted previously, the slumping is more extensive on the adjacent continental slope.

The coherence of the deeper lying sediments is not known as no samples are available below depths of a couple of m. Two subsurface horizons of possibly increased coherence are immediately beneath reflector A and at reflector B, which lies at a general subsurface depth of 65 to 150 m. These two horizons are thought to represent paleosurfaces of the continental shelf exposed at low stands of the sea during glacial epochs. If so, more coherent sand deposits probably are associated with them; also coherence may have been added by the relatively prolonged exposure to atmospheric conditions.

SUMMARY: INTERRELATIONSHIPS AND CONCLUSIONS

The summaries that follow pertain specifically to results of the baseline sampling carried out as part of the interdisciplinary studies made in 1975; they have been designed to present the essence of the findings and their meaning as concisely as possible. The maps and charts present in a diagrammatical form the environmental characteristics of the South Texas OCS.

GEOGRAPHIC PATTERNS OF ABUNDANCE

Many aspects of the South Texas OCS environment are strongly correlative in a geographic sense, others less so and a few not at all. The biological, chemical and hydrographic aspects showing the strongest correlation are summarized in the series of maps in figures 111 through 114. The maps show by pattern the spatial relationships of major abundance for each of the sample stations; the patterns are composites covering all three seasons of sampling. The composite patterns are based on the number of times during the three periods of sampling a station ranked first or second in either biological numerical abundance, or chemical concentration. For the hydrography, both the high and low measurements for salinity and temperature were composited. The number outside the parentheses indicates the number of times the station ranked first, the number in parentheses indicates the number of times it ranked second. The isopleths were drawn on the basis of the sum of the two rankings.

The composite patterns on figure 111 indicate the relative abundance of the marine organisms; those on figure 112 show the distribution of chlorophyll, ATP the nutrients and hydrographic aspects; and those on

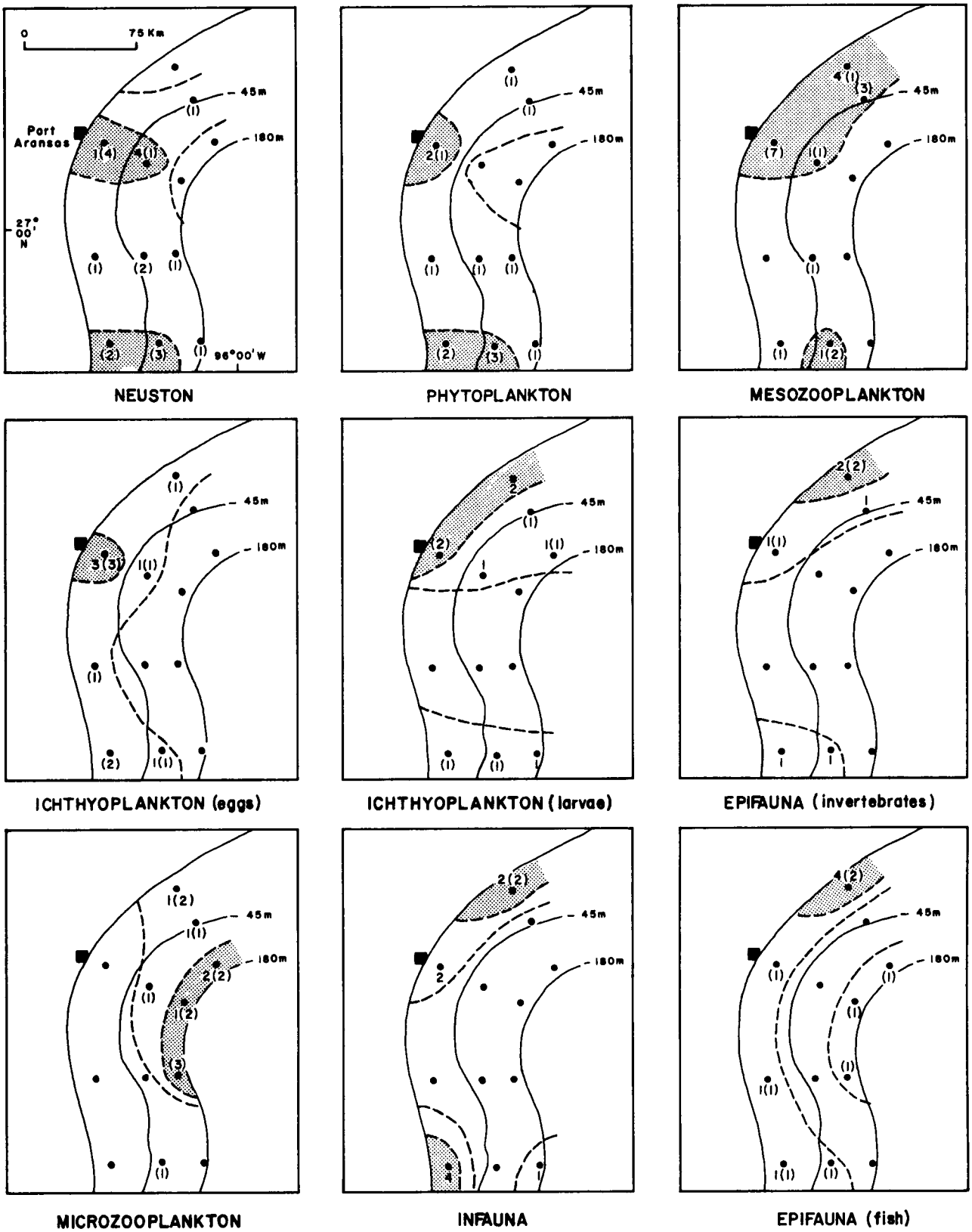

Figure 111. Composite patterns of abundance of organisms for all three periods of sampling. Number outside parentheses indicates number of times station ranked first during all three seasons; number in parentheses indicates number of times station ranked second. Dot indicates location of sample stations. Broken lines are isopleths based on sum of the two numbers, but weighted to first order rankings. Shading indicates amount above regional average.

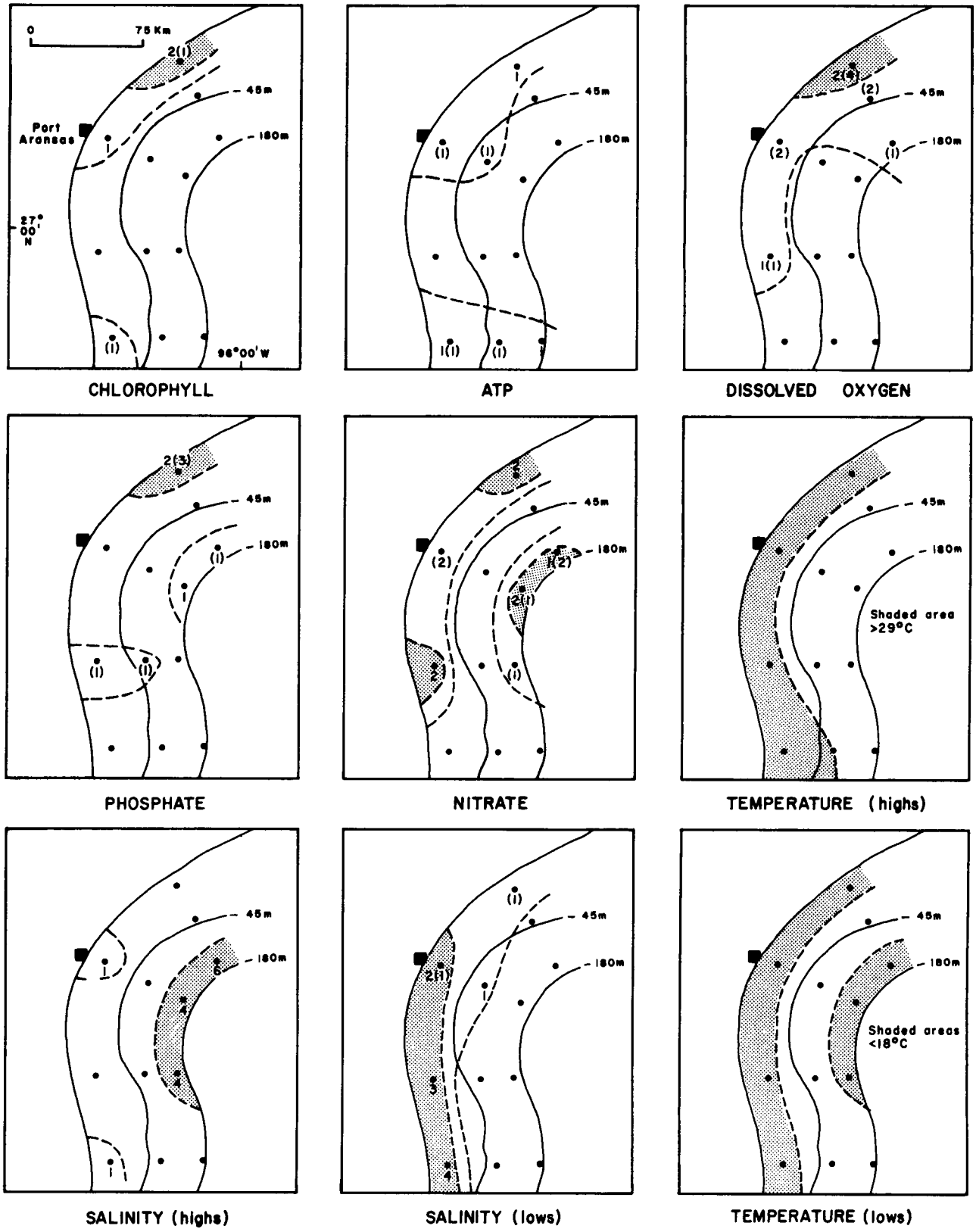

Figure 112. Composite patterns for amounts of nutrients and for hydrographic conditions for all three periods of sampling. Number outside parentheses indicates number of times station ranked first during all three seasons; number in parentheses indicates number of times station ranked second. Dot indicates location of sample stations. Broken lines are isopleths based on sum of the two numbers but weighted to first order rankings. Shading indicates amount above regional average.

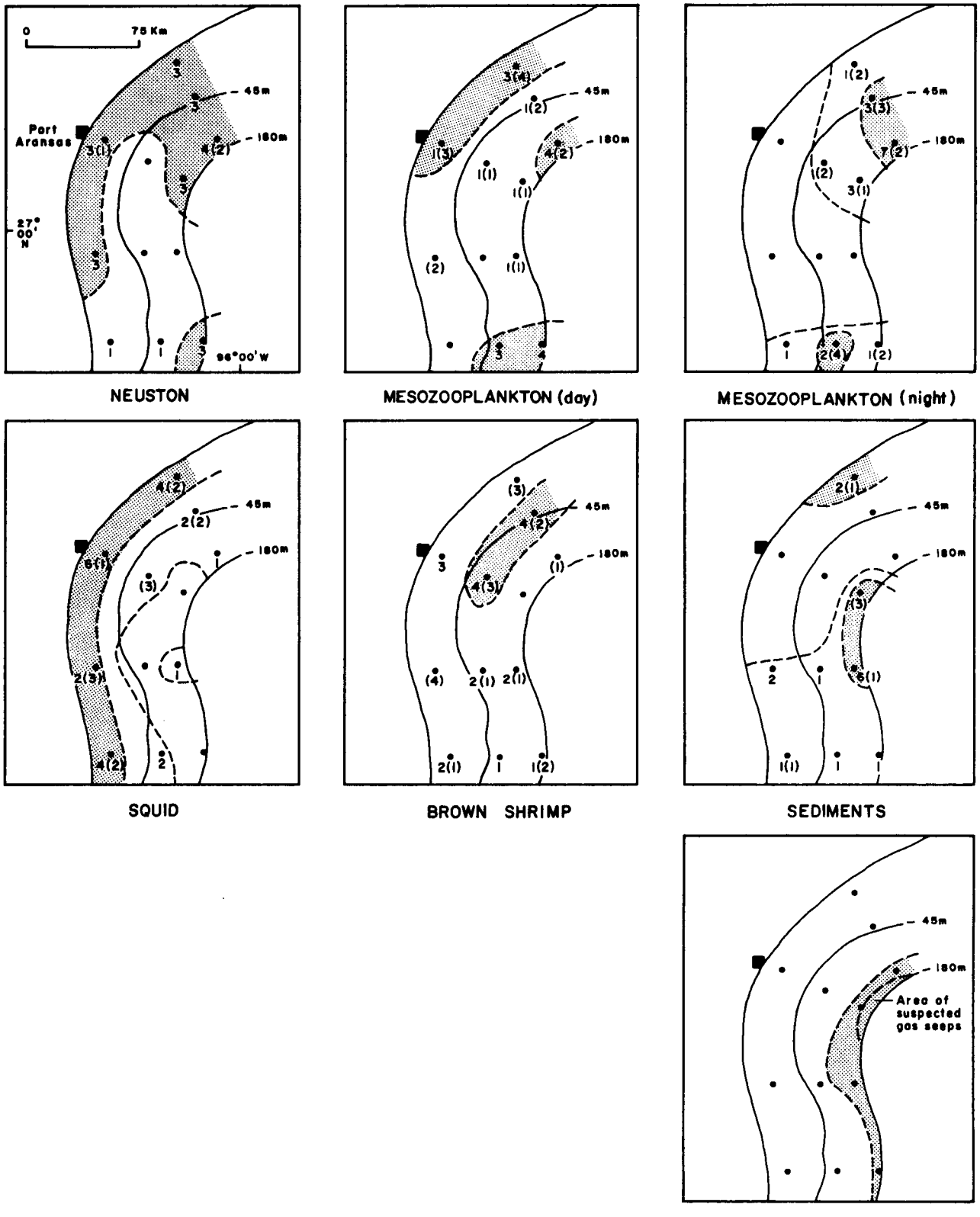

Figure 113. Composite patterns of abundance of trace metals in organisms and in bottom sediments; map of area of Holocene faulting. Number outside parentheses indicates number of times station ranked first for a specific metal during all three seasons; number in parentheses indicates number of times station ranked second. Dot indicates location of sample stations. Broken lines are isopleths based on sum of the two numbers, but weighted to first order rankings. Shading indicates amount above regional average except in map of Holocene faulting, where it indicates location of area where Holocene faulting has occurred.

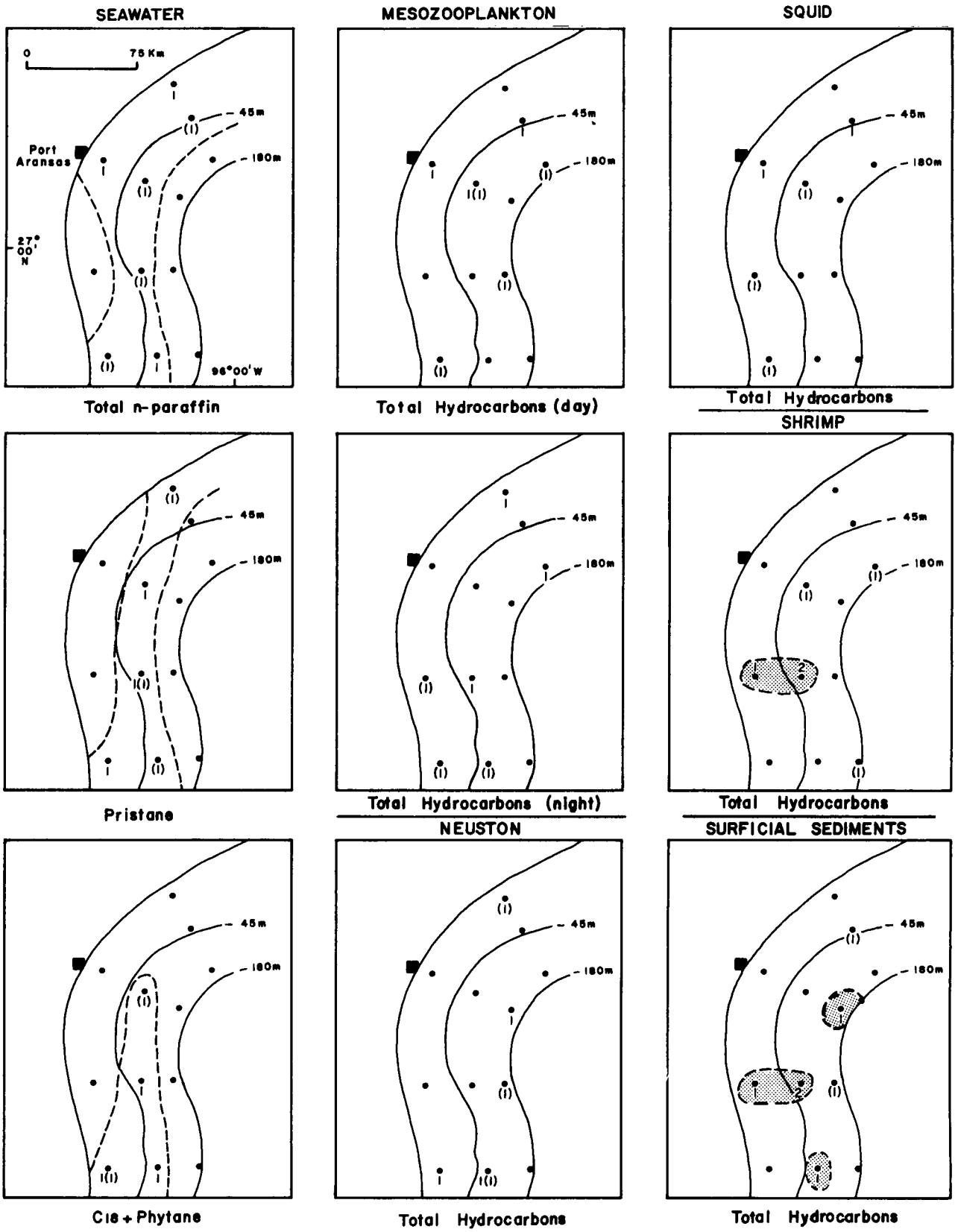

Figure 114. Major abundance of high-molecular-weight hydrocarbons by station and by category of analysis for all three periods of sampling. Number outside parentheses indicates number of times station ranked first during all three seasons; number in parentheses indicates number of times station ranked second. Dot indicates location of sample stations. Broken lines are isopleths based on sum of the two numbers, but weighted to first order rankings. Shading indicates amount above regional average.

figure 113 show the distribution of trace metals in certain of the marine organisms and in the bottom sediments. The patterns for the marine organisms in figure 111 and those for the nutrients and related components in figure 112 are strikingly similar, even though localized variations are apparent. A strong cause-and-effect relationship is evident, namely the mutual abundance of both numbers of organisms and amounts of nutrients along the inner part of the OCS where continental runoff supplies the food base for the highest level of productivity on the OCS. The productivity reaches its peak in the spring when continental runoff is greatest. The reduced salinity along the inner shelf in the spring documents the influx of fresher water.

In contrast to the composite patterns for the biota and nutrients, those for the hydrocarbons showed few direct relations to the distribution of other components. A few exceptions are worthy of note. In sea water, the several components of high-molecular-weight hydrocarbons, n-paraffins, pristane and C_{18} plus phytane, were most abundant in winter and spring along the same mid-shelf area where amounts of methane and, to a degree, propane were largest in spring and summer. In the sediments, the high-molecular-weight hydrocarbons in aggregate tended to be most abundant along much the same mid-shelf area, but in summer the area of greatest concentration was restricted to the southern part of the shelf where acoustical reflection profiling indicated a large gas content in the sediment at shallow depth. When viewed in composite for all seasons, greatest abundance of high-molecular-weight hydrocarbons was at the two stations that lie within the area of suspected high gas content. (See fig. 114). Also, several aspects of the biological data have at least a casual parallelism to the hydrocarbon data in the mid-shelf area. The patterns of numerical abundance for the

larvae of the flounder, sea basses and mackerel have an areal distribution that is almost exactly the same as that for the most abundant levels of the low-molecular-weight gases methane and propane in the spring and summer. Figure 114 shows the distribution of the high-molecular-weight hydrocarbons in the water, the bottom sediments and the organisms.

As a means of emphasizing the localized variations within the region, the individual stations were tabulated as to the number of times each ranked first or second in all three periods of sampling. The sums of first and second ranking arranged geographically by transect and by station for each category of data are shown by table 16; totals significantly higher than the regional average have been circled for emphasis. The tabulation demonstrates that the northwestern part of the shelf north of Port Aransas is biologically the most active. Significantly, the productivity is sustained largely by nutrients carried to the South Texas OCS by water inflow that comes from the northern Gulf.

Both the maps and the tabulations indicate that in terms of biologic activity, nutrient levels and hydrography, the South Texas OCS can be divided into three subareas on the basis of the composite patterns indicated and on the basis of seasonal variations:

1) Inner shelf--most productive part of shelf overall; substantial seasonal and geographic variations;

2) Outer shelf--generally low productivity; relatively high nutrient levels in all seasons; small variation in hydrographic components from season to season;

3) Southernmost shelf--generally greater productivity than shelf area immediately to the north; seasonal abundances as large as any place on shelf at individual stations and within a season but highly variable.

It should be noted that neither the low-molecular-weight hydrocarbons data nor the fish data, except for the demersal fish, have been included in

Table 16. Composite tabulations of abundance arranged geographically by transect and by station for biology and associated aspects. Number outside parentheses indicates number of times the station ranked first in abundance or content during the three sampling periods; number in parentheses is the number of times it ranked second; the number below is the sum of the first and second order rankings. Those sums higher than the regional average are circled for emphasis.

BIOLOGY (Number of organisms)

Transect Number	Station Number		
	1	2	3
I	13(11)	2(6)	3(4)
	(24)	8	7
II	9(19)	7(4)	1(3)
	(28)	11	4
III	1(4)	(4)	(6)
	5	4	6
IV	6(9)	3(12)	2(2)
	15	15	4

NUTRIENTS

	1	2	3
I	9(9)	(2)	7(4)
	(18)	2	(11)
II	4(6)	1(1)	7(1)
	(10)	2	8
III	6(2)	(1)	4(1)
	8	1	5
IV	5(2)	(1)	1
	7	1	1

TRACE METALS - BIOLOGY

	1	2	3
I	11(11)	13(9)	16(7)
	(22)	(22)	(23)
II	13(5)	5(9)	7(5)
	(18)	14	12

TRACE METALS - BIOLOGY (continued)

III	7(9) 16	2(1) 3	4(2) 6
IV	9(3) 12	10(4) 14	9(4) 13

TRACE METALS - SEDIMENTS

	1	2	3
I	2(1) 3	- 	-
II	- 	- 	(3) 3
III	2 	1 	6(1) (7)
IV	1(1) 2	1 	1

TOTALS

	1	2	3
I	35(32) (67)	15(17) 32	26(15) (41)
II	26(30) (56)	13(14) 27	15(12) 27
III	16(15) 31	3(6) 9	14(10) 24
IV	21(15) (36)	14(17) 31	13(6) 19

the tabulations. The data for those components showed no consistent regional patterns with the exception, perhaps, of the distribution of methane. Localized very high levels of methane were indicated for both mid and near-bottom depths in the water column, but no source was conclusively identified. The source is probably biogenic and the high seasonal concentrations in the water column may reflect unidentified solubility/temperature relationships in bottom sediments. Another possible explanation is that seasonal trapping of the gas as a result of thermal layering of the water and of temporarily enclosed water circulation may account for local methane abundances.

SHELF PROCESSES

The principal processes responsible for the geographic patterns indicated on the South Texas OCS are: fresh water inflow to the inner shelf, movement of open Gulf water onto the outer shelf, water mass movement or general circulation over the shelf, sedimentation and crustal deformation. The recognition of the primary processes that are generally responsible for the various environmental interactions on continental shelves was not a discovery of the 1975 studies. These processes have been known for a long time to be operative over continental shelves throughout the world. Not previously known for the South Texas OCS, nor indeed for any other segment of the continental shelves of the U.S., were the relative magnitude and geographic extent of each process, patterns of interactions within the region, seasonal and yearly variability on a quantitative basis and the extent to which the biological and chemical aspects of the environment are controlled by these processes.

The studies during 1975 have not supplied all of the data that will be necessary to quantify each of the individual processes and interactions indicated. However, they have provided a sound characterization of the region and a working outline. Perhaps, of most importance, the results for 1975 indicate clearly the types of studies that will be necessary to fill the knowledge gaps that still exist. The nature and extent of the various processes identified are shown by table 17.

BASELINE CONDITIONS

The environmental studies made during 1975 have outlined the broad characteristics of the South Texas OCS and have indicated the manner in which the operative processes interact. The degree to which the interactions vary from year to year and the extent of localized geographic variations must await the continuing studies. However, the historical data used to supplement the baseline data, though fragmentary, do substantiate the general picture outlined by the baseline data. Furthermore, the historical data give some indication that aspects of the environment, such as fresh water inflow and hydrography, do vary from year to year, largely as a response to variations in climatic conditions beyond the OCS region. For example, Mississippi River water probably reaches the South Texas OCS in some years but not in others. That it did so in 1975 is indicated by the hydrographic data and by the clay minerals in the suspended sediments. Consequently, the details of the patterns outlined by the 1975 data and the amounts of specific components can be expected to vary yearly, but the broader regional patterns very likely will not.

Table 17. Summary of principal processes operative in the South Texas OCS. [A chart of interrelationships, geographical and seasonal] W-winter; S-spring; Su-summer; F-fall

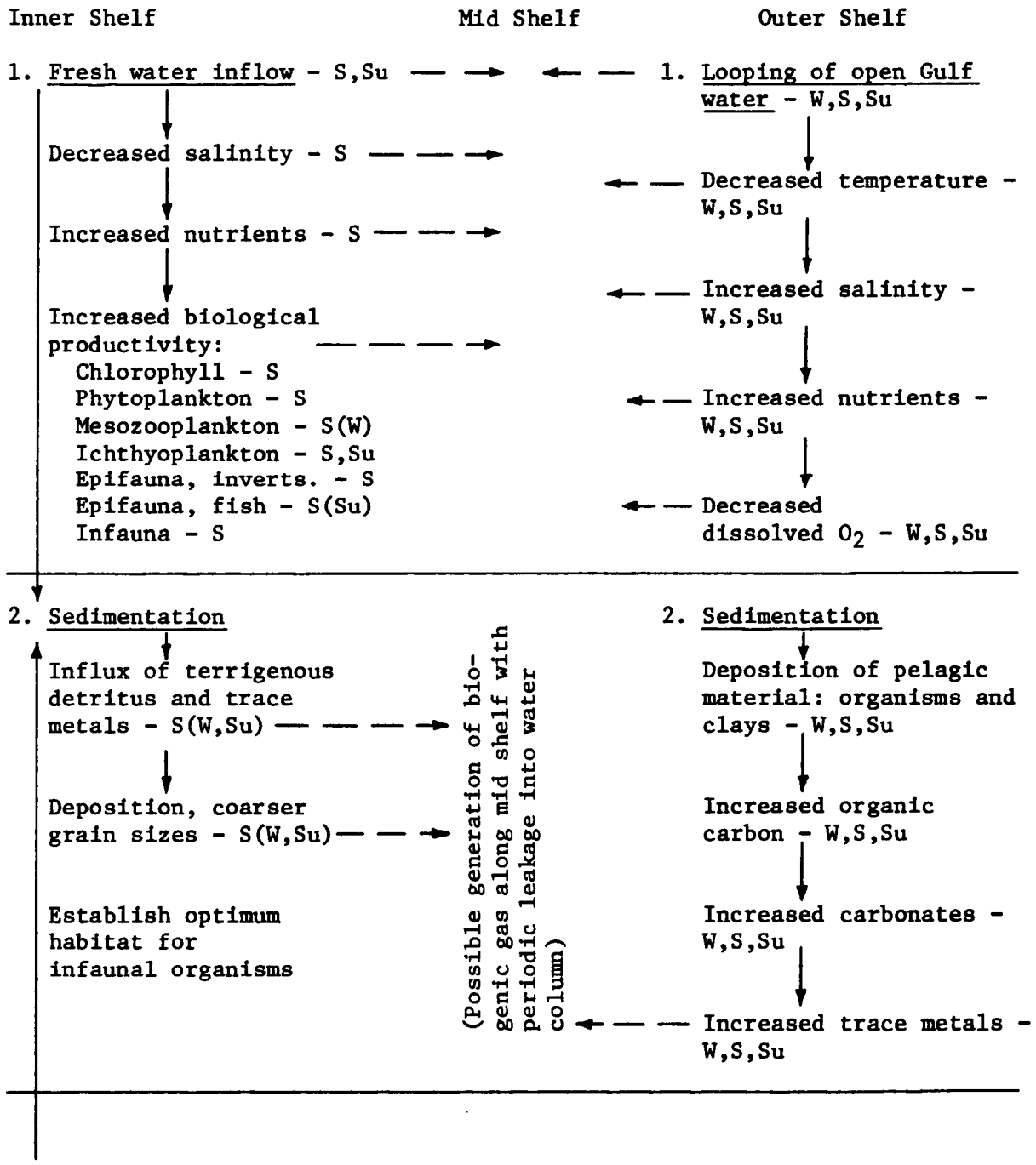

3. Water mass movement

Longshore dispersal of sediments:
- W - Southward
- S - Convergence starts s. central shelf; moves northward
- Su - Northward
- F - Convergence migrates southward

(Strongest normal effect during winter - net movement of sediments over the shelf is southward: storms carry sands beyond mid shelf)

Dispersal (or concentration) of nutrients

Dispersal (or concentration) of nekton and plankton

Dispersal of suspended sediments

3. Water mass movement

(Effects not known beyond those listed under no. 1. Intermittent influence to mid shelf indicated)

---

4. Deforming crustal movements

Holocene sequence not affected

4. Deforming crustal movements

Holocene sediments extensively faulted

Seaward tilting of shelf

Probable seepage of natural gas along faults

Possible induction of trace metals into sediments and water by gas seepage

Possible induction of hydrocarbons into water column

(Localized slumping of unstable sediments at edge of shelf)

The baseline status for the South Texas OCS, as indicated by the studies made in 1975, and an evaluation of the status of knowledge at the conclusion of the first year of study are summarized in the statements that follow. Unfortunately, the environmental characteristics of the South Texas OCS cannot be compared to those for other segments of the U.S. continental shelves because comparable data are not available. Statements of comparison are made as the limited data permit.

Physical Oceanography/Hydrography

1. Response to wind stress --Water movement relative to directions of air flow is strongly seasonal: southward in the winter, northward in the summer, and multidirectional during seasonal turn-around in the spring and fall. The patterns for the inner half of the shelf are well documented by significant amounts of historical drifter data and are predictable. Directions of drift relative to the pattern for the outer half of the shelf are poorly documented. Trajectory paths for possible surface oil spills based on seasonal drift patterns have been plotted on a tentative basis. (See figs. 43 through 46.)
2. Regional water mass movement --The patterns for currents moving over the South Texas OCS as a part of the larger Gulf-wide circulation are known only in the broadest sense. Data generated by other aspects of the OCS studies, such as nutrient content of the water, distribution of microzooplankton, and seasonal salinity and temperature variations, strongly indicate that the South Texas OCS is influenced by two regimes of water mass movement: influx of continental runoff on the inner shelf, and the movement of open Gulf water onto the outer shelf. The extent

to which Mississippi River effluent advances onto the South Texas OCS in the spring and the lag time and rates of flow are not well established; rates and specific directions of flow and the extent of encroachment and seasonal variations for the movement of water from the deeper Gulf onto the outer shelf are not known.

3. Hydrography--Over the inner half of the shelf, strong geographic and seasonal patterns of variability are indicated. Seasonal changes on the inner shelf related to climatic variations and to continental runoff are marked and predictable: lowered temperature during the winter and significantly lowered salinity in the spring. However, variations from year to year in magnitudes of change and in the geographic extent of change both southward along the shelf and seaward over the shelf are indicated. Over the outer edge of the shelf, accumulated data indicate an entirely different and more stable regime characterized by conditions that are less variable through the year.

4. Status of knowledge--The directions of movement for surficial water over the inner half of the shelf are reasonably well established; the directions of water movements at depth become progressively less known seaward. Rates and directions of water movement over periods of a few days are poorly known and for the inner shelf are known only for periods of approximately 2 weeks as based on the resultant vectors plotted from the time lapse between drifter release and drifter recovery. The magnitudes of seasonal changes in hydrographic conditions are reasonably well established and some indication of the magnitudes of yearly variations are evident from the baseline and historical data.

Nutrients

1. Geographic distribution --Amounts of the nutrients phosphate, nitrate and silicate showed strong geographic zonation: inner shelf and outer shelf. Each compound showed distinctly different seasonal patterns. Phosphate content was equally large in the two zones in winter, larger on the outer shelf in the spring and very small in both zones in the summer. Nitrate was equally abundant in all seasons on the outer shelf and relatively abundant on the inner shelf only in the spring. Silicate was equally abundant in all seasons on the inner shelf and relatively more abundant on the outer shelf only in the spring. The patterns of distribution for the nutrients present the best documentation for the two water mass regimes noted previously.
2. Relative abundance --The variations in the amounts of nutrients on the inner shelf are strictly seasonal and are directly related to two factors: greatly increased influx of continental runoff in the spring and utilization by the plankton. The specific variations for each type of nutrient is related to the degree to which the nutrient is taken up during periods of plankton blooming. Consequently, phosphate has the greatest seasonal variation, nitrate has less variation and silicate the least.
3. Status of knowledge --The studies during 1975 indicate nutrient patterns that are reasonable and that can be predicted, allowing for yearly differences in amounts because of variations in the amount of continental runoff.

Biology

1. Geographic abundance --Most of the marine organisms showed a strong geographic zonation when tabulated by numerical abundance. The plankton were most abundant along the inner shelf and their distribution is predictably similar to that for the nutrients. (Compare figures 111 and 112.) The numbers again were predictably large in the spring when nutrient content of the water was enriched by increased continental runoff. Both epifaunal and infaunal organisms were more numerous along the inner shelf where general productivity was greatest in response to the increased food supplies. Within the inner shelf zone, the organisms were clustered in the northern and southern parts. An additional factor controlling the epifaunal/infaunal communities appears to be the coarser grained bottom sediments along the inner shelf, which provide a more suitable habitat for these organisms than the finer grained mixtures of silt and clay farther out.

   The larger and more mobile organisms, such as the pelagic fish, showed less obvious geographic patterns. However, the ichthyoplankton abundance was greatest on the inner shelf. Biologically, the inner shelf is the most critical part of the South Texas OCS relative to the monitoring of future petroleum development.

2. Status of knowledge --Although the number of stations used for the baseline sampling was relatively small, the patterns of abundance for the organisms shown on figure 111 are both consistent and what might be expected on empirical grounds. Furthermore, the historical data for the mesozooplankton and ichthyoplankton corroborate the data gathered

in 1975. Several years of data almost certainly will show yearly differences at specific stations and the increased replicate sampling being done in the follow-on work will refine the patterns indicated in 1975.

Chemistry

1. Trace metals--The amounts of trace metals in the biota and sediments, both suspended and bottom, are similar to amounts measured in previous studies and in other offshore areas. No amounts significantly larger than normal were measured. Regional distribution falls into two zones: the inner shelf where amounts are predictably increased by continental runoff and the outer shelf where content in bottom sediments is predictably higher in the fine-grained sediments that are enriched in pelagic organic remains. Some of the trace metals in the outermost bottom sediments may have been introduced during seepage of natural gas. Slightly larger amounts of Pb and Cd seaward of the outlet for Matagorda Bay and on the shelf off the Rio Grande may be anthropogenic. For the larger and more mobile organisms, no obvious patterns were indicated.

   The South Texas OCS does not appear to have been contaminated by induction of excessive trace metals, thus a meaningful baseline has been established for future monitoring on a site-specific basis.

2. Hydrocarbons--No consistent patterns for the occurrence of low-molecular-weight hydrocarbons were indicated. A significant feature of the 1975 results was the very large amount of methane detected at mid and near-bottom water depths, both at mid shelf and along the edge

of the shelf. The amounts measured at mid depth during the summer were larger than amounts previously found by the same investigator on the Louisiana shelf where petroleum production has been extensive. The source for so much methane at mid-water level is not obvious, but the amount was abnormally large. The methane may be biogenic or it may be coming from petrogenic sources in the areas where natural gas seeps are suspected. However, the largest amounts of methane in the water were not in the areas of suspected gas seeps, nor were they in places where excessive biogenic gas would have been expected.

Whether the large amount of methane encountered in 1975 was normal for the South Texas OCS or whether it was an anomaly must await further work. More samples from mid-water levels are needed to resolve this mystery.

The heavy hydrocarbons showed even fewer consistent patterns than did the low-molecular-weight hydrocarbons. Few conclusions can be drawn about regional characteristics of distribution on the basis of the 1975 results. Significantly, regardless of the category of sample; water, animal or sediments, the analyses showed no concentrations larger than normal except at the innermost station of transect IV off the Rio Grande where some contamination by petrogenic hydrocarbon was suspected in the bottom sediments. Where amounts of heavy hydrocarbons were slightly larger than overall averages, they could be related to seasonal increase in the abundance of organisms. As was indicated by the trace metals, the South Texas OCS probably has not been contaminated by excessive amounts of petrogenic hydrocarbons. A reasonable baseline probably was established, but considering the great mobility of some of the organisms

analyzed and the difficulties involved in analyzing the small amounts of hydrocarbons encountered, further work is needed over a period of several years to establish meaningful regional patterns.

Sea Floor Sediments

1. Regional patterns--Patterns of sediment distribution based on differences in grain size are predictable, based on general knowledge about the energy levels of moving water relative to water depth on continental shelves. Sand-sized sediments are predominant on the inner shelf and decrease in abundance seaward. Localized rapid rates of sediment deposition or scour were not indicated. Relative to continental shelves in general, the rate of sediment accumulation during Holocene time has been relatively rapid, possibly as much as a half m or more locally per thousand years. Net long-term movement of sediment along the shelf seems to be southward.

   Cores of sediments taken up to 30 miles offshore contained discrete sand layers. The nature of these layers suggests that the sand probably was swept seaward over the shelf in the aftermath of hurricanes.

2. Sea floor stability--The surficial and near-surface bottom sediments are typically relatively soft and not suitable for bearing heavy structures at shallow depths. Some slumping of sea floor sediments has occurred along the periphery of the ancestral Rio Grande delta at the edge of the continental shelf. Over much of the ancestral Rio Grande delta where firm relict sand and soft mud are locally adjacent, sea floor stability is highly variable over short distances.

3. Status of knowledge--The data from the 264 bottom stations have

established a firm base of knowledge about textural patterns and some knowledge about rates of deposition and directions of transport over the shelf. For specific areas, such as parts of the ancestral Rio Grande delta and the outer periphery of the delta where slumping has occurred, detailed site-specific surveys prior to emplacement of structures and pipelines are needed. Furthermore, the general incoherence of the shallow sediment in an area susceptible to hurricanes suggests the need for burying any pipelines laid across the shelf.

Geologic Structure

Faulting of Holocene sediments all along the outer part of the continental terrace is indicated by the geophysical data. The data indicate that the movements have been progressive through time along many of the faults. A few of the faults intersect the sea floor, indicating recent movement. Seepage of natural gas along a number of the faults is suggested by the seismic profiles. The faults on the outer shelf seem to lie along the flank of an anticlinal fold whose axis roughly parallels the trend of the upper continental slope. Diapiric salt has penetrated almost to the sea floor in two places along the fold, producing domal structures. The nature of the faulting associated with the salt domes suggests that further movement can be expected. The need for detailed site-specific surveys is indicated prior to emplacement of structures along the outer edge of the shelf.

REFERENCES

Angelovic, J. W., and others, 1976, Environmental Studies of the South Texas Outer Continental Shelf, 1975: vol. 1, Plankton and Fisheries Investigations, 162 p., 40 figs., basic data in appendices A-F; vol. II, Physical Oceanography, 290 p., 174 figs.; A report to the U.S. Bureau of Land Management prepared by the National Oceanic and Atmospheric Administration: National Marine Fisheries Service and National Ocean Survey.

Berryhill, H. L., Jr., and others, 1976, Environmental Studies of the South Texas Outer Continental Shelf, 1975: Geology: Part I, Geologic description and interpretation, 270 p., 115 figs.; Part II, Basic analytical data. A report to the U.S. Bureau of Land Management prepared by the U.S. Geological Survey.

Bright, T. J., Rezak, Richard, and others, 1976, A Biological and Geological Reconnaissance of Selected Topographical Features on the Texas Continental Shelf: a report to the U.S. Bureau of Land Management prepared by the Texas A&M Research Foundation and the Texas A&M Department of Oceanography.

Carr, J. T., Jr., 1967, Hurricanes affecting the Texas Gulf coast: Texas Water Development Board, Report 49.

Parker, P. L., and others, 1976, Environmental Studies, South Texas Outer Continental Shelf, 1975: Biology and Chemistry, 598 p., 186 figs., basic data in appendices I-II. A report the U.S. Bureau of Land Management prepared by personnel of the University of Texas, Texas A&M University and Rice University.

The Department of the Interior Mission

As the Nation's principal conservation agency, the Department of the Interior has responsibility for most of our nationally owned public lands and natural resources. This includes fostering sound use of our land and water resources; protecting our fish, wildlife, and biological diversity; preserving the environmental and cultural values of our national parks and historical places; and providing for the enjoyment of life through outdoor recreation. The Department assesses our energy and mineral resources and works to ensure that their development is in the best interests of all our people by encouraging stewardship and citizen participation in their care. The Department also has a major responsibility for American Indian reservation communities and for people who live in island territories under U.S. administration.

The Minerals Management Service Mission

As a bureau of the Department of the Interior, the Minerals Management Service's (MMS) primary responsibilities are to manage the mineral resources located on the Nation's Outer Continental Shelf (OCS), collect revenue from the Federal OCS and onshore Federal and Indian lands, and distribute those revenues.

Moreover, in working to meet its responsibilities, the **Offshore Minerals Management Program** administers the OCS competitive leasing program and oversees the safe and environmentally sound exploration and production of our Nation's offshore natural gas, oil and other mineral resources. The MMS **Minerals Revenue Management** meets its responsibilities by ensuring the efficient, timely and accurate collection and disbursement of revenue from mineral leasing and production due to Indian tribes and allottees, States and the U.S. Treasury.

The MMS strives to fulfill its responsibilities through the general guiding principles of: (1) being responsive to the public's concerns and interests by maintaining a dialogue with all potentially affected parties and (2) carrying out its programs with an emphasis on working to enhance the quality of life for all Americans by lending MMS assistance and expertise to economic development and environmental protection.